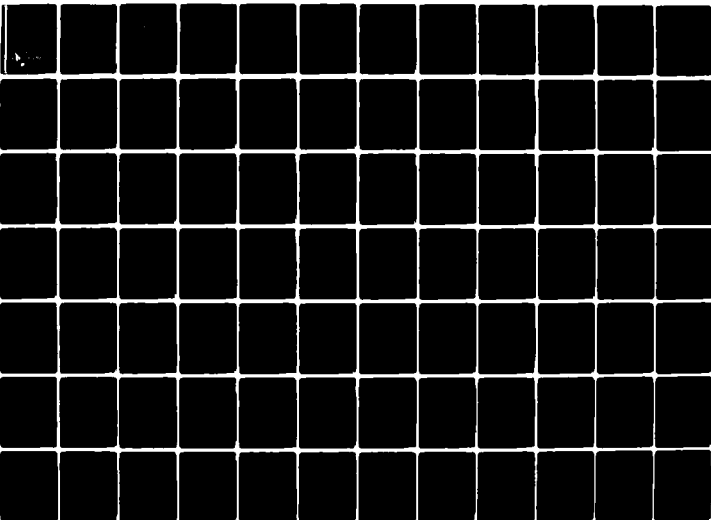


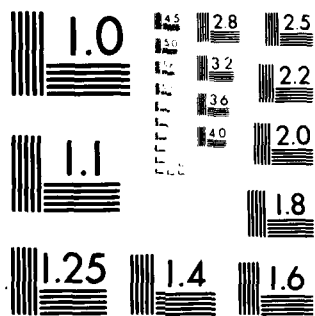
AD-A087 297

CALIFORNIA UNIV BERKELEY EARTHQUAKE ENGINEERING RES--ETC F/8 13/13
EARTHQUAKE RESPONSE OF CONCRETE GRAVITY DAMS INCLUDING HYDRODYN--ETC(U)
JAN 80 A K CHOPRA, P CHAKRABARTI, S GUPTA DACW73-71-C-0051
UCB/EERC-80/01 NL

UNCLASSIFIED

1 of 3
NO. 8
PAGE 1





MICROCOPY RESOLUTION TEST CHART

NATIONAL BUREAU OF STANDARDS-1963-A

LEVEL II

C

REPORT NO.
UCB/EERC-80/01
JANUARY 1980

✓ EARTHQUAKE ENGINEERING RESEARCH CENTER

EARTHQUAKE RESPONSE OF CONCRETE GRAVITY DAMS INCLUDING HYDRODYNAMIC AND FOUNDATION INTERACTION EFFECTS

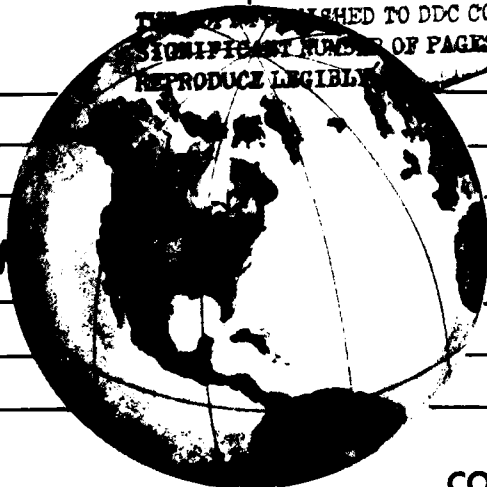
by
ANIL K. CHOPRA
P. CHAKRABARTI
SUNIL GUPTA

DTIC
JUL 31 1980
C

A report on research conducted under Contract DACW
73-71-C-0051 with the Office of the Chief of Engineers,
Washington, D.C. and Grants ATA74-20554 and
ENV76-80073 from the National Science Foundation.

THIS DOCUMENT IS BEST QUALITY PRACTICABLE.
THE COPY FURNISHED TO DDC CONTAINED A
SIGNIFICANT NUMBER OF PAGES WHICH DO NOT
REPRODUCE LEGIBLY.

This document has been approved
for public release and sale; its
distribution is unlimited.



COLLEGE OF ENGINEERING

UNIVERSITY OF CALIFORNIA • Berkeley, California

80 7 29 00

ADA087297

DDC FILE COPY

Any opinions, findings, and conclusions or recommendations expressed in this publication are those of the authors and do not necessarily reflect the views of the National Science Foundation.

For sale by the National Technical Information Service, U. S. Department of Commerce, Springfield, Virginia 22151.

See back of report for up to date listing of EERC reports.

DISCLAIMER NOTICE

**THIS DOCUMENT IS BEST QUALITY
PRACTICABLE. THE COPY FURNISHED
TO DTIC CONTAINED A SIGNIFICANT
NUMBER OF PAGES WHICH DO NOT
REPRODUCE LEGIBLY.**

(6) EARTHQUAKE RESPONSE OF CONCRETE GRAVITY DAMS
INCLUDING HYDRODYNAMIC AND FOUNDATION INTERACTION EFFECTS,

by

(10) Anil K./Chopra

P./Chakrabarti

Sunil/Gupta

(11) Jan 24 /
JUL 31 1980
C

(15) DACW 73-71-C-0051,
NSF-ATA 74-20554

A Report on Research Conducted Under
Contract DACW 73-71-C-0051 with the
Office of the Chief of Engineers, Washington, D.C.
and
Grants ATA74-20554 and ENV76-80073
from the National Science Foundation

(14)
Report No. UCB/EERC-80/01
Earthquake Engineering Research Center
University of California
Berkeley, California

January 1980

405986

ABSTRACT

A general procedure for analysis of the response of concrete gravity dams, including the dynamic effects of impounded water and flexible foundation rock, to the transverse (horizontal) and vertical components of earthquake ground motion is presented. The problem is reduced to one in two dimensions, considering the transverse vibration of a monolith of the dam. The system is analyzed under the assumption of linear behavior for the concrete, foundation rock and water.

The complete system is considered as composed of three substructures -- the dam, represented as a finite element system, the fluid domain, as a continuum of infinite length in the upstream direction, and the foundation rock region as a viscoelastic halfplane. The structural displacements of the dam are expressed as a linear combination of Ritz vectors, chosen as normal modes of an associated undamped dam-foundation system. The effectiveness of this analytical formulation lies in its being able to produce excellent results by considering only a few Ritz vectors. The modal displacements due to earthquake motion are computed by synthesizing their complex frequency responses using Fast Fourier Transform procedures. The stress responses are calculated from the modal displacements.

An example analysis is presented to illustrate results obtained from this analytical procedure. Computation times for several analyses are presented to illustrate effectiveness of the procedure.

The response of idealized dam cross-sections to harmonic horizontal or vertical ground motion is presented for a range of important system parameters characterizing the properties of the dam, foundation rock and impounded water. Based on these results, the separate effects of structure-water interaction and structure-foundation interaction, and the combined effects of the two sources of interaction, on dynamic response of dams are investigated, leading to the following conclusions.

Each source of interaction generally has significant effect on the complex frequency response functions for the dam. The fundamental resonant frequency of the dam decreases and its apparent damping increases because of structure-foundation interaction. The higher resonant frequencies and associated damping are affected similarly but to a lesser degree. These effects

are qualitatively similar whether the reservoir is empty or full, except at the resonant frequencies of the fluid domain. Because of hydrodynamic effects, the response curves are complicated in the neighborhood of the natural frequencies of water in the reservoir; the resonant frequencies of the dam are reduced -- the fundamental frequency by a significant amount but the higher resonant frequencies by relatively little; and the fundamental mode exhibits highly resonant behavior. The hydrodynamic effects in the dam response are qualitatively similar whether the foundation rock is rigid or flexible. The fundamental resonant frequency of the dam is reduced by roughly the same degree, independent of the foundation material properties. However, the apparent damping at the fundamental resonant frequency is dominated by effects of structure-foundation interaction and varies little with the depth of water. The fundamental resonant frequency of the dam is reduced by each of the two sources of interaction, with the influence of water usually being larger. However, there are no general trends regarding the comparative effects of water and foundation on the higher resonant frequencies or on the resonant responses of the dam. The response of the dam, without water, to vertical ground motion is small relative to that due to horizontal ground motion, but it becomes relatively significant when the hydrodynamic effects are included.

The displacement and stress responses of Pine Flat Dam to the S69E component of the Taft ground motion only, and to the S69E and vertical components acting simultaneously, are presented. For each of these excitations, the response of the dam is analyzed four times corresponding to the following four sets of assumptions: (1) rigid foundation, hydrodynamic effects excluded; (2) rigid foundation, hydrodynamic effects included; (3) flexible foundation, hydrodynamic effects excluded; and (4) flexible foundation, hydrodynamic effects included. These results lead to the following conclusions.

The displacements and stresses of Pine Flat Dam due to the Taft ground motion are increased significantly because of hydrodynamic effects. Compared to the response of the dam including only hydrodynamic effects, the stresses in the upper parts of the dam are significantly increased due to structure-foundation interaction. Stresses at the heel of the dam are increased to a lesser extent because of the stress relaxation due to foundation flexibility. The influence of structure-foundation interaction and structure-water interaction on the response of a dam depends in part on

the change in the earthquake response spectrum ordinate associated with changes in frequency and apparent damping due to these interaction effects. As such, these effects would depend on the resonant frequencies of the dam and the shape of the earthquake response spectrum in a neighborhood of these resonant frequencies. Although considerable stresses in Pine Flat Dam are caused by the vertical component of Taft ground motion, they partially cancel the stresses due to the horizontal component, resulting in reduced response when both ground motion components are considered simultaneously. The contribution of the vertical component of ground motion to the total response of a dam, including hydrodynamic effects, depends on the relative phasing of the responses to horizontal and vertical ground motion, which in turn depends on the phasing of the ground motion components and the vibration properties of the dam.

Accession For	
NTIS GML&I	<input checked="checked" type="checkbox"/>
DDC TAB	<input type="checkbox"/>
Unannounced	<input type="checkbox"/>
Justification	
By	
Distribution/	
Availability Codes	
Dist	Avail and/or special
A	Q3

TABLE OF CONTENTS

	<u>Page</u>
ABSTRACT	i
TABLE OF CONTENTS	v
1. INTRODUCTION	1
1.1 Objectives	1
1.2 Review of Past Work	1
1.3 Scope of this Report	4
1.4 Acknowledgments	5
2. SYSTEM AND GROUND MOTION	7
2.1 Dam-Water-Foundation System	7
2.2 Ground Motion	8
3. ANALYSIS OF GRAVITY DAMS	11
3.1 Introductory Note	11
3.2 Governing Equations	11
3.3 Earthquake Response Analysis	13
3.3.1 Time Domain Analysis	13
3.3.2 Frequency Domain Analysis	15
4. ANALYSIS OF GRAVITY DAMS INCLUDING DAM-WATER INTERACTION . .	17
4.1 Introductory Note	17
4.2 Governing Equations	17
4.2.1 Substructure 1: Dam	17
4.2.2 Substructure 2: Fluid Domain	19
4.3 Response Analysis for Harmonic Horizontal Ground Motion	20
4.4 Response Analysis for Harmonic Vertical Ground Motion .	24
4.5 Response to Arbitrary Ground Motion	27

	<u>Page</u>
5. ANALYSIS OF DAMS INCLUDING DAM-FOUNDATION INTERACTION . . .	29
5.1 Introductory Note	29
5.2 Frequency Domain Equations in Nodal Point Coordinates	29
5.2.1 Substructure 1: Dam	29
5.2.2 Substructure 2: Foundation Rock Region	30
5.2.3 Dam-Foundation System	32
5.2.4 Computational Requirements	34
5.3 Reduction of Degrees of Freedom	34
5.4 Response to Arbitrary Ground Motion	36
6. ANALYSIS OF DAMS INCLUDING HYDRODYNAMIC AND FOUNDATION INTER- ACTION EFFECTS	39
6.1 Introductory Note	39
6.2 Frequency Domain Equations	39
6.2.1 Substructure 1: Dam	39
6.2.2 Substructure 2: Foundation Rock Region	41
6.2.3 Dam-Foundation System	44
6.2.4 Reduction of Degrees of Freedom	44
6.2.5 Substructure 3: Fluid Domain	47
6.2.6 Dam-Water-Foundation System	53
6.2.7 Singularities of Response	56
6.3 Response to Arbitrary Ground Motion	56
6.4 Static Stress Analysis	57
6.5 Special Cases	62
6.5.1 Dam-Foundation System, No Water	62
6.5.2 Dam on Rigid Foundation, with Water	62
6.5.3 Dam on Rigid Foundation, No Water	63
6.6 Computer Program	64

	<u>Page</u>
7. PRELIMINARY RESULTS FOR PARAMETER SELECTION	65
7.1 Scope of the Chapter	65
7.2 Systems, Ground Motions, and Response Quantities	65
7.2.1 Systems	65
7.2.2 Ground Motions	67
7.2.3 Response Quantities	67
7.3 Comparison of Plane Strain and Plane Stress Assumption . .	68
7.4 Elastic Moduli Parameters	70
7.5 Damping Models and Parameters	70
7.5.1 Dam	70
7.5.2 Foundation	72
7.6 Number of Generalized Coordinates	76
8. COMPLEX FREQUENCY RESPONSES	79
8.1 Scope of Chapter	79
8.2 Systems, Ground Motions, Cases Analyzed and Response Quantities	79
8.2.1 Systems	79
8.2.2 Ground Motions	81
8.2.3 Cases Analyzed	81
8.2.4 Response Quantities	83
8.3 Complex Frequency Responses	83
8.3.1 Dam-Water Interaction Effects	83
8.3.2 Dam-Foundation Interaction Effects	90
8.3.3 Dam-Water and Dam-Foundation Interaction Effects .	90
9. EARTHQUAKE RESPONSE OF PINE FLAT DAM	107
9.1 Scope of the Chapter	107
9.2 Pine Flat Dam, Ground Motion, Cases Analyzed and Response Results	107

	<u>Page</u>
9.2.1 Pine Flat Dam	107
9.2.2 Ground Motion	111
9.2.3 Cases Analyzed	111
9.2.4 Response Results	114
9.3 Dam-Water Interaction Effects	115
9.4 Dam-Foundation Interaction Effects	120
9.5 Dam-Water and Dam-Foundation Interaction Effects	124
10. CONCLUSIONS	133
REFERENCES	137
APPENDIX A: USERS GUIDE TO COMPUTER PROGRAM	141
APPENDIX B: LISTING OF EAGD COMPUTER PROGRAM	159
EERC REPORT LISTING	189

1. INTRODUCTION

1.1 Objectives

It is extremely important to design dams which store large quantities of water to safely withstand earthquakes, particularly in view of the catastrophic consequences of dam failure. The damage to Koyna Dam, in India, which was designed according to standard, widely accepted procedures, shows that concrete gravity dams are not as immune to earthquake damage as has commonly been believed [1,2].

Reliable analytical procedures are necessary to design earthquake resistant dams, and to evaluate the safety of existing dams during future earthquakes. These procedures should provide the capability of evaluating the dynamic deformations and stresses in a dam subjected to a given ground motion. Special attention should be given to the interaction of the dam with the impounded water and with the foundation rock or soil. These factors complicate the otherwise routine finite element analysis of concrete gravity dams.

The objectives of the present study are: (a) to develop reliable and effective techniques for analyzing the response of concrete gravity dams to earthquake ground motion, including effects of dam-water interaction and of dam-foundation interaction, and (b) to examine the significance of these interaction effects in earthquake response of dams.

1.2 Review of Past Work

During the past 25 years, the finite element method has become the standard procedure for analysis of all types of civil engineering structures. Early in its development, it became apparent that this method had unique potentialities in the evaluation of stress in dams, and many of its earliest civil engineering applications concerned special problems associated with such structures [3,4]. The earliest dynamic finite element analyses of civil engineering structures involved the earthquake response analysis of earth dams [5]. Using the finite element method and excluding hydrodynamic effects, a number of questions were studied concerning the response of concrete gravity dams to earthquakes. These questions were prompted by the structural damage, caused by the December 1967 earthquake, to Koyna Dam.

The analysis of hydrodynamic pressures, due to horizontal ground motion, on rigid dams started with Westergaard's pioneering work of 1933 [7]. Continuing with the assumption of a rigid dam, more comprehensive analyses of hydrodynamic pressures on the dam face, due to both horizontal and vertical components of ground motion, have been developed [8,12].

In the finite element analyses mentioned, hydrodynamic effects were not considered; whereas in the studies of hydrodynamic pressures, the dam was assumed to be rigid. Additional hydrodynamic pressures will result from deformations of the upstream face of the dam, and the structural deformations in turn will be affected by the hydrodynamic pressures on the upstream face. To break this closed cycle of cause and effect, the problem formulation must recognize the dynamic interaction between the dam and water.

Finite element analysis of the complete dam-water system is one possible approach to including these interaction effects. Application of standard analysis procedures with nodal point displacements as the degrees-of-freedom was only partly successful [13]. A different finite element formulation of the complete system, in which displacements are considered as the unknowns at the nodal points for the dam, and pressures as the unknowns at the nodal points for the water, has been applied to small problems [14]; but this approach appears to require prohibitive computational effort for practical problems.

The more effective approach is to treat the dam-water system as composed of two substructures -- dam and fluid domain -- coupled through the interaction forces and appropriate continuity conditions at the face of the dam. A series of studies [15-18] led to a general analysis procedure [19] and computer program [20] for dynamic analyses of dams, including dam-water interaction. This approach conveniently permits different models to be used for the dam and water. The dam may be idealized by the finite element method, which has the ability to handle systems of arbitrary geometry. At the same time, the fluid domain may be treated as a continuum, an approach which is ideally suited to the simple geometry but great upstream extent of the impounded water [19]. The fluid domain may also be idealized by the finite element method in conjunction with infinite elements [21]. When the substructure method is employed, along with transformation of the governing equations to generalized coordinates

associated with vibration modes of the dam alone, the analysis procedure is very efficient, and little additional computational effort is required to include the hydrodynamic effects [19].

Utilizing such an analysis procedure, it was shown that the dam-water interaction and water compressibility have a significant influence on the dynamic behavior of concrete gravity dams and their responses to earthquake ground motion [22]. Because of hydrodynamic effects, the vertical component of ground motion is more important in the response of gravity dams than in other classes of structures [18,22]. A simplified analysis procedure has been developed which includes the dam-water interaction effects in the computation of lateral earthquake forces for dam design [23].

The effects of dam-foundation interaction can most simply be included in dynamic analysis of dams by including, in the finite element idealization, foundation rock or soil above a rigid horizontal boundary. The response of such a finite element system to excitation specified at the bottom, rigid boundary is then analyzed by standard procedures. Such an approach leads to enormous computational requirements and the reliability of results in some cases is questionable. For sites where similar materials extend to large depths and there is no obvious "rigid" boundary such as a soil-rock interface, the location of the rigid boundary introduced in the analysis is often quite arbitrary, and it may significantly distort the response.

These difficulties can be overcome by using the substructure method [24, 25], wherein the dam and the foundation rock or soil region are considered as two substructures of the complete system. The dam may be idealized as a finite element system which has the ability to represent arbitrary geometry and material properties. The foundation rock or soil region may be idealized as either a continuum (a viscoelastic halfspace for example), or as a finite element system, whichever is appropriate for the site. The halfspace idealization permits accurate modelling of sites where similar materials extend to large depths. For sites where layers of soil or soft rock overlie harder rock at shallow depths, finite element idealization of the foundation region would be appropriate. The governing equations for the two substructures are combined by imposing equilibrium and compatibility requirements at the base of the dam. These equations make direct use of free field ground motion specified at the dam-foundation interface. The resulting equations are transformed to generalized Ritz coordinates; the displacements are expressed as a

linear combination of the first few vibration modes of an associated dam-foundation system, thus leading to a very efficient solution.

The preceding review discussed the dam-water system and dam-foundation system separately. In each of these two cases, the impounded water and the foundation, respectively, modify the vibration properties of the dam and may significantly affect its response. However, the two problems actually are coupled and the results obtained by separate analyses will, in general, be invalid. There is need, therefore, for developing techniques for analysis of complete dam-water-foundation systems, and assessing simultaneously, the interaction due to both water and foundation. Some work on this problem has been reported in recent years [26,27]. The substructure methods developed for separately considering hydrodynamic and foundation interaction effects in the response of dams appear to be ideally suited for and extendable to complete analyses which simultaneously include both types of interaction.

1.3 Scope of this Report

Chapter 2 describes how the dam-water-foundation system and earthquake ground motion are idealized in this study. Also included in this chapter are the assumptions underlying the procedure, developed in later chapters, for analysis of earthquake response of concrete gravity dams.

For the reader's convenience, a summary is given of the procedures available for analyzing earthquake response of concrete gravity dams under restrictive conditions. Chapter 3 summarizes the standard finite element method for analysis of dams on rigid foundations with no water stored in their reservoirs. Chapter 4 summarizes the substructure method for including the effects of dam-water interaction in the analysis procedure. (This method treats the impounded water and dam on rigid foundation as two substructures of the total system.) Also based on the substructure concept is the procedure for including effects of interaction between the dam and its flexible foundation on the earthquake response of dams without water, summarized in Chapter 5.

Because the substructure concept has proven to be effective in separately including the effects of dam-water interaction and of dam-foundation interaction in the analysis, it is extended in Chapter 6 to develop an analysis procedure simultaneously including various effects of the water and the foundation. These include effects arising from interaction between the dam

and foundation, dam and water, water and foundation, and interaction among all three substructures -- dam, water, and foundation. The computer program developed to implement the procedure for analysis of dam-water-foundation systems is briefly described in this chapter; the user's guide and program listing is included in Appendices A and B.

Using this computer program, results of several preliminary analyses are presented in Chapter 7 with the aim of defining the important system and analysis parameters for the subsequent study of dynamic response behavior of dams. The behavioral study is in two parts, separated into Chapters 8 and 9.

The response of idealized dam cross-sections to harmonic horizontal or vertical ground motion is presented in Chapter 8 for a range of the important systems parameters characterizing the properties of the dam, foundation rock, and impounded water. With the aid of these results, the separate effects of dam-water interaction and dam-foundation interaction, and the combined effects of the two sources of interaction on dynamic response of dams are investigated.

Chapter 9 presents the responses of Pine Flat Dam to the S69E component of the Taft ground motion only; and to the S69E and vertical components acting simultaneously. For each of these excitations, the response of the dam is analyzed four times corresponding to the following four sets of assumptions: (1) rigid foundation, hydrodynamic effects excluded; (2) rigid foundation, hydrodynamic effects included; (3) flexible foundation, hydrodynamic effect excluded; and (4) flexible foundation, hydrodynamic effects included. These results provide insight into the effects of dam-water and dam-foundation interaction, considered separately or together, in the earthquake response of dams.

Chapter 10 briefly summarizes the significant conclusions which may be drawn from this investigation of dam-water and dam-foundation interaction effects in earthquake response of concrete gravity dams.

1.4 Acknowledgements

This study was initially supported by the Office of the Chief of Engineers, Department of the Army, Washington, D.C., under Contract No. DACW73-71-C-0051. Completion of this study was made possible by Grants ATA74-20554 and ENV76-80073 from the National Science Foundation. The authors are grateful for the support from both agencies.

Perhaps a few words regarding the history of this study would be of interest to the sponsors and the reader. The study was initiated in 1974. Dr. P. Charkabarti participated in formulating the essential aspects of the analysis procedure and developed the computer programs during 1974 and 1975, at which time he left Berkeley to accept a position in India. Thereafter, Dr. G. Dasgupta was involved in the study for a short time, incorporating some improvements in the analysis procedure and computer program. His efforts were then diverted to developing dynamic stiffness matrices for the foundation required in obtaining the numerical results for this study. At this juncture, in 1976, Sunil Gupta, a graduate research assistant, became associated with the project. He produced the large volume of computer results presented in this report, and assisted in interpreting these results and preparing the report. Because there was some discontinuity between the times Chakrabarti, Dasgupta, and Gupta worked on this project; because considerable time was required to develop the results on dynamic stiffness matrices for the foundation; and for other reasons beyond our control, our efforts on this study have been sporadic. This resulted in considerable, unanticipated delay in completion of the study.

2. SYSTEM AND GROUND MOTION

2.1 Dam-Water-Foundation System

Vibration tests on Pine Flat Dam [28] indicate that at small vibration amplitudes a concrete gravity dam will behave like a solid even though there is some slippage between monoliths. Thus, at the beginning of an earthquake, the behavior of a dam can be best described by a three-dimensional model. However, at large amplitudes of motion, the inertia forces are much larger than the shear forces that can be transmitted across joints between monoliths. The monoliths slip and tend to vibrate independently, as evidenced by the spalled concrete and increased water leakage at the joints of Koyna Dam during the Koyna earthquake of December 11, 1967. Consequently, two-dimensional models of individual monoliths appear to be more appropriate than three-dimensional models for predicting the response of concrete gravity dams to the strong phase of intense ground motion. However, a model more complicated than either of these two models will be necessary to describe the behavior of a concrete gravity dam through the complete amplitude range. .

Because the dimensions and dynamic properties of the various monoliths differ, the effects of the dam on deformations and stresses in the foundation will vary along the length of the dam. Thus even with two-dimensional models for the dam, a three-dimensional model would seem necessary for the foundation. If the dam were to behave as a solid without slippage between monoliths, and all of its properties and the ground motion did not vary along the length, it would be appropriate to assume the dam as well as the foundation to be in plane strain. A plane stress model which applies to a thin sheet-like body seems obviously inappropriate for a continuum foundation.

Although the basic concepts underlying the analysis procedure presented in this work are applicable under more general conditions, the procedure is specifically developed for two-dimensional systems; thus its application is restricted to systems in generalized plane stress or plane strain. Although neither of the two models are strictly applicable, the former is better for the dam and the latter for the foundation. However, in order to define the dam-foundation system on a consistent basis, the same model should be employed for both substructures. Results from the two models are compared in Sec. 7.3 to provide a basis for choosing one for parameter studies.

A cross-section of the system considered is shown in Fig. 2.1. The system consists of a concrete gravity dam supported on the horizontal surface of a viscoelastic half plane and impounding a reservoir of water. The system is analyzed under the assumption of linear behavior for the concrete, foundation soil or rock, and water. The dam is idealized as a two-dimensional finite element system, thus making it possible to consider arbitrary geometry and variation of material properties. However, certain restrictions on the geometry are imposed to permit solutions for the foundation and fluid domains treated as continua. For the purposes of determining hydrodynamic effects, and only for this purpose, the upstream face of the dam is assumed to be vertical. This is reasonable for an actual concrete gravity dam, because the upstream face is vertical or almost vertical for most of its height, and the hydrodynamic pressures on the dam face are insensitive to small departures of the face slope from the vertical. For the purpose of including structure-foundation interaction effects, the foundation surface is assumed to be horizontal; thus the base of the dam as well as the reservoir bottom is assumed to be horizontal. An actual system can usually be idealized to conform to this assumption.

2.2 Ground Motion

The excitation for the two-dimensional dam-foundation-water system is defined by the two components of free-field ground acceleration in the plane of a cross-section of the dam: the horizontal component transverse to the dam axis, $a_g^x(t)$, and the vertical component, $a_g^y(t)$.

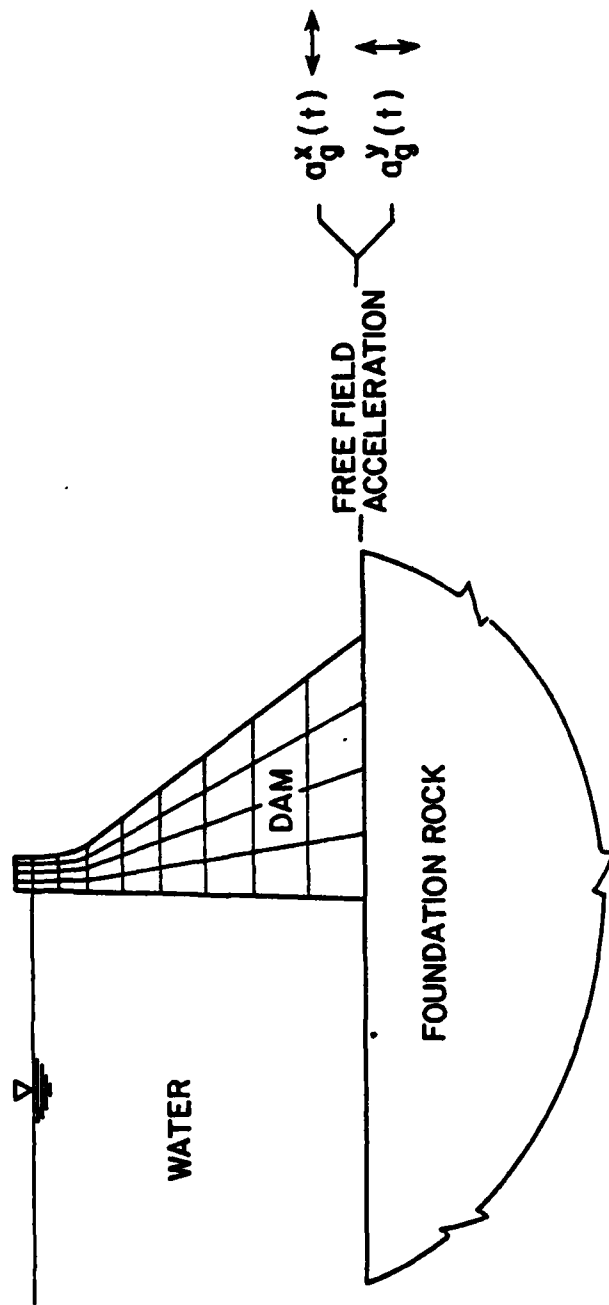


FIG. 2.1 DAM-WATER-FOUNDATION SYSTEM

3. ANALYSIS OF GRAVITY DAMS

3.1 Introductory Note

The standard finite element method for analysis of gravity dams on rigid foundations with no water stored in the reservoir is summarized in this chapter. In later chapters, the analysis will be extended to include effects of impounded water and foundation flexibility.

3.2 Governing Equations

Consider a monolith of a concrete gravity dam on a rigid foundation, with no water in the reservoir, subjected to earthquake ground motion which does not vary across the base of the monolith. The equations of motion for such a dam monolith idealized as a planar, two-dimensional finite element system are:

$$\underline{m}\ddot{\underline{r}} + \underline{c}\dot{\underline{r}} + \underline{k}\underline{r} = -\underline{m}\underline{l}^x a_g^x(t) - \underline{m}\underline{l}^y a_g^y(t) \quad (3.1)$$

In Eq. 3.1, \underline{m} , \underline{k} and \underline{c} are the mass, stiffness, and viscous damping matrices for the finite element system; \underline{r} is the vector of nodal point displacements, relative to the free-field displacement:

$$\underline{r}^T = \langle r_1^x \ r_1^y \ r_2^x \ r_2^y \ \dots \ r_n^x \ r_n^y \ \dots \ r_N^x \ r_N^y \rangle$$

where r_n^x and r_n^y are the x- and y- components of displacement of nodal point n and the number of nodal points above the base is N; $\dot{\underline{r}}$ and $\ddot{\underline{r}}$ are, respectively, the nodal point velocity and acceleration vectors.

$$\{\underline{l}^x\}^T = \langle 1 \ 0 \ 1 \ 0 \ \dots \ 1 \ 0 \ \dots \ 1 \ 0 \rangle$$

$$\{\underline{l}^y\}^T = \langle 0 \ 1 \ 0 \ 1 \ \dots \ 0 \ 1 \ \dots \ 0 \ 1 \rangle$$

$a_g^x(t)$ and $a_g^y(t)$ are the x (horizontal) and y (vertical) components of the free-field ground acceleration.

The stiffness and mass matrices of the structure are obtained from the corresponding matrices for the individual finite elements by direct assembly

procedures. The element stiffness matrices are derived using quadratic interpolation function for displacements, whereas the element mass matrices are based on a lumped mass approximation.

Energy dissipation in structures, even in the linear range of vibration, is due to various complicated phenomena. Because it is not possible to mathematically describe each of these sources of energy dissipation, it is customary to define damping in terms of damping ratios in the natural modes of vibration. Damping ratios for similar structures obtained from both the analysis of harmonic vibration tests, and responses recorded during earthquakes, are used as a basis for assigning the modal damping ratios. The modal damping ratios provide a complete description of damping properties for purposes of linear analysis and the damping matrix need not be defined explicitly.

Traditionally, analysis of dynamic response of structures has been carried out directly in the time domain. For such analyses, viscous damping is the most convenient representation of energy dissipation in the structure. When effects of dam-water interaction and dam-foundation interaction are included, the analysis is most effectively carried out by a substructure method [3,4]. As will be seen in Chapters 4,5 and 6, the substructure method is best formulated in the frequency domain. In such a formulation, constant hysteretic damping is a preferable representation -- for conceptual as well as computational reasons -- especially when structure-soil interaction effects are included [5].

The Fourier transform of Eq. 2.1 provides the governing equation in the frequency domain

$$[-\omega^2 \underline{m} + i\omega \underline{c} + \underline{k}] \underline{\hat{f}}(\omega) = -\underline{m} \underline{l}^x \hat{a}_g^x(\omega) - \underline{m} \underline{l}^y \hat{a}_g^y(\omega) \quad (3.2)$$

in which the Fourier transform of $f(t)$ is denoted by $\hat{f}(\omega)$. For constant hysteretic damping, Eq. 2.2 becomes

$$[-\omega^2 \underline{m} + (1 + i\eta) \underline{k}] \underline{\hat{f}}(\omega) = -\underline{m} \underline{l}^x \hat{a}_g^x(\omega) - \underline{m} \underline{l}^y \hat{a}_g^y(\omega) \quad (3.3)$$

where η is the constant hysteretic damping factor.

Damping ratios as obtained from forced vibration tests on dams are

essentially independent of the mode number [28]. If ξ is the damping ratio appropriate for all the natural modes of vibration of the dam, $\eta = 2\xi$ would be an appropriate value for the constant hysteretic damping factor [29]. With the damping coefficient so related, essentially the same response will be obtained for a lightly damped system with either damping mechanism.

3.3 Earthquake Response Analysis

3.3.1 Time Domain Analysis

The earthquake response of a dam is obtained by solving the equations of motion (Eq. 3.1). These equations of motion in nodal point coordinates may be solved either directly or after transformation to modal coordinates [30]. The latter approach, commonly known as the mode superposition method, is applicable if the response is within the linear range. This method is advantageous for calculating the earthquake response of many types of structures, because the response is essentially due to the first few modes of vibration.

The first step in the mode superposition analysis procedure is to obtain the lower few natural frequencies and mode shapes of vibration of the dam by solving the eigenvalue problem:

$$\underline{k} \underline{\phi} = \omega^2 \underline{m} \underline{\phi} \quad (3.4)$$

The equations of motion (Eq. 3.1) are uncoupled by the transformation

$$\underline{r}(t) = \sum_{n=1}^{2N} \underline{\phi}_n Y_n(t) \quad (3.5)$$

provided the damping matrix \underline{c} satisfies certain restrictions [6]. In Eq. 3.5, $Y_n(t)$ is the generalized coordinate and $\underline{\phi}_n$ the mode shape for the n^{th} natural mode of vibration. The uncoupled equation for the n^{th} mode of vibration is

$$M_n \ddot{Y}_n + C_n \dot{Y}_n + K_n Y_n = -L_n^x a_g^x(t) - L_n^y a_g^y(t) \quad (3.6)$$

where

$$M_n = \underline{\phi}_n^T \underline{m} \underline{\phi}_n, C_n = \xi_n (2M_n \omega_n), K_n = \omega_n^2 M_n, \omega_n \text{ and } \xi_n \text{ are the natural}$$

circular frequency and damping ratio for the n^{th} mode, $L_n^x = \phi_n^T m \ddot{x}$, and $L_n^y = \phi_n^T m \ddot{y}$.

Equation 3.6 may be solved for $Y_n(t)$ by a step-by-step integration method [30]. After computation has been repeated for all modes, the nodal displacement vector $\underline{r}(t)$ can be obtained from Eq. 3.5. In practice, it is generally sufficient to solve the equations of motion only for the lower few modes, because the contributions of the higher modes to the total response are small.

The stresses $\underline{\sigma}_p(t)$ in finite element p at any instant of time are related to the nodal displacement $\underline{r}_p(t)$ for that element by

$$\underline{\sigma}_p(t) = \underline{T}_p \underline{r}_p(t) \quad (3.7)$$

where the stress transformation matrix \underline{T}_p is based on the interpolation functions for the element as well as its elastic properties. The stresses throughout the dam at any instant of time are determined from the nodal point displacements by application of the above transformation to each finite element.

The initial stresses, before the earthquake, should be added to the stresses due to earthquake excitation, determined by the procedures presented in the preceding sections, to obtain the total stresses in the dam. Excluding the temperature and creep stresses in concrete, only the gravity loads need to be considered. The equations of static equilibrium are formulated:

$$\underline{K} \underline{r} = \underline{R} \quad (3.8)$$

where \underline{R} is the vector of static loads due to the weight of the dam and hydrostatic pressures. Solution of these algebraic equations results in the displacement vector \underline{r} . Static stresses are then determined from the displacements by applying Eq. 3.7 to each finite element.

Analytical predictions, based on the procedure summarized above, for the performance of Koyna Dam correlated well with the damage experienced by the dam during the Koyna earthquake of December 11, 1976 [2].

3.3.2 Frequency Domain Analysis

An alternative approach to solving the modal equations of motion (Eq. 3.6) exists in which, instead of step-by-step integration in the time domain, the complex frequency responses are superposed in the frequency domain utilizing the Fourier integral [30]. The complex frequency response function $\bar{z}(\omega)$ for a response quantity $z(t)$ has the property that, when the excitation is the real part of $e^{i\omega t}$, then the response is the real part of $\bar{z}(\omega)e^{i\omega t}$.

The response in the n^{th} mode of vibration due to the horizontal ground motion will be denoted by \bar{y}_n^x , and that due to the vertical ground motion by \bar{y}_n^y . The response to excitation $a_g^\ell(t) = e^{i\omega t}$ can then be expressed as

$$\bar{y}_n^\ell = \bar{\bar{y}}_n^\ell e^{i\omega t} \quad \text{where } \ell = x \text{ or } y.$$

Substitution in Eq. 3.6 leads to

$$(-\omega^2 M_n + i\omega C_n + K_n) \bar{\bar{y}}_n^\ell(\omega) = -L_n^\ell; \ell = x, y \quad (3.9)$$

from which

$$\bar{\bar{y}}_n^\ell(\omega) = \frac{-L_n^\ell}{-\omega^2 M_n + i\omega C_n + K_n}, \ell = x, y \quad (3.10)$$

If the system has constant hysteretic damping instead of viscous damping, starting from Eq. 3.3, it can be shown that Eqs. 3.9 and 3.10 become

$$[-\omega^2 M_n + (1 + i\eta)K_n] \bar{\bar{y}}_n^\ell(\omega) = -L_n^\ell; \ell = x, y \quad (3.11)$$

and

$$\bar{\bar{y}}_n^\ell(\omega) = \frac{-L_n^\ell}{-\omega^2 M_n + (1 + i\eta)K_n}; \ell = x, y \quad (3.12)$$

The response to arbitrary ground motion is the superposition of responses to individual harmonic components of the excitation through the Fourier integral:

$$\bar{y}_n^\ell(t) = \frac{1}{2\pi} \int_{-\infty}^{\infty} \bar{\bar{y}}_n^\ell(\omega) A_g^\ell(\omega) e^{i\omega t} d\omega; \ell = x, y \quad (3.13)$$

in which $A_g^\ell(\omega)$ is the Fourier transform of $a_g^\ell(t)$:

$$A_g^\ell(\omega) = \int_0^d a_g^\ell(t) e^{-i\omega t} dt; \quad \ell = x, y \quad (3.14)$$

where d is the duration of the ground motion.

The response in the n^{th} vibration mode due to simultaneous action of the horizontal and vertical components of ground motion is

$$Y_n(t) = Y_n^x(t) + Y_n^y(t) \quad (3.15)$$

Repeating this procedure for all the necessary values of n , the displacement responses may be obtained by superposition of the modal responses (Eq. 3.5) and the stress responses by calculating the stresses associated with these displacements (Eq. 3.7). The initial stresses are added to determine the total stresses.

Until the development of the Fast Fourier Transform (FFT) algorithm [31], numerical evaluation of integrals such as those in Eqs. 3.13 and 3.14 required prohibitive amounts of computer time and the errors in the results could not be predicted accurately. As a result, step-by-step integration in the time domain has conventionally been used for response analysis. With the FFT algorithm, integrals of Eqs. 3.13 and 3.14 can be evaluated accurately and efficiently. As a result, the frequency domain approach can now be employed advantageously for analysis of dynamic response of structures. It provides an alternative approach for analysis of dams without water. As will be seen in Chapters 4, 5, and 6, the analysis is best formulated by the frequency domain approach when dam-water and dam-foundation interaction effects are included.

4. ANALYSIS OF GRAVITY DAMS INCLUDING DAM-WATER INTERACTION

4.1 Introductory Note

Summarized in this chapter is the procedure presented earlier [19], for including the effects of dam-water interaction in earthquake response analyses of concrete gravity dams. The concept underlying this procedure is to treat the impounded water and the dam as two substructures of the total system. With this approach, the dam may be idealized by the finite element method, which has the ability to represent systems of arbitrary geometry and material properties (see Chapter 3). At the same time, the impounded water may be treated as a continuum, an approach which is ideally suited to the simple idealized geometry but great upstream extent of the impounded water. The equations of motion for the two substructures are coupled by including the forces of interaction between the water and the face of the dam.

4.2 Governing Equations

4.2.1 Substructure 1: Dam

A gravity dam supported on a rigid foundation and storing water to a given depth is shown in Fig. 4.1. Including hydrodynamic effects, the equations of motion are, for a dam monolith idealized as a planar two-dimensional finite element system (Chapter 3), subjected to horizontal and vertical components of ground motion:

$$\underline{m} \ddot{\underline{r}} + \underline{c} \dot{\underline{r}} + \underline{k} \underline{r} = -\underline{m} \underline{1}^x a_g^x(t) - \underline{m} \underline{1}^y a_g^y(t) + \underline{R}_h(t) \quad (4.1)$$

This is identical to Eq. 3.1 except for the inclusion of the hydrodynamic loads $\underline{R}_h(t)$ on the upstream face of the dam.

Whereas Eq. 4.1 is valid for dams of arbitrary geometry, it is assumed that for the purpose of defining hydrodynamic effects, and only for this purpose, the upstream face of the dam is vertical. Considering that the upstream face of concrete gravity dams is vertical or almost vertical for most of the height, this is a reasonable assumption. With this assumption and because the hydrodynamic loads act only on the upstream face, only those loads in $\underline{R}_h(t)$ that correspond to the x-degrees of freedom of the nodal points on the upstream face are non-zero. The sub-vector of the non-zero loads is denoted by $\underline{R}_h^{xf}(t)$. The superscript "xf" indicates that only the

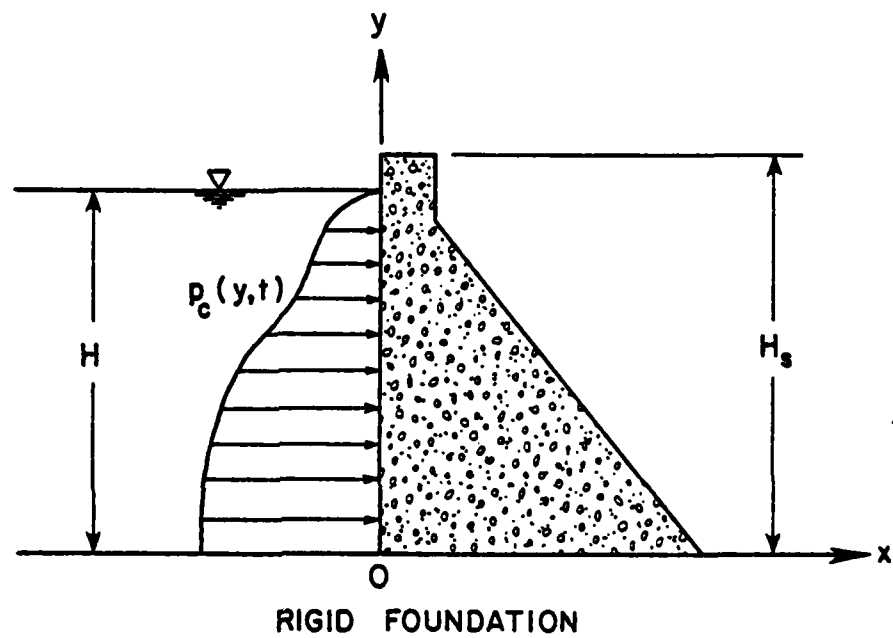


FIG. 4.1 CONCRETE GRAVITY DAM WITH IMPOUNDED WATER. THE HYDRODYNAMIC PRESSURES ON THE UPSTREAM FACE OF THE DAM ARE $p_c(y,t)$

x-component of the loads acting on the face of the dam are included in the vector.

The procedure for analyzing the response of dams without including the effects of water, presented in Chapter 3, utilized the mode-superposition concept. Although classical natural modes of vibration do not exist for the dam when hydrodynamic effects are included, expansion of displacements, including hydrodynamic effects, in terms of natural modes of vibration without water can still be used advantageously. Thus,

$$r(t) \approx \sum_{n=1}^J \phi_n Y_n(t) \quad (4.2)$$

The vectors ϕ_n , $n = 1, 2, \dots, 2N$ are linearly independent and span the vector space of dimension $2N$. Thus, the expansion of Eq. 4.2 is exact if the contributions of all the $2N$ natural modes of vibration are included. However, even when hydrodynamic effects are included, the contributions of the lower modes of vibration are expected to be more significant and relatively few terms, e.g. $J \ll 2N$, would suffice in Eq. 4.2.

Substituting Eq. 4.2 into Eq. 4.1 and utilizing the orthogonality property of mode shapes, the equation governing the generalized displacement $Y_n(t)$ in the n^{th} mode is

$$M_n \ddot{Y}_n + C_n \dot{Y}_n + K_n Y_n = -L_n^X a_g^X(t) - L_n^Y a_g^Y(t) + R_{hn}(t) \quad (4.3)$$

This is the same as Eq. 3.6, except for the additional term $R_{hn}(t) = \phi_{n-h}^T R_h(t) = \{\phi_n^{xf}\}^T R_h^{xf}(t)$ in which the vector ϕ_n^{xf} consists of the x-components of the displacements of the nodal points on the upstream face of the dam.

4.2.2 Substructure 2: Fluid Domain

The motion of the dam-water system is considered to be two-dimensional, i.e., it is the same for any vertical plane perpendicular to the axis of the dam. Assuming water to be linearly compressible and neglecting its internal viscosity, the small amplitude, irrotational motion of the fluid is governed by the two-dimensional wave equation

$$\frac{\partial^2 p}{\partial x^2} + \frac{\partial^2 p}{\partial y^2} = \frac{1}{c^2} \frac{\partial^2 p}{\partial t^2} \quad (4.4)$$

in which $p(x,y,t)$ is the hydrodynamic pressure (in excess of the hydrostatic pressure) and C is the velocity of sound in water. The hydrodynamic pressure acting on the upstream face of the dam is $p_c(y,t) \equiv p(0,y,t)$.

4.3 Response Analysis for Harmonic Horizontal Ground Motion

Specializing the equations of motion of the dam in terms of generalized modal displacements (Eq. 4.3) for the case when the ground motion acts only in the horizontal (x) direction leads to

$$M_n \ddot{Y}_n^x + C_n \dot{Y}_n^x + K_n Y_n^x = -L_n^x a_g^x(t) + R_{hn}^x(t) \quad (4.5)$$

where $L_n^x = \phi_n^T m_1^x$ and $R_{hn}^x(t) = \{\phi_n^{xf}\}^T R_h^{xf}(t)$. The vector $R_h^{xf}(t)$ consists of forces, associated with hydrodynamic pressures acting in the horizontal direction, at the nodal points on the vertical upstream face of the dam. These hydrodynamic pressures are governed by the two-dimensional wave equation (Eq. 4.4) and the following boundary conditions:

- Pressure at the free surface is zero, implying that the effects of waves at the free surface are ignored;
- Vertical motion at the base of the reservoir is zero; and
- Horizontal component of motion of the fluid boundary $x = 0$ is the same as the horizontal motion of the upstream face of the dam.

The responses to harmonic ground acceleration $a_g^x(t) = e^{i\omega t}$ can be expressed as follows:

$$\text{Generalized Displacements, } Y_n^x(t) = \bar{Y}_n^x(\omega) e^{i\omega t} \quad (4.6a)$$

$$\text{Generalized Accelerations, } \ddot{Y}_n^x(t) = \bar{\ddot{Y}}_n^x(\omega) e^{i\omega t} \quad (4.6b)$$

Horizontal accelerations at the upstream face,

$$\ddot{u}(t) = \{\hat{1} + \sum_{j=1}^J \phi_j^{xf} \bar{\ddot{Y}}_j^x(\omega)\} e^{i\omega t} \quad (4.6c)$$

in which $\hat{1}$ is a vector with all elements equal to unity.

$$\text{Hydrodynamic pressures, } p_c^x(y,t) = \bar{p}_c^x(y,\omega) e^{i\omega t} \quad (4.6d)$$

Strictly for purposes of notational convenience, the vector ϕ_j^{xf} is replaced by its continuous analog function $\phi_j(y)$. The total horizontal acceleration

of the fluid boundary at $x = 0$, the upstream face of the dam, may now be represented by the function

$$\ddot{u}(0, y, t) = \left\{ 1 + \sum_{j=1}^J \phi_j(y) \bar{Y}_j^x(\omega) \right\} e^{i\omega t} \quad (4.7)$$

With reference to Fig. 4.1, the boundary conditons for the wave equation are

$$\left. \begin{aligned} p(x, H, t) &= 0 \\ \frac{\partial p}{\partial y}(x, 0, t) &= 0 \\ \frac{\partial p}{\partial x}(0, y, t) &= -\frac{w}{g} \left\{ 1 + \sum_{j=1}^J \phi_j(y) \bar{Y}_j^x(\omega) \right\} e^{i\omega t} \end{aligned} \right\} \quad (4.8)$$

Because the governing equation as well as the boundary conditions are linear, the principal of superpostion applies. The complex frequency response function for $p_c^x(y, t)$ can therefore be expressed as

$$\bar{p}_c^x(y, \omega) = \bar{p}_0^x(y, \omega) + \sum_{j=1}^J \bar{Y}_j^x(\omega) \bar{p}_j(y, \omega) \quad (4.9)$$

where $p_0^x(y, t) = \bar{p}_0^x(y, \omega) e^{i\omega t}$ is the solution of the wave equation at $x = 0$ (Eq. 4.4) for the following boundary conditions:

$$\left. \begin{aligned} p(x, H, t) &= 0 \\ \frac{\partial p}{\partial y}(x, 0, t) &= 0 \\ \frac{\partial p}{\partial x}(0, y, t) &= -\frac{w}{g} e^{i\omega t} \end{aligned} \right\} \quad (4.10)$$

and $p_j(y, t) = \bar{p}_j(y, \omega) e^{i\omega t}$ is the solution of the wave equation at $x = 0$ for the following boundary conditons:

$$\left. \begin{aligned} p(x, H, t) &= 0 \\ \frac{\partial p}{\partial y}(x, 0, t) &= 0 \\ \frac{\partial p}{\partial x}(0, y, t) &= -\frac{w}{g} \phi_j(y) e^{i\omega t} \end{aligned} \right\} \quad (4.11)$$

Solutions of Eq. 4.4 for the above two sets of boundary conditons are

presented in Eqs. 4.12 and 4.13

$$\bar{p}_0^x(y, \omega) = \frac{4w}{\pi g} \sum_{\ell=1}^{\infty} \frac{(-1)^\ell}{(2\ell-1) \sqrt{\lambda_\ell^2 - \omega^2/c^2}} \cos \lambda_\ell y \quad (4.12)$$

$$\bar{p}_j(y, \omega) = - \frac{2w}{gH} \sum_{\ell=1}^{\infty} \frac{I_{j\ell}}{\sqrt{\lambda_\ell^2 - \omega^2/c^2}} \cos \lambda_\ell y \quad (4.13)$$

in which $\lambda_\ell = (2\ell-1) \pi/2H$ and $I_{j\ell} = \int_0^H \phi_j(y) \cos \lambda_\ell y \, dy$. The complex frequency response function $\bar{p}_0^x(y, \omega)$ is for the hydrodynamic pressures on the dam when the excitation to the fluid domain is the horizontal acceleration of the ground and the dam is rigid. The corresponding function is $\bar{p}_j^x(y, \omega)$ when the excitation is the acceleration of the dam in the j^{th} mode of vibration and there is no motion of the base of the reservoir.

The integrals $I_{j\ell}$ are computed as a summation using the elements of the vector ϕ_j^{xf} instead of the continuous function $\phi_j(y)$ which was introduced only for notational convenience. The nodal force vectors are $\bar{R}_0^x(t) = \bar{R}_0^x(\omega) e^{i\omega t}$ and $\bar{R}_j(t) = \bar{R}_j(\omega) e^{i\omega t}$, where $\bar{R}_0^x(\omega)$ and $\bar{R}_j^x(\omega)$ are the static equivalents of the corresponding pressure functions $\bar{p}_0^x(y, \omega)$ and $\bar{p}_j^x(y, \omega)$, respectively. They may be computed directly by using the principle of virtual work with the displacements between nodal points defined by the finite element interpolation functions. The complex frequency response function for the total force vector $\bar{R}_h^{xf}(t)$ is, from Eq. 4.9,

$$\bar{R}_h^{xf}(\omega) = \bar{R}_0^x(\omega) + \sum_{j=1}^J \bar{Y}_j^x(\omega) \bar{R}_j(\omega) \quad (4.14)$$

The hydrodynamic forces on the dam have thus been expressed in terms of the unknown generalized coordinate responses $\bar{Y}_j^x(\omega)$.

With the aid of Eq. 4.14 and substituting $\bar{Y}_j^x(\omega) = -\omega^2 \bar{Y}_j^x(\omega)$, Eq. 4.5 can be written as follows for the excitation $a_g^x(t) = e^{i\omega t}$:

$$\left[-\omega^2 M_n + i\omega C_n + K_n \right] \bar{Y}_n^x(\omega) = -L_n^x + \{ \phi_n^{xf} \}^T \left\{ \bar{R}_0^x(\omega) - \omega^2 \sum_{j=1}^J \bar{Y}_j^x(\omega) \bar{R}_j(\omega) \right\} \quad (4.15)$$

The set of equations 4.15 for $n = 1, 2 \dots J$ may be rearranged and expressed in matrix form as

$$\begin{bmatrix} S_{11}(\omega) & S_{12}(\omega) & \dots & S_{1J}(\omega) \\ S_{21}(\omega) & S_{22}(\omega) & \dots & S_{2J}(\omega) \\ \vdots & \vdots & \ddots & \vdots \\ S_{J1}(\omega) & S_{J2}(\omega) & \dots & S_{JJ}(\omega) \end{bmatrix} \begin{Bmatrix} \bar{Y}_1^x(\omega) \\ \bar{Y}_2^x(\omega) \\ \vdots \\ \bar{Y}_J^x(\omega) \end{Bmatrix} = \begin{Bmatrix} L_1^x(\omega) \\ L_2^x(\omega) \\ \vdots \\ L_J^x(\omega) \end{Bmatrix} \quad (4.16)$$

in which

$$\left. \begin{aligned} S_{nj}(\omega) &= \omega^2 \{\phi_n^{xf}\}^T \bar{R}_j(\omega) \text{ for } n \neq j \\ S_{nn}(\omega) &= [-\omega^2 M_n + i\omega C_n + K_n] + \omega^2 \{\phi_n^{xf}\}^T \bar{R}_n(\omega) \\ L_n^x(\omega) &= -L_n^x + \{\phi_n^{xf}\}^T \bar{R}_0^x(\omega) \end{aligned} \right\} \begin{array}{l} n = 1, 2 \dots J \\ j = 1, 2 \dots J \end{array} \quad (4.17)$$

The coefficient matrix $\underline{S}(\omega)$ in Eq. 4.17 is a frequency dependent matrix which relates the generalized displacement vector $\bar{Y}^x(\omega)$ with the corresponding generalized load vector $L^x(\omega)$. Unlike classical modal analysis, the matrix $\underline{S}(\omega)$ is not diagonal because the vectors ϕ_n are not the natural vibration modes of the dam-fluid system; they simply are the natural vibration modes of the dam without water. It can be shown that $\underline{S}(\omega)$ is a symmetric matrix.

With one change, Eqs. 4.16 and 4.17 are valid even if damping for the dam is idealized as constant hysteretic damping instead of viscous damping. The expression for the diagonal elements of $\underline{S}(\omega)$ changes to

$$S_{nn}(\omega) = [-\omega^2 M_n + (1 + i\eta) K_n] + \omega^2 \{\phi_n^{xf}\}^T \bar{R}_n(\omega) \quad (4.18)$$

Solution of Eq. 4.16 for all values of excitation frequency would give the complete frequency response functions for all the generalized coordinates $\bar{Y}_n^x(\omega)$, $n = 1, 2 \dots J$. The frequency responses for generalized accelerations may be obtained from the generalized displacements as

$$\bar{\ddot{Y}}_n^x(\omega) = -\omega^2 \bar{Y}_n^x(\omega) \quad (4.19)$$

The complex frequency response functions for the vectors of nodal displacements and accelerations relative to the ground motion are obtained by superposition of the contributions of the various modes of vibration (Eq. 4.2):

$$\bar{\underline{r}}^x(\omega) = \sum_{n=1}^J \phi_n \bar{\underline{y}}_n^x(\omega) \quad (4.20)$$

$$\bar{\underline{\ddot{r}}}^x(\omega) = -\omega^2 \sum_{n=1}^J \phi_n \bar{\underline{y}}_n^x(\omega) \quad (4.21)$$

4.4 Response Analysis for Harmonic Vertical Ground Motion

Specializing the equations of motion of the dam in terms of generalized modal displacements (Eq. 4.3) for the case when the ground motion acts only in the vertical (y) direction leads to:

$$M_n \ddot{\underline{y}}_n^y + C_n \dot{\underline{y}}_n^y + K_n \underline{y}_n^y = -L_n^y a_g^y(t) + R_{hn}^y(t) \quad (4.22)$$

where $L_n^y = \phi_n^T \underline{1}^y$ and $R_{hn}^y(t) = \{\phi_n^{xf}\}^T R_h^{xf}(t)$. The vector $R_h^{xf}(t)$ consists of forces, associated with hydrodynamic pressures acting in the horizontal direction, at the nodal points on the vertical upstream face of the dam. These hydrodynamic pressures are governed by the two-dimensional wave equation (Eq. 4.4) together with the following boundary conditions (see Fig. 4.1):

- Pressure at the free surface is zero, implying that the effects of waves at the free surface are ignored;
- Vertical component of motion of the fluid boundary $y = 0$, the base of the reservoir, is prescribed by the vertical component of ground acceleration; and
- Horizontal component of motion of the fluid boundary $x = 0$ is the same as the horizontal motion of the upstream face of the dam.

The responses to harmonic ground acceleration $a_g^y(t) = e^{i\omega t}$ can be expressed as follows:

$$\text{Generalized displacements, } \underline{y}_n^y(t) = \bar{\underline{y}}_n^y(\omega) e^{i\omega t} \quad (4.23a)$$

$$\text{Generalized accelerations, } \ddot{y}_n^Y(t) = \ddot{y}_n^Y(\omega) e^{i\omega t} \quad (4.23b)$$

Horizontal accelerations at the upstream face,

$$\ddot{u}(t) = \left\{ \sum_{j=1}^J \phi_j^{xf} \ddot{y}_j^Y(\omega) \right\} e^{i\omega t} \quad (4.23c)$$

$$\text{Hydrodynamic pressures, } p_c^Y(y, t) = \bar{p}_c^Y(y, \omega) e^{i\omega t} \quad (4.23d)$$

Replacing the vector ϕ_j^{xf} by its continuous analog function, $\phi_j(y)$, as before, the horizontal acceleration of the fluid boundary at $x = 0$, the upstream face of the dam, is represented by the function:

$$\ddot{u}(0, y, t) = \left\{ \sum_{j=1}^J \phi_j(y) \ddot{y}_j^Y(\omega) \right\} e^{i\omega t} \quad (4.24)$$

Then the boundary conditions for the wave equation are

$$\left. \begin{aligned} p(x, H, t) &= 0 \\ \frac{\partial p}{\partial y}(x, 0, t) &= -\frac{w}{g} e^{i\omega t} \\ \frac{\partial p}{\partial x}(0, y, t) &= -\frac{w}{g} \left\{ \sum_{j=1}^J \phi_j(y) \ddot{y}_j^Y(\omega) \right\} e^{i\omega t} \end{aligned} \right\} \quad (4.25)$$

Because the governing equations as well as boundary conditions are linear, the principle of superpositions applies. The complex frequency response function for $p_c^Y(y, t)$ can therefore be expressed as

$$\bar{p}_c^Y(y, \omega) = \bar{p}_0^Y(y, \omega) + \sum_{j=1}^J \ddot{y}_j^Y(\omega) \bar{p}_j(y, \omega) \quad (4.26)$$

where $p_0^Y(y, t) = \bar{p}_0^Y(y, \omega) e^{i\omega t}$ is the solution of the wave equation (Eq. 4.4) for the following boundary conditions

$$\left. \begin{aligned} p(x, H, t) &= 0 \\ \frac{\partial p}{\partial y}(x, 0, t) &= -\frac{w}{g} e^{i\omega t} \\ \frac{\partial p}{\partial x}(0, y, t) &= 0 \end{aligned} \right\} \quad (4.27)$$

and $p_j(y,t) = \bar{p}_j(y,\omega)e^{i\omega t}$ is the solution of the wave equation (Eq. 4.4) at $x = 0$ for the following boundary conditions:

$$\left. \begin{aligned} p(x,H,t) &= 0 \\ \frac{\partial p}{\partial y}(x,0,t) &= 0 \\ \frac{\partial p}{\partial x}(0,y,t) &= -\frac{w}{g} \phi_j(y)e^{i\omega t} \end{aligned} \right\} \quad (4.28)$$

Solution of Eq. 4.4 for the boundary conditions of Eq. 4.27 is

$$\bar{p}_0^y(y,\omega) = \frac{w}{g} \frac{C}{\omega} \frac{(1+\alpha) \sin \frac{\omega(H-y)}{C}}{(1+\alpha) \cos \frac{\omega H}{C} + i(1-\alpha) \sin \frac{\omega H}{C}} \quad (4.29)$$

In this equation, the reflection coefficient

$$\alpha = \frac{(C_r w_r / Cw) - 1}{(C_r w_r / Cw) + 1} \quad (4.30)$$

where w_r and C_r are the unit weight and P-wave velocity for the rock material at the bottom of the reservoir. For rigid rock, $\alpha = 1$ indicating that hydrodynamic pressure waves are completely reflected at the bottom of the reservoir. For deformable rock, $\alpha < 1$ implying that hydrodynamic pressure waves impinging at the reservoir bottom are partially reflected back in the fluid domain and partially refracted into rock. The complex frequency response function $\bar{p}_0^y(y,\omega)$ is for the hydrodynamic pressures on the dam when the excitation to the fluid domain is the vertical acceleration of the ground and the dam is rigid.

The solution of Eq. 4.4 for the boundary conditions of Eq. 4.28 has been presented earlier in Eq. 4.13. As mentioned before, $\bar{p}_j(y,\omega)$ is the complex frequency response function for the hydrodynamic pressure when the excitation is the acceleration of the dam in the j^{th} mode of vibration and there is no motion of the base.

The nodal force vectors are $\bar{R}_0^y(t) = \bar{R}_0^y(\omega)e^{i\omega t}$ and $\bar{R}_j(t) = \bar{R}_j(\omega)e^{i\omega t}$, where $\bar{R}_0^y(\omega)$ and $\bar{R}_j(\omega)$ are the static equivalents of the corresponding pressure functions $\bar{p}_0^y(y,\omega)$ and $\bar{p}_j(y,\omega)$ respectively. The complex frequency response function for the total force vector $\bar{R}_h^{xf}(t)$ is, from Eq. 4.25,

$$\bar{R}_h^{xf}(\omega) = \bar{R}_0^y(\omega) + \sum_{j=1}^J \bar{Y}_j^y(\omega) \bar{R}_j(\omega) \quad (4.31)$$

With the aid of Eq. 4.31 and substituting $\ddot{\bar{Y}}_j^Y(\omega) = -\omega^2 \bar{Y}_j^Y(\omega)$, Eq. 4.22 can be written as follows for the excitation $a_g^Y(t) = e^{i\omega t}$:

$$\left[-\omega^2 M_n + i\omega C_n + K_n \right] \bar{Y}_n^Y(\omega) = -L_n^Y + \left\{ \phi_n^{xf} \right\}^T \left\{ \bar{R}_0^Y(\omega) - \omega^2 \sum_{j=1}^J \bar{Y}_j^Y(\omega) \bar{R}_j^Y(\omega) \right\} \quad (4.32)$$

The set of Eqs. 4.32 for $n = 1, 2, \dots, J$ after rearranging may be expressed in matrix form as

$$\underline{S}(\omega) \bar{\underline{Y}}^Y(\omega) = \underline{L}^Y(\omega) \quad (4.33)$$

in which the coefficient matrix $\underline{S}(\omega)$ is identical to the case when the excitation was the horizontal component of ground motion (Eqs. 4.16-4.18), and

$$L_n^Y(\omega) = -L_n^Y(\omega) + \left\{ \phi_n^{xf} \right\}^T \bar{R}_0^Y(\omega), \quad n = 1, 2, \dots, J \quad (4.34)$$

Solution of Eq. 4.33 for all values of excitation frequency would give the complex frequency response functions for generalized displacements $\bar{Y}_n^Y(\omega)$. The frequency responses for generalized accelerations

$$\ddot{\bar{Y}}_n^Y(\omega) = -\omega^2 \bar{Y}_n^Y(\omega) \quad (4.35)$$

The complex frequency response functions for the vectors of nodal displacements and accelerations relative to the ground motion are given by expressions similar to Eqs. 4.20 and 4.21:

$$\bar{\underline{r}}^Y(\omega) \approx \sum_{n=1}^J \phi_n \bar{Y}_n^Y(\omega) \quad (4.36)$$

$$\ddot{\bar{\underline{r}}}^Y(\omega) \approx -\omega^2 \sum_{n=1}^J \phi_n \bar{Y}_n^Y(\omega) \quad (4.37)$$

4.5 Response to Arbitrary Ground Motion

Once the complex frequency response functions $\bar{Y}_n^X(\omega)$ and $\bar{Y}_n^Y(\omega)$, $n = 1, 2, \dots, J$, have been determined by solving Eqs. 4.16 and 4.33 for an appropriate range of excitation frequency ω , the responses to arbitrary ground motion can be obtained as the superposition of responses to individual harmonic components of the excitation through the Fourier integral:

$$\bar{Y}_n^\ell(t) = \frac{1}{2\pi} \int_{-\infty}^{\infty} \bar{Y}_n^\ell(\omega) A_g^\ell(\omega) e^{i\omega t} d\omega; \ell = x, y \quad (4.38)$$

in which $A_g^\ell(\omega)$ is the Fourier Transform of $a_g^\ell(t)$:

$$A_g^\ell(\omega) = \int_0^d a_g^\ell(t) e^{-i\omega t} dt; \ell = x, y \quad (4.39)$$

where d is the duration of ground motion.

The combined response $Y_n(t)$ to horizontal and vertical components of ground motion acting simultaneously is

$$Y_n(t) = Y_n^x(t) + Y_n^y(t) \quad (4.40)$$

Repeating this procedure for all the necessary values of n , the displacement response is obtained by transforming back from generalized to nodal point coordinates

$$\underline{r}(t) \approx \sum_{n=1}^J \phi_n Y_n(t) \quad (4.41)$$

The stresses $\underline{\sigma}_p(t)$ in finite element p at any instant of time are related to the nodal displacements $\underline{r}_p(t)$ for that element by

$$\underline{\sigma}_p(t) = \underline{T}_p \underline{r}_p(t) \quad (4.42)$$

where \underline{T}_p is the stress transformation matrix for the finite element p . At any instant of time, the stresses throughout the dam are determined from the nodal point displacements by applying the transformation of Eq. 4.42 to each finite element.

The total stresses are the sum of the dynamic stresses determined above and the initial static stresses due to the weight of the dam and hydrostatic pressures (Sec. 3.3).

A digital computer program was developed [20] to implement the analysis summarized in this chapter. Studies using this computer program have led to a better understanding of hydrodynamic effects in earthquake response of concrete gravity dams [18].

5. ANALYSIS OF DAMS INCLUDING DAM-FOUNDATION INTERACTION

5.1 Introductory Note

This chapter summarizes the procedure presented earlier [24,25] for including the effects of structure-foundation interaction, i.e., interaction between the structure and underlying soil or rock, in earthquake response analyses of concrete gravity dams without water. This procedure to include the dam-foundation interaction effects is based on the same basic substructure concept utilized to include the dam-water interaction. The soil or rock region and the dam are considered as two substructures of the combined system. The dam may be idealized by the finite element method, which has the ability to represent systems of arbitrary geometry and material properties (see Chapters 3 and 4). The soil or rock region may be idealized as either a finite element system or as a continuum, for example, as a viscoelastic halfspace. The halfspace idealization permits accurate modelling of sites where essentially similar rocks extend to large depths. For sites where layers of soil or soft rock are underlain by harder rock at shallow depth, finite element idealization of the soil region would be appropriate. The governing equations for the two substructures are combined by imposing equilibrium and compatibility requirements at the base of the dam, which is the structure-foundation interface.

5.2 Frequency Domain Equations in Nodal Point Coordinates

5.2.1 Substructure 1: Dam

The equations of motion for the dam idealized as a planar, two-dimensional finite element system (Chapter 3) are:

$$\underline{m}_c \ddot{\underline{r}}_c + \underline{c}_c \dot{\underline{r}}_c + \underline{k}_c \underline{r}_c = -\underline{m}_c \underline{1}_c^x a_g^x(t) - \underline{m}_c \underline{1}_c^y a_g^y(t) + \underline{R}_c(t) \quad (5.1)$$

in which \underline{m}_c , \underline{c}_c , and \underline{k}_c are the mass, damping, and stiffness matrices for the finite element system; \underline{r}_c is the vector of nodal point displacements relative to the free-field earthquake displacement at the base (Fig. 5.1):

$$\underline{r}_c^T = \langle r_1^x \ r_1^y \ r_2^x \ r_2^y \ \dots \ r_n^x \ r_n^y \ \dots \ r_{N+N_b}^x \ r_{N+N_b}^y \rangle$$

in which r_n^x and r_n^y are the x and y components of the displacement of nodal

point n ; N is the number of nodal points above the base, N_b is the number on the base, and the total number is $N+N_b$;

$$\{\underline{1}_C^x\}^T = \langle 1 \ 0 \ 1 \ 0 \ \dots \ 1 \ 0 \ \dots \ 1 \ 0 \rangle$$

$$\{\underline{1}_C^y\}^T = \langle 0 \ 1 \ 0 \ 1 \ \dots \ 0 \ 1 \ \dots \ 0 \ 1 \rangle$$

$\underline{R}_C(t)$, the vector of forces due to structure-foundation interaction, will have non zero elements only at the base of the dam; $a_g^x(t)$ and $a_g^y(t)$ are the x and y components of the specified free-field ground acceleration, assumed to be identical at all nodal points on the dam base.

For harmonic ground acceleration in the x (horizontal) or y (vertical) directions $a_g^l(t) = e^{i\omega t}$, $l = x$ or y , the displacements and interaction forces can be expressed in terms of their complex frequency responses: $\underline{r}_C(t) = \underline{\bar{r}}_C^l(\omega) e^{i\omega t}$ and $\underline{R}_C(t) = \underline{\bar{R}}_C^l(\omega) e^{i\omega t}$ and the governing equation as

$$[-\omega^2 \underline{m}_C + i\omega \underline{c}_C + \underline{k}_C] \underline{\bar{r}}_C^l(\omega) = -\underline{m}_C \underline{1}_C^l + \underline{\bar{R}}_C^l(\omega); \quad l = x \text{ or } y \quad (5.2)$$

If the structure has constant hysteretic damping, Eq. 5.2 becomes

$$[-\omega^2 \underline{m}_C + (1 + i\eta) \underline{k}_C] \underline{\bar{r}}_C^l(\omega) = -\underline{m}_C \underline{1}_C^l + \underline{\bar{R}}_C^l(\omega); \quad l = x \text{ or } y \quad (5.3)$$

Partitioning \underline{r}_C into \underline{r} , the vector of displacements of nodal points above the base, and \underline{r}_b the vector of interaction displacements at the base (Fig. 5.1), Eq. 5.3 can be expressed as

$$\left(-\omega^2 \begin{bmatrix} \underline{m} & 0 \\ 0 & \underline{m}_b \end{bmatrix} + (1+i\eta) \begin{bmatrix} \underline{k} & \underline{k}_b \\ (\underline{k}_b)^T & \underline{k}_{bb} \end{bmatrix} \right) \begin{Bmatrix} \underline{\bar{r}}^l(\omega) \\ \underline{\bar{r}}_b^l(\omega) \end{Bmatrix} = - \begin{Bmatrix} \underline{m} \underline{1}^l \\ \underline{m}_b \underline{1}_b^l \end{Bmatrix} + \begin{Bmatrix} 0 \\ \underline{\bar{R}}_b^l(\omega) \end{Bmatrix} \quad (5.4)$$

5.2.2 Substructure 2: Foundation Rock Region

The dynamics of the foundation soil or rock region are considered separately. The interaction forces, $\underline{R}_f(t)$, at the foundation surface can be expressed in terms of the corresponding displacements, $\underline{r}_f(t)$, relative to the free-field earthquake ground displacement [24]:

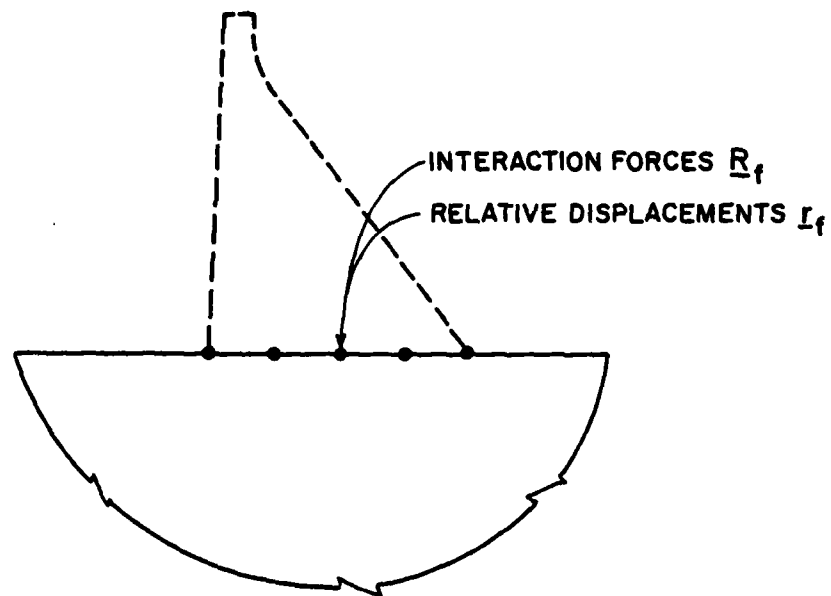
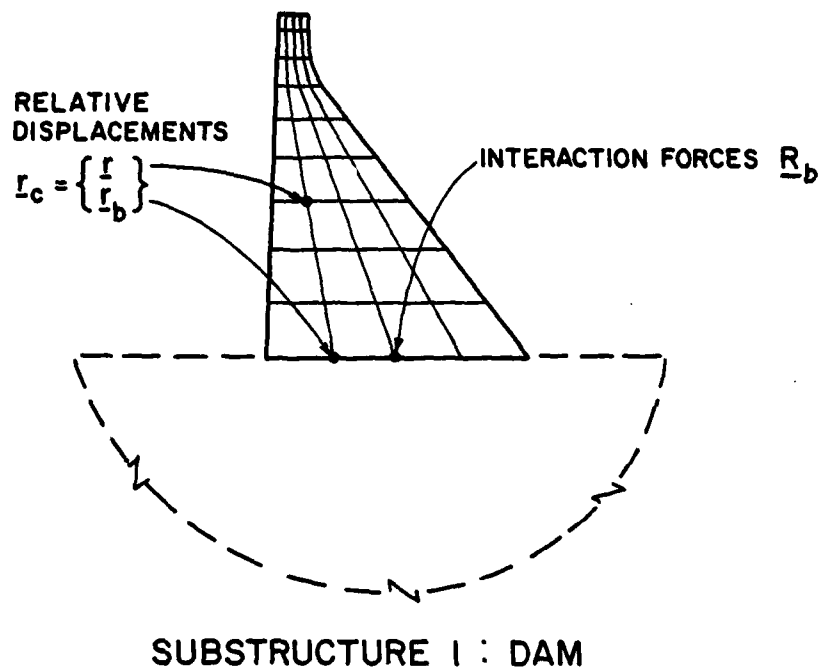


FIG. 5.1 SUBSTRUCTURE REPRESENTATION OF DAM-FOUNDATION SYSTEM

$$\underline{\underline{g}}_f(\omega) \underline{\underline{r}}_f(\omega) = \underline{\underline{R}}_f(\omega) \quad (5.5)$$

where $\underline{\underline{g}}_f(\omega)$ is the complex valued, dynamic stiffness matrix for the foundation soil region. The ij^{th} element of this matrix, $\underline{\underline{g}}_f(\omega)_{ij}$ is defined in Fig. 5.2 where displacements as shown have been imposed at nodal points within the base of the dam and tractions outside the base are zero.

The foundation stiffness matrix $\underline{\underline{g}}_f(\omega)$ is to be determined by a separate analysis of the substructure representing the foundation soil or rock region. For sites where formations of soft rock or soil overlie hard rock, it would be reasonable to hypothesize that the boundary between the two types of rock is rigid. Then the foundation region may be idealized as a finite element system, in which material non-homogeneity and irregular geometry can be conveniently handled. Techniques for determining $\underline{\underline{g}}_f(\omega)$ for a finite element idealization of the foundation soil region are discussed elsewhere [29]. For sites where similar rock extends to large depths, it may be more appropriate to idealize the foundation as a viscoelastic half-plane. Assuming that the dam is supported at the surface of a viscoelastic half-plane with homogeneous material properties, $\underline{\underline{g}}_f(\omega)$ can be determined from the available data and procedures [32]. These results, in contrast to those from many earlier studies, are not restricted to a rigid plate at the base of the structure.

5.2.3 Dam-Foundation System

Equilibrium of interaction forces between the two substructures -- dam and foundation -- at the base of the dam requires that

$$\underline{\underline{R}}_b^{\ell}(\omega) = -\underline{\underline{R}}_f(\omega) \quad (5.6)$$

Similarly, compatibility of interaction displacements in the two substructures at the dam base requires that

$$\underline{\underline{r}}_b^{\ell}(\omega) = \underline{\underline{r}}_f(\omega) \quad (5.7)$$

Consequently, Eq. 5.5 becomes

$$\underline{\underline{R}}_b^{\ell}(\omega) = -\underline{\underline{g}}_f(\omega) \underline{\underline{r}}_b^{\ell}(\omega) \quad (5.8)$$

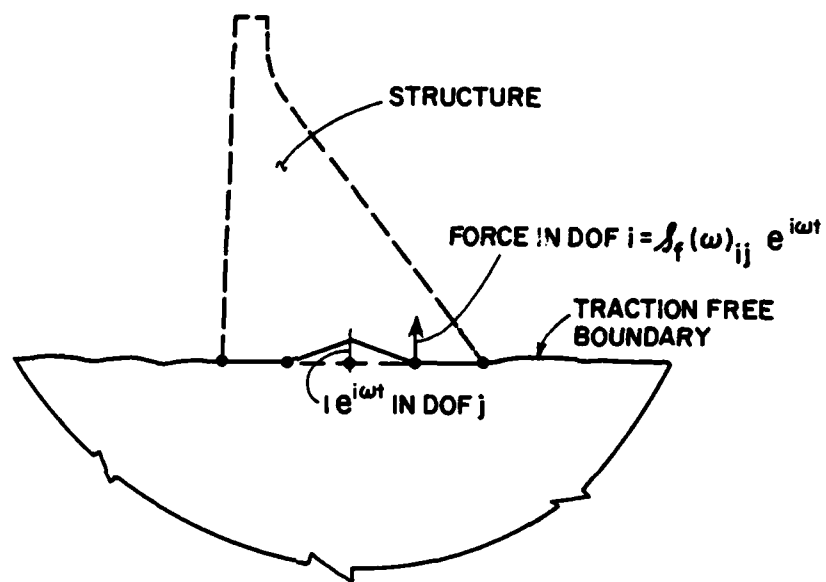


FIG. 5.2 DEFINITION OF $g_f(\omega)_{ij}$, THE ij -ELEMENT OF THE DYNAMIC STIFFNESS MATRIX $\underline{g}_f(\omega)$ FOR THE FOUNDATION REGION

which is substituted in Eq. 5.4 to obtain

$$\left[-\omega^2 \underline{\underline{m}}_c + (1 + i\eta) \underline{\underline{k}}_c + \tilde{\underline{\underline{g}}}_f(\omega) \right] \underline{\underline{r}}_c^\ell(\omega) = -\underline{\underline{m}}_c \underline{\underline{1}}_c^\ell \quad (5.9)$$

where

$$\tilde{\underline{\underline{g}}}_f(\omega) = \begin{bmatrix} \underline{\underline{0}} & \underline{\underline{0}} \\ \underline{\underline{0}} & \underline{\underline{g}}_f(\omega) \end{bmatrix} \quad (5.10)$$

For a particular excitation frequency ω , Eq. 5.9 represents $2(N+N_b)$ algebraic equations with complex-valued coefficients, in the unknown nodal point displacements $\underline{\underline{r}}_c^\ell$.

5.2.4 Computational Requirements

Analysis of structural response to earthquake motion via the frequency domain requires that the complex frequency response functions be determined for a range of frequencies over which the ground motion and structural response have significant components. For each excitation frequency, this entails solution of Eq. 5.9, a set of as many algebraic equations as the number of degrees of freedom for the dam. Finite element systems with a few hundred degrees of freedom are typically employed to represent concrete gravity dams. Enormous computational effort would be required for repeated solutions of these equations for many values of the excitation frequency. Furthermore, the entire displacement vector, $\underline{\underline{r}}_c^\ell$, at each ω has to be stored for future Fourier synthesis, requiring very large amounts of computer storage. Fourier synthesis calculations would have to be performed for each of the few hundred displacements, requiring large computational effort even when the very efficient FFT procedure is employed. The need for judiciously reducing the number of degrees of freedom in the analysis is therefore apparent.

5.3 Reduction of Degrees of Freedom

At any instant of time, the structural displacements in the DOF above the base may be separated into static displacements due to the interaction displacements at the base and the remaining dynamic displacements. The

latter can be expressed as a linear combination of the first few natural modes of vibration of the structure on a fixed base. This has been demonstrated to be effective in reducing the number of DOF for one-dimensional structural systems on rigid footing supported on the surface of a halfspace and also for complex structures on a deformable base. If J vibration modes are adequate to represent the structural response, the number of unknowns in Eq. 5.9 would be reduced to $J+2N_b$, the latter being the number of DOF at the base. While this approach is conceptually appealing, the number of unknowns can not be reduced below $2N_b$, the number of DOF at the base, which in finite element models of dams might be of the order of 20.

For such systems the number of unknowns in Eq. 5.9 can be most effectively reduced by use of the Ritz concept. The displacements \underline{r}_c are expressed as linear combinations of the Ritz vectors, chosen as the normal modes of an associated undamped structure-foundation system. The associated system considered is one in which $\underline{g}_f(\omega)$ is replaced by a frequency-independent value, say the static value $\underline{g}_f(0)$. The frequencies λ_n and mode shapes $\underline{\psi}_n$ of the associated system are solutions of the eigenvalue problem

$$\left[\underline{k}_c + \underline{\tilde{g}}_f(0) \right] \underline{\psi}_n = \lambda_n^2 \underline{m}_c \underline{\psi}_n \quad (5.11)$$

where $\underline{\tilde{g}}_f(0)$ was defined in Eq. 5.10.

If the first J modes $\underline{\psi}_1, \underline{\psi}_2, \dots, \underline{\psi}_J$ are considered as the Ritz vectors, the structural displacements are expressed as

$$\underline{r}_c^l(t) \approx \sum_{j=1}^J \underline{z}_j^l(t) \underline{\psi}_j \quad l = x, y \quad (5.12)$$

where \underline{z}_j 's are the generalized coordinates. In terms of the complex frequency response functions, Eq. 5.12 is

$$\underline{r}_c^l(\omega) = \sum_{j=1}^J \underline{\bar{z}}_j^l(\omega) \underline{\psi}_j \quad (5.13)$$

Introducing the transformations of Eq. 5.13 into Eq. 5.9, premultiplying by $\underline{\psi}_n^T$, and utilizing the orthogonality property of modes of the associated structure-foundation system with respect to the "stiffness" and mass matrices of Eq. 5.11, results in

$$\underline{s}(\omega) \underline{\bar{z}}^l(\omega) = \underline{l}^l(\omega) \quad (5.14)$$

In Eq. 5.14, the diagonal elements of $\underline{S}(\omega)$ are

$$S_{nn}(\omega) = \left[-\omega^2 + (1 + i\eta)\lambda_n^2 \right] \psi_n^T \underline{m}_c \psi_n + \psi_n^T \left[\tilde{\underline{g}}_f(\omega) - (1 + i\eta)\tilde{\underline{g}}_f(0) \right] \psi_n \quad (5.15a)$$

whereas the off-diagonal elements are

$$S_{nj}(\omega) = \psi_n^T \left[\tilde{\underline{g}}_f(\omega) - (1 + i\eta)\tilde{\underline{g}}_f(0) \right] \psi_j \quad (5.15b)$$

where n and $j = 1, 2, 3, \dots, J$; $\tilde{\underline{Z}}(\omega)$ is a column vector of the complex frequency response functions for the generalized coordinates \underline{Z}_n ; \underline{l} is a column vector with the n^{th} element

$$l_n^\ell = -\psi_n^T \underline{m}_c \underline{l}_c^\ell; \quad \ell = x, y \quad (5.15c)$$

For a particular excitation frequency ω , Eq. 5.14 represents J simultaneous algebraic equations in the generalized coordinates $\tilde{\underline{Z}}_n(\omega)$, $n = 1, 2, \dots, J$.

If all the $2(N+N_b)$ vibration modes of the associated structure-foundation system were included in the Ritz method, the results obtained by solving the simultaneous equations 5.14 would be identical to the "exact" results from solution of Eq. 5.9. There would, however, be no advantage in choosing to solve Eq. 5.14 instead of Eq. 5.9 because the number of equations is not reduced nor are they uncoupled. On the other hand, if sufficiently accurate results can be obtained with $J \ll 2(N+N_b)$, there would be profound computational advantages in working with Eq. 5.14.

That this is indeed the case has been demonstrated for one-dimensional structural systems on rigid footings supported on the surface of a halfspace [33] and also for concrete gravity dams [24]. The number of generalized coordinates that should be included in analysis depends on the properties of the structure-foundation system, the response quantities, and the frequency range of interest. The number necessary in analysis of concrete gravity dams studied in this report is determined in Section 7.6.

5.4 Response to Arbitrary Ground Motion

The complex frequency response functions $\tilde{\underline{Z}}_n^x(\omega)$ and $\tilde{\underline{Z}}_n^y(\omega)$, $n = 1, 2, \dots, J$, are determined by solving Eq. 5.14 for an appropriate range of excitation frequency ω . The response to arbitrary ground motion can be

computed using the equations of Sec. 4.5 with the following changes in notation: replace y_n^l by z_n^l , r by r_c , and ϕ_n by ψ_n .

6. ANALYSIS OF DAMS INCLUDING HYDRODYNAMIC AND FOUNDATION INTERACTION EFFECTS

6.1 Introductory Note

The substructure concept was employed to separately include the effects of dam-water interaction (Chapter 4) and dam-foundation interaction (Chapter 5) in the analysis. Using the same concept the analysis procedure is extended to analyze earthquake response of dams, simultaneously including various effects of the water and the foundation. These include effects arising from interaction between the dam and foundation, dam and water, water and foundation, and from interaction among all three substructures -- dam, water and foundation.

6.2 Frequency Domain Equations

6.2.1 Substructure 1: Dam

A cross-section of the dam-water-foundation system is shown in Fig. 2.1. The equations of motion for the dam idealized as a planar, two-dimensional finite element system are:

$$\underline{m}_c \ddot{\underline{r}}_c + \underline{c}_c \dot{\underline{r}}_c + \underline{k}_c \underline{r}_c = -\underline{m}_c \underline{1}_c^x a_g^x(t) - \underline{m}_c \underline{1}_c^y a_g^y(t) + \underline{R}_c(t) \quad (6.1)$$

in which \underline{m}_c , \underline{c}_c , and \underline{k}_c are the mass, damping and stiffness matrices for the finite element system; \underline{r}_c is the vector of nodal point displacements relative to the free-field earthquake displacement at the base (Fig. 6.1):

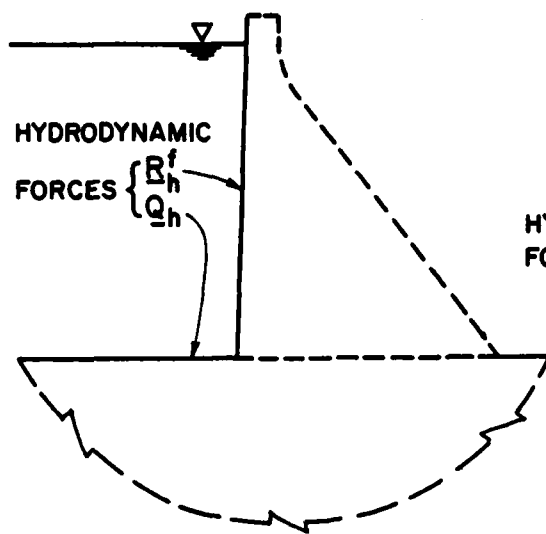
$$\underline{r}_c^T = \langle r_1^x \ r_1^y \ r_2^x \ r_2^y \ \dots \ r_n^x \ r_n^y \ \dots \ r_{N+N_b}^x \ r_{N+N_b}^y \rangle$$

in which r_n^x and r_n^y are the x and y components of the displacement of nodal point n; N is the number of nodal points above the base, N_b is the number of nodal points on the base, and the total number is $N+N_b$;

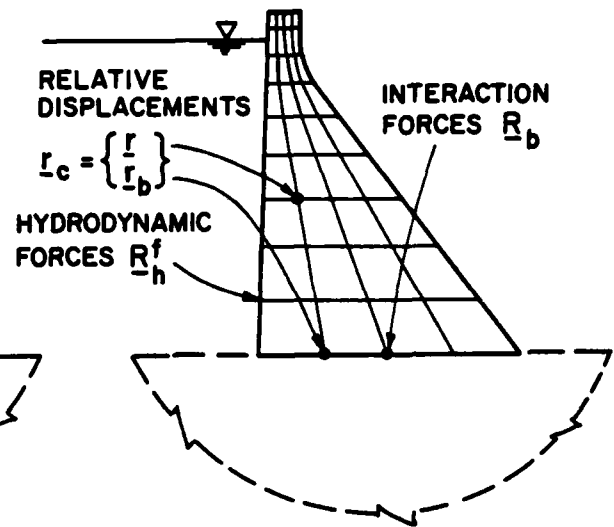
$$\{\underline{1}_c^x\}^T = \langle 1 \ 0 \ 1 \ 0 \ \dots \ 1 \ 0 \ \dots \ 1 \ 0 \rangle$$

$$\{\underline{1}_c^y\}^T = \langle 0 \ 1 \ 0 \ 1 \ \dots \ 0 \ 1 \ \dots \ 0 \ 1 \rangle$$

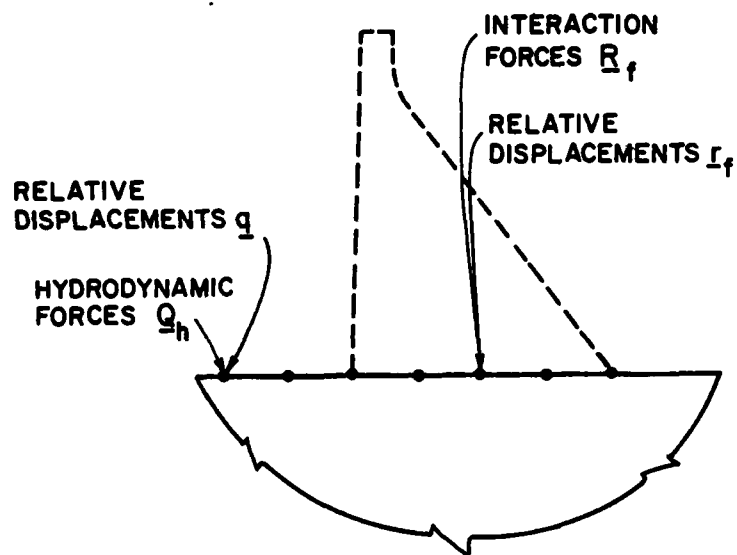
The force vector $\underline{R}_c(t)$ includes hydrodynamic forces $\underline{R}_h(t)$ at the upstream face of the dam and forces $\underline{R}_b(t)$ at the base of the dam due to structure-



SUBSTRUCTURE 3:
FLUID DOMAIN



SUBSTRUCTURE 1:
DAM



SUBSTRUCTURE 2:
FOUNDATION ROCK REGION

FIG. 6.1 SUBSTRUCTURE REPRESENTATION OF DAM-WATER-FOUNDATION SYSTEM

foundation interaction; $a_g^x(t)$ and $a_g^y(t)$ are the x and y components of the specified free-field ground acceleration, assumed to be identical at all nodal points on the dam base.

For harmonic ground acceleration in the x (horizontal) or y (vertical) directions $a_g^l(t) = e^{i\omega t}$, $l = x$ or y , the displacements and forces can be expressed in terms of their complex frequency responses: $r_c(t) = \bar{r}_c^l(\omega) e^{i\omega t}$, $R_c(t) = \bar{R}_c^l(\omega) e^{i\omega t}$, $R_h(t) = \bar{R}_h^l(\omega) e^{i\omega t}$ and $R_b(t) = \bar{R}_b^l(\omega) e^{i\omega t}$. The governing equation, Eq. 6.1, then becomes

$$\left[-\omega^2 \underline{m}_c + i\omega \underline{c}_c + \underline{k}_c \right] \bar{r}_c^l(\omega) = -\underline{m}_{c-b} \underline{1}^l + \bar{R}_c^l(\omega) ; l = x \text{ or } y \quad (6.2)$$

If the structure has constant hysteretic damping, Eq. 6.2 becomes

$$\left[-\omega^2 \underline{m}_c + (1+i\eta) \underline{k}_c \right] \bar{r}_c^l(\omega) = -\underline{m}_{c-b} \underline{1}^l + \bar{R}_c^l(\omega) ; l = x \text{ or } y \quad (6.3)$$

Partitioning \bar{r}_c into \bar{r} , the vector of displacements of nodal points above the base, and \bar{r}_b , the vector of interaction displacements at the base (Fig. 6.1), Eq. 6.3 can be expressed as

$$\left(-\omega^2 \begin{bmatrix} \underline{m} & \underline{0} \\ \underline{0} & \underline{m}_b \end{bmatrix} + (1+i\eta) \begin{bmatrix} \underline{k} & \underline{k}_b \\ (\underline{k}_b)^T & \underline{k}_{bb} \end{bmatrix} \right) \begin{Bmatrix} \bar{r}^l(\omega) \\ \bar{r}_b^l(\omega) \end{Bmatrix} = - \begin{Bmatrix} \underline{m} \underline{1}^l \\ \underline{m}_{b-b} \underline{1}^l \end{Bmatrix} + \begin{Bmatrix} \bar{R}_h^l(\omega) \\ \bar{R}_b^l(\omega) \end{Bmatrix} \quad (6.4)$$

The forces at the base of the dam, $\bar{R}_b^l(\omega)$, are next expressed in terms of interaction displacements by appropriate analyses of substructure 2, the foundation (Sec. 6.2.2). Later (Sec. 6.2.5) the hydrodynamic forces $\bar{R}_h^l(\omega)$ are expressed in terms of displacements or accelerations at the upstream face of the dam by appropriate analyses of substructure 3, the fluid region.

6.2.2 Substructure 2: Foundation Rock Region

The forces acting at the surface of the foundation include the forces R_f at the base of the dam due to structure-foundation interaction and the hydrodynamic forces Q_h at the bottom of the reservoir. Beyond a certain distance upstream of the dam, the hydrodynamic pressures will become small enough to be negligible. Only the significant forces are included in Q_h . For unit harmonic ground acceleration these forces can be expressed in

terms of their complex frequency response functions $\underline{R}_f(t) = \underline{\bar{R}}_f(\omega)e^{i\omega t}$ and $\underline{Q}_h(t) = \underline{\bar{Q}}_h(\omega)e^{i\omega t}$. The corresponding displacements relative to the free-field ground displacement are $\underline{r}_f(t) = \underline{\bar{r}}_f(\omega)e^{i\omega t}$ and $\underline{q}(t) = \underline{\bar{q}}(\omega)e^{i\omega t}$. The forces and displacements can be related through the complex valued, dynamic foundation stiffness matrix $\underline{g}(\omega)$:

$$\begin{bmatrix} \underline{g}_{rr}(\omega) & \underline{g}_{rq}(\omega) \\ \underline{g}_{rq}^T(\omega) & \underline{g}_{qq}(\omega) \end{bmatrix} \begin{Bmatrix} \underline{\bar{r}}_f \\ \underline{\bar{q}} \end{Bmatrix} = \begin{Bmatrix} \underline{\bar{R}}_f \\ \underline{\bar{Q}}_h \end{Bmatrix} \quad (6.5)$$

The ij^{th} element of this matrix, $\underline{g}_{ij}(\omega)$, is defined in Fig. 6.2 where displacements as shown have been imposed at nodal points contained in \underline{r}_f and \underline{q} and tractions outside these nodal points are zero.

The second matrix equation from Eq. 6.5 can be expressed as

$$\underline{\bar{q}} = \underline{g}_{qq}^{-1}(\omega) \left[\underline{\bar{Q}}_h - \underline{g}_{rq}^T(\omega) \underline{\bar{r}}_f \right] \quad (6.6)$$

Substituting this expression into the first matrix equation from Eq. 6.5 leads to

$$\left[\underline{g}_{rr}(\omega) - \underline{g}_{rq}(\omega) \underline{g}_{qq}^{-1}(\omega) \underline{g}_{rq}^T(\omega) \right] \underline{\bar{r}}_f = \underline{\bar{R}}_f - \underline{g}_{rq}(\omega) \underline{g}_{qq}^{-1}(\omega) \underline{\bar{Q}}_h$$

or

$$\underline{g}_f(\omega) \underline{\bar{r}}_f = \underline{\bar{R}}_f - \underline{g}_{rq}(\omega) \underline{g}_{qq}^{-1}(\omega) \underline{\bar{Q}}_h \quad (6.7a)$$

where

$$\underline{g}_f(\omega) = \underline{g}_{rr}(\omega) - \underline{g}_{rq}(\omega) \underline{g}_{qq}^{-1}(\omega) \underline{g}_{rq}^T(\omega) \quad (6.7b)$$

The matrix $\underline{g}_f(\omega)$ of Eq. 6.7b is the same as the matrix $\underline{g}_f(\omega)$ in Eq. 5.5. In particular, without hydrodynamic forces, $\underline{\bar{Q}}_h = \underline{0}$ and Eq. 6.6 reduces to Eq. 5.5.

The dynamic stiffness matrices for the foundation appearing in Eqs. 6.5, 6.7a, and 6.7b are to be determined by a separate analysis of the substructure representing the foundation soil or rock region. At many sites of concrete gravity dams, similar rocks extend to large depths, and it is therefore appropriate to idealize the foundation as a viscoelastic half plane. The surface of the half plane is assumed to be horizontal and its material properties to be homogeneous. Available data and methods [32] are utilized in this investigation to determine dynamic stiffness for such idealized foundations.

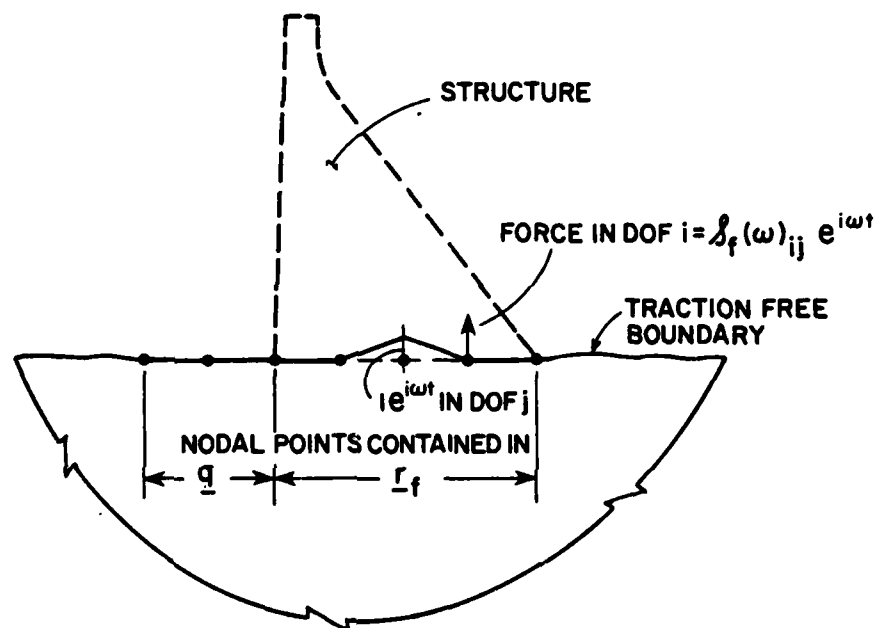


FIG. 6.2 DEFINITION OF $S_f(\omega)_{ij}$, THE ij -ELEMENT OF THE DYNAMIC STIFFNESS MATRIX $\underline{S}_f(\omega)$ FOR THE FOUNDATION REGION

6.2.3 Dam-Foundation System

Equilibrium of interaction forces between the two substructures -- dam and foundation -- at the base of the dam requires that

$$\bar{\underline{R}}_b^{\ell}(\omega) = -\bar{\underline{R}}_f^{\ell}(\omega) \quad (6.8)$$

Similarly, compatibility of interaction displacements at the dam base in the two substructures requires that

$$\bar{\underline{r}}_b^{\ell}(\omega) = \bar{\underline{r}}_f^{\ell}(\omega) \quad (6.9)$$

Consequently, Eq. 6.6 because

$$\bar{\underline{R}}_b^{\ell}(\omega) = -\underline{g}_f(\omega) \bar{\underline{r}}_b^{\ell}(\omega) - \underline{g}_{rq} \underline{g}_{qq}^{-1} \underline{Q}_h \quad (6.10)$$

Thus, the forces $\bar{\underline{R}}_b^{\ell}(\omega)$ at the base of the dam due to structure-foundation interaction have been expressed in terms of the interaction displacements $\bar{\underline{r}}_b^{\ell}(\omega)$ and hydrodynamic forces \underline{Q}_h through dynamic stiffness matrices for the foundation region. Substituting Eq. 6.10 into Eq. 6.4 leads to

$$\begin{aligned} & \left(-\omega^2 \begin{bmatrix} \underline{m} & 0 \\ 0 & \underline{m}_b \end{bmatrix} + (1+i\eta) \begin{bmatrix} \underline{k} & \underline{k}_b \\ \underline{k}_b^T & \underline{k}_{bb} \end{bmatrix} + \begin{bmatrix} 0 & 0 \\ 0 & \underline{g}_f(\omega) \end{bmatrix} \right) \begin{Bmatrix} \bar{\underline{r}}^{\ell}(\omega) \\ \bar{\underline{r}}_b^{\ell}(\omega) \end{Bmatrix} \\ & = - \begin{Bmatrix} \underline{m} \underline{1}^{\ell} \\ \underline{m}_b \underline{1}_b^{\ell} \end{Bmatrix} + \begin{Bmatrix} \bar{\underline{R}}_h^{\ell}(\omega) \\ -\underline{g}_{rq} \underline{g}_{qq}^{-1} \underline{Q}_h \end{Bmatrix} \end{aligned} \quad (6.11)$$

or

$$[-\omega^2 \underline{m}_c + (1+i\eta) \underline{k}_c + \tilde{\underline{g}}_f(\omega)] \bar{\underline{r}}_c^{\ell}(\omega) = -\underline{m}_c \underline{1}_c^{\ell} + \tilde{\underline{R}}_c^{\ell}(\omega) \quad (6.12)$$

where

$$\tilde{\underline{g}}_f(\omega) = \begin{bmatrix} 0 & 0 \\ 0 & \underline{g}_f(\omega) \end{bmatrix} \quad (6.13)$$

The hydrodynamic forces $\bar{\underline{R}}_h$ and $\bar{\underline{Q}}_h$ will be expressed in terms of accelerations of the upstream face of the dam and the bottom of the reservoir by analyses of the fluid region, to be described later.

6.2.4 Reduction of Degrees of Freedom

For each excitation frequency Eq. 6.11 is a set of $2(N+N_b)$ algebraic equations, as many as the number of DOF of the dam, which typically would

be a few hundred. Enormous computational effort would be required for repeated solutions of these equations for many values of the excitation frequency and subsequent Fourier synthesis of the harmonic responses in each DOF. Thus, it is important to judiciously reduce the number of unknowns in the analysis. As mentioned in Chapter 5, two approaches have proven to be effective in reducing the number of DOF.

In the first approach [25, 33], the structural displacements $\underline{r}^{\ell}(t)$ at some time t in the DOF above the base are separated into two parts: static displacements due to base displacements $\underline{r}_b^{\ell}(t)$ at the same time plus the remaining "dynamic" displacements; and the latter are expressed as a linear combination of the first few natural modes of vibration of the structure on a fixed base. If J vibration modes are adequate to represent the structural response, the number of unknowns in Eq. 6.11 would reduce to $J+2N_b$, where $2N_b$ = the number of DOF at the base. While this approach is conceptually appealing, the number of unknowns cannot be reduced below $2N_b$, which in finite element models of dams may be, say, 20.

The second approach [24,33], based on the Ritz concept, is more effective for such systems. The displacements \underline{r}_c are expressed as linear combinations of the Ritz vectors, chosen as the normal modes of an associated undamped structure-foundation system. The associated system chosen here and in earlier studies is one in which $\underline{g}_f(\omega)$ is replaced by a frequency independent value, say the static value $\underline{g}_f(0)$. The vibration frequencies λ_n and mode shapes $\underline{\psi}_n$ of the associated system are solutions of the eigenvalue problem

$$[\underline{k}_c + \underline{\tilde{g}}_f(0)]\underline{\psi}_n = \lambda_n^2 \underline{m}_c \underline{\psi}_n \quad (6.14)$$

where $\underline{\tilde{g}}_f(0)$ was defined in Eq. 6.13.

If the first J modes $\underline{\psi}_1, \underline{\psi}_2, \dots, \underline{\psi}_J$ are considered as the Ritz vectors, the structural displacements are expressed as

$$\underline{r}_c^{\ell}(t) = \sum_{j=1}^J \underline{z}_j^{\ell}(t) \underline{\psi}_j \quad (6.15)$$

where \underline{z}_j 's are the generalized coordinates. In terms of the complex frequency response functions, Eq. 6.15 is

$$\underline{r}_c^{\ell}(\omega) = \sum_{j=1}^J \underline{\bar{z}}_j^{\ell}(\omega) \underline{\psi}_j \quad (6.16)$$

Equation 6.16 contains the following equation for the displacements at the base of the structure:

$$\underline{\bar{r}}_b^\ell(\omega) = \sum_{j=1}^J \underline{\bar{z}}_j^\ell(\omega) \underline{\psi}_{bj} \quad (6.17)$$

where $\underline{\psi}_{bj}$ is the subvector of $\underline{\psi}_j$ corresponding to the base DOF. Because $\underline{r}_f = \underline{r}_b$, and $\underline{\psi}_j$ were determined from Eq. 6.14 involving $\underline{g}_f(0)$, the static foundation stiffness matrix, \underline{g} may be expressed in terms of generalized coordinates by setting $\omega = 0$ in Eq. 6.6 and ignoring the hydrodynamic loads \underline{Q} ; thus

$$\underline{g} = -\underline{g}_{qq}^{-1}(0) \underline{g}_{rq}^T(0) \underline{r}_b \quad (6.18)$$

Combining Eqs. 6.17 and 6.18 leads to

$$\underline{g} = \sum_{j=1}^J \underline{\bar{z}}_j^\ell(\omega) \underline{\chi}_j \quad (6.19)$$

where

$$\underline{\chi}_j = -\underline{g}_{qq}^{-1}(0) \underline{g}_{rq}^T(0) \underline{\psi}_{bj} \quad (6.20)$$

Introducing the transformation of Eq. 6.16 into Eq. 6.12, premultiplying by $\underline{\psi}_n^T$ and utilizing the orthogonality property of eigenvectors of the associated structure-foundation system with respect to the stiffness and mass matrices of Eq. 6.14, results in

$$\underline{S}(\omega) \underline{\bar{z}}^\ell(\omega) = \underline{L}^\ell(\omega) \quad (6.21)$$

In Eq. 6.21, the diagonal elements of $\underline{S}(\omega)$ are

$$S_{nn}(\omega) = \left[-\omega^2 + (1+i\eta)\lambda_n^2 \right] \underline{\psi}_{n-c}^T \underline{\psi}_n + \underline{\psi}_n^T \left[\underline{\bar{g}}_f(\omega) - (1+i\eta)\underline{\bar{g}}_f(0) \right] \underline{\psi}_n \quad (6.22a)$$

whereas the off-diagonal elements are

$$S_{nj}(\omega) = \underline{\psi}_n^T \left[\underline{\bar{g}}_f(\omega) - (1+i\eta)\underline{\bar{g}}_f(0) \right] \underline{\psi}_j \quad (6.22b)$$

where n and $j = 1, 2, 3, \dots, J$; $\underline{\bar{z}}^\ell(\omega)$ is a column vector of the complex frequency response functions for the generalized coordinates \underline{z}_n^ℓ ; \underline{L}^ℓ is a column vector with the n^{th} element

$$L_n^\ell = -L_n^\ell + \underline{\psi}_{n-c}^T \underline{\bar{R}}(\omega) \quad (6.23)$$

where

$$L_n^\ell = \underline{\psi}_{n-c}^T \underline{1}_c^\ell \quad (6.24)$$

For a particular excitation frequency ω , Eq. 6.21 represents J simultaneous algebraic equations in the generalized coordinates $Z_n^l(\omega)$, $n = 1, 2, \dots, J$. These equations need to be solved for several hundred values of the excitation frequency to determine the complex frequency responses.

Equation 6.21 would contain $2(N+N_b)$ equations if all the vibration modes of the associated structure-foundation system were included as Ritz vectors. Solution of these equations would then be identical to the solution of Eq. 6.11 in nodal point coordinates. There would, however, be no advantage in choosing to solve Eq. 6.21 instead of Eq. 6.11 because the number of equations is not reduced nor are the equations uncoupled by the transformation. However, there would be profound computational advantages in working with Eq. 6.21 if sufficiently accurate results can be obtained by including only a few Ritz vectors. The number necessary depends on the properties of the structure-foundation system, the response quantities, and the frequency range of interest; for concrete dams this number is determined in Section 7.6.

6.2.5 Substructure 3: Fluid Domain

The motion of the dam-water system is assumed to be two-dimensional, and the same for any vertical plane perpendicular to the axis of the dam (Chapter 2). Assuming water to be linearly compressible and neglecting its internal viscosity, the small amplitude irrotational motion of water is governed by the two-dimensional wave equation

$$\frac{\partial^2 p}{\partial x^2} + \frac{\partial^2 p}{\partial y^2} = \frac{1}{C^2} \frac{\partial^2 p}{\partial t^2} \quad (6.25)$$

in which $p(x, y, t)$ is the hydrodynamic pressure (in excess of the hydrostatic pressure) and the velocity of sound in water $C = \sqrt{gK/w}$ where K and w are bulk modulus and unit weight of water, respectively, and g = acceleration of gravity. For harmonic ground motion $a_g^l(t) = e^{i\omega t}$, $l = x$ or y ,

$$p(x, y, t) = \bar{p}(x, y, \omega) e^{i\omega t} \quad (6.26)$$

where \bar{p} is the complex frequency response function for the pressure and Eq. 6.25 becomes the Helmholtz equation:

$$\frac{\partial^2 \bar{p}}{\partial x^2} + \frac{\partial^2 \bar{p}}{\partial y^2} + \frac{\omega^2}{C^2} \bar{p} = 0 \quad (6.27)$$

Whereas Eqs. 6.11 and 6.17 are valid for dams of arbitrary geometry, it is assumed that for purposes of defining hydrodynamic loads, and only for this purpose, the upstream face of the dam is vertical. This is a reasonable assumption, given that the upstream face of concrete gravity dams is vertical or almost vertical for most of the height.

Dynamic water pressures are generated by horizontal motions of the vertical upstream face of the dam and by vertical motions of the horizontal bottom of the reservoir. The vector of horizontal accelerations at the nodal points on the upstream face of the dam is

$$\ddot{\underline{u}}(t) = \left\{ \hat{1} + \sum_{j=1}^J \psi_j^{xf} \bar{z}_j^x(\omega) \right\} e^{i\omega t} \quad (6.28a)$$

if the excitation is horizontal ground motion $a_g^x(t) = e^{i\omega t}$; and

$$\ddot{\underline{u}}(t) = \left\{ \sum_{j=1}^J \psi_j^{xf} \bar{z}_j^y(\omega) \right\} e^{i\omega t} \quad (6.28b)$$

if the excitation is vertical ground motion $a_g^y(t) = e^{i\omega t}$. In Eq. 6.28 the vector ψ_j^{xf} is a subvector of ψ_j containing only the elements corresponding to the x-DOF of the nodal points on the upstream face of the dam. From Eq. 6.19, the vector of vertical accelerations at the nodal points at the bottom of the reservoir is

$$\ddot{\underline{v}}(t) = \left\{ \sum_{j=1}^J \chi_j^y \bar{z}_j^x(\omega) \right\} e^{i\omega t} \quad (6.29a)$$

if the excitation is horizontal ground motion; and

$$\ddot{\underline{v}}(t) = \left\{ 1 + \sum_{j=1}^J \chi_j^y \bar{z}_j^y(\omega) \right\} e^{i\omega t} \quad (6.29b)$$

if the excitation is vertical ground motion, where χ_j^y is a subvector of χ_j containing only the elements corresponding to the y-DOF of the nodal points at the bottom of the reservoir.

Strictly for purposes of notational convenience, the vectors ψ_j^{xf} and χ_j^y are replaced by their continuous analogue functions $\psi_j(y)$ and $\chi_j(x)$, respectively in Eq. 6.28 to obtain

$$\ddot{u}(0, y, t) = \left[1 + \sum_{j=1}^J \psi_j(y) \bar{z}_j^x(\omega) \right] e^{i\omega t} \quad (6.30a)$$

$$\ddot{u}(0, y, t) = \left[\sum_{j=1}^J \psi_j(y) \bar{z}_j^y(\omega) \right] e^{i\omega t} \quad (6.30b)$$

and in Eq. 6.29 to obtain

$$\ddot{v}(x, 0, t) = \left[\sum_{j=1}^J \chi_j(x) \bar{z}_j^x(\omega) \right] e^{i\omega t} \quad (6.31a)$$

$$\ddot{v}(x, 0, t) = \left[1 + \sum_{j=1}^J \chi_j(x) \bar{z}_j^y(\omega) \right] e^{i\omega t} \quad (6.31b)$$

When the excitation is horizontal ground motion $a_g^x(t) = e^{i\omega t}$, neglecting effects of the waves at the free surface of water [11], the boundary conditions for Eq. 6.27 governing \bar{p} are (with reference to Fig. 6.1)

$$\left. \begin{aligned} \bar{p}(x, H, \omega) &= 0 \\ \frac{\partial \bar{p}}{\partial y}(x, 0, \omega) &= -\frac{w}{g} \sum_{j=1}^J \chi_j(x) \bar{z}_j^x(\omega) \\ \frac{\partial \bar{p}}{\partial x}(0, y, \omega) &= -\frac{w}{g} \left[1 + \sum_{j=1}^J \psi_j(y) \bar{z}_j^x(\omega) \right] \end{aligned} \right\} \quad (6.32)$$

For the case of vertical ground motion $a_g^y(t) = e^{i\omega t}$ the boundary conditions are

$$\left. \begin{aligned} \bar{p}(x, H, \omega) &= 0 \\ \frac{\partial \bar{p}}{\partial y}(x, 0, \omega) &= -\frac{w}{g} \left[1 + \sum_{j=1}^J \chi_j(x) \bar{z}_j^y(\omega) \right] \\ \frac{\partial \bar{p}}{\partial x}(0, y, \omega) &= -\frac{w}{g} \left[\sum_{j=1}^J \psi_j(y) \bar{z}_j^y(\omega) \right] \end{aligned} \right\} \quad (6.33)$$

Because the governing equation as well as the boundary conditions are linear, the principle of superposition applies. The complex frequency response functions $\bar{p}^x(x, y, \omega)$ and $\bar{p}^y(x, y, \omega)$, associated respectively with x and y components of ground motion, can therefore be expressed as

$$\bar{p}^{\ell}(x, y, \omega) = \bar{p}_0^{\ell}(x, y, \omega) + \sum_{j=1}^J \bar{z}_j^{\ell}(\omega) \left[\bar{p}_j^f(x, y, \omega) + \bar{p}_j^b(x, y, \omega) \right] \quad (6.34)$$

In Eq. 6.34, $\bar{p}_0^x(x, y, \omega)$ is the solution of Eq. 6.27 for the following boundary conditions:

$$\left. \begin{aligned} \bar{p}(x, H, \omega) &= 0 \\ \frac{\partial \bar{p}}{\partial y}(x, 0, \omega) &= 0 \\ \frac{\partial \bar{p}}{\partial x}(0, y, \omega) &= -\frac{w}{g}; \end{aligned} \right\} \quad (6.35)$$

$\bar{p}_0^y(x, y, \omega)$ is the solution of Eq. 6.27 for the following boundary conditions:

$$\left. \begin{aligned} \bar{p}(x, H, \omega) &= 0 \\ \frac{\partial \bar{p}}{\partial y}(x, 0, \omega) &= -\frac{w}{g} \\ \frac{\partial \bar{p}}{\partial x}(0, y, \omega) &= 0; \end{aligned} \right\} \quad (6.36)$$

$\bar{p}_j^f(x, y, \omega)$ is the solution of Eq. 6.27 for the following boundary conditions:

$$\left. \begin{aligned} \bar{p}(x, H, \omega) &= 0 \\ \frac{\partial \bar{p}}{\partial y}(x, 0, \omega) &= 0 \\ \frac{\partial \bar{p}}{\partial x}(0, y, \omega) &= -\frac{w}{g} \psi_j(y); \end{aligned} \right\} \quad (6.37)$$

and $\bar{p}_j^b(x, y, \omega)$ is the solution of Eq. 6.27 for the following boundary conditions:

$$\left. \begin{aligned} \bar{p}(x, H, \omega) &= 0 \\ \frac{\partial \bar{p}}{\partial y}(x, 0, \omega) &= -\frac{w}{g} \chi_j(x) \\ \frac{\partial \bar{p}}{\partial x}(0, y, \omega) &= 0 \end{aligned} \right\} \quad (6.38)$$

The complex frequency response functions \bar{p}_0^x and \bar{p}_0^y are for the hydrodynamic pressures due to accelerations of the ground in the horizontal and vertical directions, respectively, and the dam is rigid; $\bar{p}_j^f(x, y, \omega)$ is the corresponding function when the excitation is the horizontal acceleration $\psi_j(y)$ of the dam in the j^{th} vibration mode of the associated dam-foundation system, with no motion of the reservoir bottom; $\bar{p}_j^b(x, y, \omega)$ is due to vertical acceleration $\chi_j(x)$ of the reservoir bottom, associated with the j^{th} vibration mode of the associated dam-foundation system, and with no motion of the dam.

Solution of Eq. 6.27 in fluid domains of infinite extent in the upstream direction (Fig. 6.1) and the boundary conditions of Eqs. 6.35, 6.37 and 6.36 have been reported earlier and are presented in Eqs. 6.39, 6.40 and 6.41, respectively:

$$\bar{p}_0^x(x, y, \omega) = \frac{4w}{\pi g} \sum_{\ell=1}^{\infty} \frac{(-1)^\ell}{(2\ell-1)\sqrt{\lambda_\ell^2 - \frac{\omega^2}{c^2}}} \exp\left(x\sqrt{\lambda_\ell^2 - \frac{\omega^2}{c^2}}\right) \cos \lambda_\ell y \quad (6.39)$$

$$\bar{p}_j^f(x, y, \omega) = -\frac{2w}{gH} \sum_{\ell=1}^{\infty} \frac{I_{j\ell}}{\sqrt{\lambda_\ell^2 - \frac{\omega^2}{c^2}}} \exp\left(x\sqrt{\lambda_\ell^2 - \frac{\omega^2}{c^2}}\right) \cos \lambda_\ell y \quad (6.40)$$

in which $\lambda_\ell = (2\ell-1) \pi/2H$ and $I_{j\ell} = \int_0^H \psi_j(y) \cos \lambda_\ell y \, dy$.

$$\bar{p}_0^y(x, y, \omega) = \frac{wC}{g\omega} \frac{(1+\alpha) \sin \frac{\omega(H-y)}{C}}{(1+\alpha) \cos \frac{\omega H}{C}} \quad (6.41)$$

where the reflection coefficient

$$\alpha = \frac{(C_r w_r / Cw) - 1}{(C_r w_r / Cw) + 1} \quad (6.42)$$

where w_r and C_r are the unit weight and P-wave velocity for the foundation rock at the bottom of the reservoir; $\alpha = 1$ for rigid rock indicating that hydrodynamic pressure waves are completely reflected at the reservoir bottom; and $\alpha < 1$ for deformable rock implying that hydrodynamic pressure waves impinging at the reservoir bottom are partially reflected back in the fluid

domain and partially refracted into rock.

Solution of Eq. 6.27 in fluid domains of infinite extent in the upstream direction (Fig. 6.1) and the boundary conditions of Eq. 6.38 may be obtained by procedures similar to those used in obtaining the above solutions of Eqs. 6.39 and 6.41 [34] and by employing the Fourier transform with respect to the spatial coordinate X . Such a general solution is not necessary, however, because the resulting pressures have little influence on the response of the dam (see discussion preceeding Eqs. 6.52).

The complex frequency response function for $\bar{R}_h^f(t)$, the vector of total hydrodynamic forces at the upstream face of the dam, is, from Eq. 6.34,

$$\bar{R}_h^f(\omega) = \bar{R}_0^l(\omega) + \sum_{j=1}^J \bar{Z}_j^l(\omega) \left[\bar{R}_j^f(\omega) + \bar{R}_j^b(\omega) \right] \quad (6.43)$$

in which $\bar{R}_0^l(\omega)$, $\bar{R}_j^f(\omega)$, and $\bar{R}_j^b(\omega)$ are the nodal forces statically equivalent to the corresponding pressure functions at the dam face: $\bar{p}_0^l(0, y, \omega)$, $\bar{p}_j^f(0, y, \omega)$, and $\bar{p}_j^b(0, y, \omega)$, respectively. They are computed by using the principle of virtual work with the displacements between nodal points defined by the interpolation functions used in the finite element idealization of the dam. Because the pressures act in the horizontal direction on a vertical upstream face, elements of \bar{R}_h^f that correspond to the y -DOF will be zero. Similarly, from Eq. 6.34, the complex frequency response function for $\bar{Q}_h(t)$, the vector of hydrodynamic forces at the reservoir bottom, is

$$\bar{Q}_h(\omega) = \bar{Q}_0^l(\omega) + \sum_{j=1}^J \bar{Z}_j^l(\omega) \left[\bar{Q}_j^f(\omega) + \bar{Q}_j^b(\omega) \right] \quad (6.44)$$

in which $\bar{Q}_0^l(\omega)$, $\bar{Q}_j^f(\omega)$, and $\bar{Q}_j^b(\omega)$ are the nodal forces statically equivalent to the corresponding pressure functions at the reservoir bottom: $\bar{p}_0^l(x, 0, \omega)$, $\bar{p}_j^f(x, 0, \omega)$ and $\bar{p}_j^b(x, 0, \omega)$, respectively. Because the pressures act in the vertical direction on a horizontal bottom of the reservoir, elements of \bar{Q}_h that correspond to the x -DOF will be zero.

Thus, by analyses of the fluid domain for appropriate conditions, the hydrodynamic forces in Eq. 6.21 have been expressed in terms of the unknown generalized accelerations $\bar{Z}_j^l(\omega)$ and by substituting

$$\bar{z}_j^{\ell}(\omega) = -\omega^2 \bar{z}_j^{\ell}(\omega) \quad (6.45)$$

in terms of the unknown generalized displacements.

6.2.6 Dam-Water-Foundation System

The n^{th} equation contained in Eq. 6.21 is

$$\begin{aligned} S_{nn}(\omega) \bar{z}_n^{\ell}(\omega) + \sum_{\substack{j=1 \\ j \neq n}}^J S_{nj}(\omega) \bar{z}_j^{\ell}(\omega) \\ = -L_n^{\ell} + \{\psi_n^f\}^T \bar{R}_h^f(\omega) - \{\psi_{bn}\}^T \underline{g}_{-rq-qq}^{-1} \bar{Q}_h(\omega) \end{aligned} \quad (6.46)$$

in which $S_{nj}(\omega)$ were defined in Eq. 6.22, L_n^{ℓ} in Eq. 6.24, and ψ_n^f is the sub-vector of ψ_n containing only the elements corresponding to the face (f) DOF. Expressing hydrodynamic forces $\bar{R}_h^f(\omega)$ and $\bar{Q}_h(\omega)$ in terms of generalized displacements from Eqs. 6.43 - 6.45 leads to

$$\begin{aligned} S_{nn}(\omega) \bar{z}_n^{\ell}(\omega) + \sum_{\substack{j=1 \\ j \neq n}}^J S_{nj}(\omega) \bar{z}_j^{\ell}(\omega) \\ = -L_n^{\ell} + \{\psi_n^f\}^T \left[\bar{R}_0^{\ell}(\omega) - \omega^2 \sum_{j=1}^J \bar{z}_j^{\ell}(\omega) \{\bar{R}_j^f(\omega) + \bar{R}_j^b(\omega)\} \right] \\ - \{\psi_{bn}\}^T \underline{g}_{-rq}(\omega) \underline{g}_{-qq}^{-1}(\omega) \left[\bar{Q}_0^{\ell}(\omega) - \omega^2 \sum_{j=1}^J \bar{z}_j^{\ell}(\omega) \{\bar{Q}_j^f(\omega) + \bar{Q}_j^b(\omega)\} \right] \end{aligned} \quad (6.47)$$

The set of equations 6.47 for $n = 1, 2 \dots J$ may be rearranged and expressed in matrix form as

$$\begin{bmatrix} \tilde{S}_{11}(\omega) & \tilde{S}_{12}(\omega) & \dots & \tilde{S}_{1J}(\omega) \\ \tilde{S}_{21}(\omega) & \tilde{S}_{22}(\omega) & \dots & \tilde{S}_{2J}(\omega) \\ \vdots & \vdots & \ddots & \vdots \\ \tilde{S}_{J1}(\omega) & \tilde{S}_{J2}(\omega) & \dots & \tilde{S}_{JJ}(\omega) \end{bmatrix} \begin{Bmatrix} \bar{z}_1^{\ell}(\omega) \\ \bar{z}_2^{\ell}(\omega) \\ \vdots \\ \bar{z}_J^{\ell}(\omega) \end{Bmatrix} = \begin{Bmatrix} \tilde{L}_1^{\ell}(\omega) \\ \tilde{L}_2^{\ell}(\omega) \\ \vdots \\ \tilde{L}_J^{\ell}(\omega) \end{Bmatrix} \quad (6.48)$$

in which

$$\begin{aligned} \tilde{S}_{nj}(\omega) = S_{nj}(\omega) + \omega^2 \left\{ \psi_n^f \right\}^T \left\{ \bar{R}_j^f(\omega) + \bar{R}_j^b(\omega) \right\} \\ - \omega^2 \left\{ \psi_{bn} \right\}^T \bar{g}_{-rq}(\omega) \bar{g}_{-qq}^{-1}(\omega) \left\{ \bar{Q}_j^f(\omega) + \bar{Q}_j^b(\omega) \right\} \end{aligned} \quad (6.49)$$

valid for diagonal as well as off-diagonal elements of $S(\omega)$
and

$$\tilde{L}_n^\ell(\omega) = -L_n^\ell + \left\{ \psi_n^f \right\}^T \bar{R}_0^\ell(\omega) - \left\{ \psi_{bn} \right\}^T \bar{g}_{-rq}(\omega) \bar{g}_{-qq}^{-1}(\omega) \bar{Q}_0^\ell(\omega) \quad (6.50)$$

Equation 6.49, after substitution of Eq. 6.22, becomes

$$\begin{aligned} \tilde{S}_{nn}(\omega) = \left[-\omega^2 + (1+i\eta)\lambda_n^2 \right] \psi_n^T \bar{m} \psi_n + \psi_n^T \left[\tilde{g}_f(\omega) - (1+i\eta)\tilde{g}_f(0) \right] \psi_n \\ + \omega^2 \left\{ \psi_n^f \right\}^T \left\{ \bar{R}_n^f(\omega) + \bar{R}_n^b(\omega) \right\} \\ - \omega^2 \left\{ \psi_{bn} \right\}^T \bar{g}_{-rq}(\omega) \bar{g}_{-qq}^{-1}(\omega) \left\{ \bar{Q}_n^f(\omega) + \bar{Q}_n^b(\omega) \right\} \end{aligned} \quad (6.51a)$$

and

$$\begin{aligned} \tilde{S}_{nj}(\omega) = \psi_n^T \left[\tilde{g}_f(\omega) - (1+i\eta)\tilde{g}_f(0) \right] \psi_j + \omega^2 \left\{ \psi_n^f \right\}^T \left\{ \bar{R}_j^f(\omega) + \bar{R}_j^b(\omega) \right\} \\ - \omega^2 \left\{ \psi_{bn} \right\}^T \bar{g}_{-rq}(\omega) \bar{g}_{-qq}^{-1}(\omega) \left\{ \bar{Q}_j^f(\omega) + \bar{Q}_j^b(\omega) \right\} \end{aligned} \quad (6.51b)$$

Equations 6.48 and 6.49 contain effects of the foundation and water in various forms:

- Dam-foundation interaction effects appear in eigenvalues λ_n and eigenvectors of the associated dam-foundation system and through the foundation stiffness matrix $\bar{g}_f(\omega)$ (Eqs. 6.7b and 6.13).
- Additional hydrodynamic loads \bar{R}_0^ℓ on the dam due to the free-field ground motions computed on the assumption of a rigid dam.
- Dam-water interaction effects appear through the hydrodynamic forces \bar{R}_j^f on the face of the dam and \bar{Q}_j^f on the reservoir bottom due to deformational motions of the dam.
- Water-foundation interaction effects appear through the hydrodynamic

forces \underline{R}_j^b on the face of the dam and \underline{Q}_j^b on the reservoir bottom due to deformational motions of the reservoir bottom.

- Dam-water-foundation interaction effects appear through the hydrodynamic forces \underline{Q}_0^l , \underline{Q}_j^f , and \underline{Q}_j^b at the bottom of the reservoir which influences the forces at the dam-foundation interface.

It can be argued and shown through numerical examples that several terms in Eqs. 6.49 - 6.51 are relatively small and can be dropped without introducing any significant errors. One group of such terms arises from the hydrodynamic forces \underline{Q}_0^l , \underline{Q}_j^f and \underline{Q}_j^b at the reservoir bottom which are due to the various excitations mentioned earlier. The other such term involves \underline{R}_j^b , the hydrodynamic forces at the upstream face of the dam due to deformational motions of the reservoir bottom.

Dropping these terms from Eqs. 6.49 - 6.51 leads to their simplified version:

$$\tilde{\underline{S}}(\omega) \tilde{\underline{Z}}^l(\omega) = \tilde{\underline{L}}^l(\omega), \quad l=x, y \quad (6.52)$$

in which

$$\begin{aligned} \tilde{\underline{S}}_{nn}(\omega) = & \left[-\omega^2 + (1+i\eta)\lambda_n^2 \right] \underline{\psi}_{n-c}^T \underline{\psi}_n + \underline{\psi}_n^T \left[\tilde{\underline{g}}_f(\omega) - (1+i\eta)\tilde{\underline{g}}_f(0) \right] \underline{\psi}_n \\ & + \omega^2 \left\{ \underline{\psi}_n^f \right\}^T \underline{\bar{R}}_n^f(\omega) \end{aligned} \quad (6.53a)$$

$$\tilde{\underline{S}}_{nj}(\omega) = \underline{\psi}_n^T \left[\tilde{\underline{g}}_f(\omega) - (1+i\eta)\tilde{\underline{g}}_f(0) \right] \underline{\psi}_j + \omega^2 \left\{ \underline{\psi}_n^f \right\}^T \underline{\bar{R}}_j^f(\omega) \quad (6.53b)$$

$$\tilde{\underline{L}}_n^l(\omega) = -\underline{\psi}_{n-c}^T \underline{l}_c^l + \left\{ \underline{\psi}_n^f \right\}^T \underline{\bar{R}}_0^l(\omega) \quad (6.53c)$$

These are the final equations governing the response of the dam to horizontal or vertical ground motions, applied separately. Included in these equations are the hydrodynamic effects and dam-foundation interaction effects that are significant in the response of the dam. Equation 6.52 represents J algebraic equations in the unknown complex frequency response functions in the generalized coordinates $\tilde{\underline{Z}}_j^l(\omega)$, $j = 1, 2, \dots, J$, corresponding to the J Ritz vectors included in the analysis. The coefficient matrix $\tilde{\underline{S}}(\omega)$ is to be determined for each excitation frequency and simultaneous solution of the equations leads to the values of $\tilde{\underline{Z}}_j^l$ at that excitation frequency. Repeated solution for several hundred excitation frequencies, covering the frequency range over which the ground motion and structural response have significant components, leads to the complete functions $\tilde{\underline{Z}}_j^l(\omega)$.

The number of Ritz vectors that need be included in the analysis depends on the system properties, the response quantities, and frequency range of interest. The number necessary in analysis of concrete gravity dams is determined in Sec. 7.6. As will be seen later, a few generalized coordinates (ten to twenty) are sufficient in the analysis of dams idealized as finite element systems with say 200 DOF, thus leading to very efficient procedures.

6.2.7 Singularities of Response

Elements of matrix $\tilde{S}(\omega)$ and load vector $\tilde{L}^l(\omega)$ are to be computed for a frequency ω by using Eq. 6.53 together with the pressure functions \bar{p}_0^l and \bar{p}_j of Eqs. 6.39 and 6.40. The pressure functions, and hence the corresponding nodal forces \bar{R}_0^l and \bar{R}_j , are unbounded at $\omega = \omega_m^r$ where $\omega_m^r = (2m-1)\pi C/2H$, is the m^{th} resonant frequency of the fluid domain. Consequently, the elements of $\tilde{S}(\omega)$ and $\tilde{L}^x(\omega)$ are unbounded at these frequencies.

When $J = 1$, i.e. when only one vibration mode of the dam is considered in the analysis, the J equations of Eq. 6.53 reduce to one equation and the response at $\omega = \omega_m^r$ can be obtained through a limiting process. However, when $J > 1$, i.e. when more than one mode is considered in the analysis, the limiting process yields a system of equations such that $\tilde{S}(\omega)$ is singular at $\omega = \omega_m^r$. In particular, all the M equations become identical to each other and no solution can be obtained.

This degeneracy of the equations may be considered as a limitation of the substructure method of analysis. However, this limitation is of no practical consequence in obtaining earthquake responses. Numerical values for the frequency responses may be obtained for values of ω arbitrarily close to ω_m^r . The singularities at ω_m^r constitute a discrete set and will therefore not affect the values of the Fourier integrals which will lead to earthquake responses (Sec. 6.3).

6.3 Response to Arbitrary Ground Motion

Once the complex frequency response functions $\bar{Z}_n^x(\omega)$ and $\bar{Z}_n^y(\omega)$, $n = 1, 2, \dots, J$, have been determined by solving Eq. 6.52 for an appropriate range of excitation frequency ω , the responses to arbitrary ground motion can be obtained as the superposition of responses to individual harmonic components of the excitation through the Fourier integral:

$$\bar{z}_n^{\ell}(t) = \frac{1}{2\pi} \int_{-\infty}^{\infty} \bar{z}_n^{\ell}(\omega) A_g^{\ell}(\omega) e^{i\omega t} d\omega; \quad \ell = x, y \quad (6.54)$$

in which $A_g^{\ell}(\omega)$ is the Fourier transform of $a_g^{\ell}(t)$:

$$A_g^{\ell}(\omega) = \int_0^d a_g^{\ell}(t) e^{-i\omega t} dt; \quad \ell = x, y \quad (6.55)$$

where d is the duration of ground motion.

The combined response $Z_n(t)$ to horizontal and vertical components of ground motions acting simultaneously is

$$Z_n(t) = Z_n^x(t) + Z_n^y(t) \quad (6.56)$$

Repeating this procedure for all the necessary values of n , the displacement response is obtained by transforming back from generalized to nodal point coordinates

$$\underline{r}_c(t) = \sum_{n=1}^J Z_n(t) \underline{\psi}_n \quad (6.57)$$

The stresses $\underline{\sigma}_p(t)$ in finite element p at any instant of time are related to the nodal point displacements $\underline{r}_p(t)$ for that element by

$$\underline{\sigma}_p(t) = \underline{T}_p \underline{r}_p(t) \quad (6.58)$$

where \underline{T}_p is the stress transformation matrix for the finite element p . At any instant of time, the stresses throughout the dam are determined from the nodal point displacements by applying the transformations of Eq. 6.58 to each finite element.

6.4 Static Stress Analysis

The standard procedure for analysis of stresses due to static loads (Chapter 3) applies to structures on rigid base. Including foundation flexibility, the equilibrium equations for a dam subjected only to hydrostatic pressures and forces associated with its own weight can be obtained as a

special case of the equations of dynamics (Eq. 6.11)

$$\begin{bmatrix} \underline{k} & \underline{k}_b \\ (\underline{k}_b)^T & \underline{k}_{bb} + \underline{g}_f(0) \end{bmatrix} \begin{Bmatrix} \underline{r} \\ \underline{r}_b \end{Bmatrix} = \begin{Bmatrix} \underline{R} \\ 0 \end{Bmatrix} \quad (6.59)$$

The vector of static loads is denoted by \underline{R} and the effects of foundation deformations are represented by the foundation stiffness matrix at zero frequency.

In principle, Eq. 6.59 may be directly solved for the desired nodal point displacements resulting from the gravity loads. In practice, this direct approach may be unsatisfactory because the displacements \underline{r} and \underline{r}_b include large rigid body components which have no effect on the stresses in the dam. To avoid this difficulty, the total displacements are expressed as the sum of rigid body displacements plus an increment due to deformations, i.e.,

$$\begin{Bmatrix} \underline{r} \\ \underline{r}_b \end{Bmatrix} = \begin{Bmatrix} \underline{r}_0 \\ \underline{r}_{0b} \end{Bmatrix} + \begin{Bmatrix} \tilde{\underline{r}} \\ \tilde{\underline{r}}_b \end{Bmatrix} \quad (6.60)$$

in which the subscript "0" refers to rigid body displacements, and the "tilde" identifies the relative displacement components. The rigid body and relative displacements at the base of the dam are shown in Fig. 6.3.

Introducing Eq. 6.60 into Eq. 6.59 yields:

$$\begin{bmatrix} \underline{k} & \underline{k}_b \\ (\underline{k}_b)^T & \underline{k}_{bb} + \underline{g}_f(0) \end{bmatrix} \begin{Bmatrix} \underline{r}_0 \\ \underline{r}_{0b} \end{Bmatrix} + \begin{bmatrix} \underline{k} & \underline{k}_b \\ (\underline{k}_b)^T & \underline{k}_{bb} + \underline{g}_f(0) \end{bmatrix} \begin{Bmatrix} \tilde{\underline{r}} \\ \tilde{\underline{r}}_b \end{Bmatrix} = \begin{Bmatrix} \underline{R} \\ 0 \end{Bmatrix} \quad (6.61)$$

But since the rigid body displacements produce no forces in the structure, this may be written as

$$\begin{bmatrix} 0 & 0 \\ 0 & \underline{g}_f(0) \end{bmatrix} \begin{Bmatrix} \underline{r} \\ \underline{r}_b \end{Bmatrix} + \begin{bmatrix} \underline{k} & \underline{k}_b \\ (\underline{k}_b)^T & \underline{k}_{bb} + \underline{g}_f(0) \end{bmatrix} \begin{Bmatrix} \tilde{\underline{r}} \\ \tilde{\underline{r}}_b \end{Bmatrix} = \begin{Bmatrix} \underline{R} \\ 0 \end{Bmatrix} \quad (6.62)$$

Designating the foundation forces associated with rigid body displacements by \underline{R}_{0b} , where

$$\underline{R}_{0b} = \underline{g}_f(0) \underline{r}_{0b} \quad (6.63)$$

Eq. 6.62 may be written as follows:

$$\begin{bmatrix} \underline{k} & \underline{k}_b \\ \underline{k}_b^T & \underline{k}_{bb} + \underline{g}_f(0) \end{bmatrix} \begin{Bmatrix} \underline{\tilde{r}} \\ \underline{\tilde{r}}_b \end{Bmatrix} = \begin{Bmatrix} \underline{R} \\ -\underline{R}_{0b} \end{Bmatrix} \quad (6.64)$$

Equation 6.64 thus provides a means to solve directly for the relative displacements; the rigid body displacements enter only in the evaluation of the rigid body foundation forces \underline{R}_{0b} . To evaluate these forces, it is convenient to express the rigid body displacements \underline{r}_{0b} in terms of

$$\underline{r}_{cg} = \begin{Bmatrix} u_{cg} \\ v_{cg} \\ \theta_{cg} \end{Bmatrix}$$

the three components of displacement of the center of gravity (c.g) of the base (Fig. 6.4):

$$\underline{r}_{0b} = \underline{D} \underline{r}_{cg} \quad (6.65)$$

where the transformation matrix \underline{D} involves only the geometry of the location of the base nodal points and the c.g of the base.

Similarly, the resultant base forces \underline{R}_{cg} corresponding with the displacements \underline{r}_{cg} can be expressed in terms of the nodal forces \underline{R}_{0b} as follows:

$$\underline{R}_{cg} = \underline{D}^T \underline{R}_{0b} \quad (6.66)$$

where

$$\underline{R}_{cg} = \begin{Bmatrix} U \\ V \\ M \end{Bmatrix}$$

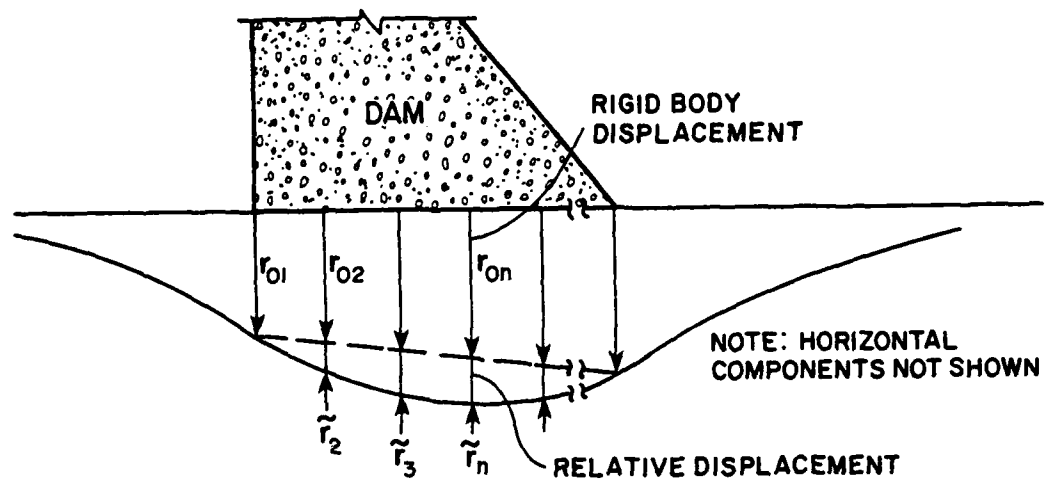


FIG. 6.3 RIGID BODY AND RELATIVE DISPLACEMENTS AT BASE OF THE DAM

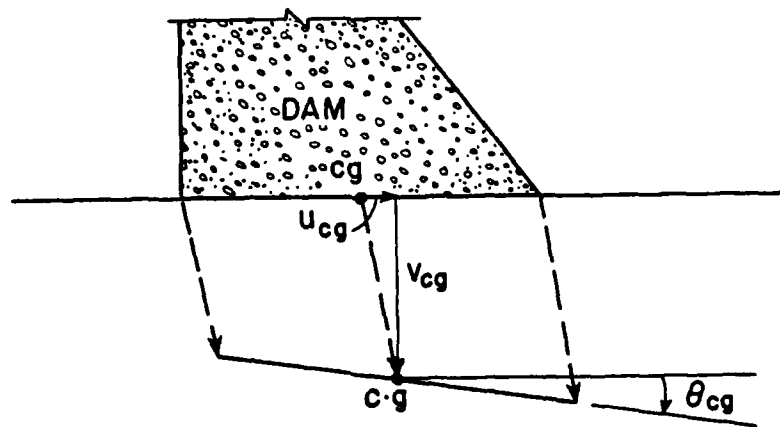


FIG. 6.4 RIGID BODY DISPLACEMENTS AT THE CENTER OF GRAVITY OF THE DAM BASE

in which

U = resultant horizontal force

V = resultant vertical force

M = resultant moment about the center of gravity

Introducing Eqs. 6.63 and 6.65 into Eq. 6.66 yields

$$\underline{R}_{cg} = \underline{D}^T \underline{R}_{Ob} = \underline{D}^T \underline{g}_f(0) \underline{r}_{Ob} = \underline{D}^T \underline{g}_f(0) \underline{D} \underline{r}_{cg}$$

from which

$$\underline{R}_{cg} = \underline{g}_{f0} \underline{r}_{cg} \quad (6.67)$$

if the symbol

$$\underline{g}_{f0} = \underline{D}^T \underline{g}_f(0) \underline{D} \quad (6.68)$$

is used to represent the rigid body foundation stiffness matrix.

Solving Eq. 6.67 for the rigid body displacements:

$$\underline{r}_{cg} = \underline{g}_{f0}^{-1} \underline{R}_{cg}$$

and making use of Eqs. 6.65 and 6.63, the nodal forces \underline{R}_{Ob} associated with rigid body displacements are expressed in terms of \underline{R}_{cg} , the resultant forces at the base due to all applied loads R:

$$\underline{R}_{Ob} = \underline{g}_f(0) \underline{D} \underline{g}_{f0}^{-1} \underline{R}_{cg} \quad (6.69)$$

With this result the right hand side of Eq. 6.64 is known. This equation can be solved for the relative nodal displacements, from which all desired stresses in the dam can be found, without any specific consideration of the rigid body displacements.

6.5 Special Cases

6.5.1 Dam-Foundation System, No Water

The frequency-domain equations for the dam, without any impounded water and including dam-foundation interaction effects, can be obtained from the general Eqs. 6.52 and 6.33 by simply dropping the hydrodynamic terms $\underline{R}_0^\ell(\omega)$ and $\underline{R}_j^f(\omega)$. The resulting equations are

$$\underline{S}(\omega) \underline{\bar{Z}}^\ell(\omega) = \underline{L}^\ell(\omega); \quad \ell = x, y \quad (6.70)$$

in which

$$\underline{S}_{nn}(\omega) = \left[-\omega^2 + (1+i\eta)\lambda_n^2 \right] \underline{\psi}_{n-c}^T \underline{\psi}_n + \underline{\psi}_n^T \left[\underline{\bar{g}}_f(\omega) - (1+i\eta)\underline{\bar{g}}_f(0) \right] \underline{\psi}_n \quad (6.71a)$$

$$\underline{S}_{nj}(\omega) = \underline{\psi}_n^T \left[\underline{\bar{g}}_f(\omega) - (1+i\eta)\underline{\bar{g}}_f(0) \right] \underline{\psi}_j \quad (6.71b)$$

$$\underline{L}_n^\ell = -\underline{\psi}_{n-c}^T \underline{1}_c^\ell \quad (6.71c)$$

Equations 6.70 and 6.71 are the same as those presented in Chapter 5 for dynamic response of dams including structure-foundation interaction.

6.5.2 Dam on Rigid Foundation, with Water

In this case, the base DOF can be eliminated from the analysis; the associated structure-foundation system defined in Sec. 6.2.4 is simply the dam on rigid foundation. Denoting the mass and stiffness matrices of the dam on rigid base by \underline{m} and \underline{k} , the natural vibration frequencies ω_n and corresponding mode shapes $\underline{\phi}_n$ of this system are solutions of the eigenvalue problem

$$\underline{k} \underline{\phi}_n = \omega_n^2 \underline{m} \underline{\phi}_n \quad (6.72)$$

The structural displacements are expressed as a linear combination of the first J mode shapes:

$$\underline{r}^\ell(t) = \sum_{j=1}^J \underline{y}_j^\ell(t) \underline{\phi}_j \quad \text{and} \quad \underline{\bar{r}}^\ell(\omega) = \sum_{j=1}^J \underline{\bar{y}}_j^\ell(\omega) \underline{\phi}_j \quad (6.73)$$

Thus, the frequency domain equations for the dam on a rigid foundation,

including hydrodynamic effects, can be obtained by appropriately specializing Eqs. 6.52 and 6.53. The resulting equations are

$$\underline{S}(\omega) \underline{\bar{Y}}^\ell(\omega) = \underline{L}^\ell(\omega) ; \ell = x, y \quad (6.74)$$

in which

$$S_{nn}(\omega) = \left[-\omega^2 + (1+i\eta)\omega^2 \right] \phi_n^T \underline{\bar{m}} \phi_n + \omega^2 \{ \phi_n^f \}^T \underline{\bar{R}}_n^f(\omega) \quad (6.75a)$$

$$S_{nj}(\omega) = \omega^2 \{ \phi_n^f \}^T \underline{\bar{R}}_j^f(\omega) \quad (6.75b)$$

$$L_n^\ell(\omega) = - \phi_n^T \underline{\bar{m}} \underline{\bar{l}}^\ell + \{ \phi_n^f \}^T \underline{\bar{R}}_0^\ell(\omega) \quad (6.75c)$$

These equations are equivalent to those in Chapter 4 (Eqs. 4.16-4.18 and 4.34-4.35) developed directly for dams with water on rigid foundation.

6.5.3 Dam on Rigid Foundation, No Water

Equations governing complex frequency responses of a dam without water are obtained by further specializing Eqs. 6.74 and 6.75, simply by setting to zero the hydrodynamic forces $\underline{\bar{R}}_0^\ell(\omega)$ and $\underline{\bar{R}}_j^\ell(\omega)$. The coefficients of Eq. 6.74 are then given by:

$$S_{nn}(\omega) = \left[-\omega^2 + (1+i\eta)\omega^2 \right] \phi_n^T \underline{\bar{m}} \phi_n \quad (6.76a)$$

$$S_{nj}(\omega) = 0 \quad (6.76b)$$

$$L_n^\ell(\omega) = - \phi_n^T \underline{\bar{m}} \underline{\bar{l}}^\ell \quad (6.76c)$$

The matrix $\underline{S}(\omega)$ is now diagonal since the chosen Ritz vectors are the natural modes of vibration of the system considered.

Comparing Eqs. 6.76 and 6.75, it is apparent that $\underline{S}(\omega)$ and $\underline{L}(\omega)$ are modified due to the presence of water. The diagonal terms of $\underline{S}(\omega)$ are modified by an additional frequency-dependent mass. Off-diagonal mass terms appear because the Ritz vectors, the natural modes of vibration of the dam (without water), are not the vibration modes of the combined dam-water system, and they become coupled due to hydrodynamic interaction effects. An additional term appears in $\underline{L}^\ell(\omega)$ due to hydrodynamic loads.

These equations are equivalent to those in Chapter 3 (Eq. 3.11) derived directly for the dam without water on rigid foundation.

6.6 Computer Program

Based on the analytical procedures developed in this chapter, a computer program has been written in FORTRAN IV to numerically evaluate the responses of concrete gravity dams, including various effects of both the water and the foundation. These include effects arising from interaction between the dam and foundation, dam and water, water and foundation, and from interaction among all three substructures--dam, water, and foundation. The dynamic stiffness matrix for the foundation is not computed within the computer program. Thus it should be computed externally and supplied to the computer program. Available data and methods [32] may be utilized to determine the dynamic stiffness matrix for a foundation region idealized as a viscoelastic half plane.

The computer program is capable of analyzing the response of a dam for four conditions: Dam on rigid foundation excluding hydrodynamic effects, dam on rigid foundation including hydrodynamic effects, dam on flexible foundation excluding hydrodynamic effects, and dam on flexible foundation including hydrodynamic effects.

The response of dam-water-foundation systems, idealized as described in Chapter 2, to horizontal and vertical components of ground motion can be analyzed. The dam is treated as an assemblage of two-dimensional finite elements; the impounded water and foundation are treated as continua.

The output from the computer program includes the complex frequency response functions describing the response to harmonic ground motions and the complete time-history of displacements and stresses throughout the dam. Because the program is capable of including any number of Ritz shape vectors, results can be obtained to any desired degree of accuracy.

The users guide and listing of the program are included in Appendices A and B.

7. PRELIMINARY RESULTS FOR PARAMETER SELECTION

7.1 Scope of the Chapter

Several preliminary analyses were carried out to assist in the selection of parameters defining the system and also those necessary to carry out the analyses for the dynamic response study presented in Chapter 8. Results from two analyses of a dam foundation system, assuming the system to be in plane stress in one and in plane strain in the other, are presented to provide a basis for selecting one of the two assumptions. Similarly, response of the dam is presented and compared for two damping models, viscous damping and constant hysteretic damping. With the aid of response results, the minimum number of parameters -- those that have the most important influence on the dam response -- defining the elastic moduli of the dam and foundation are identified. The number of generalized coordinates necessary to obtain accurate responses over the desired range of excitation frequency is determined with the aid of response results obtained with varying numbers of these coordinates.

7.2 Systems, Ground Motions, and Response Quantities

7.2.1 Systems

The dam is idealized as having a triangular cross section with a vertical upstream face and a downstream face with a slope of 0.8:1. The dam is assumed to be homogeneous with linearly elastic and isotropic properties for mass concrete: Young's modulus $E_s = 2$ or 4 million psi; Poisson's ratio $= 0.2$; and unit weight $= 155 \text{ lbs/ft}^3$. Representative values for the latter two parameters have been chosen. The possible small variation around the chosen values will have little influence on the dam response. Two damping assumptions are considered: Viscous damping with damping ratio $\xi_s = 0.05$ in each natural mode of vibration of the dam alone (without water) on a fixed base, and constant hysteretic damping with the energy loss coefficient $\eta_s = 0.1$.

The finite element idealization for a monolith of the dam (Fig. 7.1) consists of 20 quadrilateral elements and 26 nodal points which provide 42 degrees of freedom on a fixed base and 52 on a flexible base.

The dam monolith is supported on the surface of a homogeneous, isotro-

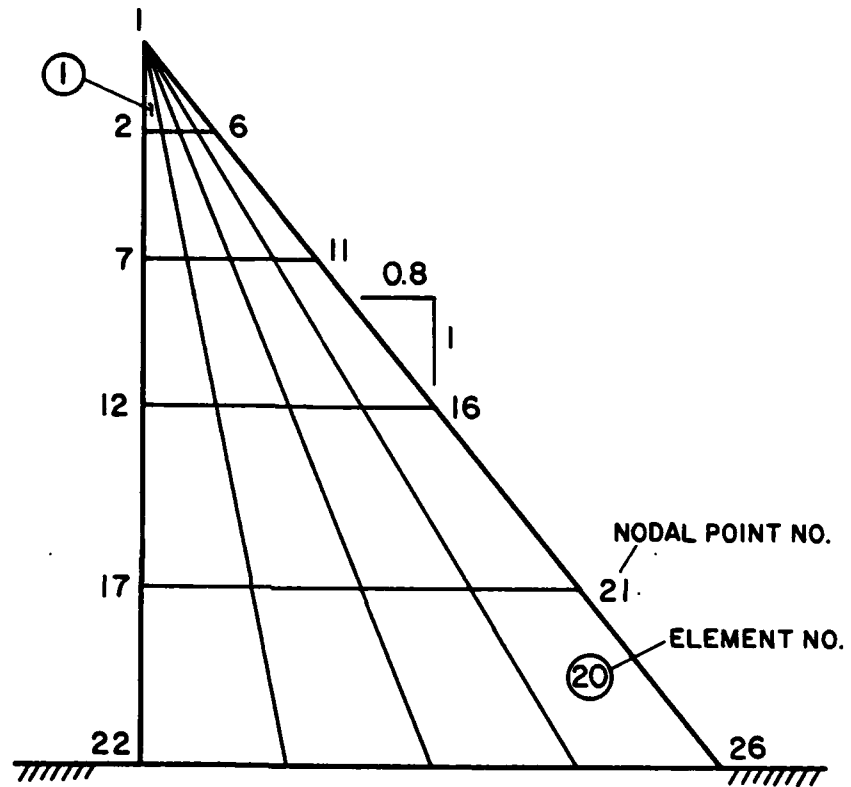


FIG. 7.1 FINITE ELEMENT IDEALIZATION OF A DAM MONOLITH WITH TRIANGULAR CROSS-SECTION

pic, linearly viscoelastic half space. The following properties are assumed for the foundation materials: $E_f = 2E_s$; Poisson's ratio = $1/3$; and unit weight, $w_f = 165 \text{ lbs/ft}^3$. The latter two parameter values are not varied because the response is insensitive to the small variations in those parameter values that can occur in practical problems. The foundation soil or rock is idealized as a constant hysteretic solid with several values of energy loss coefficient $\eta_f = 0.1, 0.25, \text{ and } 0.5$, or as a Voigt solid with energy loss coefficient $\xi_f = 0.1$. Impounded water in the reservoir has a constant depth H and is idealized as extending to infinity in the upstream direction. The unit weight of water $w = 62.5 \text{ lbs/ft}^3$ and the velocity of sound in water = 4720 ft/sec . Two values of the depth of water H , relative to the height of the dam H_s , are considered: $H/H_s = 0$ (no water) and 1 (full water).

The dam and foundation both are assumed to be in a state of generalized plane stress or plane strain.

7.2.2 Ground Motions

The excitation for the dam-water-foundation system is defined by the two components of free-field ground motion in the plane of a monolith of the dam: the horizontal component transverse to the dam axis; and the vertical component. Each component of ground acceleration is assumed to be harmonic, $a_g^x(t) = a_g^y(t) = e^{i\omega t}$, with the excitation frequency to be varied over a relevant range.

7.2.3 Response Quantities

The response of the dam to harmonic free field ground motion was determined by the analytical procedures presented in Chapter 6. Five mode shapes on fixed base or generalized coordinates, as appropriate, were included in the analysis. Although the analysis led to response at all nodal points, only the results for a few selected degrees-of-freedom are presented. For dams on rigid foundations, the complex frequency response functions for horizontal acceleration at the crest of the dam are presented. In addition, the complex frequency response functions for the horizontal acceleration at the center of the base of the dam and for vertical accelerations at the upstream and downstream edges of the base are presented when the interaction between the structure and flexible foundation material is included.

The absolute value (or modulus) of the complex-valued acceleration response is plotted against normalized excitation frequency parameter ω/ω_1 , where ω_1 = fundamental fixed base natural frequency of the dam alone.

7.3 Comparison of Plane Strain and Plane Stress Assumption

Because, at the present time, the analysis procedure presented in Chapter 6 has been implemented only for two-dimensional systems, its application is restricted to systems in plane stress or plane strain. Although, as mentioned in Chapter 2, neither of the two models are strictly valid, the former is better for the dam and the latter for the foundation. However, in order to define the dam-foundation system on a consistent basis, the same model should be employed for both substructures.

The results of two analyses of the dam-foundation system described in Section 7.2.1, assuming the system to be in plane stress in one and in plane strain in the other, are presented in Fig. 7.2. Constant hysteretic damping with energy loss coefficient $\eta = 0.1$ was assumed for the dam and foundation materials. The results presented are for systems with $E_f/E_s = 2$, independent of the E_f and E_s value separately. It is obvious from Fig. 7.2 that the response of the dam, including effects of dam-foundation interaction, is essentially the same under two assumptions -- plane stress or plane strain.

The dam-foundation system is assumed to be in plane stress for all the results in this and later chapters. As discussed in Chapter 2, based on physical behavior, this assumption is appropriate for describing the behavior of a concrete gravity dam vibrating at large amplitudes of motion, but not for the foundation. However, based on the above results, the same assumption may be made for the foundation behavior without significant loss in accuracy.

7.4 Elastic Moduli Parameters

The complex frequency acceleration response functions describe the steady-state acceleration response of dams to harmonic excitations. These functions for a dam on a rigid foundation and no water, plotted against normalized excitation frequency parameter ω/ω_1 , apply to dams of all heights provided they all have the same cross-sectional shape. Furthermore, they are independent of the unit weight w_s and Young's modulus E_s for the dam

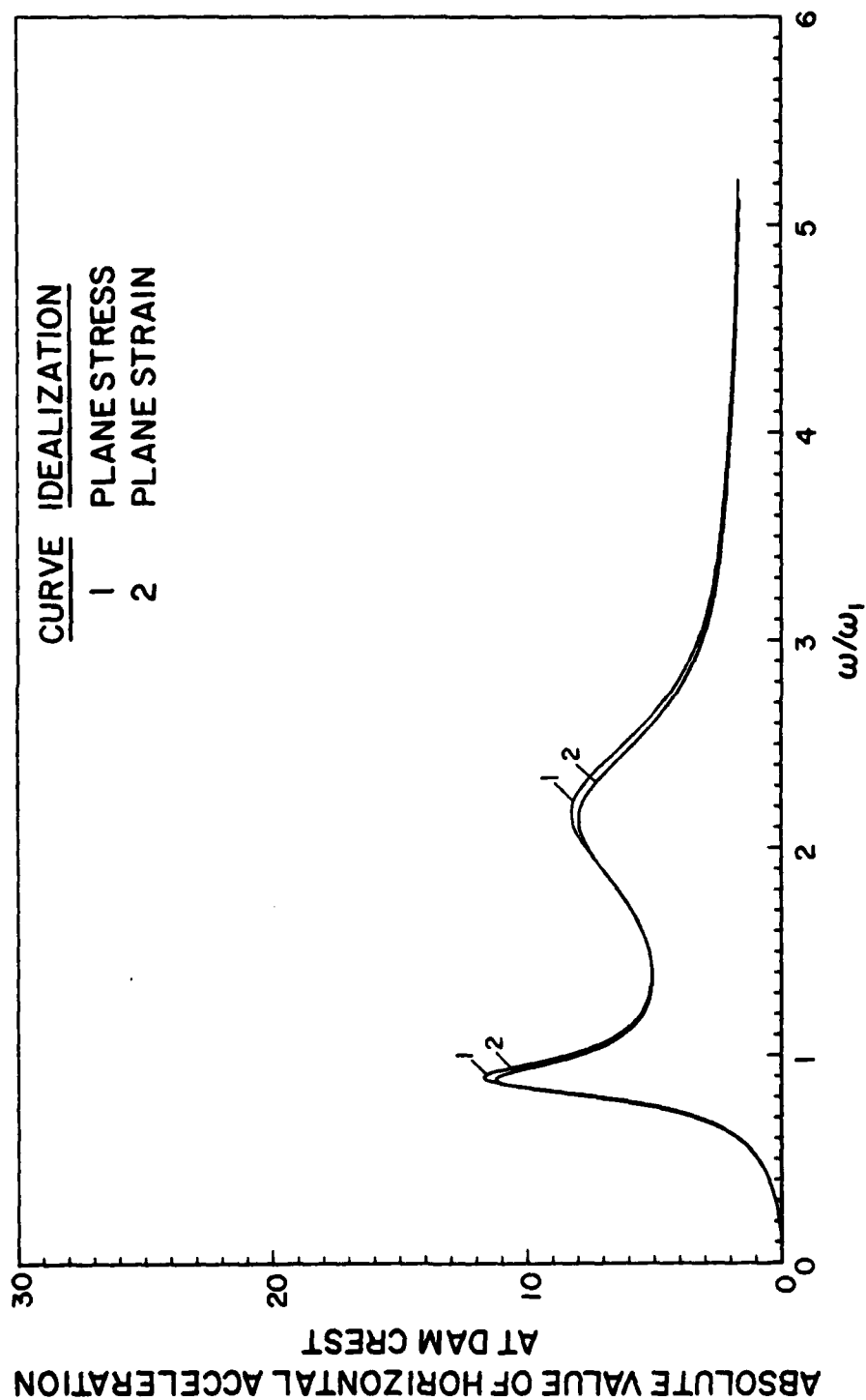


FIG. 7.2 RESPONSE OF A DAM WITHOUT WATER, INCLUDING DAM-FOUNDATION INTERACTION, TO HARMONIC HORIZONTAL GROUND ACCELERATION OBTAINED UNDER TWO ASSUMPTIONS FOR THE SAME SYSTEM:
(1) PLANE STRESS; AND (2) PLANE STRAIN

concrete. It can be concluded from the equations of motion for the dam, including the dam-foundation interaction but excluding hydrodynamic effects, that the complex frequency response functions plotted against normalized excitation frequency do not depend separately on E_s and E_f but only the ratio E_f/E_s . These functions for dams on rigid foundations vary significantly with E_s when hydrodynamic effects are considered [22]. They vary even for dams on flexible foundations: for a fixed value of E_f/E_s , the value of E_s has influence on the response of the dam including dam-water interaction effects. Figure 7.3 demonstrates that this influence is minor in the response to horizontal ground motion but significant in the response to vertical ground motion.

7.5 Damping Models and Parameters

7.5.1 Dam

The analytical procedures presented in Chapters 3-6 included two models -- viscous damping and constant hysteretic damping -- for energy dissipation in the dam. Viscous damping had been selected earlier [22], in studying hydrodynamic effects in earthquake response of dams. Constant hysteretic damping is preferable for conceptual as well as computational reasons, especially when structure-soil interaction is included in the analysis [29]. Therefore, all numerical results presented in Chapters 8 and 9 are for dams with constant hysteretic damping. In order to provide a basis for comparing these results with those presented earlier [22], response results using both damping models are presented in this section and compared.

Using the analysis procedure in Chapter 6, the steady-state response of the idealized dam monolith (Fig. 7.1) to harmonic ground acceleration in the horizontal direction is determined for several cases. Assuming the concrete properties listed in Section 7.2.1, with Young's modulus = 4×10^6 psi, and considering the foundation to be rigid, the complex frequency response functions for the dam were determined for the following four cases. (The first five vibration modes were included in the analysis.)

1. Viscous damping, $\xi_s = 0.05$ for all vibration modes; no water
2. Constant hysteretic damping, $\eta_s = 0.10$; no water
3. Viscous damping, $\xi_s = 0.05$ for all vibration modes; full water
4. Constant hysteretic damping, $\eta_s = 0.10$; full water

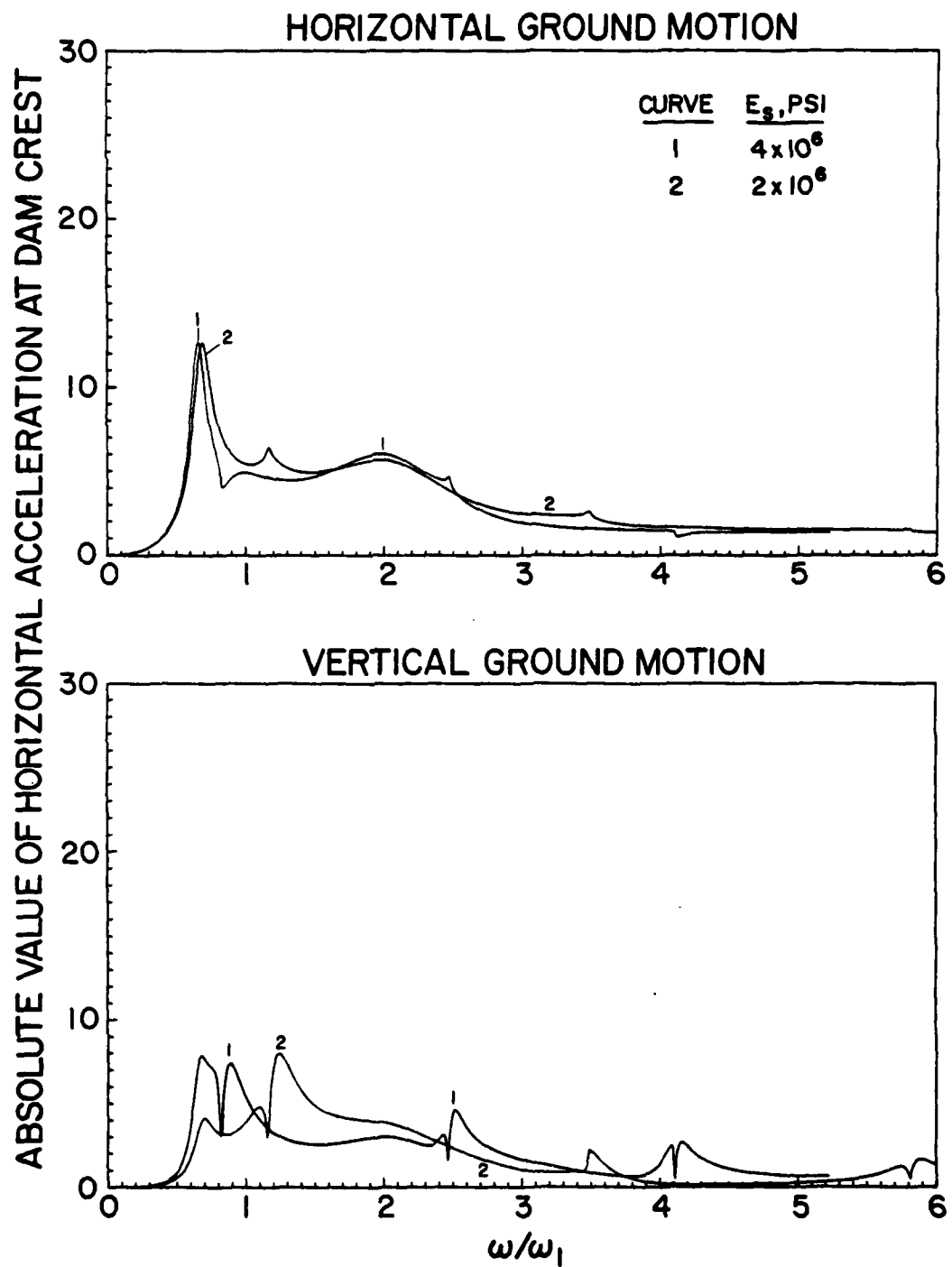


FIG. 7.3 INFLUENCE OF YOUNG'S MODULUS E_s OF DAM CONCRETE ON RESPONSE OF A DAM, INCLUDING EFFECTS OF WATER AND FOUNDATION, TO HARMONIC GROUND MOTION. E_f/E_s IS THE SAME IN BOTH CASES.

The selected values of damping factor η_s in constant hysteretic damping and viscous damping ratio ξ_s for all modes of vibration are related by $\eta_s = 2\xi_s$. As a result, the energy dissipated per vibration cycle in each natural mode of vibration at the resonant excitation frequency would be the same for the two damping models. The energy dissipated per cycle in constant hysteretic damping is independent of excitation frequency, but varies linearly with frequency for viscous damping.

Because the energy dissipated at the fundamental resonant frequency of the dam alone is the same for the two damping models and the selected parameters, the dam response is independent of the type of damping (Fig. 7.4). At the fundamental resonant frequency of the dam, including hydrodynamic effects, the energy dissipated in constant hysteretic damping will be the same but reduced in viscous damping, compared to the energy dissipated at the natural frequency of the dam alone. As a result, the resonant response is significantly smaller for the dam with constant hysteretic damping, compared to the results for viscous damping (Fig. 7.4). The differences in resonant responses for the two damping models are directly related to the reduction in resonant frequencies due to dam-water interaction effects. Because such reduction is relatively small for higher resonant frequencies, the corresponding resonant responses are affected less by the damping model (Fig. 7.4). At excitation frequencies not close to resonant frequencies, damping has little effect on the response and it is essentially the same with the two damping models.

Constant hysteretic damping with $\eta_s = 0.1$ is assumed for the dam in obtaining all subsequent results in Chapters 7, 8, and 9.

7.5.2 Foundation

Numerical results and analytical procedures have been presented to determine dynamic stiffness matrices for a viscoelastic half-plane of Voigt or constant hysteretic materials [32]. In this section, computed responses of the dam including structure-soil interaction effects are presented to aid in selecting the damping model and parameters for the foundation material.

The response of the idealized dam monolith (Fig. 7.1) without water but including dam-foundation interaction effects is computed by the procedures of Chapter 6. The following properties are selected for the dam in addition to those listed in Section 7.2.1: Young's modulus $E_s = 4 \times 10^6$ psi, constant hysteretic damping factor $\eta_s = 0.1$. The foundation modulus E_f is twice that of the dam and, in addition to the properties of the foundation material listed

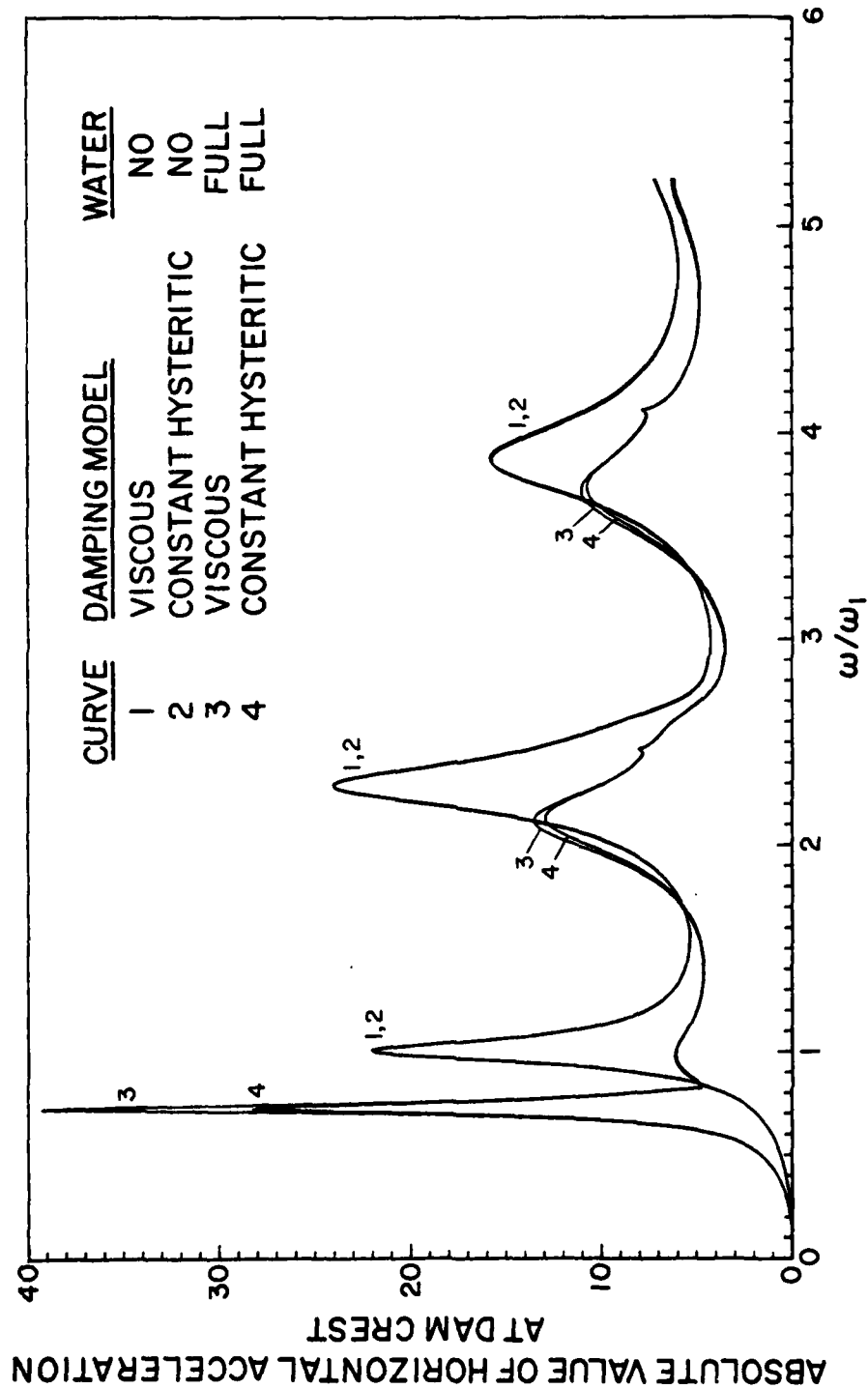


FIG. 7.4 INFLUENCE OF DAMPING MODEL, VISCOUS OR CONSTANT HYSTERETIC, ON RESPONSE OF A DAM ON RIGID FOUNDATION TO HARMONIC, HORIZONTAL GROUND MOTION

in Section 7.2.1, the following are selected: $E_f/E_s = 2$, energy loss coefficients $\xi_f = 0.1$ for the Voigt solid; and $\eta_f = 0.1$ for the constant hysteretic solid. The two dam-foundation systems analyzed have identical properties with one exception: the foundation is of Voigt material in one case, and constant hysteretic material in the other case. Including five generalized coordinates in the analysis, the complex frequency response functions for the dam were obtained for the two systems. The results presented in Fig. 7.5a demonstrate that the damping model for the foundation has little effect on the resonant frequencies of the dam or on the response except at the fundamental resonant frequency. The fundamental resonant response of the dam is somewhat larger with Voigt foundation material.

For a Voigt solid, the energy loss per cycle of harmonic vibration is proportional to the excitation frequency. However, over a considerable range of frequencies, rocks and soils exhibit energy loss essentially independent of the frequency of vibration. Such materials are better idealized as constant hysteretic solids. This is the model adopted for the foundation material for the dam responses presented in Chapters 8 and 9. Based on the above discussion, however, those results are also indicative of the response of dams on Voigt foundation materials.

Using the properties mentioned above for the dam and foundation, the analysis was repeated for two other values of damping coefficient for a constant hysteretic foundation: $\eta_f = 0.25$ and 0.50 . The complex frequency response functions for the dam with constant hysteretic damping, $\eta_s = 0.1$, on a constant hysteretic foundation are presented in Fig. 7.5b for three values of the damping factor $\eta_f = 0.1, 0.25$, and 0.50 . The responses are insensitive to the foundation damping except in a neighborhood of the fundamental resonant frequency. Even this resonant response is not influenced greatly by damping; increasing $\eta_f = 0.1$ to 0.25 reduces the resonant response by only 13%. Damping in the foundation is modeled as a constant hysteretic solid with $\eta_f = 0.1$ in obtaining all subsequent results in Chapters 7, 8, and 9. The assumed value of damping factor is appropriate for sound rocks at sites of major concrete dams. Because the dam response is not very sensitive to foundation damping, however, those results are approximately indicative of the dam response with other levels of foundation damping.

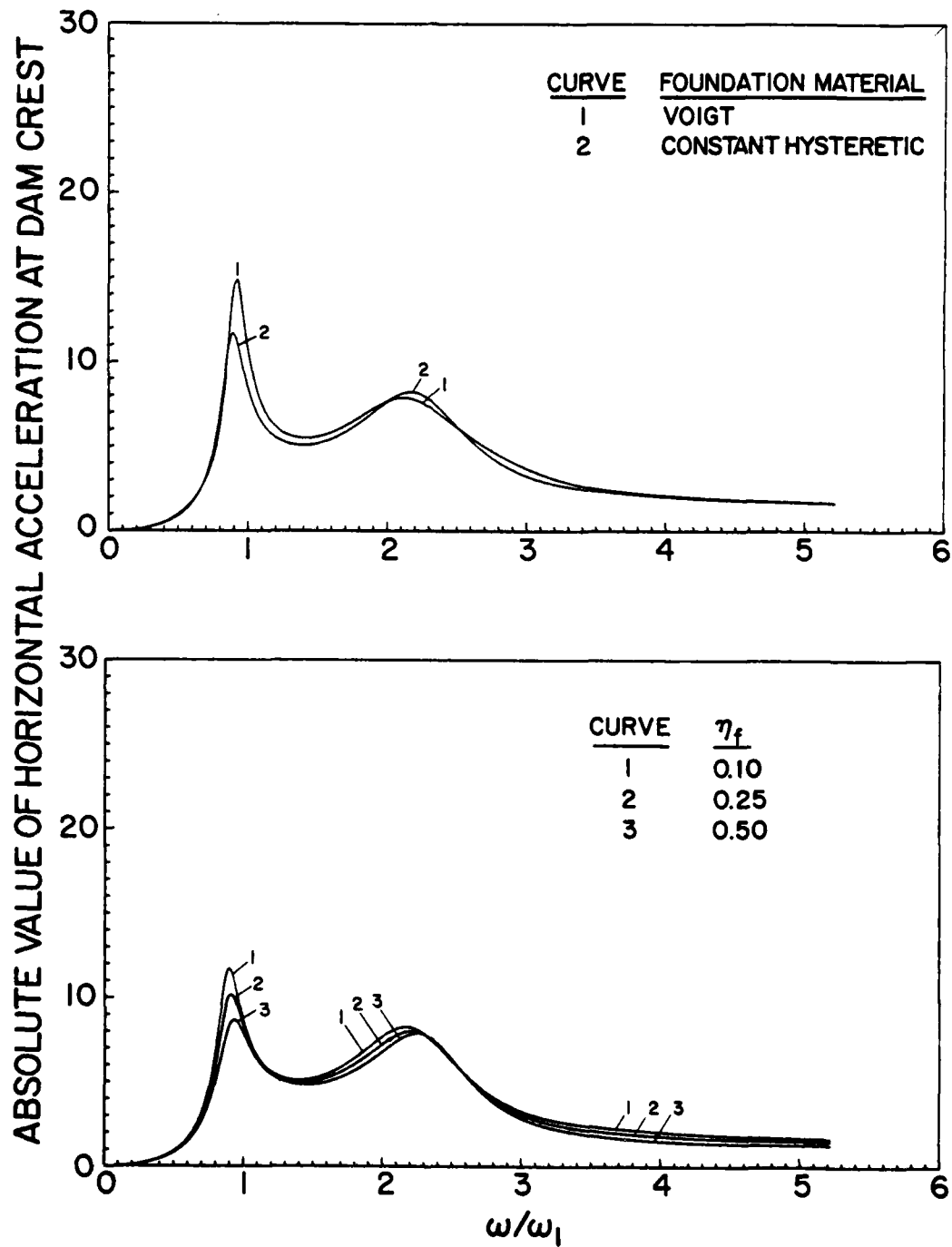


FIG. 7.5 RESPONSE OF A DAM WITHOUT WATER TO HARMONIC, HORIZONTAL GROUND ACCELERATION: (A) INFLUENCE OF DAMPING MODEL, VOIGT OR CONSTANT HYSTERETIC, FOR THE FOUNDATION. (B) INFLUENCE OF DAMPING COEFFICIENT η_f OF A CONSTANT HYSTERETIC FOUNDATION.

7.6 Number of Generalized Coordinates

The governing equations in the frequency domain were transformed from the physical nodal point displacement coordinates to generalized coordinates (Chapters 3-6). As many of these generalized coordinates should be included in the analysis as necessary to obtain accurate responses over a desired range of excitation frequencies. The required number of generalized coordinates will generally be a small fraction of the number of degrees-of-freedom in the finite element idealization of the dam.

The natural modes of vibration of the dam alone were selected as the generalized coordinates for analysis of the dam on rigid foundation, with or without water (Chapters 3 and 4). In order to accurately obtain the response of the dam without water on a rigid base, all the modes of vibration should be included which have natural frequencies within and close to the range of excitation frequencies of interest, and contribute significantly to the response in this frequency range. Accelerograph records accurately reproduce ground motion components with frequencies up to approximately 25 cps. The first few, say five, natural vibration modes, would generally be sufficient to obtain accurate responses of concrete gravity dams -- they have relatively high natural frequencies -- in this frequency range. Dam-water interaction significantly reduces the fundamental resonant frequency but has little influence on the higher resonant frequencies. Thus, usually, the same number of natural vibration modes would be sufficient for analysis of the response of the dam, with or without water.

The eigenvectors (vibration mode shapes) of an associated dam-foundation system, the dam with the foundation characterized by the stiffness matrix $\underline{g}_f(0)$ equal to the dynamic stiffness matrix $\underline{g}_f(\omega)$ at $\omega = 0$, were selected as the generalized coordinates for response analysis of the dam including dam-foundation interaction effects (Chapter 5). Unlike the natural modes of vibration of the dam on a rigid base, these generalized coordinates are not physically meaningful. Thus the number of these generalized coordinates that need to be included in the analysis is not as obvious. The complex frequency response functions for the dam with horizontal ground acceleration as the excitation was obtained from four analyses using the procedure of Chapters 5 and 6, including 5, 7, 19, and 15 generalized coordinates, respectively. The results presented in Fig. 7.6 are for the idealized dam

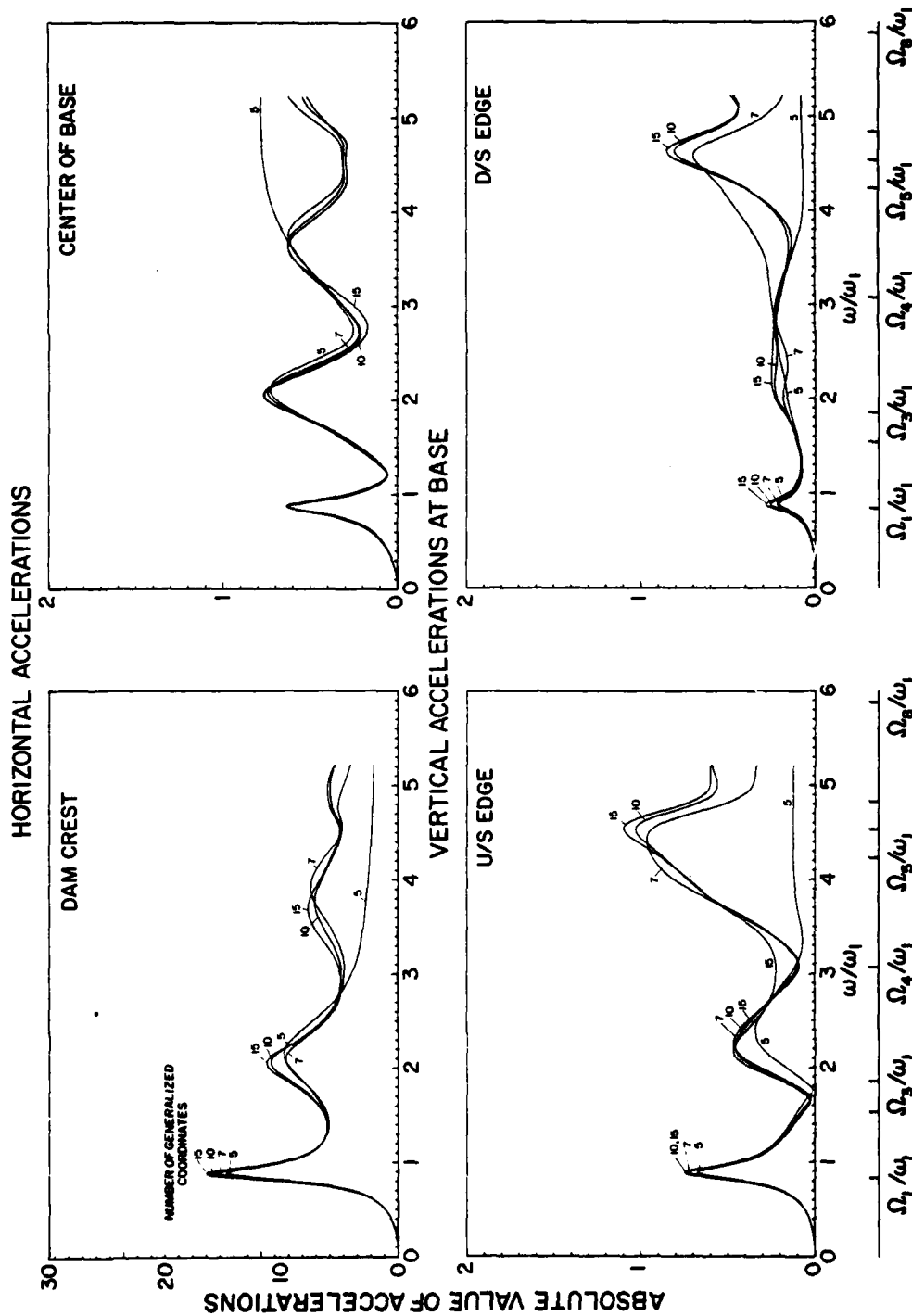


FIG. 7.6 INFLUENCE OF THE NUMBER OF GENERALIZED COORDINATES INCLUDED IN THE ANALYSIS ON RESPONSE OF A DAM, WITHOUT WATER BUT INCLUDING DAM-FOUNDATION INTERACTION, TO HARMONIC, HORIZONTAL GROUND MOTION

monolith, without water, but including dam-foundation interaction effects. The first 8 eigenvalues Ω_n (vibration frequencies) of the associated dam-foundation system are identified along the frequency axis. It is apparent that, in order to obtain satisfactory results for responses over some frequency range, all the generalized coordinates associated with eigenvalues within the frequency range plus a few, say three, more should be included in the analysis. Based on this criterion, the frequency-range represented in earthquake ground motion, and the fact that complex frequency response functions decrease at larger excitation frequencies, ten generalized coordinates were considered sufficient for the results presented in Chapters 8 and 9.

8. COMPLEX FREQUENCY RESPONSES

8.1 Scope of Chapter

The analysis procedure developed in Chapter 6 can be used to evaluate the response of concrete gravity dams subjected to earthquake ground motion. In this procedure, the complex frequency response functions describing the response to harmonic ground motion are determined, followed by the Fourier transform procedures to compute responses to arbitrary ground motion. In this chapter, the complex frequency response functions for an idealized cross section representative of concrete gravity dams are determined for a range of the important system parameters characterizing the properties of the dam, foundation soil or rock, and impounded water. The effects of dam-water interaction and of dam-foundation interaction on the dynamic response of the dam are studied.

8.2 Systems, Ground Motions, Cases Analyzed and Response Quantities

8.2.1 Systems

The idealized cross section considered as representative of concrete gravity dams is a triangle with a vertical upstream face and a downstream face with a slope of 0.8:1. The dam is assumed to be homogeneous with linearly elastic and isotropic properties for mass concrete: Young's modulus $E_s = 3, 4$ or 5 million psi; Poisson's ratio $= 0.2$; and unit weight $= 155$ lbs/cu.ft. Energy dissipation in the structure is represented by constant hysteretic damping, with the energy loss coefficient η_s selected as 0.1 . This is equivalent to a damping ratio of 0.05 in all the natural modes of vibration of the dam alone (without water) on a fixed base.

The finite element idealization for a monolith of the dam is shown in Fig. 8.1, consisting of 20 quadrilateral elements and 26 nodal points, which provide 42 degrees of freedom on a fixed base and 52 on a flexible base.

The dam is supported on the surface of a homogeneous, isotropic, linearly viscoelastic half space. For the foundation material, several values for the Young's modulus E_f are considered, Poisson's ratio $= 1/3$, and unit weight $= w_f = 165$ lbs/cu.ft. The foundation soil or rock is idealized as a constant hysteretic solid with energy loss coefficient $\eta_f = 0.1$.

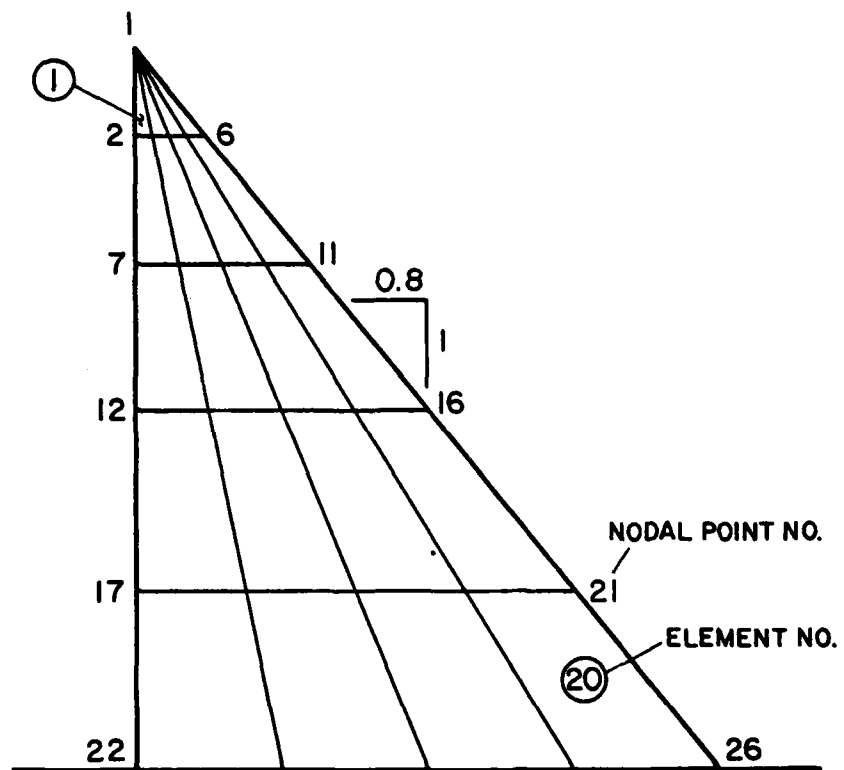


FIG. 8.1 FINITE ELEMENT IDEALIZATION OF A DAM MONOLITH WITH TRIANGULAR CROSS-SECTION

Impounded water in the reservoir has constant depth H and is idealized as extending to infinity in the upstream direction. Several different values for H , the depth of water, relative to H_s , the height of dam, are considered: $H/H_s = 0$ (empty reservoir), 0.8 (partially filled reservoir), and 1 (full reservoir). The unit weight of water $w = 62.5$ lbs/cu.ft. and the velocity of sound in water $= 4720$ ft/sec.

The dam and foundation are assumed to be in a state of generalized plane stress. This assumption, although not most appropriate for the foundation material, is dictated by the expected behavior of the dam (see Chapter 2).

8.2.2 Ground Motions

The excitation for the dam-water-foundation system is defined by the two components of free-field ground motion in the plane of a monolith of the dam: the horizontal component transverse to the dam axis, and the vertical component. Each component of ground acceleration is assumed to be harmonic, $a_g^x(t) = a_g^y(t) = e^{i\omega t}$, with the excitation frequency to be varied over a relevant range.

8.2.3 Cases Analyzed

As concluded in Chapter 7, the most important parameters influencing the complex frequency response functions for dams on rigid foundations are E_s , the Young's modulus of elasticity for mass concrete in the structure, and H/H_s , the ratio of water depth to dam height. When dam-foundation interaction is considered, an additional parameter is important: E_f/E_s , the ratio of Young's moduli for the foundation and dam materials. For a fixed value of E_f/E_s , the value of E_s influences the response of the structure to a minor extent for horizontal ground motion and significantly for vertical ground motion. However, to keep the number of cases analyzed to a minimum, the E_s value is not varied. Several dam-water-foundation systems were defined by values for parameters shown in Table 8.1. The complex frequency response functions for each case were determined. The following figures are presented in a manner to facilitate study of: the effects of structure-water interaction and structure-foundation interaction, considered separately; and the combined effects of these two sources of interaction, on the response of the dam.

TABLE 8.1 RESPONSE TO HORIZONTAL AND VERTICAL GROUND MOTION SEPARATELY: CASES ANALYZED

CASE	E_s - psi	FOUNDATION PROPERTIES		WATER IN RESERVOIR	
		Rigid or Flexible	E_f/E_s	Condition	H/H_s
1	Any*	Rigid	∞	Empty	0
2	4×10^6	Rigid	∞	Partially Filled	0.8
3	4×10^6	Rigid	∞	Full	1
4	3×10^6	Rigid	∞	Full	1
5	5×10^6	Rigid	∞	Full	1
6	Any*	Flexible	4	Empty	0
7	4×10^6	Flexible	4	Full	1
8	Any*	Flexible	2	Empty	0
9	4×10^6	Flexible	2	Partially Filled	0.8
10	4×10^6	Flexible	2	Full	1
11	Any*	Flexible	1	Empty	0
12	4×10^6	Flexible	1	Full	1

Results for all cases are presented in a form applicable to dams of all heights with the idealized triangular cross-section and chosen E_s value.

* Results for these cases, when presented in an appropriately normalized form, are valid for all E_s .

E_s = Young's modulus of elasticity of concrete in the dam | H = depth of water in reservoir
 E_f = Young's modulus of elasticity of foundation material | H_s = height of the dam

The hydrodynamic pressures due to vertical ground motion depend on, among other parameters, the reflection coefficient at the reservoir bottom $\alpha = [(C_r w_r / Cw) - 1] / [(C_r w_r / Cw) + 1]$ where w_r and C_r are the unit weight and P-wave velocity for the rock, w and C are the unit weight and sound velocity in water. It can be easily seen that $\alpha \leq 1$ with the maximum value corresponding to rigid rock. For $E_s = 4 \times 10^6$ psi and $E_r/E_s = \infty, 4, 2, 1$, and the values of w and w_r mentioned earlier, the values of α are 1, 0.85, 0.80 and 0.72, respectively.

8.2.4 Response Quantities

The response of the dam to harmonic free-field ground motion was determined by the analytical procedures presented in Chapter 6. Ten generalized coordinates were included in the analysis. Based on Sec. 7.6, the resulting complex frequency response functions should be accurate for excitation frequencies up to approximately 25 cps. Although the analysis led to response at all nodal points, only the results for a few selected degrees-of-freedom are presented. For dams on rigid foundations, the complex frequency response functions for horizontal and vertical accelerations at the crest of the dam are presented. In addition, the complex frequency response functions for horizontal acceleration at the center of the base of the dam and for the vertical accelerations at the upstream edge of the base are presented when interaction between the dam and flexible foundation material is included.

All the complex frequency response functions presented are for accelerations relative to the prescribed free-field ground acceleration. They are not direct measures of deformations within the dam. The absolute value (or modulus) of the complex valued acceleration response is plotted against the normalized excitation frequency parameter ω/ω_1 , where ω_1 = fundamental fixed-base natural frequency of the dam alone. When presented in this form, the results apply to dams of all heights with the idealized triangular cross section and chosen E_s value. Furthermore, if the reservoir is empty, the plotted results are also independent of the E_s value.

8.3 Complex Frequency Responses

8.3.1 Dam-Water Interaction Effects

In order to identify the effects of water on the dynamic response of the dam, the results of analysis cases 1, 2, and 3 (Table 8.1) to horizontal and vertical ground motion, separately, are presented in Figs. 8.2 and 8.3,

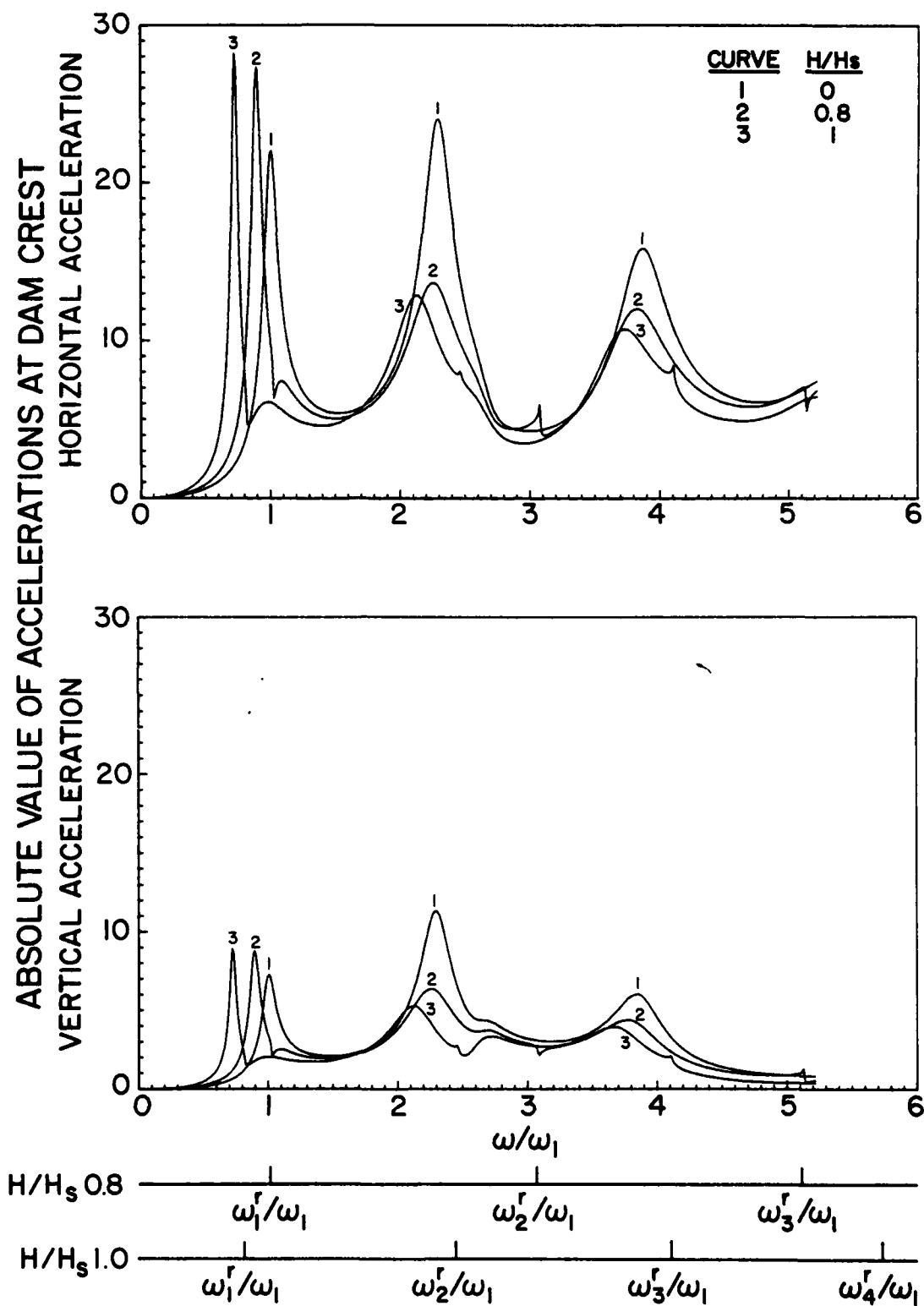


FIG. 8.2 HYDRODYNAMIC EFFECTS IN THE RESPONSE OF DAMS TO HARMONIC, HORIZONTAL GROUND MOTION. RESULTS ARE PRESENTED FOR VARYING WATER DEPTH: CASES 1, 2, AND 3 OF TABLE 8.1

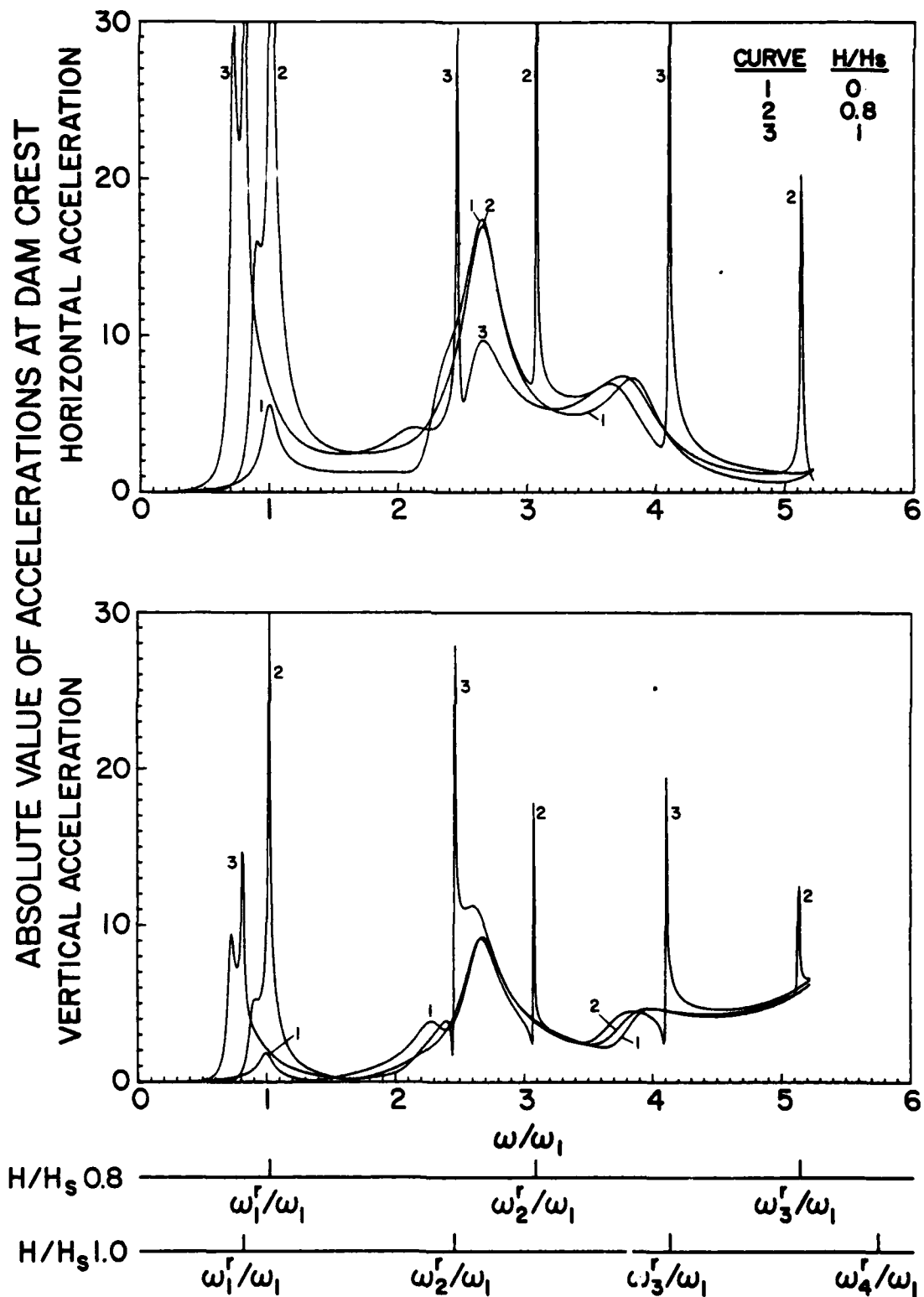


FIG. 8.3 HYDRODYNAMIC EFFECTS IN THE RESPONSE OF DAMS TO HARMONIC, VERTICAL GROUND MOTION. RESULTS ARE PRESENTED FOR VARYING WATER DEPTH: CASES 1, 2, AND 3 OF TABLE 8.1

respectively. The response curve for the dam without water ($H/H_s = 0$) is representative of a multi-degree-of-freedom system with constant mass, stiffness, and damping parameters. However, dam-water interaction introduces frequency dependent terms in the equations of motion of the dam, resulting in complicated shapes of the response curves. The response behavior is especially complicated at excitation frequencies in the neighborhood of the natural frequencies of water in the reservoir. In particular, the response curve has a double resonant peak near ω_1 and ω_1^r , which is especially pronounced for the case of vertical ground motion. At these frequencies the hydrodynamic terms in the equations of motion become unbounded but the response has finite limits (see Section 6.2.7). Based on the results of Figs. 8.2 and 8.3, the following observations can be made.

Presence of water results in a significant decrease in the fundamental resonant frequency of the dam but relatively little decrease in the higher resonant frequencies. At an excitation frequency ω smaller than ω_1^r , the fundamental resonant frequency of water in the reservoir, the effect of dam-water interaction is equivalent to an added mass and real-valued load; their magnitude depends on the excitation frequency. This added mass, in addition to reducing the fundamental resonant frequency of the dam, has the indirect effect of reducing the apparent damping ratio for the fundamental mode, resulting in narrower band width at resonance and larger resonant response. Some of the reduction in the resonant band width is, however, a consequence of the double resonant peak. At $\omega > \omega_1^r$, the effect of dam-water interaction is equivalent to frequency dependent additional mass, damping and load; the load is complex valued for horizontal and vertical ground motion except that it is real valued for vertical ground motion with $\alpha = 1$. The added mass is relatively small, which has relatively little effect on the higher resonant frequencies, but the added damping is significant, resulting in decrease in the response at the higher resonant frequencies. The fundamental resonant frequency of the dam, including hydrodynamic effects, is less than both the fundamental natural frequency of the dam with no water ω_1 , and of water in the reservoir, ω_1^r .

Comparing the results for cases 1 ($H/H_s = 0$), 2 ($H/H_s = 0.8$), and 3 ($H/H_s = 1$), it is seen that the fundamental resonant frequency is affected most by water in the upper parts of the dam height. At higher excitation frequencies, there is little difference in the responses for $H/H_s = 0.8$ and 1,

except that the response to vertical ground motion in the neighborhood of the second resonant frequency is strongly affected by increasing H/H_s from 0.8 to 1.

The vertical and horizontal motions at the crest of the dam are obviously related by the horizontal and vertical components of the vibration mode shapes. Vertical motion at the crest of the dam, while smaller than the horizontal motion, as expected, is not negligible for either horizontal or vertical ground motions.

Comparing the responses of the dam to horizontal and vertical ground motions (Figs. 8.2 and 8.3), it is apparent, consistent with common view, that without water the response to vertical ground motion is relatively small. However, with a full reservoir the response to vertical ground motion is almost as large as that due to horizontal ground motion when $\alpha < 1$ and it is even larger when $\alpha = 1$. The response to vertical ground motion is large because the hydrodynamic forces act in the horizontal direction on the vertical upstream face of the dam, causing significant lateral response of the dam. Hydrodynamic effects are seen to have especially large influence on the response to vertical ground motion.

The response of the dam alone without water ($H/H_s = 0$), when presented in the form of Figs. 8.2 and 8.3, is independent of the modulus of elasticity E_s of the concrete. Similarly, the response curves including hydrodynamic effects, do not vary with E_s if water compressibility is neglected [22]. However, results from analysis of cases 3, 4, and 5 (Table 8.1) presented in Figs. 8.4 and 8.5 demonstrate that the E_s value affects the response functions when compressibility of water is included. This effect is primarily on the fundamental resonant frequency and on the response in the neighborhood of this frequency. The fundamental resonant frequency of the dam decreases due to hydrodynamic effects to a greater degree for the larger values of E_s . Increase in E_s causes larger amplification of response but over a narrower frequency band. The resonant response to horizontal ground motion is affected little by variations in E_s but is influenced substantially for vertical ground motion. At higher excitation frequencies, the response functions for both components of ground motion are insensitive to E_s . With decreasing E_s the effects of water compressibility on response become smaller and the response approaches the incompressible case.

AD-A087 297

CALIFORNIA UNIV BERKELEY EARTHQUAKE ENGINEERING RES--ETC F/G 13/13
EARTHQUAKE RESPONSE OF CONCRETE GRAVITY DAMS INCLUDING HYDRODYN--ETC(U)
JAN 80 A K CHOPRA, P CHAKRABARTI, S GUPTA DACW73-71-C-0051

UNCLASSIFIED

UCB/EERC-80/01

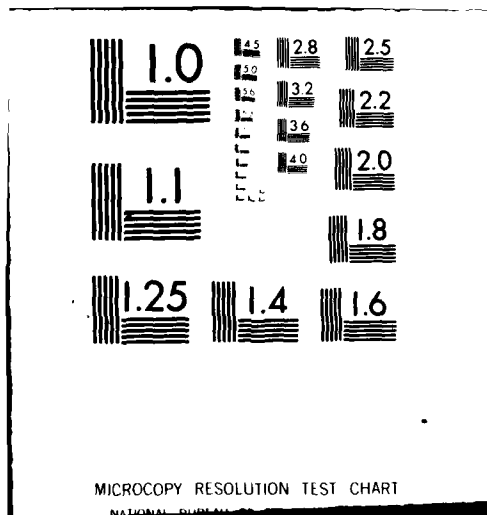
NL

2 of 3

Page 1

■

1



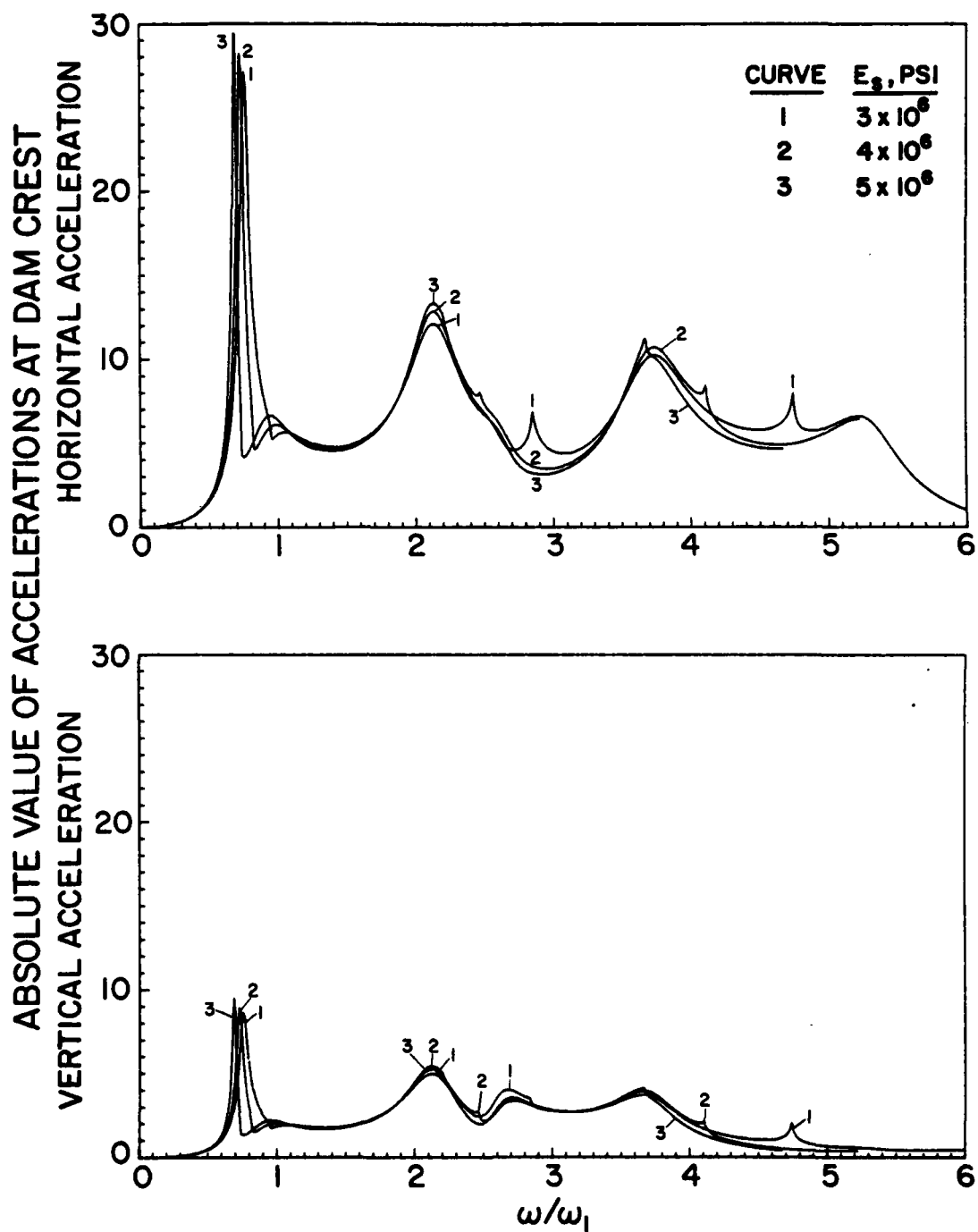


FIG. 8.4 INFLUENCE OF YOUNG'S MODULUS E_s OF DAM CONCRETE ON RESPONSE OF DAMS TO HARMONIC, HORIZONTAL GROUND MOTION. E_s IS VARIED AS SHOWN: CASES 3, 4, AND 5 OF TABLE 8.1

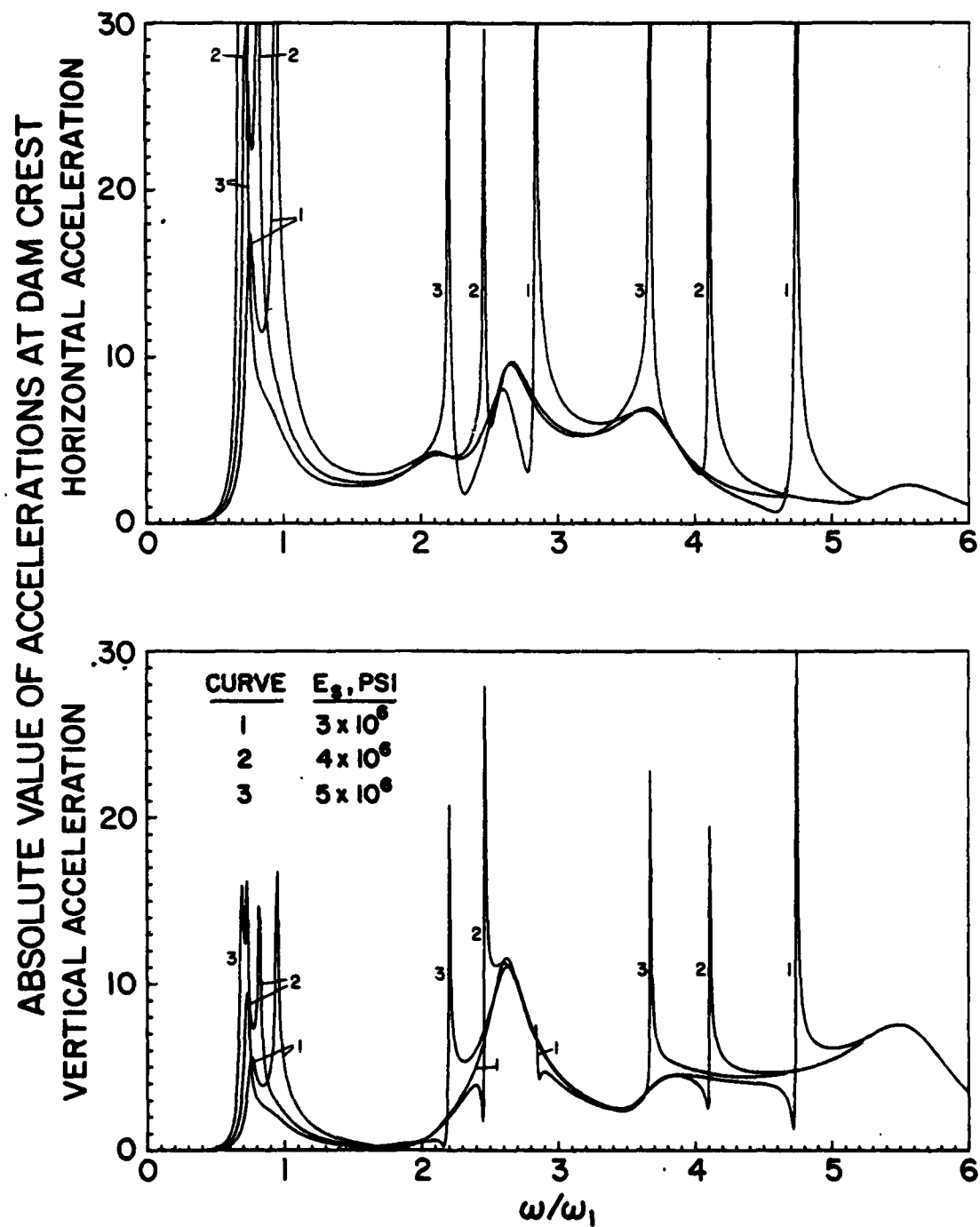


FIG. 8.5 INFLUENCE OF YOUNG'S MODULUS E_s OF DAM CONCRETE ON RESPONSE OF DAMS TO HARMONIC, VERTICAL GROUND MOTION. E_s IS VARIED AS SHOWN: CASES 3, 4 AND 5 OF TABLE 8.1

8.3.2 Dam-Foundation Interaction Effects

Complex frequency response functions for the dam, including effects of dam-foundation interaction, are presented in Figs. 8.6 and 8.7 for varying foundation stiffness (cases 1, 6, 8 and 11 in Table 8.1). When presented in this form, these functions do not depend separately on E_s and E_f but only on the ratio E_f/E_s . Results are presented for four values; $E_f/E_s = \infty, 4, 2$ and 1. The first represents rigid foundation material, thus reducing the system to dam on fixed base, and the smallest value represents the same elastic moduli for the foundation material and dam concrete.

Unlike water in the reservoir, the half plane does not have any resonant frequencies; the foundation impedances are smooth, slowly varying functions of the frequency [32]. As a result, structure-foundation interaction affects the response of the dam in a simpler manner than does structure-water interaction. As the E_f/E_s ratio decreases, which for a fixed E_s implies decrease of foundation modulus, the fundamental resonant frequency of the dam decreases; the response at the crest of the dam at this frequency decreases and the frequency band width at resonance increases, implying an increase in the apparent damping of the structure (Figs. 8.6 and 8.7). Accompanying this decrease in the resonant response at the crest of the dam is an increasing response at the base of the dam--which is, however a small fraction of the response at the crest -- with increasingly flexible soils (Figs. 8.6 and 8.7). Similar influences of decreasing the E_f/E_s ratio is observed at higher resonant frequencies, resulting in reduced response at the crest of the dam and increased response at the base over a wide range of excitation frequencies; however, the higher resonant frequencies are decreased to a lesser degree by structure-foundation interaction. The above mentioned effects of structure-foundation interaction are similar in response to horizontal and to vertical ground motions.

8.3.3 Dam-Water and Dam-Foundation Interaction Effects

In order to understand the effects of structure-water interaction and of structure-foundation interaction on the complex frequency response functions for the dam, the results of several cases in Table 8.1 are presented in different ways.

The results of analysis cases 8, 9, and 10 for horizontal and vertical

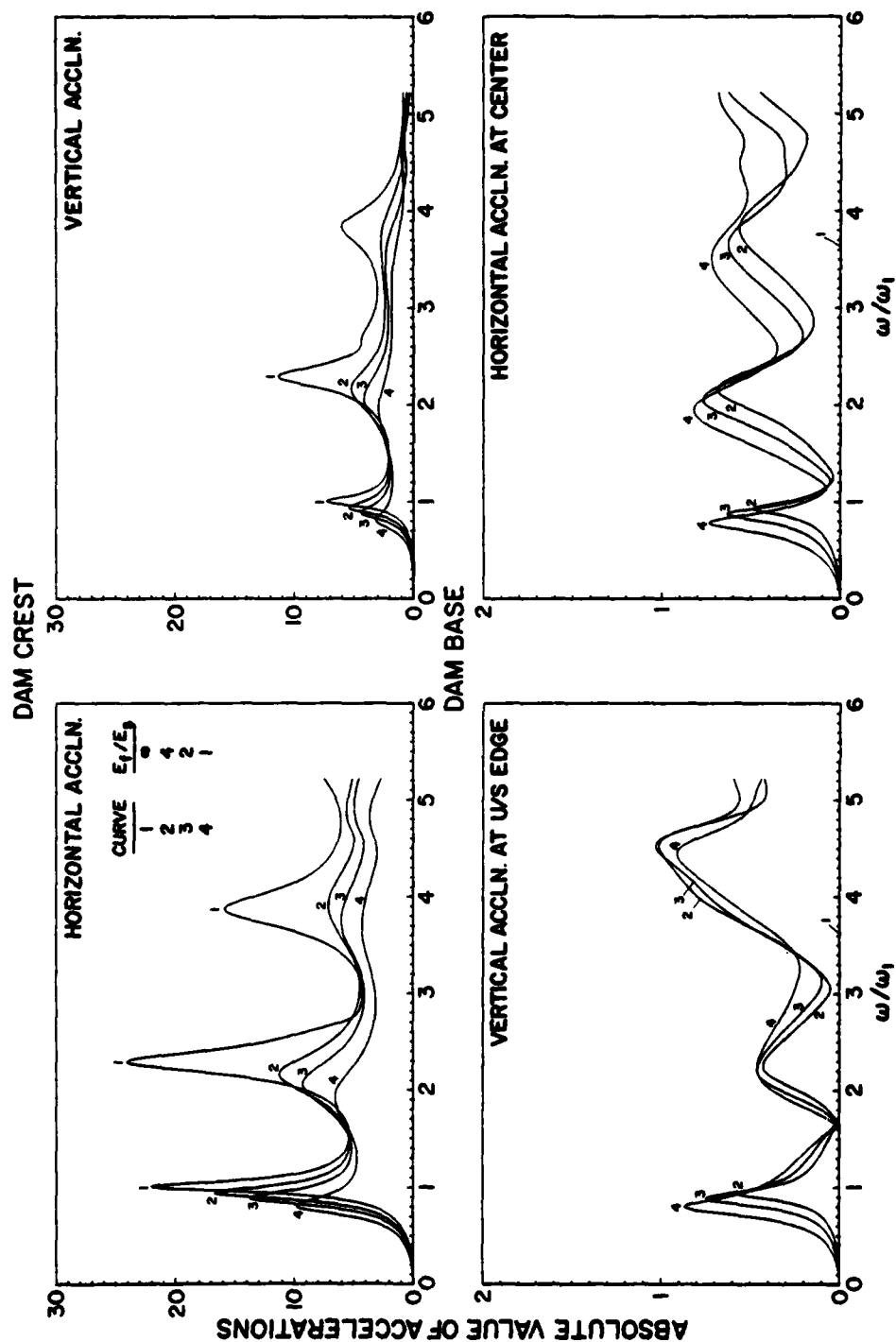


FIG. 8.6 INFLUENCE OF THE RATIO E_f/E_b ON RESPONSE OF DAMS, WITHOUT WATER BUT INCLUDING DAM-FOUNDATION INTERACTION, TO HARMONIC, HORIZONTAL GROUND ACCELERATION. CASES 1, 6, 8, AND 11 OF TABLE 8.1

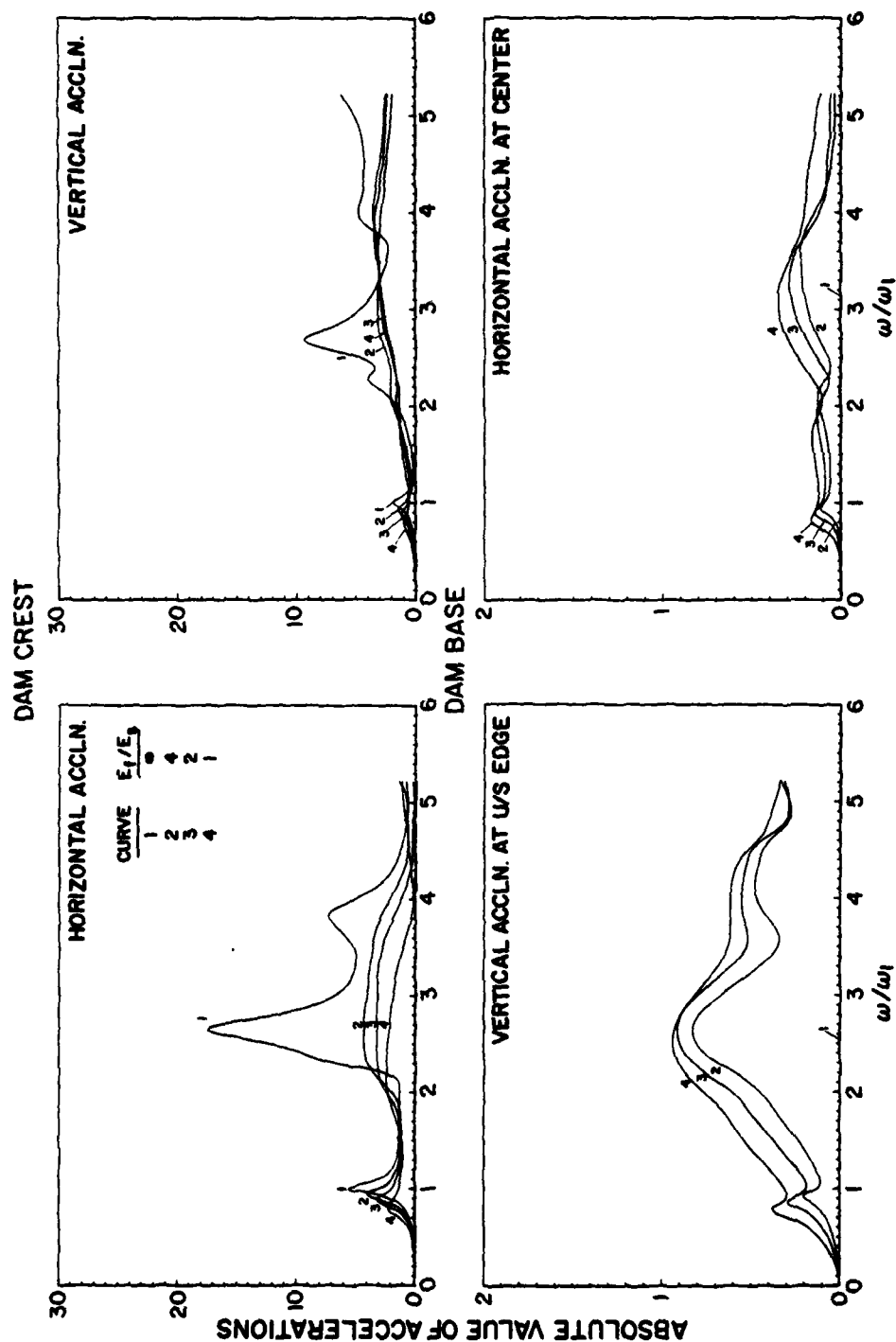


FIG. 8.7 INFLUENCE OF THE RATIO E_f/E_s ON RESPONSE OF DAMS, WITHOUT WATER BUT INCLUDING DAM-FOUNDATION INTERACTION, TO HARMONIC, VERTICAL GROUND MOTION. CASES 1, 6, 8, AND 11 OF TABLE 8.1

ground motion are presented in Figs. 8.8 and 8.9. These results, for a fixed $E_f/E_s = 2$, indicate the influence of varying depths of water in the reservoir. Whereas the response function for the dam without water ($H/H_s = 0$) is influenced by structure-foundation interaction effects, for the other two cases ($H/H_s = 0.8, 1$) dam-water interaction is also involved. Qualitatively, the effects of water on the response at the crest of the dam are generally similar whether the foundation material is rigid or flexible. However, some of the effects are relatively small. Whereas the fundamental resonant frequency is decreased by roughly the same degree as before, the apparent damping for the fundamental vibration mode is now dominated by effects of structure-foundation interaction and varies little with the depth of water. The effects of dam-water interaction on the response of a dam on flexible foundation are significant primarily at excitation frequencies in a neighborhood of the fundamental resonant frequency. At higher frequencies, dam-water interaction has little influence on the response of the dam on flexible foundation medium, except locally near the resonant frequencies of the reservoir. The principal effect of dam-water interaction on the response at the base of the dam permitted by flexible foundation medium is to decrease the fundamental resonant frequency and to increase the amplitude of response in the neighborhood of this resonant frequency. At higher frequencies the response at the base of the dam is not affected strongly by the water, except locally at the resonant frequencies of the water contained in the reservoir.

The conclusion presented in Sec. 8.3.1 is also confirmed by the results of Figs. 8.8 and 8.9. Without water the response of the dam to vertical ground motion is a small fraction of the response to horizontal ground motion, but with water the two responses at the fundamental resonant frequency are similar; at some higher frequencies the response to vertical ground motion exceeds that due to horizontal ground motion. Because of the hydrodynamic effects, the vertical ground motion is especially significant in the response of concrete gravity dams to earthquakes.

Complex frequency response functions for the dam with the reservoir full of water and varying modulus for foundation rock (cases 3, 7, 10, and 12 in Table 8.1) are presented in Figs. 8.10 and 8.11 for horizontal and vertical ground motion, respectively. Results are presented for a fixed value of $E_s = 4 \times 10^6$ psi and four values of $E_f/E_s = \infty, 4, 2$, and 1. By

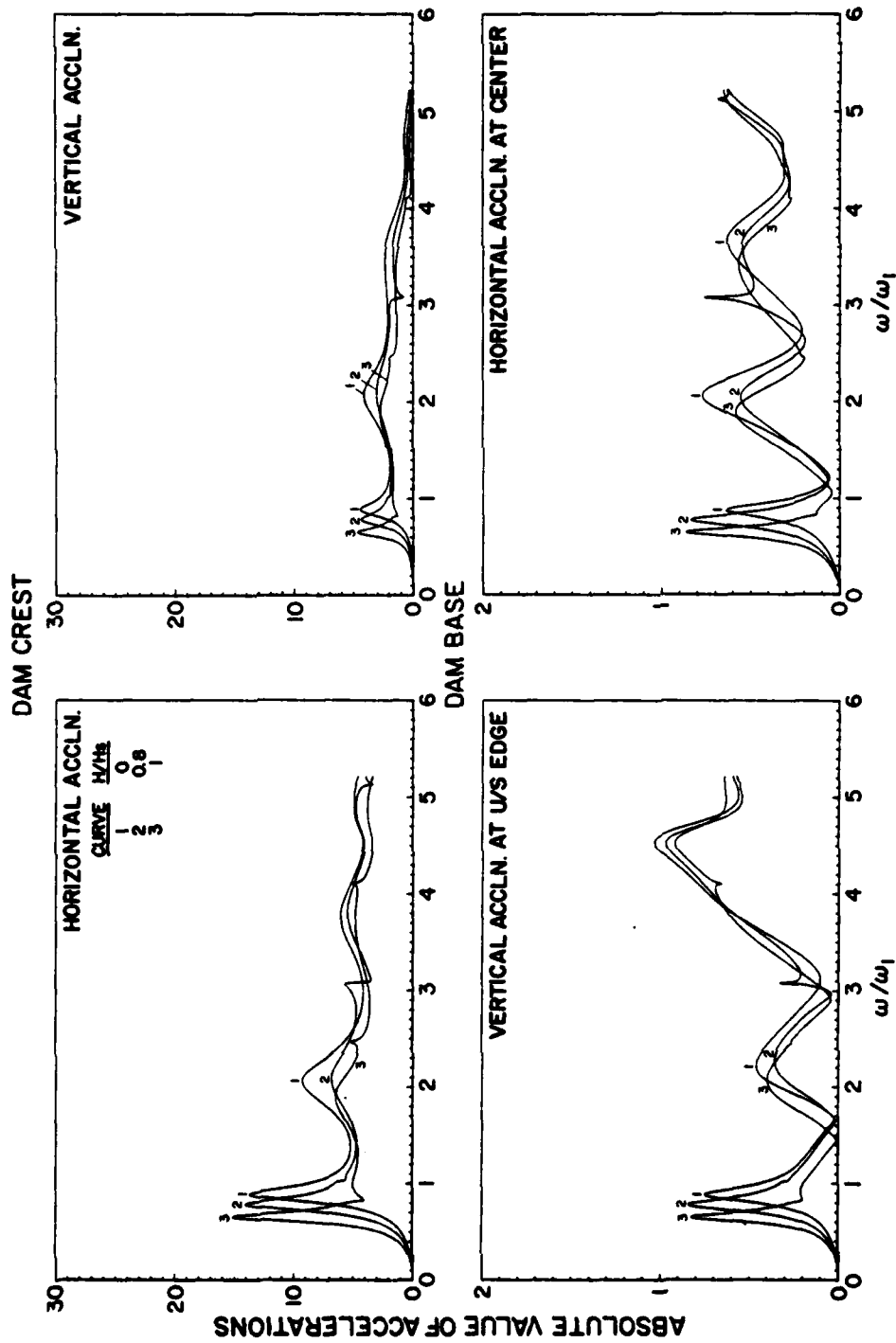


FIG. 8.8 INFLUENCE OF WATER DEPTH ON THE RESPONSE OF DAMS, INCLUDING DAM-FOUNDATION INTERACTION, TO HARMONIC, HORIZONTAL GROUND MOTION. CASES 8, 9, AND 10 OF TABLE 8.1

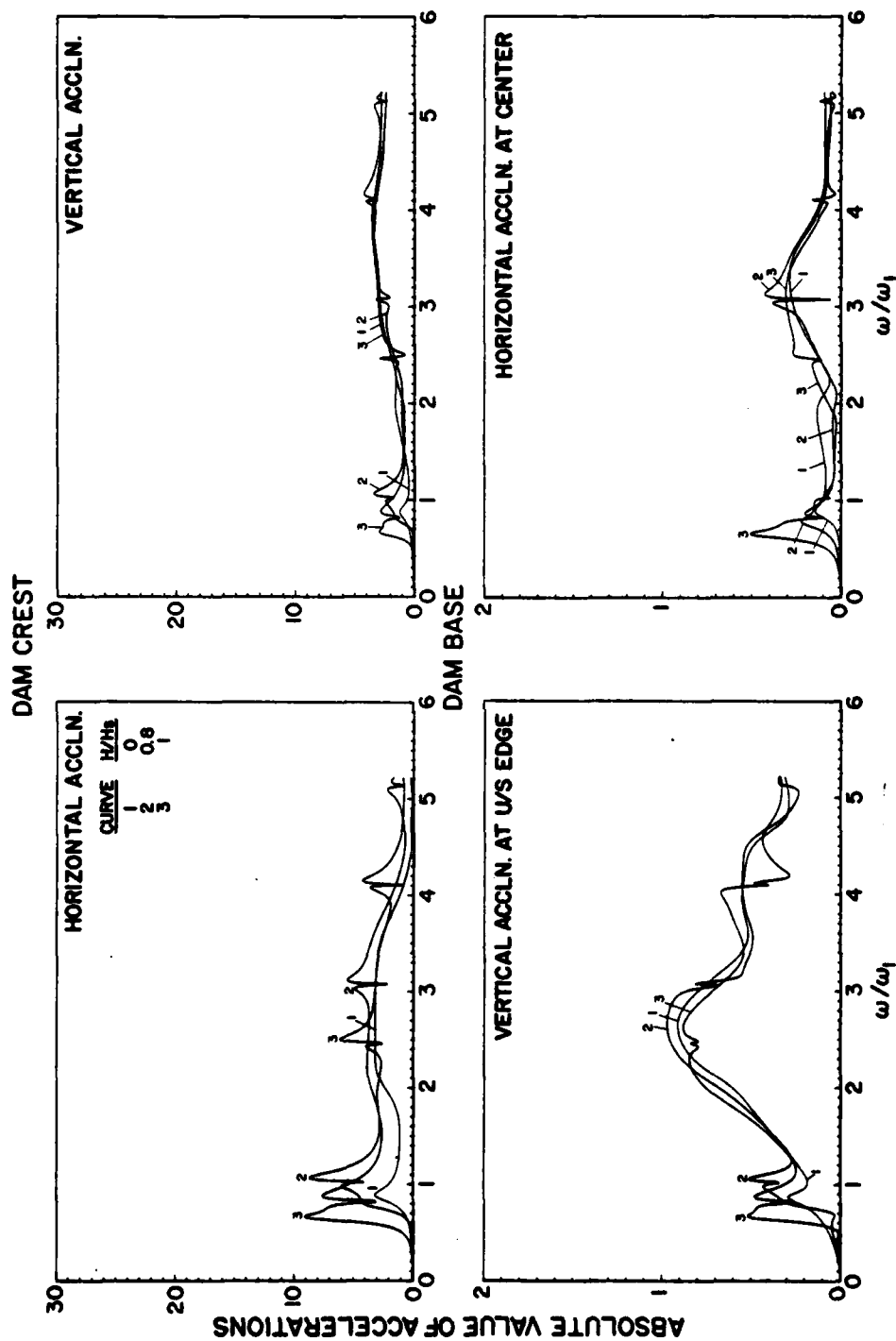


FIG. 8.9 INFLUENCE OF WATER DEPTH ON THE RESPONSE OF DAMS, INCLUDING DAM-FOUNDATION INTERACTION, TO HARMONIC, VERTICAL GROUND MOTION. CASES 8, 9, AND 10 OF TABLE 8.1

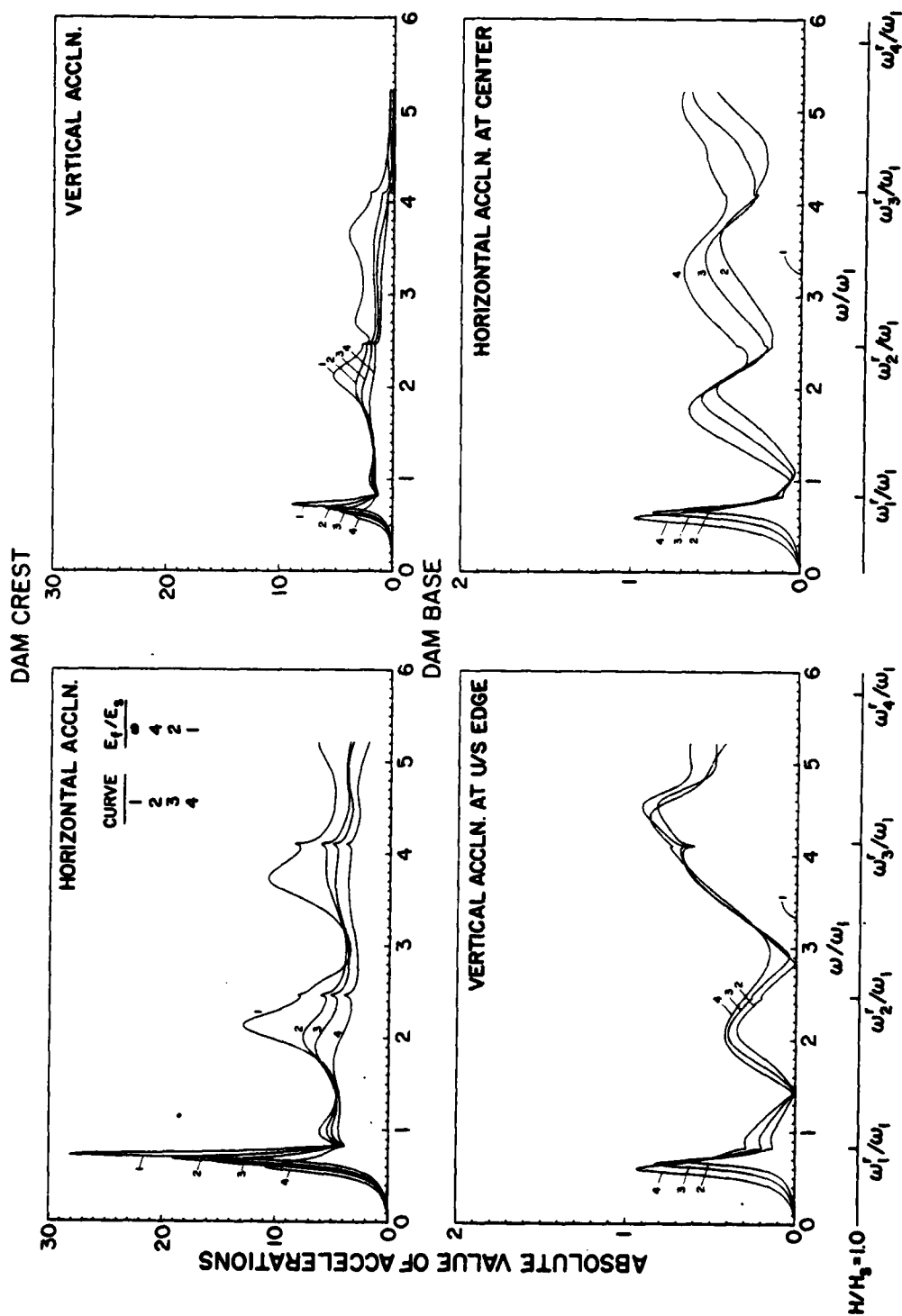


FIG. 8.10 INFLUENCE OF E_f/E_s RATIO ON RESPONSE OF DAMS WITH FULL RESERVOIR TO HARMONIC, HORIZONTAL GROUND MOTION. CASES 3, 7, 10, AND 12 OF TABLE 8.1

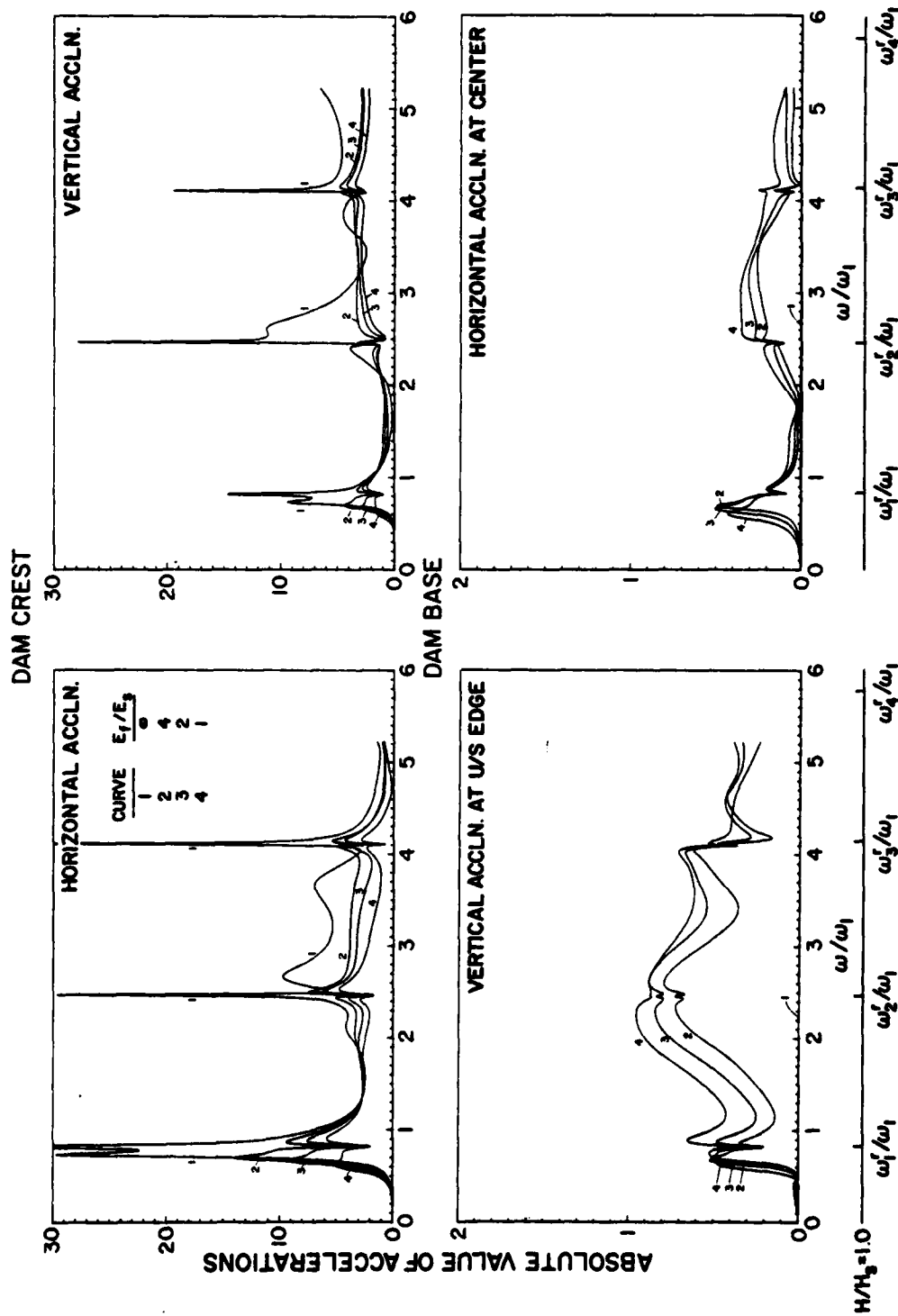


FIG. 8.11 INFLUENCE OF E_f/E_s RATIO ON RESPONSE OF DAMS WITH FULL RESERVOIR TO HARMONIC VERTICAL GROUND MOTION. CASES 3, 7, 10, AND 12 OF TABLE 8.1

comparing the results with those presented in Figs. 8.6 and 8.7, it is apparent that the effects of dam-foundation interaction are generally similar, independent of the effects of dam-water interaction.

As the E_f/E_s ratio decreases, which for a fixed E_s implies an increasingly flexible foundation, the fundamental resonant frequency decreases. The response at the crest of the dam at this frequency decreases and the frequency bandwidth at resonance increases, implying an increase in the apparent damping of the structure. The response behavior near the fundamental resonant frequency is complicated, especially for vertical ground motion, because of the double resonant peak created by hydrodynamic effects. The response at the base of the dam, although only a small fraction of the response at the crest of the dam, is also affected by E_f/E_s . In the case of horizontal ground motion, the base accelerations at and near the fundamental resonant frequency increase with decreasing E_f/E_s , but there is no clear trend in the case of vertical ground motion. Similar influence of increasingly flexible soils is observed at higher resonant frequencies, resulting in reduced response at the crest of the dam and increased response at the base over a wide range of excitation frequencies. Structure-foundation interaction has little influence on the higher resonant frequencies and tends to suppress the response at the dam crest at these frequencies.

At excitation frequencies $\omega = \omega_n^r$, the resonant frequencies of the water in the reservoir, the response at the crest of the dam is controlled by dam-water interaction and is essentially independent of the properties of the foundation rock (Figs. 8.10 and 8.11).

In order to compare the effects of structure-water interaction and structure-foundation interaction on the complex frequency response functions for the dam, results from analyses of four systems are presented together: dam on rigid foundation with no water, dam on rigid foundation with full reservoir, dam on flexible foundation with no water, dam on flexible foundation with full reservoir. The results for the first two systems (cases 1 and 3 in Table 8.1) along with those for the latter two systems for $E_f/E_s = 4$ (cases 6 and 7), $E_f/E_s = 2$ (cases 8 and 10), and $E_f/E_s = 1$ (cases 11 and 12) are presented in Figs. 8.12 to 8.14 for horizontal ground motion and Figs. 8.15 to 8.17 for vertical ground motion.

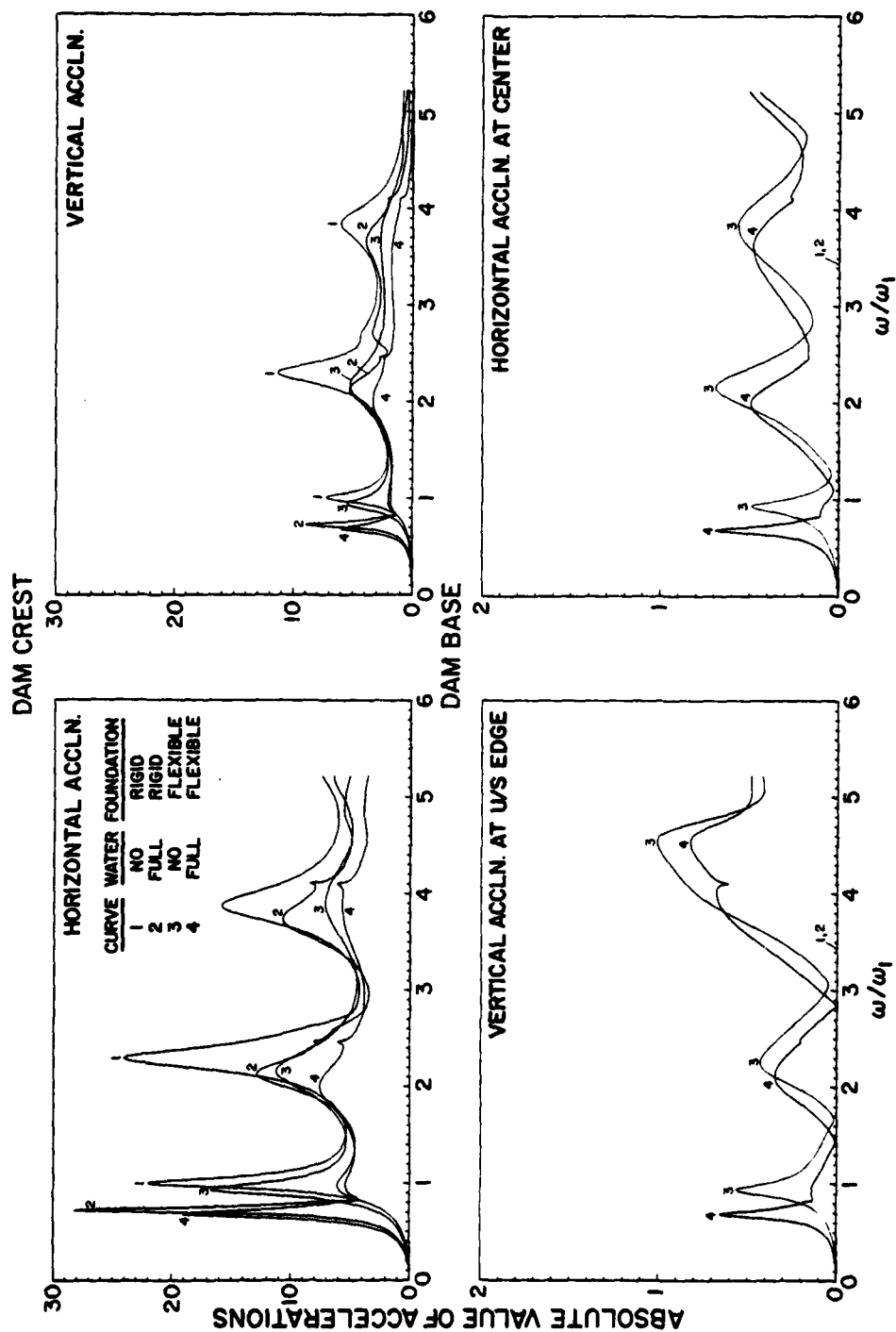


FIG. 8.12 RESPONSES OF DAMS TO HARMONIC, HORIZONTAL GROUND MOTION FOR FOUR CONDITIONS:
 DAM WITH NO WATER ON RIGID FOUNDATION (CASE 1); DAM WITH FULL RESERVOIR ON
 RIGID FOUNDATION (CASE 3); DAM WITH NO WATER ON FLEXIBLE FOUNDATION ($E_f/E_g = 4$)
 (CASE 6); AND DAM WITH FULL RESERVOIR ON FLEXIBLE FOUNDATION (CASE 7)

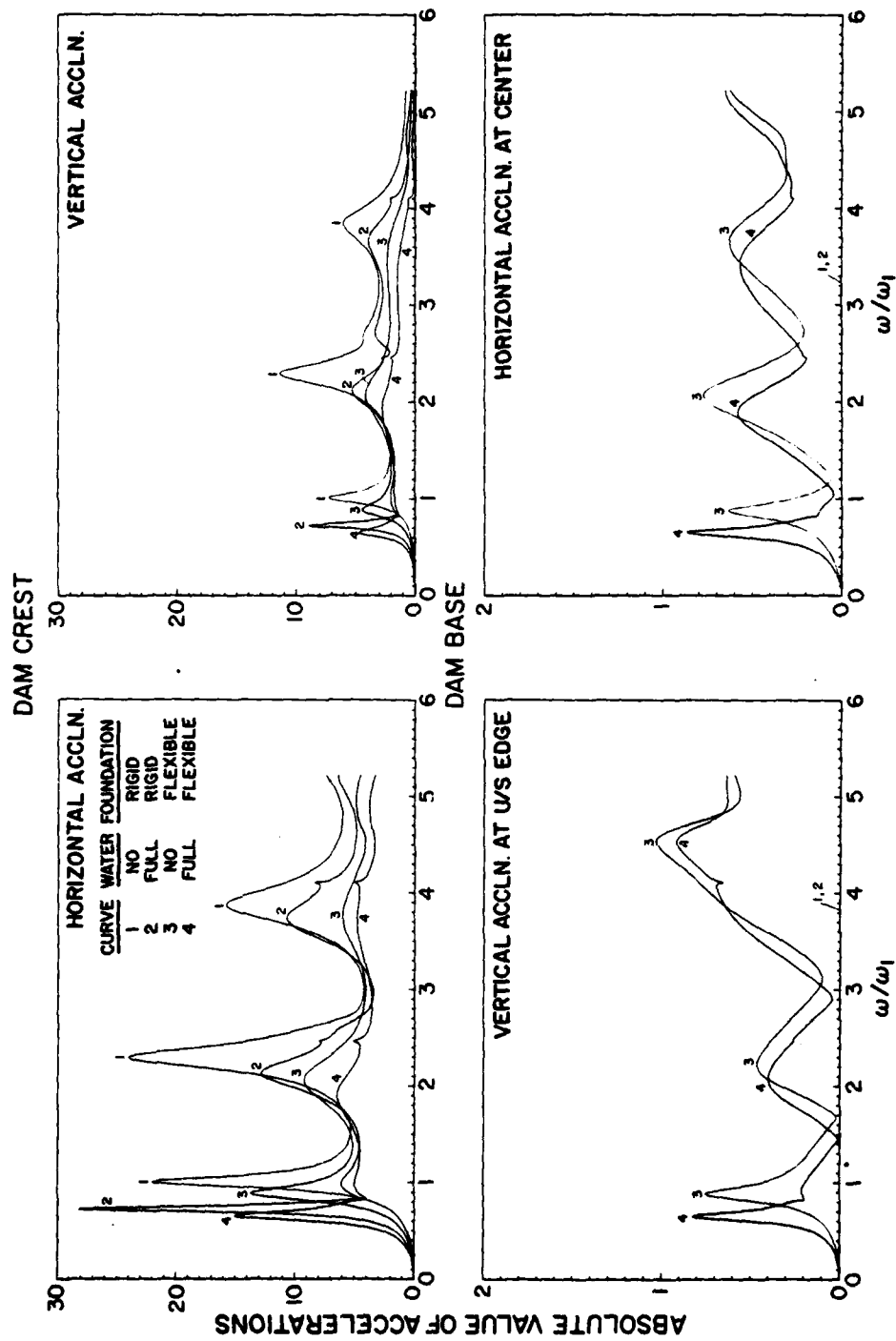


FIG. 8.13 RESPONSE OF DAMS TO HARMONIC, HORIZONTAL GROUND MOTION FOR FOUR CONDITIONS:
 DAM WITH NO WATER ON RIGID FOUNDATION (CASE 1); DAM WITH FULL RESERVOIR ON
 RIGID FOUNDATION (CASE 3); DAM WITH NO WATER ON FLEXIBLE FOUNDATION ($E_f/E_s = 2$)
 (CASE 8); AND DAM WITH FULL RESERVOIR ON FLEXIBLE FOUNDATION (CASE 10)

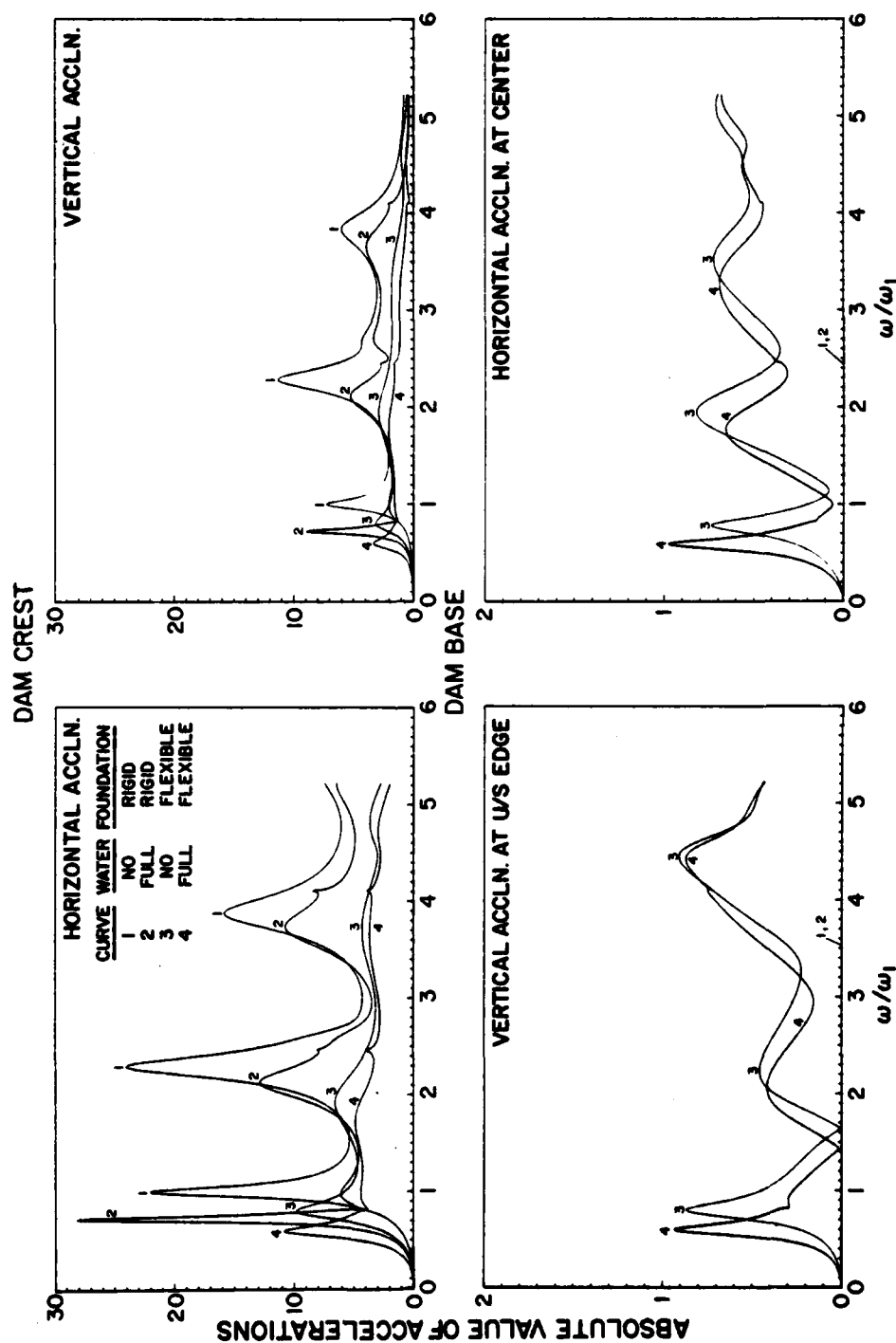


FIG. 8.14 RESPONSE OF DAMS TO HARMONIC, HORIZONTAL GROUND MOTION FOR FOUR CONDITIONS:
 DAM WITH NO WATER ON RIGID FOUNDATION (CASE 1); DAM WITH FULL RESERVOIR ON
 RIGID FOUNDATION (CASE 3); DAM WITH NO WATER ON FLEXIBLE FOUNDATION ($E_f/E_s = 1$)
 (CASE 11); AND DAM WITH FULL RESERVOIR ON FLEXIBLE FOUNDATION (CASE 12)

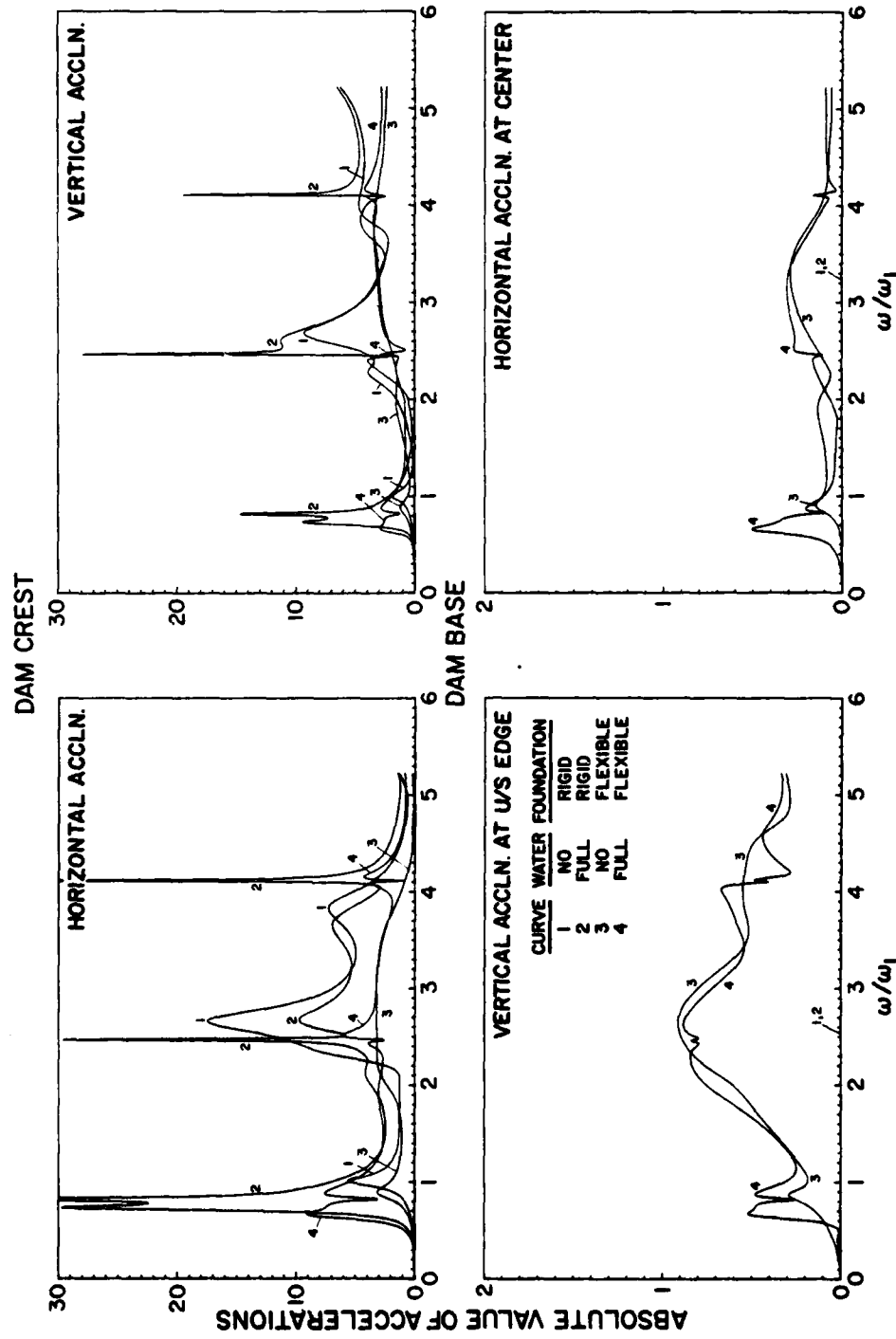


FIG. 8.16 RESPONSE OF DAMS TO HARMONIC, VERTICAL GROUND MOTION FOR FOUR CONDITIONS:
 DAM WITH NO WATER ON RIGID FOUNDATION (CASE 1); DAM WITH FULL RESERVOIR ON
 RIGID FOUNDATION (CASE 3); DAM WITH NO WATER ON FLEXIBLE FOUNDATION ($E_f/E_s = 2$)
 (CASE 8); AND DAM WITH FULL RESERVOIR ON FLEXIBLE FOUNDATION (CASE 10)

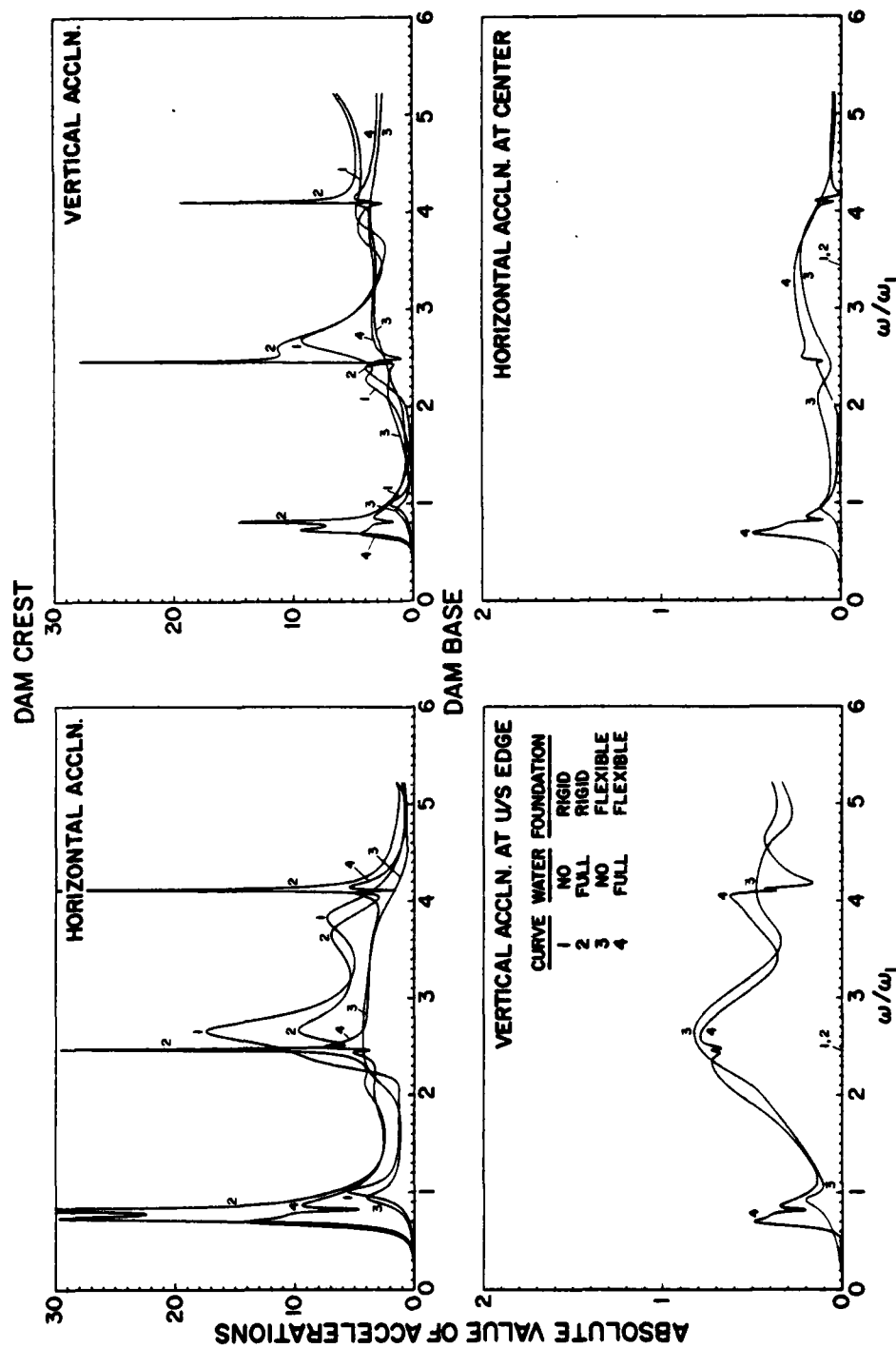


FIG. 8.15 RESPONSES OF DAMS TO HARMONIC, VERTICAL GROUND MOTION FOR FOUR CONDITIONS: DAM WITH NO WATER ON RIGID FOUNDATION (CASE 1); DAM WITH FULL RESERVOIR ON RIGID FOUNDATION (CASE 3); DAM WITH NO WATER ON FLEXIBLE FOUNDATION ($E_f/E_s = 4$) (CASE 6); AND DAM WITH FULL RESERVOIR ON FLEXIBLE FOUNDATION (CASE 7)

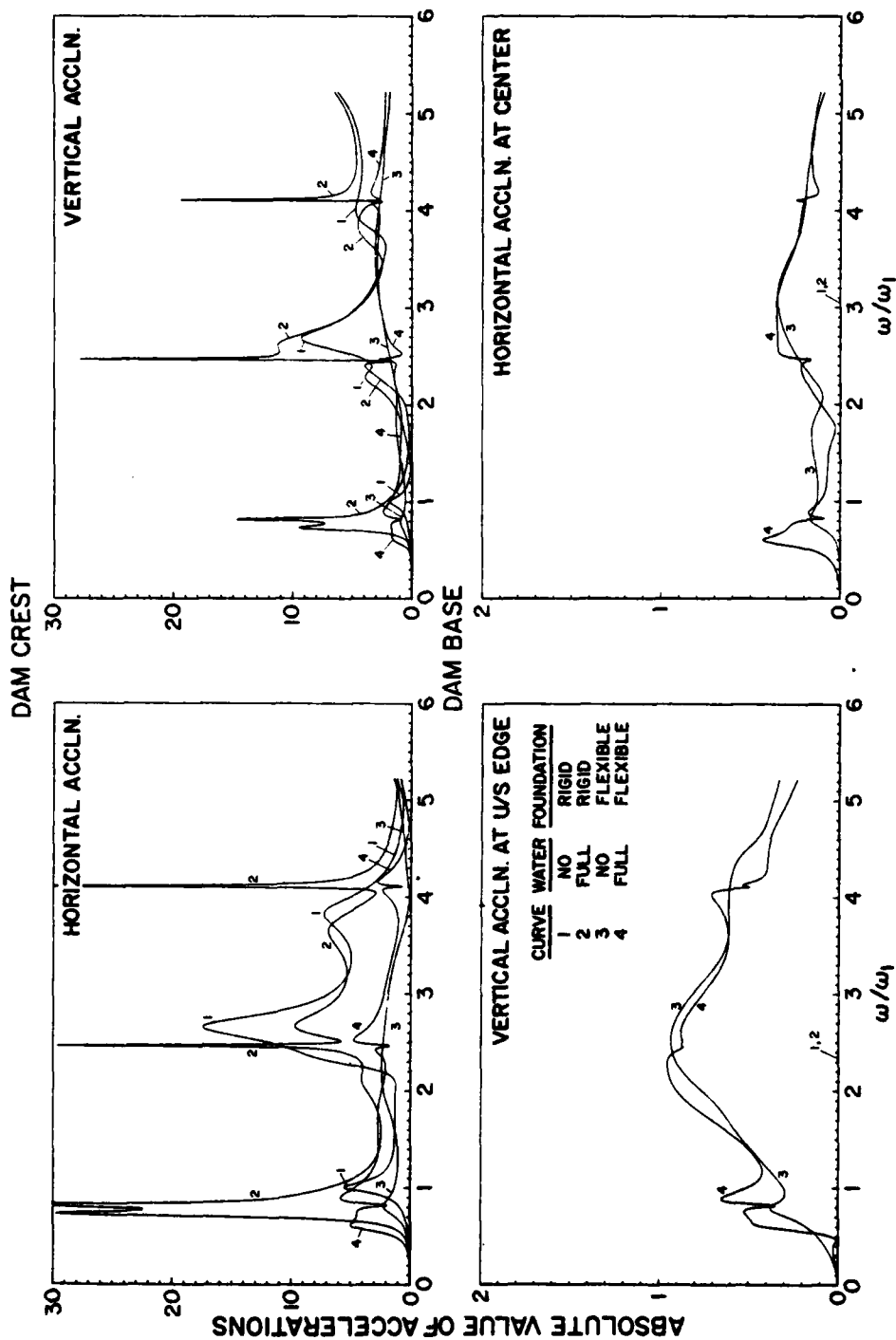


FIG. 8.17 RESPONSE OF DAMS TO HARMONIC, VERTICAL GROUND MOTION FOR FOUR CONDITIONS:
 DAM WITH NO WATER ON RIGID FOUNDATION (CASE 1); DAM WITH FULL RESERVOIR ON
 RIGID FOUNDATION (CASE 3); DAM WITH NO WATER ON FLEXIBLE FOUNDATION ($E_f/E_s = 1$)
 (CASE 11); AND DAM WITH FULL RESERVOIR ON FLEXIBLE FOUNDATION (CASE 12)

The fundamental resonant frequency of the dam decreases because of dam-water interaction and dam-foundation interaction, with the influence of the water being larger. For the most flexible foundations considered ($E_f = E_s$), the decrease in the fundamental frequency due to dam-foundation interaction is about the same as that due to dam-water interaction. This trend may or may not exist for higher resonant frequencies.

As mentioned earlier, the response at the crest of the dam is increased at the fundamental resonant frequency, but, in many cases, decreased at higher resonant frequencies because of dam-water interaction. These effects of dam-water interaction are similar whether the foundation is rigid or flexible for all values of E_f/E_s considered.

As mentioned earlier, the response at the crest of the dam is reduced and motions at the base of the dam, relative to the free-field motion, are possible due to flexibility of the soil. These effects of dam-foundation interaction are similar whether the reservoir is empty or full. The above mentioned effects of dam-foundation interaction tend to increase as E_f/E_s decreases, i.e., for a fixed E_s , as the foundation rock becomes increasingly flexible.

Comparing the effects of dam-water interaction and dam-foundation interaction on the resonant responses at the crest of the dam to horizontal ground motion (Figs. 8.12 to 8.14), it is apparent that the effects of the stiff rock ($E_f/E_s = 4$) are similar to those of the water, but for softer rocks ($E_f/E_s = 2$ and 1) the effects of dam-foundation interaction are relatively more significant. Whereas the amplitude of the response at the crest of the dam at the fundamental resonant frequency is increased by dam-water interaction but reduced due to dam-foundation interaction, both sources of interaction contribute towards a decrease in the response at higher resonant frequencies.

Because, as mentioned earlier, dam-water interaction influences the dam response to vertical ground motion to a much greater degree than it influences the response to horizontal ground motion, the relative effect of dam-water interaction and dam-foundation interaction on dam response to vertical ground motion (Figs. 8.15 to 8.17) is different than the above observations from responses to horizontal ground motion (Figs. 8.12 to 8.14). At the fundamental resonant frequency, the response of the dam is affected by dam-water interaction to a greater degree than it is affected by dam-foundation interaction. However, at higher resonant frequencies, the influence of dam-foundation interaction is greater. Whereas the amplitude of the response at the crest of the dam

at the fundamental resonant frequency is increased by dam-water interaction but reduced due to dam-foundation interaction, both sources of interaction contribute towards a decrease in the response at higher resonant frequencies, but with one exception: Vertical acceleration response at the crest of the dam is increased by dam-water interaction even at the second resonant frequency.

The effects of water on the response at the base of the dam, permitted by a flexible foundation, are closely tied to the corresponding effects on the responses at the crest of the dam. Dam-water interaction has the effect of decreasing the resonant frequencies for the base response and modifying the response amplitudes. These effects are relatively large in the responses to vertical ground motion.

9. EARTHQUAKE RESPONSE OF PINE FLAT DAM

9.1 Scope of the Chapter

Chapter 8 presented the effects of dam water interaction and of dam-foundation interaction, separately or together, on the complex frequency response functions of idealized gravity dams with triangular cross-section. This chapter presents the responses of Pine Flat Dam to a selected earthquake ground motion, analyzed using the procedures of Chapter 6 under various assumptions. The objective of this chapter is to identify the effects of dam-water interaction and dam-foundation interaction on the response of the dam.

9.2 Pine Flat Dam, Ground Motion, Cases Analyzed and Response Results

9.2.1 Pine Flat Dam

Located on the King's River near Fresno, California, Pine Flat Dam consists of thirty-six 50 ft and one 40 ft wide monoliths. The crest length is 1840 ft and the height of the tallest monolith is 400 ft. The dam is shown in Fig. 9.1 and its downstream elevation is shown in Fig. 9.2.

The tallest, non-overflow monolith of the dam with water at El. 951.00 is selected for purposes of this study. The two-dimensional finite element idealization for this monolith in plane stress is shown in Fig. 9.3, consisting of 136 quadrilateral elements with 162 nodal points. The nine nodal points at the base of the dam are equally spaced, as required for developing the dynamic stiffness matrix for the foundation [32]. This finite element system has 306 degrees of freedom analysis of the dam on rigid base. In analyses considering the foundation flexibility and the resulting motion at the dam-foundation interface, the system has 324 degrees of freedom. The mass concrete in the dam is assumed to be a homogeneous, isotropic, elastic solid with the following properties: Young's modulus of elasticity = 3.25 million psi, unit weight = 155 pcf, and Poisson's ratio = 0.2. The selected elastic modulus, determined by forced vibration tests on the dam [28], is different from that used in earlier analyses [22]. The damping factors associated with the modes of vibration of the dam, determined from the above mentioned forced vibration tests, were in the range of 2 to 3.5 percent of critical damping. A constant hysteretic damping coefficient of 0.1,

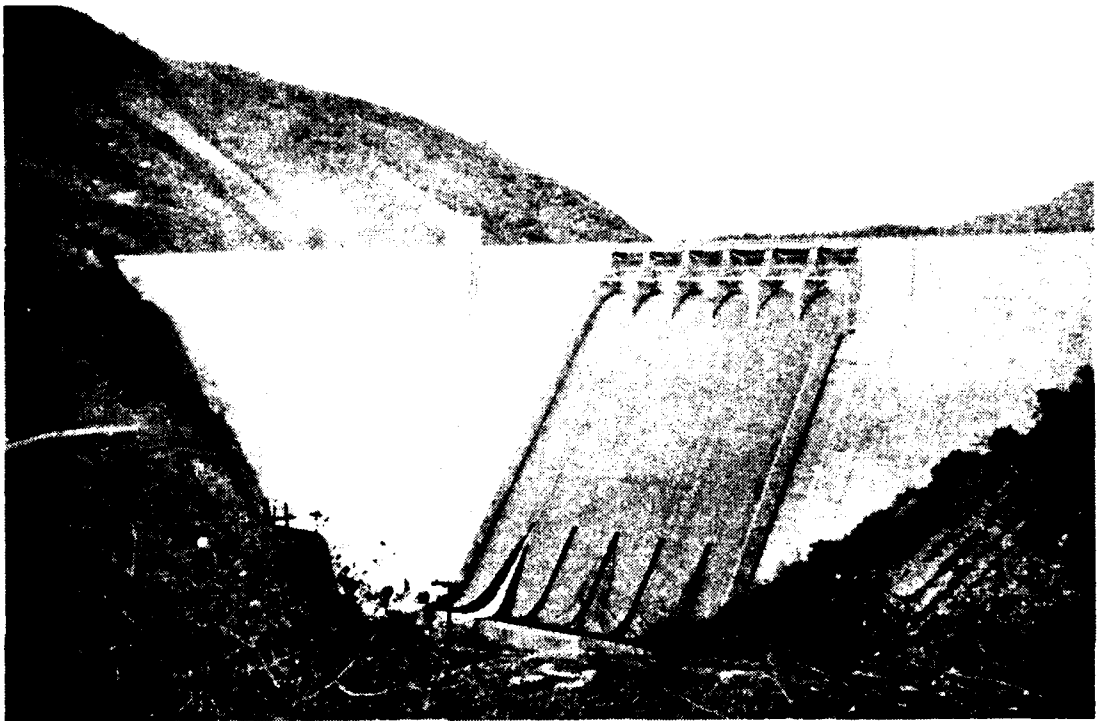


FIG. 9.1 PINE FLAT DAM

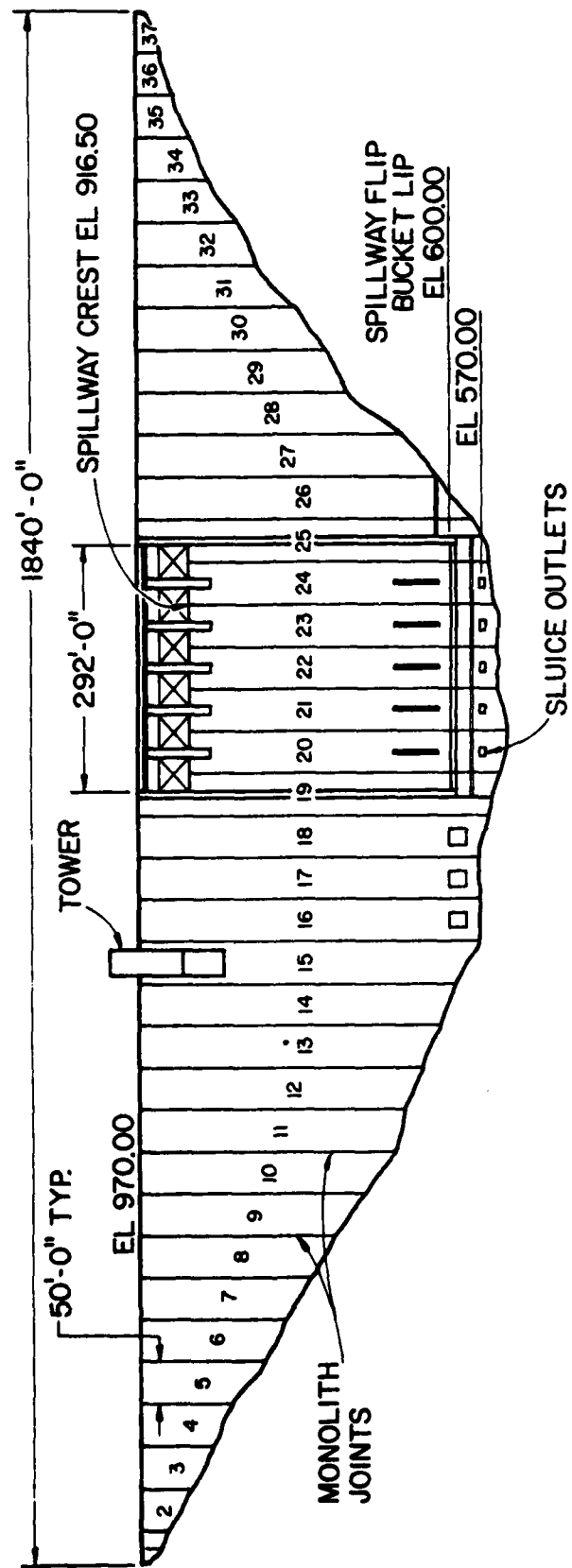


FIG. 9.2 PINE FLAT DAM - DOWNSTREAM ELEVATION

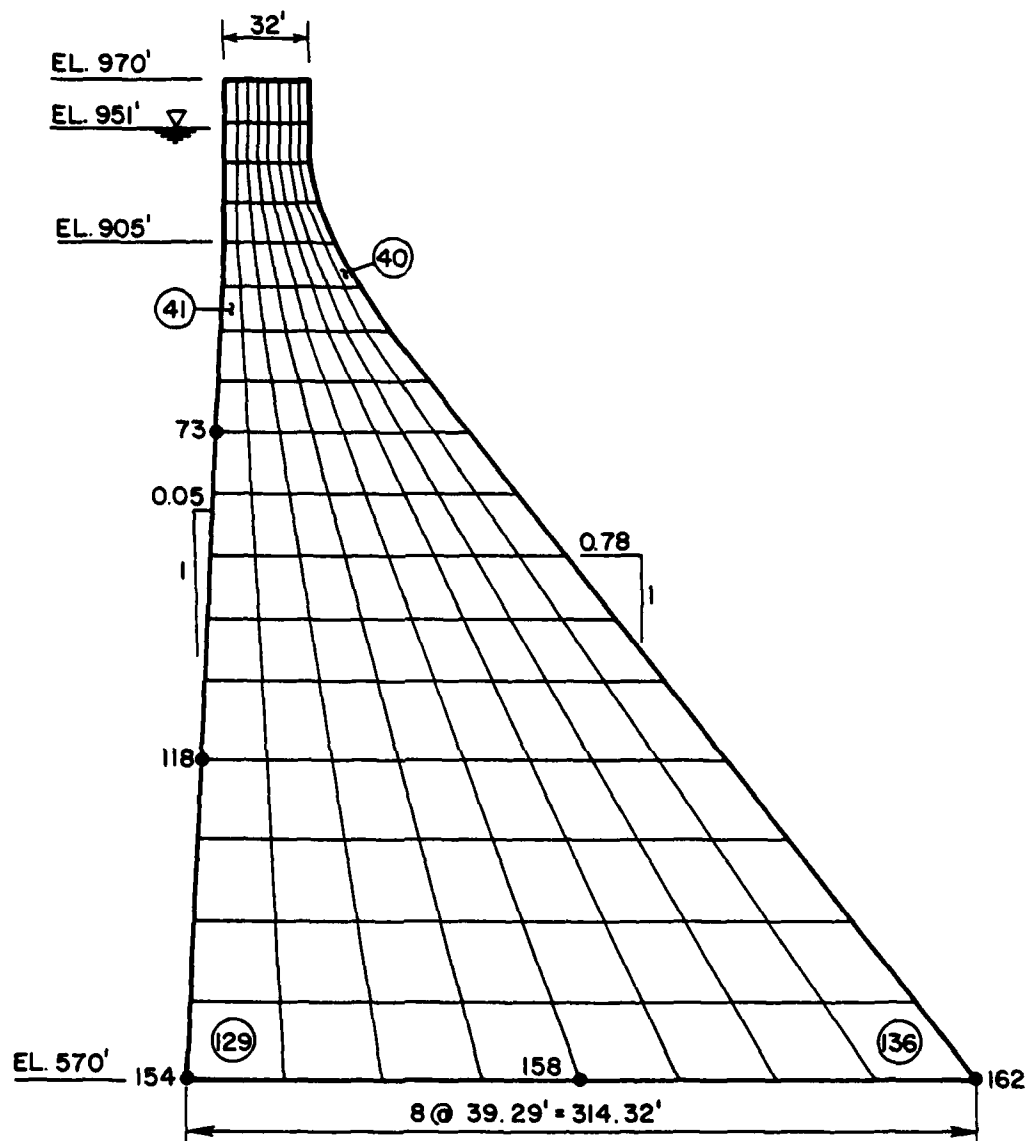


FIG. 9.3 FINITE ELEMENT IDEALIZATION OF TALLEST, NON-OVERFLOW MONOLITH OF PINE FLAT DAM

which corresponds to a 5 percent damping factor in all modes of vibration of the dam, has been selected. This is considered appropriate for the much larger motions and stress levels expected during strong earthquake ground shaking.

The foundation rock is idealized as a homogenous, isotropic, visco-elastic half plane (in plane stress) of constant hysteretic solid with the following properties: Young's modulus of elasticity = 10 million psi, a value which is appropriate for the granites and basalts at the site; Poisson's ratio = $1/3$, unit weight = 165 pcf, and damping coefficient for constant hysteretic solid = 0.05. The P-wave velocity for this rock = 10,266 ft/sec.

The following properties are assumed for water: unit weight = 62.5 pcf, wave velocity = 4720 ft/sec. For these properties of water and rock, the wave reflection coefficient at the bottom of the reservoir is $\alpha = 0.817$.

9.2.2 Ground Motion

The ground motion recorded at the Taft Lincoln School Tunnel during the Kern County, California, earthquake of July 21, 1952, is selected as the excitation for analyses of Pine Flat Dam. The ground motion acting transverse to the axis of the dam and in the vertical direction is defined by the S69E and vertical components of the recorded motion, respectively. These two components of the recorded ground motion and the maximum values of acceleration are shown in Fig. 9.4.

9.2.3 Cases Analyzed

Using the computer program described in Appendix A based on the analysis procedure presented in Chapter 6, responses of the tallest monolith of Pine Flat Dam to the selected ground motion are analyzed. The dam monolith and the foundation are assumed to be in plane stress.

Responses of the dam to the S69E component of the Taft ground motion only and to the S69E and vertical components acting simultaneously are analyzed. For each of these excitations the response of the dam is separately analyzed four times, corresponding to the following four sets of assumptions for the foundation and hydrodynamic effects.

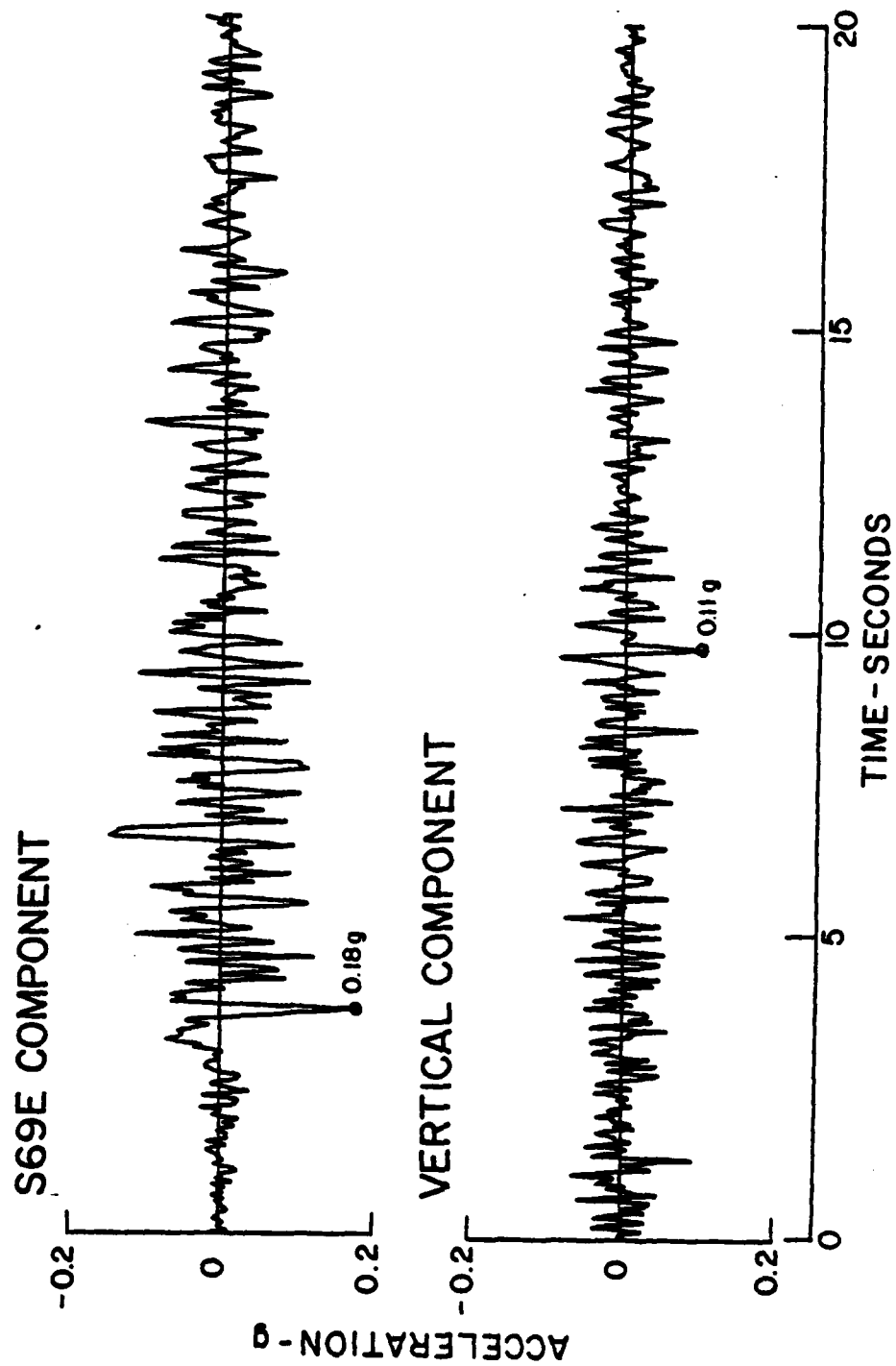


FIG. 9.4 GROUND MOTION AT TAFT LINCOLN SCHOOL TUNNEL; KERN COUNTY, CALIFORNIA, EARTHQUAKE, JULY 21, 1952

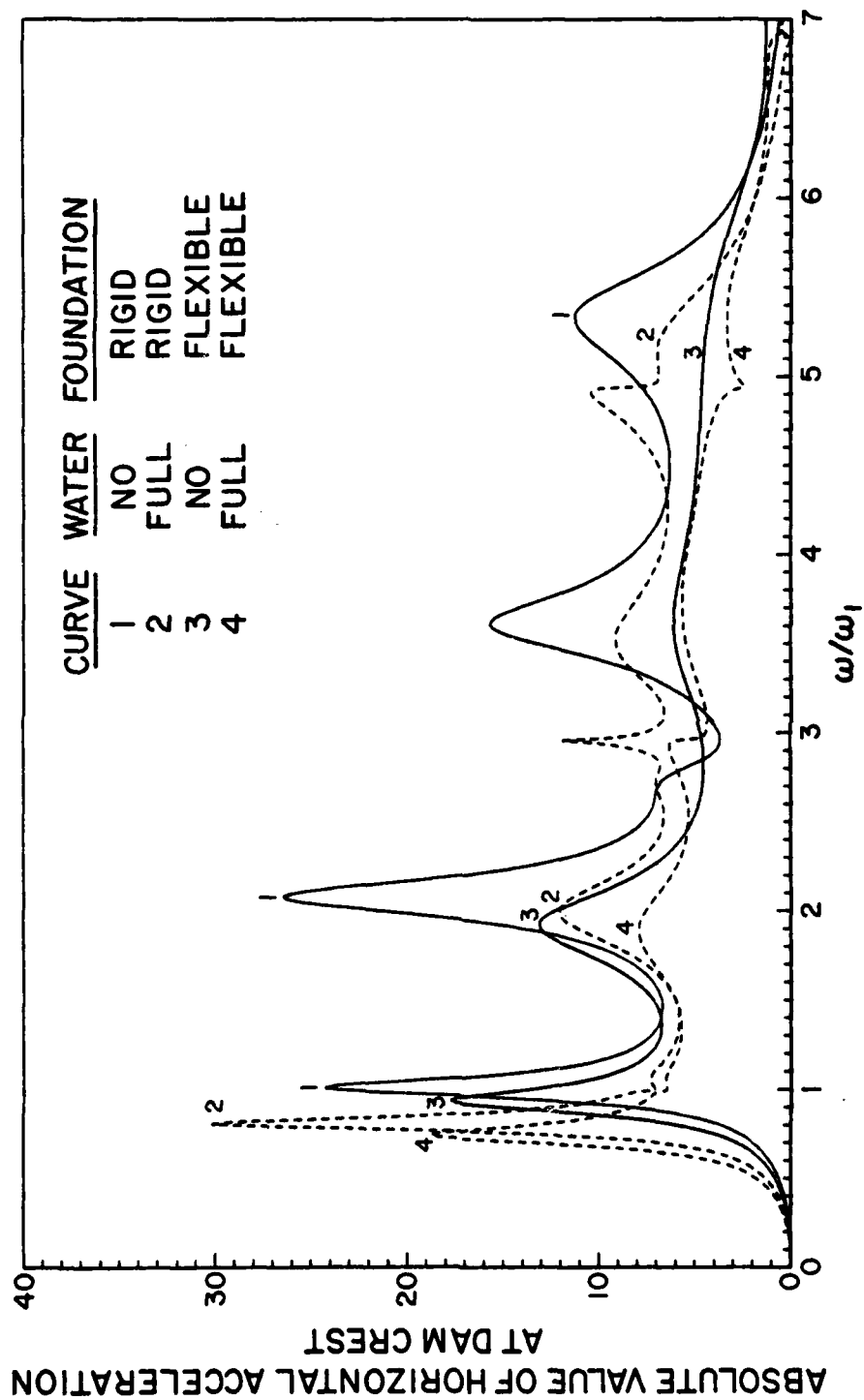


FIG. 9.5 RESPONSES OF PINE FLAT DAM TO HARMONIC, HORIZONTAL GROUND MOTION
COMPUTED FOR FOUR CONDITIONS: DAM WITH NO WATER ON RIGID FOUNDATION,
DAM WITH FULL RESERVOIR ON RIGID FOUNDATION, DAM WITH NO WATER ON
FLEXIBLE FOUNDATION, AND DAM WITH FULL RESERVOIR ON FLEXIBLE FOUNDATION

Case	Foundation	Hydrodynamic Effects
1	Rigid	Excluded
2	Rigid	Included
3	Flexible	Excluded
4	Flexible	Included

In order to consider hydrodynamic effects realistically, compressibility of water is included. The displacements and stresses due to the weight of the dam and to hydrostatic pressures are included in all analyses. As mentioned in Chapter 6, the rigid body displacements of the dam due to a deformable foundation have been excluded.

All the vibration modes or generalized coordinates, as appropriate, necessary to obtain accurate results for complex frequency response up to excitation frequencies of approximately 20 cps were included in the analysis. The first five natural modes of vibration of the dam were included in the analyses assuming a rigid base. The first ten generalized coordinates, were included in analyses considering dam-foundation interaction effects (see Sec. 6.2.6).

9.2.4 Response Results

The complex frequency response functions for the horizontal acceleration at the crest of Pine Flat Dam, with horizontal ground motion as the excitation, for the four sets of assumptions for foundation and hydrodynamic effects (Sec. 9.2.3) are presented in Fig. 9.5. From these results, the fundamental resonant period of vibration and the effective damping, determined by the half-power band width method, are as follows:

Case	Foundation	Hydrodynamic Effects	Fundamental Resonance	
			Vibration Period sec.	Damping Factor %
1	Rigid	Excluded	0.317	5.0
2	Rigid	Included	0.397	3.2
3	Flexible	Excluded	0.341	6.7
4	Flexible	Included	0.429	5.2

These vibration periods are identified on the response spectrum of the S69E component of the Taft ground motion (Fig. 9.6). The spectrum ordinates at these vibration periods corresponding to damping ratio of 5 percent can be observed in the same figure.

The response of Pine Flat Dam was determined for each of the two excitations listed in Sec. 9.2.2 and the four sets of assumptions in Sec. 9.2.3. In each case, the computer results of dynamic analysis represent the total response, including the effects of the weight of the dam and hydrostatic pressures. These results consisted of the complete time-history of the horizontal and vertical components of displacement of all the nodal points and of three components of stress in all the finite elements. For each of the cases analyzed only a small part of the total result is presented. The maximum crest displacement and maximum tensile stresses in three critical parts of the monolith are summarized in Table 9.1. Presented in Figs. 9.7 to 9.17 are the time-history of displacements at nodal points 1, 73, and 118, located at different levels on the upstream face, and at nodal points 154, 158, and 162 at the base when foundation flexibility is considered; and the distribution of envelope values of maximum principal stress (maximum tensile stress or minimum compressive stress) during the earthquake.

9.3 Dam-Water Interaction Effects

Without hydrodynamic effects, the response of the dam is typical of a multi-degree-of-freedom system with mass, stiffness, and damping properties independent of excitation frequency. Dam-water interaction introduces frequency dependent terms in the equations of motion, resulting in complicated response curves, especially in the neighborhood of the resonant frequencies for the impounded water (Fig. 9.5). A decrease in the fundamental resonant frequency of the dam is apparent from a comparison of the responses with and without hydrodynamic effects.

When the excitation is the S69E component of Taft ground motion, the inclusion of hydrodynamic effects increases the maximum displacement at the crest of the dam from 1.38" to 1.83" (Fig. 9.7). The maximum tensile stresses in the dam are increased at the upstream face from 153 to 223 psi, from 208 to 254 psi at the downstream face, and from 257 to 366 psi at the heel (Fig. 9.8). The area enclosed by a particular stress contour increases due to hydrodynamic effects, indicating that stresses exceed the value

TABLE 9.1 SUMMARY OF RESPONSES OF PINE FLAT DAM TO TAFT GROUND MOTION

Case	System Properties		Excitation	Max. Horizontal Crest Displ., in.	Max. Tensile Stresses, psi		
	Foundation	Hydrodynamic Effects			Upstream Face	Downstream Face	Heel
1	Rigid	Excluded	S69E Component,	1.38	153	208	257
2	Rigid	Included	Taft Ground	1.83	223	254	366
3	Flexible	Excluded	Motion, 1952	1.46	143	158	150
4	Flexible	Included		2.55	297	355	428
5	Rigid	Excluded	S69E and	1.46	177	225	276
6	Rigid	Included	Vertical	1.72	238	233	329
7	Flexible	Excluded	Components, Taft Ground	1.57	166	183	170
8	Flexible	Included	Motion, 1952	2.42	274	347	406

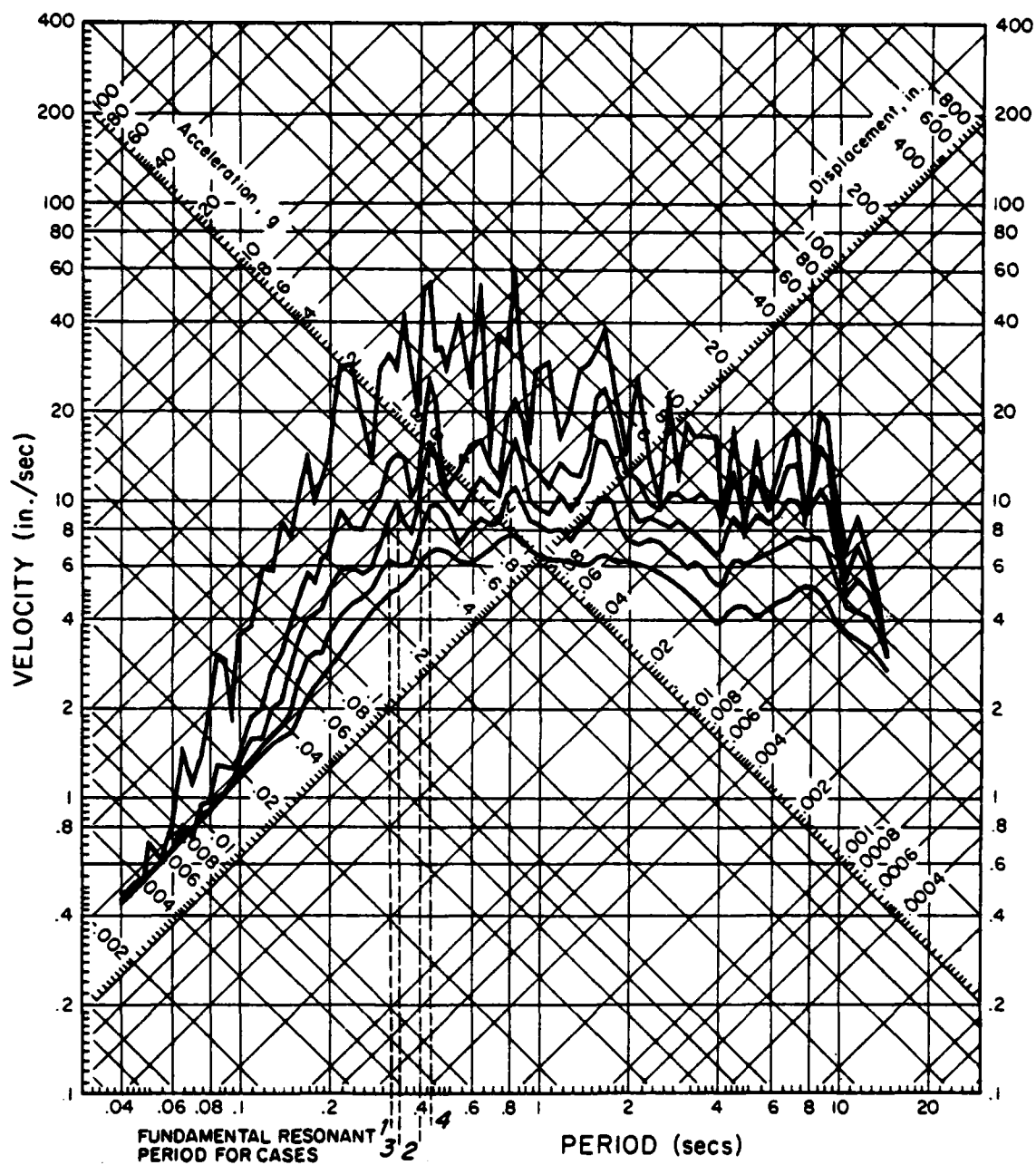


FIG. 9.6 RESPONSE SPECTRUM FOR THE S69E COMPONENT OF TAFT GROUND MOTION. THE FUNDAMENTAL VIBRATION PERIOD OF PINE FLAT DAM COMPUTED FOR THE FOUR SETS OF ASSUMPTIONS (SEC. 9.2.4) FOR FOUNDATION AND HYDRODYNAMIC EFFECTS ARE AS NOTED

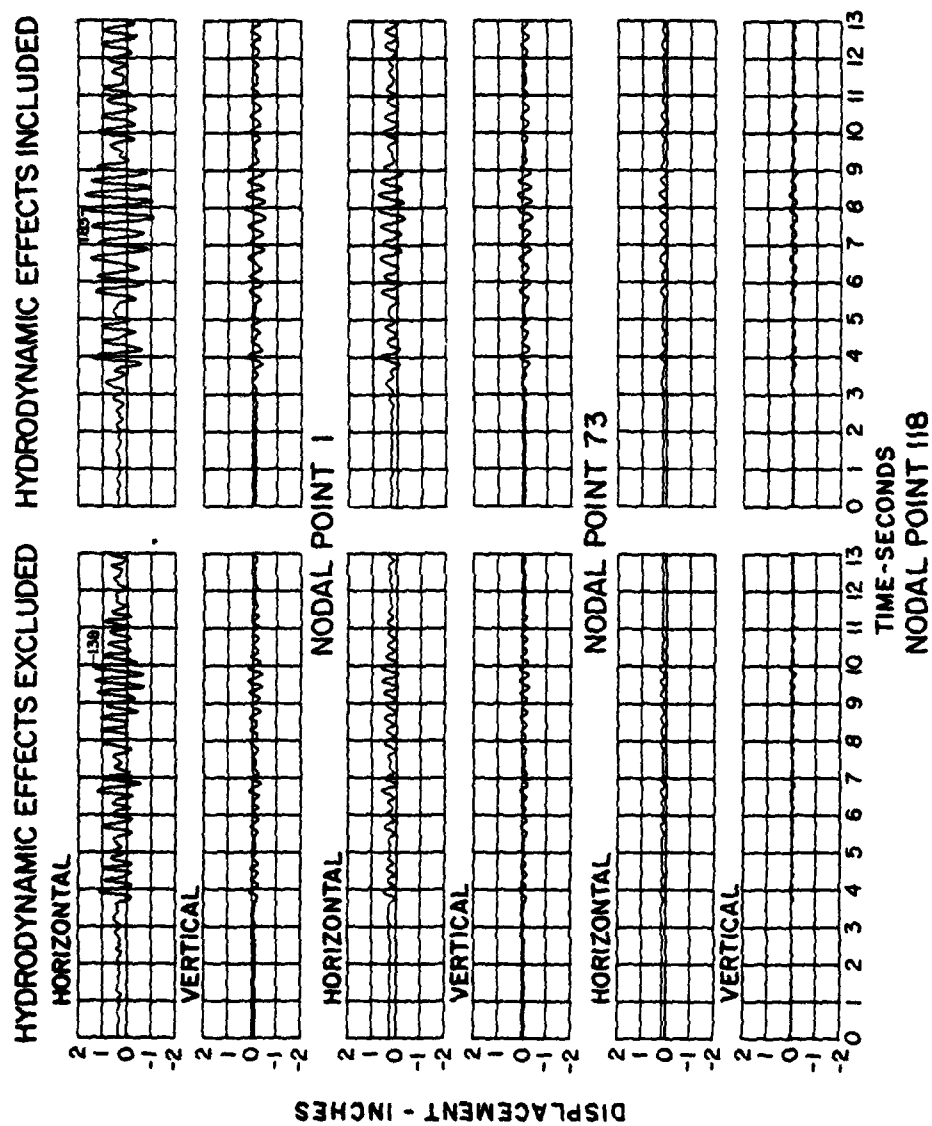


FIG. 9.7 DISPLACEMENT RESPONSE OF PINE FLAT DAM ON RIGID FOUNDATION TO S69E COMPONENT OF TAFT GROUND MOTION: (A) HYDRODYNAMIC EFFECTS EXCLUDED, AND (B) HYDRODYNAMIC EFFECTS INCLUDED

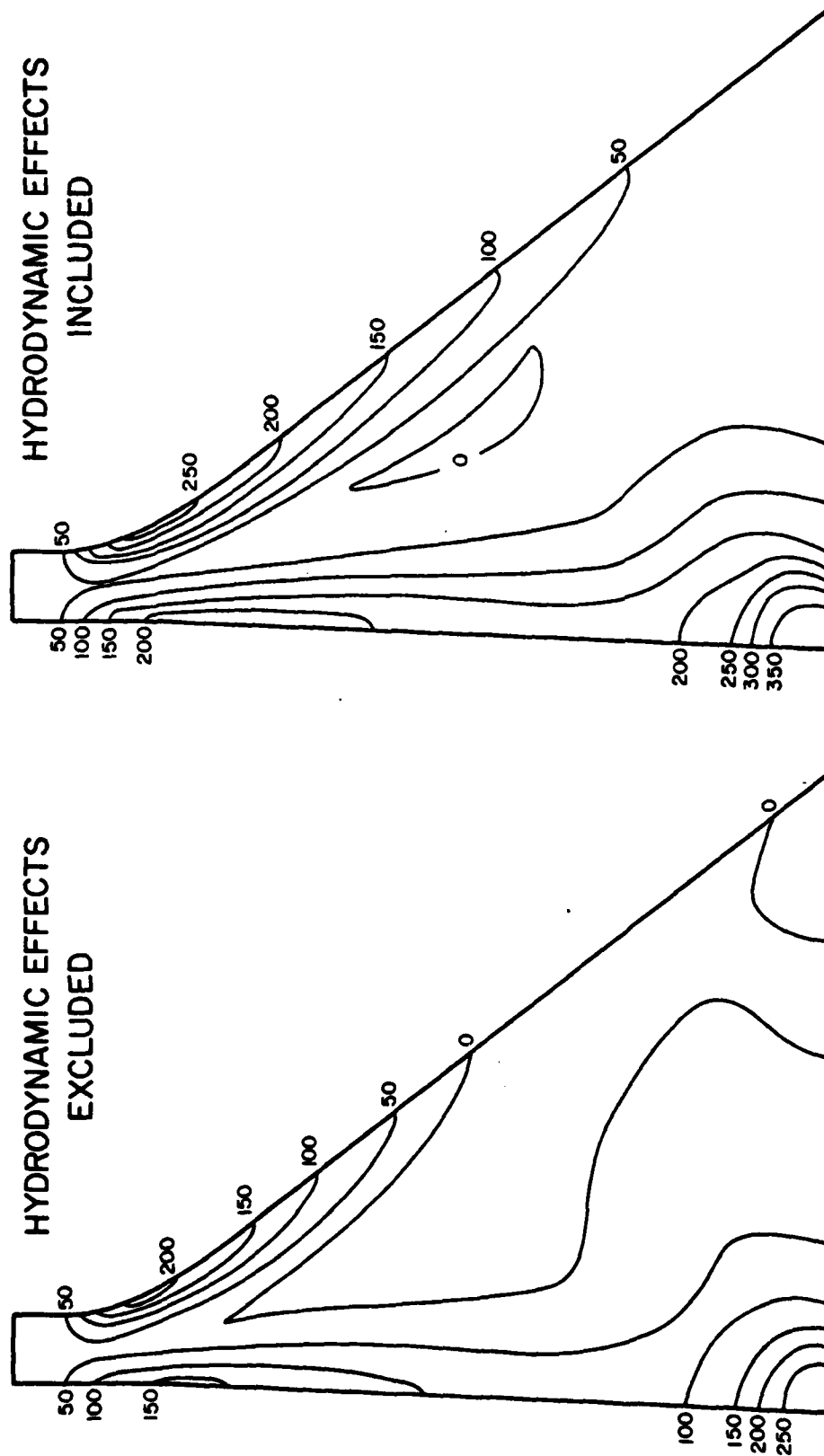


FIG. 9.8 ENVELOPE VALUES OF MAXIMUM PRINCIPAL (MAXIMUM TENSILE OR MINIMUM COMPRESSIVE) STRESSES IN PINE FLAT DAM ON RIGID FOUNDATION DUE TO S69E COMPONENT OF TAF T GROUND MOTION: (A) HYDRODYNAMIC EFFECTS EXCLUDED, AND (B) HYDRODYNAMIC EFFECTS INCLUDED.

corresponding to that stress contour over a larger portion of the monolith.

Consistent with the observations in Sec. 8.3.1, when hydrodynamic effects are excluded, the response of the dam is only slightly increased by the contribution of the vertical component of ground motion (compare Figs. 9.7-9.8 with 9.9-9.10). But, contrary to the observations in Sec. 8.3.1 and earlier results for Pine Flat Dam (18), the displacements and stresses in the dam with hydrodynamic effects included are slightly decreased by the contributions of the vertical component of ground motion (compare Figs. 9.7-9.8 with 9.9-9.10).

Earlier results (18) for the response of Pine Flat Dam subjected to the same Taft ground motion but assuming a different value of Young's modulus, demonstrated that the vertical component of ground motion causes considerable increase in the response of the dam. The vertical ground motion causes lateral hydrodynamic forces resulting in significant lateral displacements and associated stresses. Because the principal change in the system properties and ground motion from the earlier results to those presented here is in the value of assumed Young's modulus for the dam (the other change is the damping model discussed in Sec. 7.5.1); it is surprising that the results presented here are not consistent with the earlier conclusions. In order to resolve what appears to be an anomaly, the earthquake stresses (excluding initial static stresses) due to horizontal and vertical ground motions, separately, and including hydrodynamic effects, for selected finite elements (Nos. 40, 41, 129 in Fig. 9.3), are presented in Fig. 9.11. Although considerable stresses are caused by vertical ground motion, they partially cancel the stresses due to horizontal ground motion, resulting in reduced response when both ground motion components are considered simultaneously. The contribution of the vertical component of ground motion to the total response of a dam, including hydrodynamic effects, therefore depends on the relative phasing of the responses to horizontal and vertical ground motion, which in turn, depends on the phasing of the ground motion components and the vibration properties of the dam.

9.4 Dam-Foundation Interaction Effects

The foundation impedances for a half plane are smooth, slowly varying functions of the excitation frequency. However, the hydrodynamic terms are

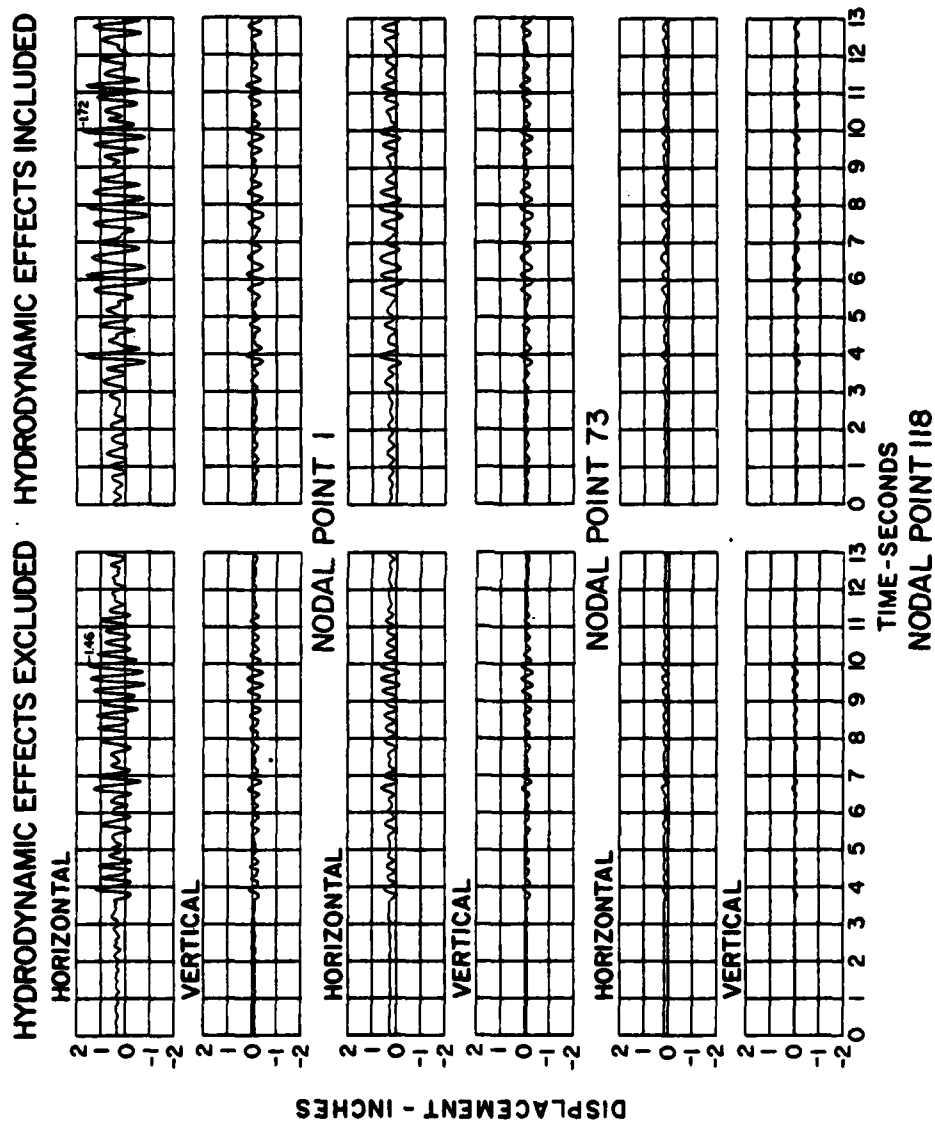


FIG. 9.9 DISPLACEMENT RESPONSE OF PINE FLAT DAM ON RIGID FOUNDATION TO S69E AND VERTICAL COMPONENTS, SIMULTANEOUSLY, OF TAFT GROUND MOTION: (A) HYDRODYNAMIC EFFECTS EXCLUDED, AND (B) HYDRODYNAMIC EFFECTS INCLUDED

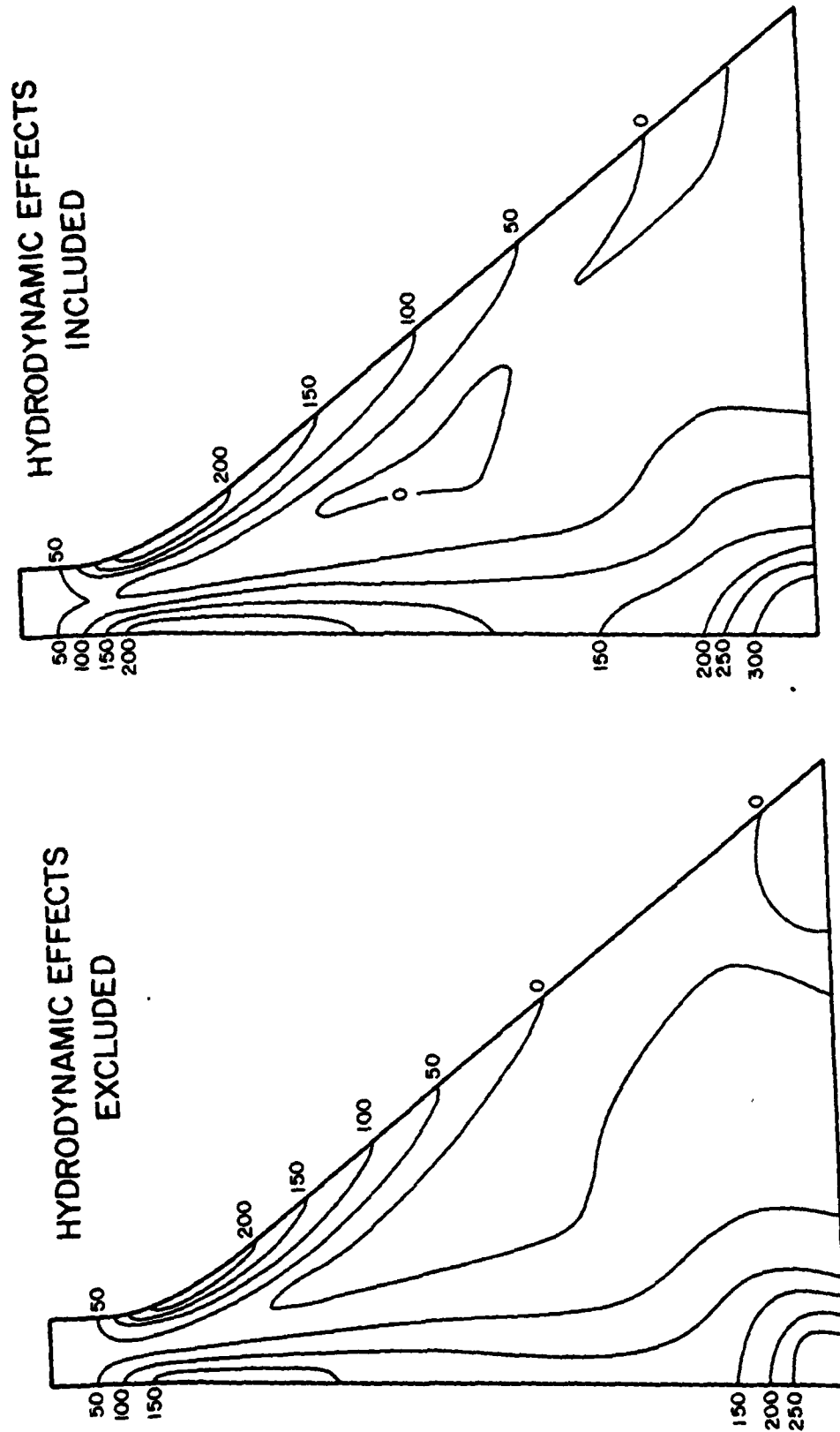


FIG. 9.10 ENVELOPE VALUES OF MAXIMUM PRINCIPAL (MAXIMUM TENSILE OR MINIMUM COMPRESSIVE) STRESSES IN PINE FLAT DAM ON RIGID FOUNDATION DUE TO S69E AND VERTICAL COMPONENTS, SIMULTANEOUSLY, OF TAFT GROUND MOTION: (A) HYDRODYNAMIC EFFECTS EXCLUDED, AND (B) HYDRODYNAMIC EFFECTS INCLUDED.

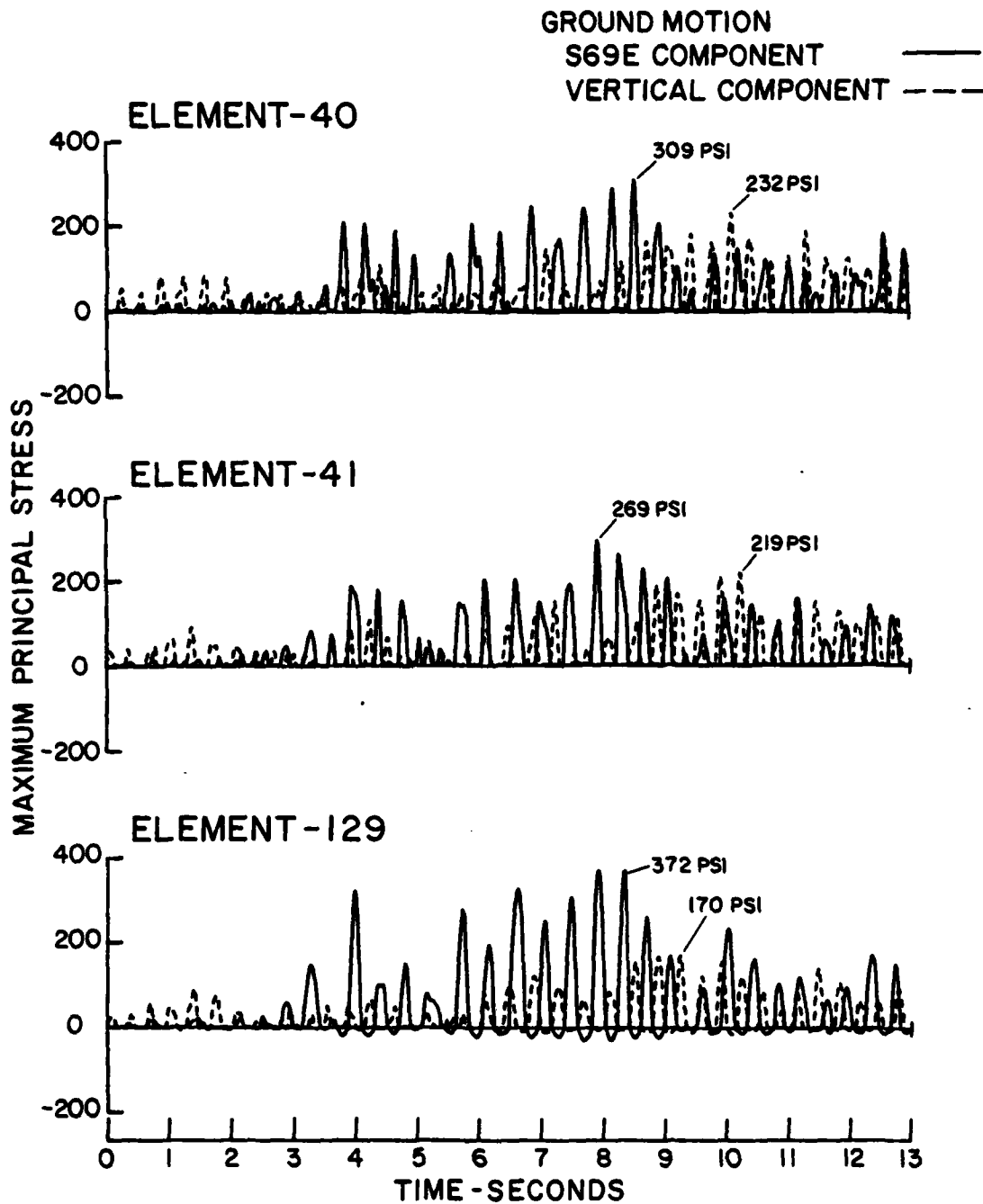


FIG. 9.11 STRESSES AT SELECTED LOCATIONS OF PINE FLAT DAM ON RIGID FOUNDATIONS DUE TO THE SEPARATE ACTION OF S69E AND VERTICAL COMPONENT OF TAFT GROUND MOTION. HYDRODYNAMIC EFFECTS INCLUDED. STATIC STRESSES EXCLUDED.

unbounded at the natural frequencies of water in the reservoir. As a result, structure-foundation interaction influences the response of the dam in a simpler manner than the hydrodynamic effects do (Fig. 9.5). The fundamental resonant frequency is decreased and the corresponding damping ratio is increased due to structure-foundation interaction (Fig. 9.5). This decrease in frequency is, however, smaller than the frequency reduction due to hydrodynamic effects. The ordinate of the pseudo-acceleration response spectrum for the S69E component of Taft ground motion is essentially unaffected by the increase in vibration period but would be reduced due to the increased damping (Fig. 9.6). This leads to increase in displacements (compare Figs. 5.7a and 5.12) and reduction in stresses (compare Figs. 9.8a and 9.13a). The displacements increase due to lengthening of the vibration period (Figs. 9.7a and 9.12). Flexibility of the soil permits motions at the base of the dam (Fig. 9.12) but these are much smaller than the motions at the crest of the dam. Comparison of Figs. 9.8a and 9.13a indicates that the stresses near the base of the dam are relaxed because of soil flexibility.

The effects of structure-foundation interaction on the response of the dam to horizontal and vertical components of ground motion acting simultaneously can be observed by comparing Figs. 9.9a and 9.14 with Figs. 9.10a and 9.15a, respectively. These effects are generally similar to those observed above in the responses to horizontal ground motion alone. The contributions of the vertical component of ground motion to the total response of the dam are rather small (compare Fig. 9.13a and 9.15a).

9.5 Dam-Water and Dam-Foundation Interaction Effects

Structure-foundation interaction affects the response of the dam in a similar manner, reducing the fundamental resonant frequency and increasing the effective damping, whether hydrodynamic effects are included or not (Fig. 9.5). The fundamental resonant frequency is reduced by dam-foundation interaction and by dam-water interaction. The two reductions are additive, resulting in further reduction in frequency when both interaction effects are considered (Fig. 9.5), and in considerably smaller resonant response as compared with either the response of the dam alone or the response including hydrodynamic effects.

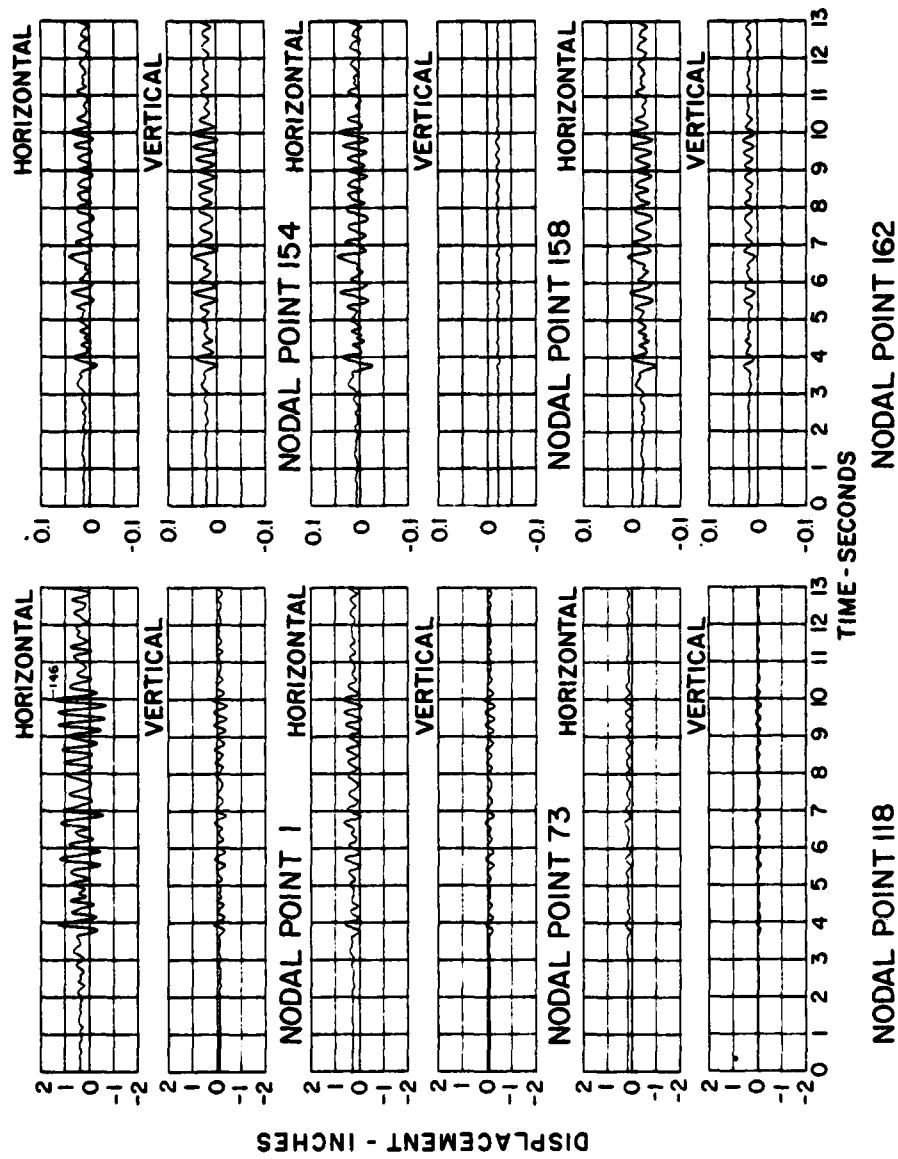


FIG. 9.12 DISPLACEMENT RESPONSE OF PINE FLAT DAM, INCLUDING DAM-FOUNDATION INTERACTION, BUT EXCLUDING HYDRODYNAMIC EFFECTS, TO S69E COMPONENT OF TAFT GROUND MOTION

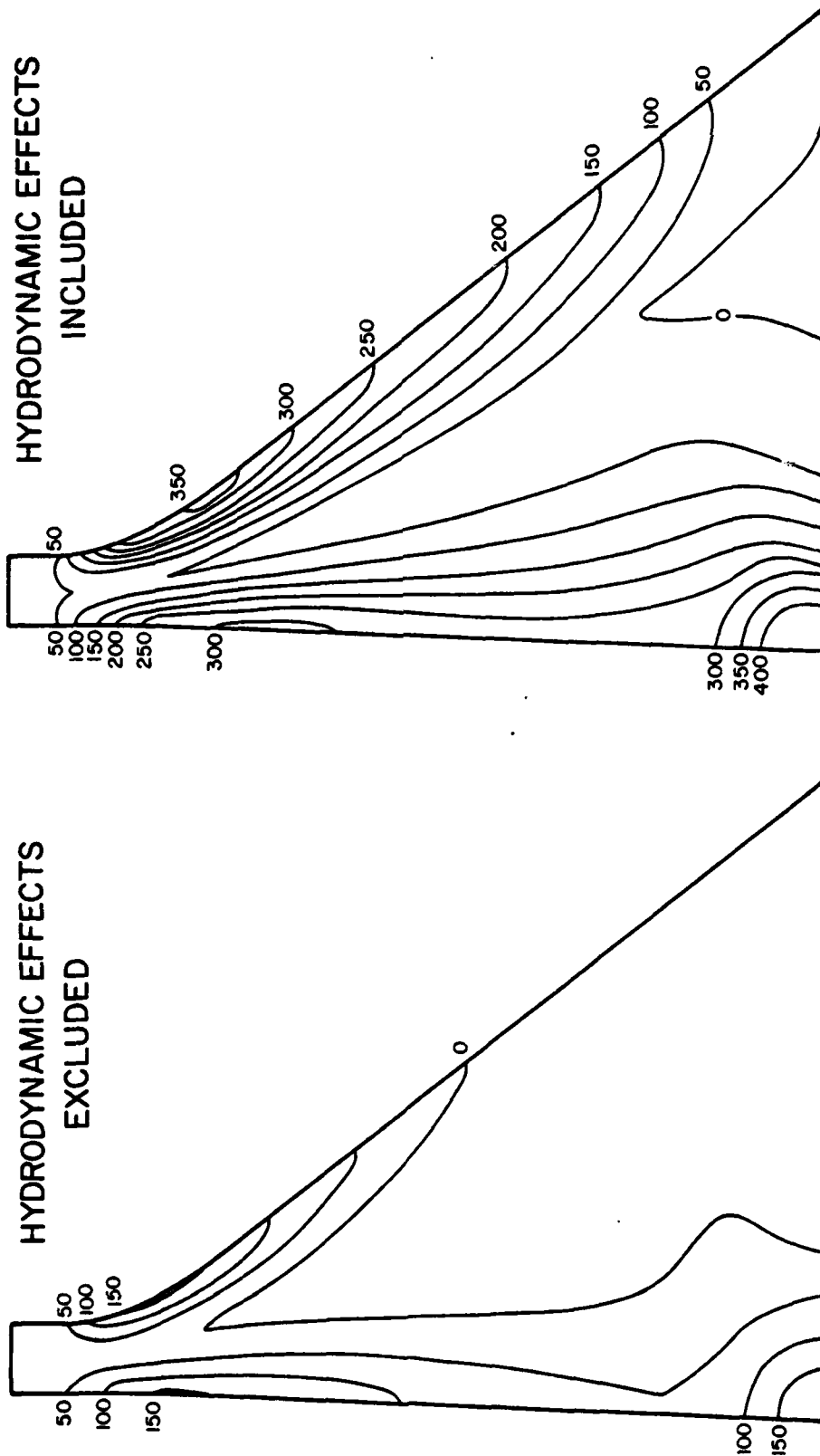


FIG. 9.13 ENVELOPE VALUES OF MAXIMUM PRINCIPAL (MAXIMUM TENSILE OR MINIMUM COMPRESSIVE) STRESSES IN PINE FLAT DAM ON FLEXIBLE FOUNDATION DUE TO S69E COMPONENT OF TAFT GROUND MOTION: (A) HYDRODYNAMIC EFFECTS INCLUDED, AND (B) HYDRODYNAMIC EFFECTS EXCLUDED.

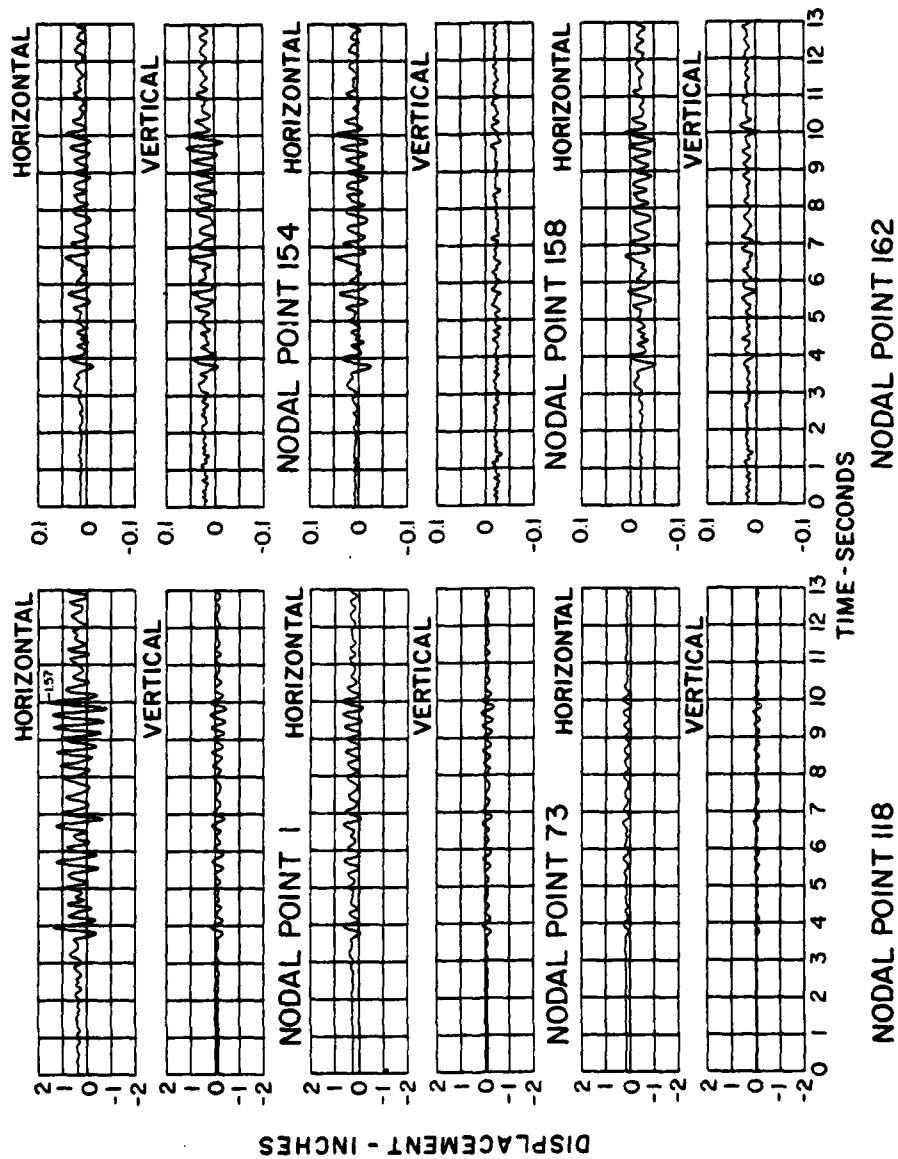


FIG. 9.14 DISPLACEMENT RESPONSE OF PINE FLAT DAM, INCLUDING DAM-FOUNDATION INTERACTION BUT EXCLUDING HYDRODYNAMIC EFFECTS, TO S69E AND VERTICAL COMPONENTS, SIMULTANEOUSLY, OF TAFT GROUND MOTION

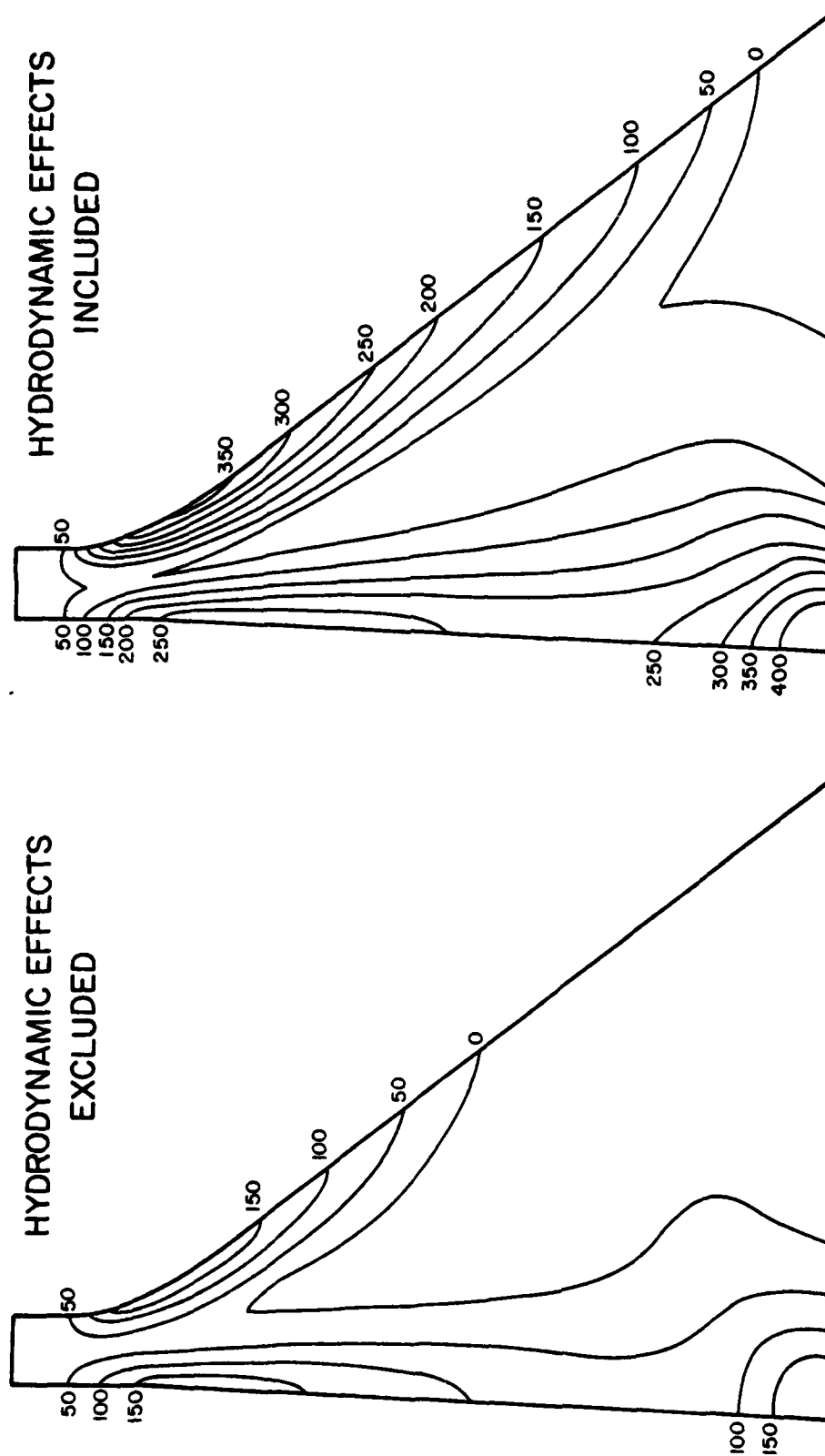


FIG. 9.15 ENVELOPE VALUES OF MAXIMUM PRINCIPAL (MAXIMUM TENSILE OR MINIMUM COMPRESSIVE) STRESSES IN PINE FLAT DAM ON FLEXIBLE FOUNDATION DUE TO S69E AND VERTICAL COMPONENTS OF TAFT GROUND MOTION:
 (A) HYDRODYNAMIC EFFECTS EXCLUDED, AND (B) HYDRODYNAMIC EFFECTS INCLUDED.

However, the displacements and stresses due to either excitation--horizontal ground motion only or horizontal and vertical ground motions simultaneously--are considerably increased due to structure-foundation interaction, (compare Figs. 9.7b and 9.16, 9.8b and 9.13b, 9.9b and 9.17, 9.10b and 9.19b). Compared to the response of the dam including only hydrodynamic effects, the stresses in upper parts of the dam are increased due to structure-foundation interaction when the excitation is only the horizontal component of ground motion (Figs. 9.8b and 9.13b); also, when the excitation included the vertical component of ground motion (Figs. 9.10b and 9.15b). Stresses at the heel of the dam are increased to a much lesser extent because of the stress-relaxation due to foundation flexibility. The area enclosed by a particular stress contour increases due to dam-foundation interaction, indicating that the dam is stressed beyond that contour value over a larger portion. This increase in earthquake response occurs in spite of the decreased response indicated by complex frequency responses, because structure-foundation interaction shifts the fundamental resonant period to correspond with a peak of the response spectrum (Fig. 9.6). Thus, the effects of dam-foundation interaction and dam-water interaction on earthquake response of the dam depend partly on the relative ordinates of the response spectrum at resonant periods of the dam with and without these interaction effects.

The effects of structure-foundation interaction on the response of the dam are generally similar with or without the vertical component of ground motion. For reasons mentioned in Sec. 9.3, the contributions of the vertical component of ground motion to the response of the dam, including both sources of interaction, are rather small.

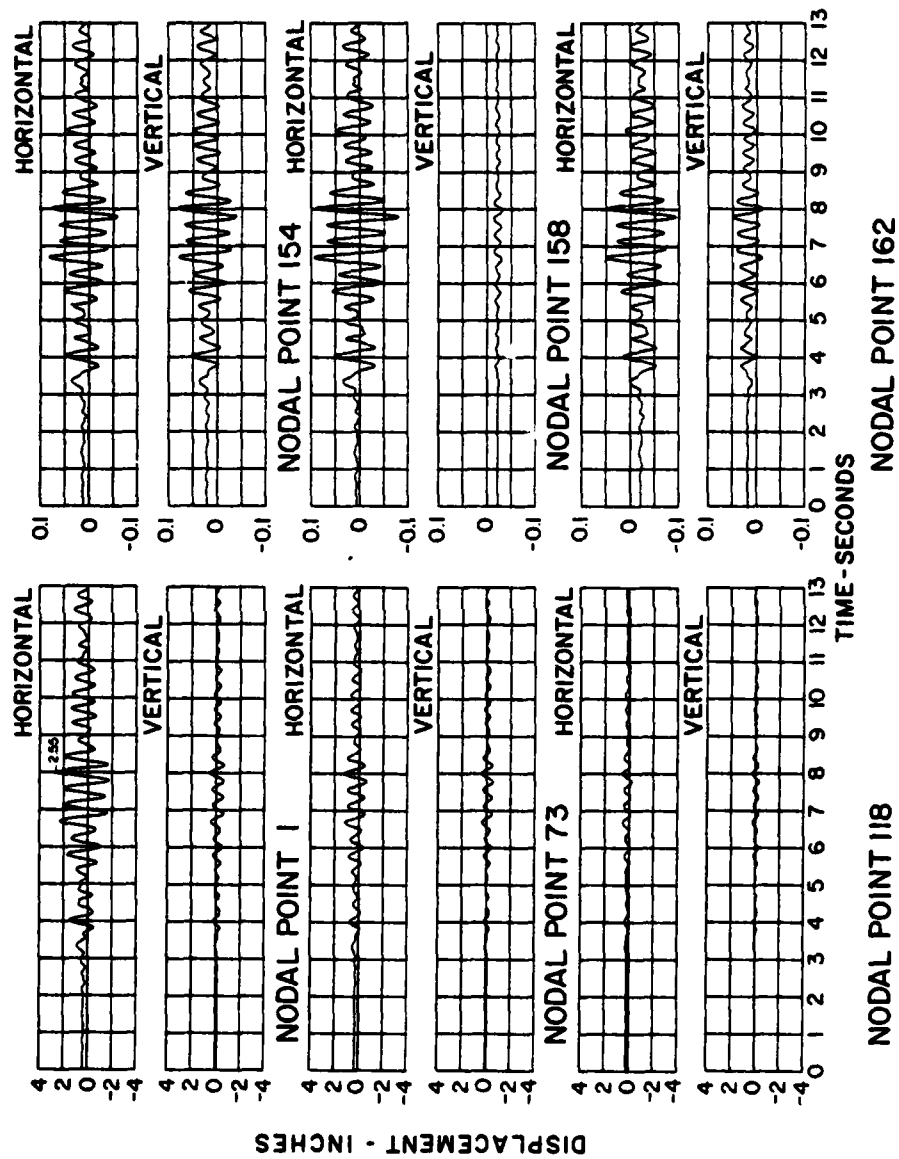


FIG. 9.16 DISPLACEMENT RESPONSE OF PINE FLAT DAM, INCLUDING DAM-FOUNDATION INTERACTION AND HYDRODYNAMIC EFFECTS, TO S69E COMPONENT OF TAFT GROUND MOTION

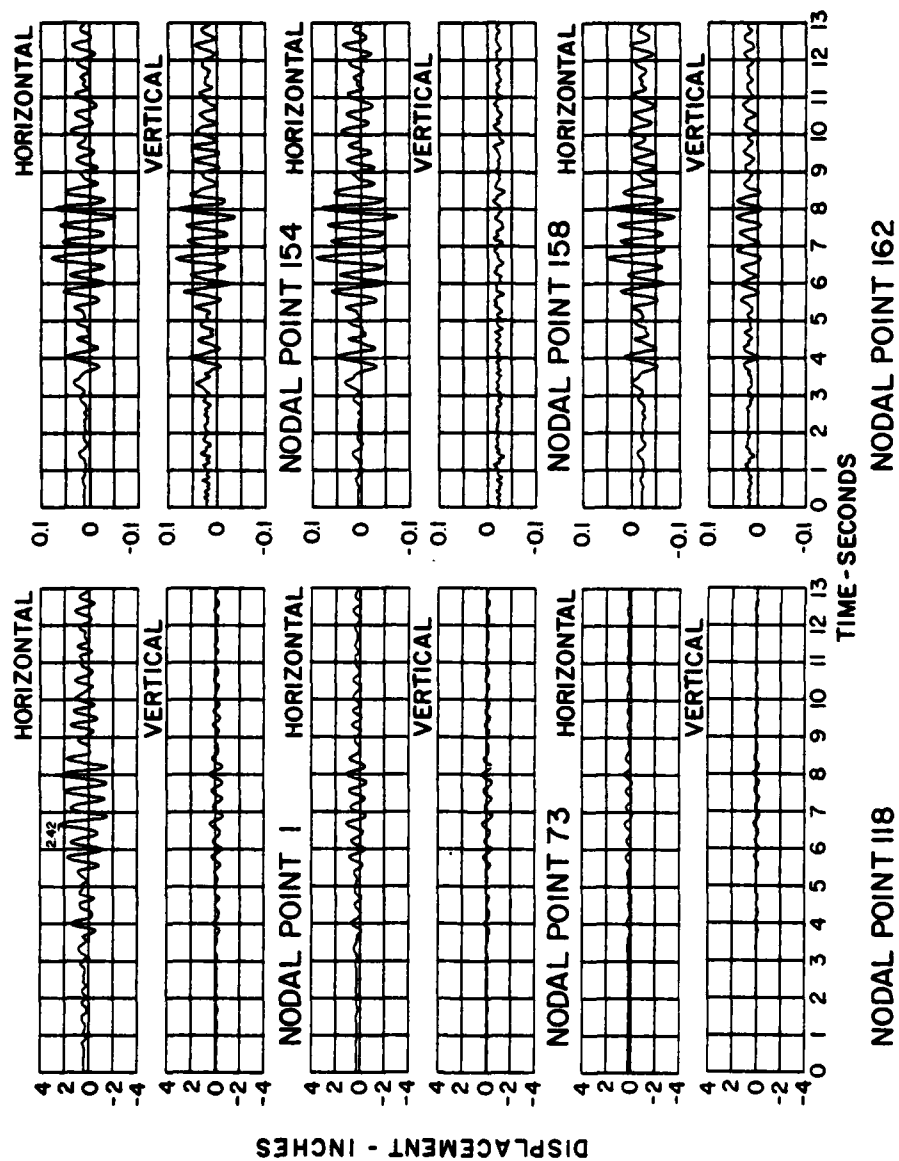


FIG. 9.17 DISPLACEMENT RESPONSE OF PINE FLAT DAM, INCLUDING DAM-FOUNDATION INTERACTION AND HYDRODYNAMIC EFFECTS, TO S69E AND VERTICAL COMPONENTS, SIMULTANEOUSLY, OF TAFT GROUND MOTION

10. CONCLUSIONS

The method presented for two-dimensional linear analysis of earthquake response of gravity dam monoliths is effective for practical problems. Included in this analysis are the effects of dynamic interaction among dam, impounded water, and foundation rock on the dam response. The dam, impounded water, and foundation rock are considered as three substructures of the complete system. Displacements of the dam are expressed as linear combinations of generalized coordinates, which are selected as the normal modes of an associated dam-foundation system. Results can be obtained to any desired degree of accuracy by including the necessary number of generalized coordinates. The substructure approach, combined with transformation of displacements to generalized coordinates, leads to an efficient analysis procedure.

The analysis procedure is developed specifically for two-dimensional analyses of gravity dam monoliths supported on the surface of a viscoelastic halfplane and impounding water in the reservoir with horizontal bottom. The dam is discretized as a two-dimensional finite element system, but the foundation and fluid domains are treated as continua. The general approach and concepts embodied in the substructure method are also applicable to more complex systems where, because of irregular geometry and/or nonhomogeneous material properties, the foundation and/or fluid domains must also be discretized.

In general, dam-water interaction, including water compressibility and dam-foundation interaction, have significant influence on the response of the dam and should be considered in the analysis. Because the foundation impedances are smooth, slowly varying functions of excitation frequency, but the hydrodynamic terms are unbounded at the resonant frequencies of the fluid domain, structure-foundation interaction affects the response of the dam in a simpler manner than does structure-water interaction.

Dam-foundation interaction effects in the response of dams depend on several factors, the most important of which is the ratio E_f/E_s of the elastic moduli of the foundation and dam materials. As the E_f/E_s ratio decreases (which for a fixed E_s implies a decrease of the foundation modulus), the fundamental resonant frequency of the dam decreases; the response at the crest of the dam at this frequency decreases; and the frequency bandwidth at resonance increases, implying an increase in the apparent damping of the structure. The influence of decreasing the E_f/E_s ratio is similar at higher resonant frequencies; however,

the higher resonant frequencies are decreased to a lesser degree by structure-foundation interaction. The effects of structure-foundation interaction are essentially independent of the effects of dam-water interaction, except at the resonant frequencies of the fluid domain. The dam response at these frequencies is controlled by dam-water interaction and is essentially independent of the properties of the foundation rock.

The influence of structure-foundation interaction on the earthquake response of a dam depends in part on the change in the earthquake response spectrum ordinate due to the decrease in frequency and increase in damping. In addition, the stresses near the base of the dam are relaxed because of foundation flexibility.

The frequency response curves are complicated in the neighborhood of the natural frequencies of water in the reservoir. In particular, the response curves have a double resonant peak near the fundamental frequencies of the dam and fluid domain, considered separately. In comparison with the response behavior of a dam without water, the response in the fundamental mode exhibits highly resonant behavior when the reservoir is full; the peak response at the fundamental frequency is especially large compared to that at higher resonant frequencies. Because of dam-water interaction, the fundamental resonant frequency of the dam is decreased by an amount depending on the depth of water -- with water in the upper parts of the dam having the most influence -- and modulus of elasticity of the dam. The higher resonant frequencies of the dam are reduced relatively little by dam-water interaction. Qualitatively, the effects of water on the dam response are generally similar whether the foundation rock is rigid or flexible. Hydrodynamic effects reduce the fundamental resonant frequency of the dam, including dam-foundation interaction, by roughly the same degree, independent of the foundation material properties. However, the apparent damping for the fundamental vibration mode is dominated by effects of structure-foundation interaction and varies little with the depth of water.

The displacements and stresses of Pine Flat Dam due to the Taft ground motion are increased significantly because of hydrodynamic effects.

The fundamental resonant frequency of the dam is reduced by dam-water interaction and by dam-foundation interaction. The two reductions are additive with the influence of the water usually being larger. This trend may

or may not exist at higher resonant frequencies. Similarly there are no general trends regarding the comparative effects of the water and foundation on the resonant responses of the dam. Which effect is more significant depends on the E_f/E_g ratio, the depth of water, the order of the resonant frequency (fundamental or higher), and the ground motion component (horizontal or vertical).

Compared to the response of Pine Flat Dam including only hydrodynamic effects, the stresses in the upper parts of the dam are significantly increased due to structure-foundation interaction. Stresses at the heel of the dam are increased to a much lesser extent because of the stress relaxation due to foundation flexibility.

The response of the dam, without water, to vertical ground motion is small relative to that due to horizontal ground motion, but it becomes relatively significant when hydrodynamic effects are included. However, the contribution of the vertical component of ground motion to the total response, including hydrodynamic effects, depends on the relative phasing of the responses to horizontal and vertical ground motion, which in turn depends on the phasing of the ground motion components and the vibration properties of the dam.

REFERENCES

1. "Koyna Earthquake of December 11, 1967", Report of the UNESCO Committee of Experts, New Delhi, April 1968.
2. A. K. Chopra and P. Chakrabarti, "The Koyna Earthquake and the Damage to Koyna Dam," Bulletin of the Seismological Society of America, Vol. 63, No. 2, April 1973, pp. 381-397.
3. R. W. Clough, F. W. Sims, J. A. Rhodes, "Cracking in Norfork Dam", Proc. ACI Vol. 61, No. 3, March 1964.
4. R. W. Clough and J. M. Raphael, "Construction Stresses in Dworshak Dam", Structural Engineering Laboratory Report No. 65-3, University of California, April 1965.
5. R. W. Clough and A. K. Chopra, "Earthquake Stress Analysis in Earth Dams," Journal of the Engineering Mechanics Division, ASCE, Vol. 92, No. EM2, April 1966.
6. A. K. Chopra and P. Chakrabarti, "The Earthquake Experience at Koyna Dam and Stresses in Concrete Gravity Dams," International Journal of Earthquake Engineering and Structural Dynamics, Vol. 1, No. 2, October-December 1972, pp. 151-164.
7. H. M. Westergaard, "Water Pressures on Dams During Earthquakes," Transactions, ASCE, Vol. 98, 1933.
8. S. Kotsubo, "Dynamic Water Pressures on Dam due to Irregular Earthquakes", Memoirs, Faculty of Engineering, Kyushu University, Fukoka, Japan, Vol. 18, No. 4, 1959.
9. J. I. Bustamante, E. Rosenblueth, I. Herrera and A. Flores, "Presion Hidrodinamica en Presas y Depositos", Boletin Sociedad Mexicana de Ingenieria Sismica, Vol. 1, No. 2, October 1963.
10. A. K. Chopra, "Hydrodynamic Pressures on Dams during Earthquakes", Journal of the Engineering Mechanics Division, ASCE, Vol. 93, No. EM6, Proc. Paper 5695, December 1967, pp. 205-223.
11. E. Rosenblueth, "Presion Hidrodinamica en presas Debida a Acceleration Vertical con Refraccion en el Fondo", II Congreso Nacional de Ingenieria Sismica, Veracruz, Mexico, 1968.
12. A. Flores, I. Herrera and C. Lozano, "Hydrodynamic Pressure Generated by Vertical Earthquake Component", Proceedings, Fourth World Conference on Earthquake Engineering, Santiago, Chile, 1969.
13. A. K. Chopra, E. L. Wilson and I. Farhoomand, "Earthquake Analysis of Reservoir-Dam Systems," Proceedings, Fourth World Conference on Earthquake Engineering, Santiago, Chile, January 1969.

14. O. C. Zienkiewicz and R. E. Newton, "Coupled Vibrations of a Structure Submerged in a Compressible Fluid," International Symposium on Finite Element Techniques, Stuttgart, May 1969.
15. A. K. Chopra, "Reservoir-Dam Interaction During Earthquakes", Bulletin of the Seismological Society of America, Vol. 57, No. 4, August 1967, pp. 675-687.
16. A. K. Chopra, "Earthquake Behavior of Reservoir-Dam Systems," Journal of Engineering Mechanics Division, ASCE, Vol. 94, No. EM6, December 1968.
17. A. K. Chopra, "Earthquake Response of Concrete Gravity Dams," Journal of the Engineering Mechanics Division, ASCE, Vol. 96, No. EM4, August 1970.
18. P. Chakrabarti and A. K. Chopra, "Hydrodynamic Pressures and Response of Gravity Dams to Vertical Earthquake Component," International Journal of Earthquake Engineering and Structural Dynamics, Vol. 1, No. 4, April-June 1973, pp. 325-335.
19. P. Chakrabarti and A. K. Chopra, "Earthquake Analysis of Gravity Dams Including Hydrodynamic Interaction," International Journal of Earthquake Engineering and Structural Dynamics, Vol. 2, pp. 143-160, 1973.
20. P. Chakrabarti and A. K. Chopra, "A Computer Program for Earthquake Analysis of Gravity Dams Including Hydrodynamic Interaction," Report No. EERC 73-7, Earthquake Engineering Research Center, University of California, Berkeley, May 1973, 39 pages.
21. S. S. Saini, P. Bettess and O. C. Zienkiewicz, "Coupled Hydrodynamic Response of Concrete Gravity Dams Using Finite and Infinite Elements," Earthquake Engineering and Structural Dynamics, Vol. 6, No. 4, pp. 363-374, July-August 1978.
22. P. Chakrabarti and A. K. Chopra, "Hydrodynamic Effects in Earthquake Response of Gravity Dams," Journal of the Structural Division, ASCE, Vol. 100, No. ST6, June 1974, pp. 1211-1224.
23. A. K. Chopra, "Earthquake Resistant Design of Concrete Gravity Dams," Journal of the Structural Division, ASCE, Vol. 104, No. ST6, June 1978, pp. 953-971.
24. A. K. Vaish and A. K. Chopra, "Earthquake Finite Element Analysis of Structure-Foundation Systems," Journal of the Engineering Mechanics Division, ASCE, Vol. 100, No. EM6, December 1974, pp. 1101-1116.
25. J. A. Gutierrez and A. K. Chopra, "A Substructure Method for Earthquake Analysis of Structures Including Structure-Soil Interaction," International Journal of Earthquake Engineering and Structural Dynamics, Vol. 6, No. 1, Jan-Feb. 1978, pp. 31-70.
26. W. D. Liam Finn, E. Varoglu and S. Cherry, "Seismic Water Pressure Against Dams," Chapter 21, pp. 420-442, in Structural and Geotechnical

Mechanics, W. J. Hall, editor, Prentice-Hall, Inc., 1977.

27. H. Parbat, V. Breaban, C. D. Ionescu, "Dam-Reservoir Interaction for a Dam with Flat Upstream Face during Earthquakes," Proceedings, Sixth World Conference on Earthquake Engineering, Vol II, New Delhi, India 1977, pp. 1301-1306.
28. D. Rea, C. Y. Liaw and A. K. Chopra, "Mathematical Models for the Dynamic Analysis of Concrete Gravity Dams," International Journal of Earthquake Engineering and Structural Dynamics, Vol. 3, No. 3, pp. 249-258, Jan-March 1975.
29. J. A. Gutierrez, "A Substructure Method for Earthquake Analysis of Structure-Soil Interaction," Report No. EERC 76-9, Earthquake Engineering Research Center, Univ. of Calif., Berkeley, April 1976.
30. R. W. Clough and J. Penzien, "Dynamics of Structures, Mc Graw-Hill Book Company, 1975.
31. J. W. Cooley and J. W. Tukey, "An Algorithm for the Machine Calculation of Complex Fourier Series," Mathematics of Computation, Vol. 19, April 1965, pp. 297-301.
32. G. Dasgupta and A. K. Chopra, "Dynamic Stiffness Matrices for Homogeneous Viscoelastic Half Planes," Journal of the Engineering Mechanics Division, ASCE, Vol. 105, No. EM5, October 1979; also see Report No. UCB/EERC-77/26, November 1977.
33. A. K. Chopra and J. A. Gutierrez, "Earthquake Response Analysis of Multistory Buildings Including Foundation Interaction," International Journal of Earthquake Engineering and Structural Dynamics, Vol. 3, 1974, pp. 65-67. Also see Report No. EERC 73-13, Univ. of Calif. Berkeley, June 1973.
34. A. K. Chopra, "Hydrodynamic Pressures on Dams during Earthquakes," Report No. 66-2, Structural Engineering Laboratory, Univ. of Calif., Berkeley, April 1966.

APPENDIX A - USERS GUIDE TO COMPUTER PROGRAM

IDENTIFICATION

EAGD Earthquake Analysis of Gravity Dams

Programmed: P. Chakrabarti, Sunil Gupta, G. Dasgupta

PURPOSE

This computer program has been developed to determine the elastic dynamic response of monoliths of concrete gravity dams to earthquake ground motion. The effects of dam-water interaction and dam-foundation interaction on the response of a dam are included. The computer program is based on the sub-structure analysis procedure developed in Chapter 6, in which the dam is treated as a finite element system, the impounded water as continuum, and the foundation rock or soil region as a finite element system or a viscoelastic halfspace, as appropriate for the site conditions.

The computer program is applicable to two-dimensional structural systems. Thus, the dam monolith and foundation must be idealized as a system in plane stress or plane strain. Compressibility of water is recognized in the analysis. The excitation includes the transverse (to dam axis) and vertical components of free-field ground motion, assumed to be the same across the base of the dam.

In order to define the input to the computer program, a cross-section or monolith of the dam must be idealized as an assemblage of planar, quadrilateral finite elements as shown by the example later in this appendix. Elements in the idealization are identified by a sequence of numbers starting with one. All nodal points are identified by a separate numbering sequence starting with one.

Because of dam-foundation interaction, a dynamic stiffness matrix for the foundation appears in the equation of motion. This matrix depends on the excitation frequency and is defined with respect to the degrees-of-freedom of nodal points at the dam-foundation interface. This matrix must be determined by a separate analysis and provided to the computer program as an input.

The computer program is written in FORTRAN IV and was developed on the CDC 6400 Computer at the University of California, Berkeley. It can be executed on other computers with minimal changes. However, the Fast Fourier Transform package included is partly written in COMPASS, developed specifically for the CDC 6400 computer. In using this computer program on other computer systems, a comparable subroutine package for FFT computations should be provided.

INPUT DATA

The following sequence of punched cards and data on a tape numerically define the dam-water-foundation system, the ground motion and control parameters for the analysis.

A. TITLE CARD (8A W)

Columns 1-80: Contain title or any information to be printed with results.

B. CONTROL CARD (5I5, F10.0, 2I5, F5.0, 5I5)

Columns 1 - 5 NUMNP: Number of nodal points.
6 - 10 NUMEL: Number of elements.
11 - 15 NUMMAT: Number of different materials.
16 - 20 NBASE: Number of nodal points at base of the dam.
21 - 25 NEV: Number of eigenvalues ($NEV \leq MBAND + 1$).
 If $NEV = 0$ and $IGRAV \neq 0$ only static analysis
 is performed.
26 - 35 WL: Water level in the reservoir, in feet.
36 - 40 NPP: Number of nodal points on the upstream face
 of the dam affected by the water pressure
 (see G).
41 - 45 IGRAV: $\neq 0$, to perform static analysis.
46 - 50 PSP: = 0., if plane stress problem.
 = 1., if plane strain problem.
51 - 55 IRES: = 0, to perform dynamic response analysis,
 otherwise, only static analysis and mode
 shapes are computed.
56 - 60 IOPR: $\neq 0$, to skip calculation of frequencies and
 mode shapes. They are read from cards in
 this case.
61 - 65 IOPP: $\neq 0$, to punch frequencies and mode shapes on
 cards.
66 - 70 IRIG: $\neq 0$, if the foundation is rigid.

C. FOUNDATION CARD (3F10.0)

Omit this card if $IRIG \neq 0$, (i.e. for rigid foundation).

Columns 1 - 10 E: Modulus of elasticity of foundation, in Ksf.
 11 - 20 RHO: Mass density of foundation, in K-sec²/ft 4.
 21 - 30 RBASE: Spacing between equally-spaced nodal points
 at base of the dam.

D. DAM MATERIAL PROPERTY CARD (I5,3F10.0)

The following cards must be supplied for each different material (NUMMAT cards).

Columns 1 - 5 Material identification number.
 6 - 15 Modulus of elasticity, in Ksf.
 16 - 25 Posson's ratio.
 26 - 35 Mass density of material, in K-sec²/ft 4.

E. NODAL POINT CARDS (I5,F5.0,2F10.0,2I5,2F10.0)

Columns 1 - 5 Nodal Point Number.
 6 - 10 Boundary condition code "p".
 11 - 20 X-ordinate, in ft.
 21 - 30 Y-ordinate, in ft.
 31 - 60 Used for layer generation, otherwise leave blank.

Specification for Code "p":

p = 0. Both displacements unknown.

p = 1. Zero displacement in the X-direction.
 Unknown displacement in the Y-direction.

p = 2. Unknown displacement in the X-direction.
 Zero displacement in the Y-direction.

p = 3. Zero displacement in the X-direction.
 Zero displacement in the Y-direction.

Nodal point cards must be in numerical sequence. If cards are omitted and Cols. 31 - 60 are left blank, the omitted nodal points are generated along a straight line between the defined nodal points (see Note 1). Or, if Cols. 31 - 60 are used they are generated in layers (see Note 2).

Note 1: Straight line generation.

If the (L-1) cards for nodal points N+1, N+2 N+L-1 are omitted and Cols. 31-60 of the card for nodal point N are left blank, the omitted nodal points are generated at equal intervals on the straight line joining nodes N and (N+L).

Note 2: Layer generation.

Layer generation may be used after two rows of nodal points are completely defined. If on the card for node N the following data is specified:

Columns 31 - 35 MOD: Module, m (> 0).
36 - 40 NLIM: Limit of generation (> N).
41 - 50 FACX: Amplification factor f_x .
(if left blank, assumed to be 1)
51 - 60 FACY: Amplification factor f_y .
(if left blank, assumed to be 1)

the X-Y coordinates of points N+1, N+2 NLIM are generated by the formulas

$$X_k = X_{k-m} + f_X (X_{k-m} - X_{k-2m})$$

$$Y_k = Y_{k-m} + f_Y (Y_{k-m} - Y_{k-2m})$$

for $k = N+1, \dots, NLIM$. If $NLIM = NUMNP$ no more nodal cards are needed. If $NLIM < NUMNP$, the card for point (NLIM+1) must follow.

The boundary condition code for generated nodal points is set equal to zero.

F. ELEMENT CARDS (6I5)

Columns 1 - 5 Element number
6 - 10 Nodal Point I
11 - 15 Nodal Point J
16 - 20 Nodal Point K
21 - 25 Nodal Point L
26 - 30 Material identification

The maximum difference "b" between these numbers is an indication of the band width of the Stiffness Matrix. "b" may be minimized by a judicious numbering of nodal points.

For a right-hand coordinate system the nodal point number I, J, K, and L must be in sequence in a counter-clockwise direction around the element (see Fig. A.1). Element cards must be in element number sequence. If element cards are omitted the program automatically generated the omitted information by incrementing by one the preceeding I, J, K, and L. The material identification for the generated card is set equal to the corresponding value on the last card. The last element card

must always be supplied. Triangular elements are also permissible; they are identified by repeating the last nodal number (i.e. I, J, K, K).

G. WATER PRESSURE CARDS (16I5)

These cards are necessary only if $NPP > 0$.

Columns 1 - 5 = 0, if the reservoir is to the left of the dam.
= 1, if the reservoir is to the right of the dam.

6 - 10	}	Nodal point numbers affected by the water starting from the top as shown in Fig. A.2.
11 - 15		
16 - 20		
etc.		

H. BASE CONNECTION NODE CARDS (16I5)

Omit if $IRIG \neq 0$ (i.e. for a rigid foundation).

Columns 1 - 5	}	Nodal point numbers at the base of the dam which are connected to the foundation rock, starting from left to right; a total of NBASE numbers, as shown in Fig. A.3.
6 - 10		
11 - 15		
:		

I. FREQUENCY CARDS (1I2,F15.8)

This array is necessary only if the control variable (Card B) $IOPR \neq 0$.

Columns 1 - 12 mode number.
13 - 22 frequency in rad/sec.

J. MODE SHAPE CARDS (1I2,2E15.6)

This array is also necessary only if the control variable (Card B) $IOPR \neq 0$. The mode shapes of the associated dam-foundation system have to be normalized in the sense $\psi^T m \psi = I$, where ψ is the mode shape matrix, m is the mass matrix, and I the identity matrix. If the array is the output of a previous run of this program on punched cards, then the mode shapes are already normalized. This array is as follows:

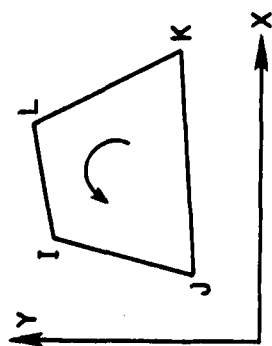


FIG. A.1 NODAL POINT NUMBERS FOR A FINITE ELEMENT

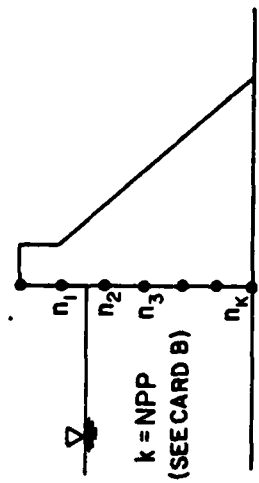


FIG. A.2 HYDROSTATIC AND HYDRO-DYNAMIC FORCES ACT AT NODAL POINTS n_i

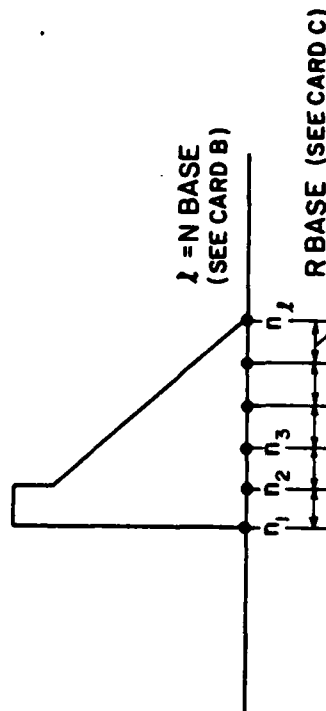


FIG. A.3 NODAL POINTS AT DAM-FOUNDATION INTERFACE

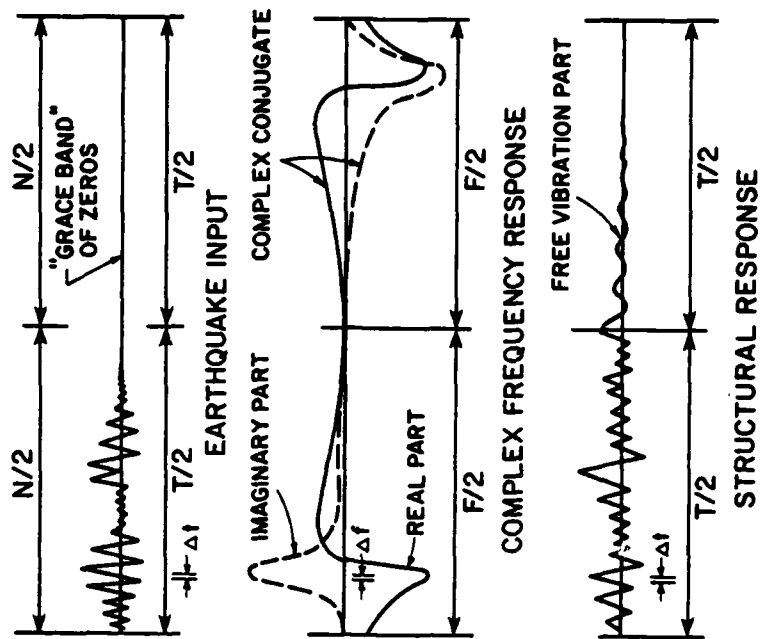


FIG. A.4 DEFINITION OF N , T , F , AND "GRACE BAND"

One card for each nodal point

Columns	1 - 12	Nodal point number	}	one set for each mode shape.
	13 - 27	X-ordinate		
	28 - 42	X-ordinate		

K. RESPONSE CONTROL CARD (3I5,2F10.0)

Columns	1 - 5	IHV: Code for ground motion component
		= 0, if only horizontal ground accelerations are to be included.
		= 1, if only vertical ground accelerations are to be included.
		= 2, if both the horizontal and vertical ground accelerations are to be included.
	6 - 10	NEXP: Defines the number of values of excitation frequency for which complex frequency response is to be evaluated. The number of excitation frequency values is $2NEXP$.
	11 - 15	IHYD: Code for hydrodynamic interaction. $IHYD \neq 0$ if hydrodynamic interaction is to be neglected. In this case only hydrostatic effects are included. (If $NPP = 0$ and $WL = 0$ in card B then this must be non-zero).
	16 - 25	DT: Time interval at which dynamic response is generated. The frequency increment for computing complex frequency response is determined from DT and NEXP. (See note 3.)
	26 - 35	ALPHA: Coefficient of reflection between water and ground rock below reservoir. This may be computed as $ALPHA = (k-1)/(k+1)$, where $k = C_r w_r / C_w$ with w_r and w being the unit weights of rock and water respectively, C_r the P-wave velocity in rock and C the velocity of sound in water (4720 ft/sec). $ALPHA \leq 1$.

Note 3: Choice of DT and NEXP.

For using the FFT algorithm any earthquake ground motion input data (see Card Group M) is interpolated at equal intervals of time $\Delta t \equiv DT$. The total number of ordinates is determined by NEXP, and is given by $\frac{N}{2} = 2NEXP$. Thus, the total duration of ground excitation used in the computations is $\frac{T}{2} = \Delta t \cdot \frac{N}{2}$ (See Fig. A.4.) A "grace band" of $\frac{N}{2}$ additional zeros are appended to the record to minimize the aliasing errors in the FFT computations. The uniform frequency increment Δf

and the frequency range $\frac{F}{2}$ for which the complex frequency response function has to be computed is given by the following relationships

$$\Delta f = \frac{1}{T}$$

$$\frac{F}{2} = \frac{N}{2} \cdot \Delta f$$

After the Fourier transform computations, which include the forward transform of the ground motion and the inverse transforms of the responses are obtained at the first $\frac{N}{2}$ points spaced at equal intervals of time Δt . By specifying TD less than T (see Card Group M), response may be obtained for a shorter duration. As is shown in Fig. A.4 the second part of the response contains free vibration response of the structure after the ground excitation has ceased.

It has been stated earlier that Δt (i.e., DT) and N (or $NEXP$) determine the values of T , Δf and F . It is crucial to choose these appropriately so that maximum accuracy in the results is ensured. The following considerations govern the selection of the time step Δt and total number of points $\frac{N}{2}$:

1. The frequency increment is small enough to permit an accurate description, especially near the resonant frequencies, of the frequency responses in the generalized coordinates. It is recommended that

$$\Delta f < \frac{f_1}{50}$$

where f_1 is the fundamental frequency of vibration of the dam in cps. An estimate of this may be obtained from a preliminary mode shape analysis of the structure using this computer program.

2. The frequency range should be large enough to include the significant portion of the frequency response function for generalized displacement in the highest mode of vibration included in the analysis. If f_ℓ is the frequency of vibration of the highest mode included in the analysis, it is recommended that

$$\frac{F}{2} > 2 f_\ell$$

3. The frequency range should include all the significant frequencies contained in typical earthquake records. Earthquake data processed by modern techniques accurately reproduces frequencies up to about 25 cps. Based on these considerations, in general, it is recommended that

$$\frac{F}{2} > 25 \text{ cps.}$$

4. For good resolution of the time-variation of response, it is recommended that

$$\Delta t < \frac{T_\ell}{8}$$

where $T_\ell = \frac{1}{f_\ell}$ is the period of vibration of the highest mode of the dam-foundation system included in the analysis. (If this criterion is satisfied then the one in (2) is automatically satisfied).

5. In order to reduce errors due to aliasing, inherent in the discrete Fourier transform computations, below acceptable limits,

$$T > \frac{1.5T_1}{\eta}$$

where

T_1 = vibration period for first mode of associated dam-foundation system.

η = constant hysteretic damping coefficient, same for all modes.

ℓ = the highest mode number included in the analysis.

L. DAMPING CARD (F10.0)

Columns 1 - 10 η : Constant hysteretic damping coefficient.

M. GROUND ACCELERATION INFORMATION CARDS.

1. CONTROL CARD (2I5,F10.0)

Columns 1 - 5 NXUGH: Number of ordinates describing time-history of horizontal ground acceleration.

6 - 10 NXUGV: Number of ordinates describing time-history of vertical ground acceleration.

11 - 20 TD: Time duration for which response is desired. $TD \leq DT \cdot (2^{NEXP} - 1)$.

2. HORIZONTAL GROUND ACCELERATION CARDS (6(F6.3,F6.4))

These cards are to be omitted if IHV = 1. NXUGH time-acceleration pairs describing the time-history of transverse horizontal ground acceleration are to be specified on these cards, with six pairs per card. Time must be expressed in seconds and the acceleration as multiples of g, the acceleration due to gravity.

3. VERTICAL GROUND ACCELERATION CARDS (6(F6.3,F6.4))

These cards are to be omitted if $IHV = 0$. NXUGV time acceleration points describing the time-history of vertical ground acceleration are to be specified on these cards, with six pairs per card. Time must be expressed in seconds and the acceleration as multiples of g , the acceleration due to gravity.

N. OUTPUT INFORMATION CARDS

1. OUTPUT CONTROL CARD (5I5)

Columns	1 - 5	NPRINT:	Print interval. Nodal point displacements and element stresses are printed every NPRINT time intervals.
	6 - 10	ICOMB:	= 0, if dynamic response is needed separately. = 1, if the static and dynamic responses are to be combined.
	11 - 15	ISEL:	Selection code ≠ 0, if output is desired for only selected nodal points and elements; otherwise displacements of all nodal points and stresses in all elements are printed.
	16 - 20	NNODE:	Total number of nodes for which displacements are to be printed, ≥ 1 .
	21 - 25	NNELM:	Total number of elements for which stresses are to be printed, ≥ 1 .

NNODE and NNELM may be left blank if $ISEL = 0$.

2. NODAL POINT SELECTION CARDS (16I5)

These cards are to be omitted if $ISEL = 0$ or $NNODE = 0$. List the NNODE nodal point numbers at which displacements are to be printed.

3. ELEMENT SELECTION CARDS (16I5)

These cards are to be omitted if $ISEL = 0$ or $NNELM = 0$. List the NNELM element numbers for which stresses are to be printed.

O. FOUNDATION MATRIX TAPE

If $IRIG = 0$, the dynamic stiffness matrix for the foundation region should be available on a tape. To be compatible with this program, this data should have been generated by Computer Programs described in "Dynamic Stiffness Matrices for Homogenous Viscoelastic Half Planes," by G. Dasgupta and A. K. Chopra, Report No. UCB/EERC-77/26; otherwise

the input statements in this program should be modified by the user.

The data read from the tape should then be copied onto a scratch file called TAPE90, which is read by the computer program. After execution, the data is destroyed.

OUTPUT

The following is printed by the program. (Note that some of these may be suppressed according to the options provided in card B.)

1. First set of input data: structural and material properties, foundation properties, options, etc.
2. Hydrostatic Loads: i.e. equivalent nodal point loads due to hydrostatic pressure of water in the reservoir.
Nodal point displacements and element stresses for static loads.
3. Frequencies and Mode Shapes.
4. Second set of input: response data including damping, time step, etc.
5. Absolute value of complex frequency responses for generalized accelerations of the dam due to horizontal and vertical ground motions separately.
6. Third set of input: earthquake acceleration data, etc.
7. Displacements of selected nodal points (according to ISEL and NNODE in Card Group N) and stresses in selected elements (according to ISEL and NNELM in Card Group N) at instants of time determined by the print interval (NPRINT in Card Group N).
8. The peak values of major and minor principal stresses in each element during the earthquake and the times at which they occur.
9. The following quantities are written on tape unit 3.

Logical Record 1: NUMNP, NUMEL, NEV, ND, DT.ND is the total number of time intervals of response determined from TD and DT using integer arithmetic.

Starting with Record 2, for each of the ND time intervals, two records are written using the following two statements:

```
WRITE (3) X
```

```
WRITE (3) STRES
```

where X and STRES are one-dimensional arrays, dimensioned properly, so that $X(2 * I - 1)$ and $X(2 * I)$ are the X-component and the

Y-component of the displacement at node number I, $I = 1, 2, \dots, \text{NUMNP}$, Similarly STRES ($3 * N - 2$), STRES ($3 * N - 1$), and STRES ($3 * N$) are the three components of stress, i.e. σ_x , σ_y , and σ_{xy} in the element number N, $N = 1, 2, \dots, \text{NUMEL}$. A physical tape has to be requested, with the file name TAPE3, in the program control cards if these results are to be saved for subsequent use. Plotting programs are available to read from this tape and plot time-history of nodal point displacements and element stresses.

EXAMPLE

The preparation of input data for this program is illustrated by an example. A very coarse finite element idealization of a cross-section of a concrete gravity dam is shown in Fig. A.5, followed by the input data required for the analysis of this structure subjected to horizontal earthquake motion.

COMPUTER PROGRAM INFORMATION, LIMITATIONS, AND TIMING

The program is written in FORTRAN IV and was developed on a CDC6400 computer at the University of California, Berkeley. The core storage requirements of the program are separated into fixed and variable parts with the fixed part consisting of instructions, non-subscripted variables, and those arrays which do not depend on the size of the individual problem. The variable part is stored in array A which appears in the blank COMMON statement.

The high speed storage requirements of the program can be changed depending on the size of the problem to be solved. This is done by changing two FORTRAN statements at the start of the program, i.e.

COMMON A (N)

MSTOR = N

The value specified for N must exceed each of the following.

1. $N_0 + 2 * \text{NUMNP} * \text{MBAND} + 6 * \text{NB2}$
2. $N_0 + 41 * \text{NUMEL}$
3. $N_0 + 6 * \text{NUMNP} + \text{NEV} * \text{NEV}$
4. $N_0 + 3 * \text{NNB} + 2 * \text{NB2} + \text{NPP} + 4 * \text{NTERM} + \text{NEV} * \text{NEV} * (4 + \text{NTERM})$
 $+ \text{NEV} * (2 * \text{NUMNP} + 3 * \text{NCOMP} + 2 * \text{NWR} * \text{NCOMP} + 2 * \text{NTERM} + 2)$
5. $\text{NDATA} * (4 + 2 * \text{NEV}) + \text{NEV} * (1 + 2 * \text{NWR}) + \text{NXUG}$
6. $\text{NUMNP} * (5 + \text{NEV}) + \text{NEV} * (2 * \text{NWR} + 1) + 42 * \text{NUMEL}$

where,

$$N_0 = 6 * \text{NUMNP} + \text{NBC} + \text{NPP} + \text{NEV} + \text{NNB} + \text{NB2}$$

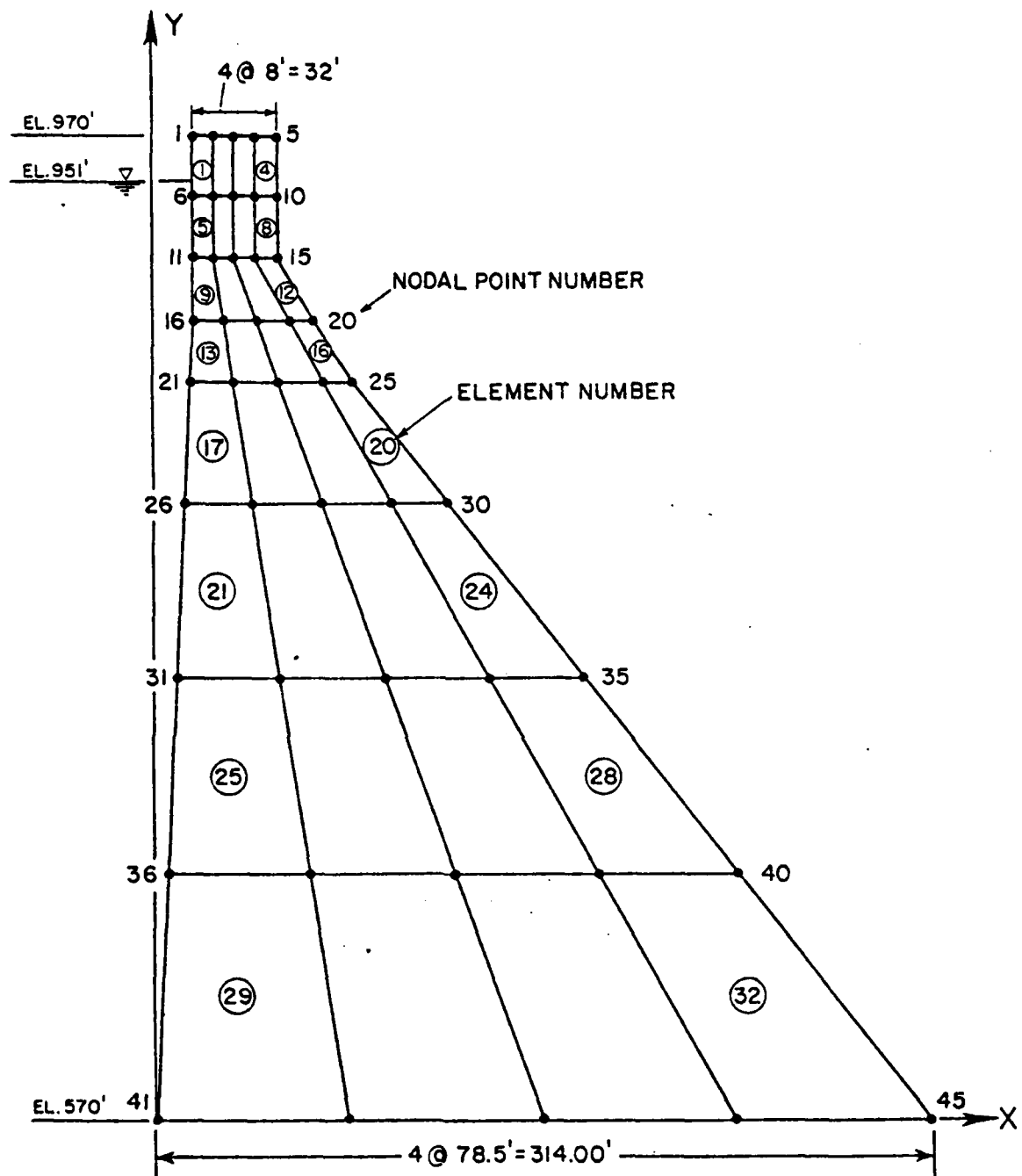


FIG. A.5 EXAMPLE FINITE ELEMENT MESH FOR A CONCRETE GRAVITY DAM TO ILLUSTRATE PREPARATION OF INPUT DATA FOR COMPUTER PROGRAM

```

***** PINE FLAT DAM -- COARSE MESH *****
45 32 1 5 4 391. 9 1
1152000. .00516 78.5
1576000. .2 .004814
1 16.75 400.
2 24.75 400.
3 32.75 400.
4 40.75 400.
5 48.75 400.
6 16.75 375.
7 24.75 375.
8 32.75 375.
9 40.75 375.
10 48.75 375.
11 16.75 350.
12 24.75 350.
13 32.75 350.
14 40.75 350.
15 50. 350.
16 15. 325.
17 29. 325.
18 43. 325.
19 55. 325.
20 64. 325.
21 15. 300.
22 32. 300.
23 51.5 300.
24 69. 300.
25 90. 300.
26 12. 250.
27 40.5 250.
28 70. 250.
29 98. 250.
30 120. 250.
31 9. 180.
32 51.5 180.
33 94.5 180.
34 137.5 180.
35 175. 180.
36 5. 100.
37 64. 100.
38 123. 100.
39 180. 100.
40 236. 100.
41 0. 0.
42 78.5 0.
43 157. 0.
44 235.5 0.
45 314. 0.
1 1 6 7 2 1
4 4 9 10 5 1
5 6 11 12 7 1
8 9 14 15 10 1
9 11 16 17 12 1
12 14 19 20 15 1
13 15 21 22 17 1

```


16	19	24	25	20	1
17	21	26	27	22	1
20	24	29	30	25	1
21	26	31	32	27	1
24	29	34	35	30	1
25	31	36	37	32	1
28	34	39	40	35	1
29	36	41	42	37	1
32	39	44	45	40	1
41	1	6	11	16	21
42	2	7	12	17	22
43	3	8	13	18	23
44	4	9	14	19	24
45	5	10	15	20	25

.1
246 0 10.

0.	94	0.340	59	0.380	149	0.140	59	0.200	97	0.260	112	TF52NW	1
0.320	44	0.350	21	0.400	174	0.440	17	0.500	17	0.540	113	TF52NW	2
0.600	122	0.660	179	0.700	121	0.740	61	0.800	147	0.820	192	TF52NW	3
0.860	252	0.920	114	0.940	120	0.980	62	1.020	264	1.060	159	TF52NW	4
1.080	212	1.140	115	1.200	120	1.260	50	1.280	41	1.320	90	TF52NW	5
1.380	207	1.460	132	1.520	234	1.580	158	1.620	118	1.700	54	TF52NW	6
1.760	249	1.820	12	1.880	327	1.940	117	2.020	91	2.060	392	TF52NW	7
2.120	340	2.140	143	2.200	287	2.280	301	2.340	470	2.380	64	TF52NW	8
2.400	142	2.440	158	2.480	92	2.520	299	2.560	181	2.620	299	TF52NW	9
2.640	93	2.680	119	2.740	237	2.780	172	2.820	185	2.860	37	TF52NW	10
2.880	67	2.920	67	2.940	120	2.980	89	3.040	434	3.120	186	TF52NW	11
3.200	775	3.240	474	3.340	605	3.420	69	3.500	488	3.680	151	TF52NW	12
3.820	750	3.860	646	3.900	410	3.940	737	4.020	191	4.120	54	TF52NW	13
4.200	1015	4.260	254	4.320	897	4.360	700	4.400	648	4.420	529	TF52NW	14
4.480	411	4.520	1485	4.600	451	4.640	438	4.680	661	4.780	817	TF52NW	15
4.900	1329	4.940	542	5.040	5	5.080	84	5.140	609	5.200	112	TF52NW	16
5.300	754	5.420	1182	5.560	610	5.600	296	5.700	1016	5.760	593	TF52NW	17
5.820	297	5.880	1377	5.940	398	5.980	304	6.060	474	6.160	179	TF52NW	18
6.220	487	6.280	206	6.340	1115	6.500	1568	6.560	1332	6.600	1411	TF52NW	19
6.740	997	6.800	338	6.920	643	7.000	705	7.180	1179	7.260	469	TF52NW	20
7.400	132	7.360	705	7.420	51	7.460	522	7.580	1191	7.620	943	TF52NW	21
7.700	1087	7.800	1230	7.820	45	7.960	392	8.000	942	8.080	1073	TF52NW	22
8.140	104	8.220	209	8.240	52	8.300	275	8.340	601	8.480	982	TF52NW	23
8.560	771	8.620	274	8.680	326	8.720	51	8.760	745	8.860	459	TF52NW	24
9.000	1333	9.120	1362	9.240	1202	9.320	207	9.360	102	9.460	643	TF52NW	25
9.520	172	9.560	316	9.620	901	9.800	787	9.860	159	9.920	787	TF52NW	26
9.980	10210	0.040	65710	0.100	75610	0.200	34310	0.220	6210	0.280	395	TF52NW	27
10.340	23210	0.400	13310	0.440	18010	0.480	19010	0.540	62510	0.600	193	TF52NW	28
10.640	36310	0.680	2910	0.740	55910	0.760	14010	0.820	40210	0.960	998	TF52NW	29
11.080	89911	1.160	81511	1.200	57911	1.260	45411	1.340	63711	1.420	292	TF52NW	30
11.480	7411	1.500	5611	1.560	51911	1.680	64511	1.720	44911	1.780	590	TF52NW	31
11.860	36211	1.960	4712	0.020	62312	1.180	58012	1.240	412	1.300	318	TF52NW	32
12.360	70212	1.440	56712	1.480	24012	1.500	13512	1.560	28312	1.600	152	TF52NW	33
12.660	47912	1.760	31912	1.800	22712	1.860	47612	1.980	42613	0.020	121	TF52NW	34
13.100	55713	1.220	113013	1.340	64913	1.440	33213	1.500	33413	1.600	136	TF52NW	35
13.640	713	1.700	15113	1.740	9913	1.780	51813	1.840	26713	1.880	70	TF52NW	36
13.920	4413	1.980	42614	0.080	90814	1.120	39814	1.160	39814	1.220	229	TF52NW	37
14.260	19814	1.320	13814	1.340	16214	1.400	26714	1.440	39814	1.480	306	TF52NW	38
14.500	29314	1.560	46514	1.620	46514	1.660	29514	1.700	62214	1.840	843	TF52NW	39
15.000	68715	1.120	715	1.160	715	1.200	31915	1.260	8415	1.320	607	TF52NW	40
15.400	57015	1.520	29315	1.600	63515	1.660	79215	1.780	28015	1.860	292	TF52NW	41

10 1 1 2 1
1 21
8

and

NUMNP = Number of nodal points
NUMEL = Number of elements
NBC = Number of displacement constraints
NPP = Number of nodal points affected by water pressure
NCOMP = Number of components of earthquake included in the analysis.
NDATA = 2 ** NEXP
NEV = Number of generalized coordinates included.
NEXP = Exponent for the number of ordinates to define complex frequency responses.
MBAND = 2 * (MB + 1)
MB = $\max_i MB_i, i = 1, \text{NUMEL}$
MB_i = difference between the largest and smallest nodal point numbers for element i.
NTERM = 50
NXUG = max (NXUGH, NXUGV)
NXUGH = Number of horizontal ground acceleration ordinates
NXUGV = Number of vertical ground acceleration ordinates
NBASE = Number of nodal points at base of the dam.
NB2 = NBASE*2
NNB = NB2*NB2*2
NWR = max(100, NDATA+1)

If only frequencies and mode shapes are desired along with static analysis it suffices to check (1) and (2) above.

The computer time required for solution depends on a number of factors. The more important ones are the number of time ordinates (which is determined by NEXP) the number of nodal points, the bandwidth of the stiffness matrix (the nodal points should be numbered in a manner which minimizes the bandwidth), the number of elements, the number of generalized coordinates to be included, and the interval for printing and writing the output.

Some representative execution times on a CDC 6400 computer are given for four cases of analysis (Tables A.1 and A.2) for Pine Flat dam (Chapter 8),

with NUMNP = 162, NUMEL = 136, MBAND = 22, and NEXP = 10, NEV = 5 for cases 1 and 2, 10 for cases 3 and 4, NBASE = 9. Table A.1 pertains to analysis for transverse ground motion only. Table A.2 is for analyses considering transverse and vertical ground motions, simultaneously. The results include the complete history of displacements and stresses during the earthquake.

Tables A.1 and A.2 provide some indication of the increase in computational effort required to include dam-water and dam-foundation interaction effects in the analysis. Considering that these interaction effects complicate the analysis greatly, the additional computer time required is modest. Comparatively, more computational effort is required to include dam-foundation interaction effects, primarily because a larger number of generalized coordinates need to be included in the analysis. The efficiency of the analysis lies in use of the substructure method along with transformation to generalized coordinates.

TABLE A.1 COMPUTATION TIMES: PINE FLAT DAM, HORIZONTAL GROUND MOTION ONLY

CASE	FOUNDATION	HYDRODYNAMIC EFFECTS	NO. OF GENERALIZED COORDINATES	CENTRAL PROCESSOR TIME (SEC.)	REMARKS
1	RIGID	EXCLUDED	5	314	Eigenvalues, Eigenvectors, and Dynamic Foundation Stiffness Matrix are read as input
2	RIGID	INCLUDED	5	474	
3	FLEXIBLE	EXCLUDED	10	810	
4	FLEXIBLE	INCLUDED	10	1313	

TABLE A.2 COMPUTATION TIMES: PINE FLAT DAM, HORIZONTAL AND VERTICAL GROUND MOTION

CASE	FOUNDATION	HYDRODYNAMIC EFFECTS	NO. OF GENERALIZED COORDINATES	CENTRAL PROCESSOR TIME (SEC.)	REMARKS
1	RIGID	EXCLUDED	5	325	Eigenvalues, Eigenvectors, and Dynamic Foundation Stiffness Matrix are read as input
2	RIGID	INCLUDED	5	500	
3	FLEXIBLE	EXCLUDED	10	832	
4	FLEXIBLE	INCLUDED	10	1356	

APPENDIX B

LISTING OF EAGD COMPUTER PROGRAM


```

DO 130 I=1,NP2
  L=BASE(I)
  DO 130 J=1,NP2
    K=BASE(J)-L
    IF (K.LF.0).OR.(K.GT.NPAND1) GO TO 170
    AIL(K)=AIL(K)+HALF(AKF(I),J)
  130 CONTINUE
C
C
C 135 CALL BANGEIGEN,MAMP,NEV,NBC,EV,MERC,SMASH,A,W1,A,W2,W1,W2,INATEP,ICM
C
C 140 OUTPUT EIGENVALUES AND EIGENVECTORS
C
  WRITE (6,2005)NEV
  DO 140 I=1,NEV
    EV(I)=EIGENVECT(I)
  140 WRITE (6,2006) I,EV(I)
  CALL MPRINT (A,NEV,NP)
  WRITE (6,2007)
  DO 140 I=1,NEV
    DO 140 J=1,NP
      SUM=0.0
      DO 140 K=1,NPQ
        SUM=SUM+EV(I)*SPASS(K)*A(K,J)
      140 CC(I,J)=SUM
      II=I-1
      IF (II.LT.100) GO TO 170
      DO 140 L=1,II
        CC(I,L)=CC(I,L)
      140 CONTINUE
      CALL MPRINT (CC,NEV,NEV)
C
C 150 PUNCH FREQUENCIES AND MODE SHAPES
C
  IF (IUMP.EQ.0) GO TO 160
  DO 200 M=1,NEV
    PUNCH 2005,M,EV(M)
  200 CONTINUE
  DO 210 M=1,NEV
    DO 210 N=1,NPAMP
      L=NP+1
      210 PUNCH 1020,M,AIL(M),AIL(N),AIL(1),N)
    RETURN
C
C 220 READ FREQUENCIES AND MODE SHAPES
C
  DO 230 M=1,NEV
    DO 230 N=1,NPAMP
      L=NP+1
      230 READ (5,1010) EV(M),N,NEV)
      WRITE (6,2006)M,N
      DO 240 I=1,NEV
        240 WRITE (6,2007) I,EV(I)
      CALL MPRINT (A,NEV,NP)

```


- 171 -

[illegible]

- 177 -


```

C
COMPLEX FOUR(1),UG(1),VINC(1)
DIMENSION X(1),XUG(1)
COMMON /CTRL/ MDATA,NR,DT,NRST,NRUF,NR,NL,NCK,IMV,MCMUP,ISEL,
      ICMN,NPRINT,ND
C
FAC=22.2601
NR2=NRUF
NR2*MDATA
N2=NR+2
C
TRANSFORM COMPUTATIONS
C
DO 400 I=1,NRNP
C
C READ EARTHQUAKE DATA
C
ITAPE=2
IF (I=2) GO TO 50
IF (IMV=1) 40,40,40
40 READ (5,1000) (X(I),XUG(I),K=1,NRUG)
WRITE (6,2000) (X(I),XUG(I),K=1,NRUG)
NR=XUG
GO TO 70
50 ITAPE=3
60 READ (5,1000) (X(I),XUG(I),K=1,NRUG)
WRITE (6,2001) (X(I),XUG(I),K=1,NRUG)
NR=XUG
70 DO 140 K=1,NR
140 XUG(K)=XUG(K)*FAC
C
INTERPOLATE EARTHQUAKE DATA AT DT STEPS AND ITS ALIASING
C
DO 150 K=1,NR
150 UG(K)=0.
ND=(10/DT)*511
IF (IND,GT,MDATA) ND=MDATA
CALL (INTER(XI,XI*,MD,DT,UG))
C
FOURIER TRANSFORM OF EARTHQUAKE ACCELERATION
C
CALL FFT(UG,N)
C
READ COMPLEX FREQUENCY RESPONSE FROM TAPE AND
STORE AS 2-DIMENSIONAL ARRAY
C
REWIND ITAPE
DO 110 N=1,NR,NCK
NR2=NRUF
DO 100 LL=1,NR2
JJ=JJ+1
DO 100 NR=1,NR2
NR2=NR+2
100 Y(JJ,KK)=YRUF(NR)
C
DO 110 K=1,NR
110 X(JJ,K)=XUG(K)
DO 110 J=1,NR2
110 Y(JJ,K)=X(JJ,K)
CALL READY(YRUF,NR,ITAPE)
DO 170 KK=1,NR2
NR2=NR+2
170 Y(JJ,KK)=YRUF(NR)
180 Y(JJ,KK)=YRUF(NR)
195 Y(JJ,KK)=YRUF(NR)
200 Y(JJ,KK)=YRUF(NR)
210 Y(JJ,KK)=YRUF(NR)
220 Y(JJ,KK)=YRUF(NR)
230 Y(JJ,KK)=YRUF(NR)
240 Y(JJ,KK)=YRUF(NR)
250 Y(JJ,KK)=YRUF(NR)
260 Y(JJ,KK)=YRUF(NR)
270 Y(JJ,KK)=YRUF(NR)
280 Y(JJ,KK)=YRUF(NR)
290 Y(JJ,KK)=YRUF(NR)
300 Y(JJ,KK)=YRUF(NR)
310 Y(JJ,KK)=YRUF(NR)
320 Y(JJ,KK)=YRUF(NR)
330 Y(JJ,KK)=YRUF(NR)
340 Y(JJ,KK)=YRUF(NR)
350 Y(JJ,KK)=YRUF(NR)
360 Y(JJ,KK)=YRUF(NR)
370 Y(JJ,KK)=YRUF(NR)
380 Y(JJ,KK)=YRUF(NR)
390 Y(JJ,KK)=YRUF(NR)
400 Y(JJ,KK)=YRUF(NR)
410 Y(JJ,KK)=YRUF(NR)
420 Y(JJ,KK)=YRUF(NR)
430 Y(JJ,KK)=YRUF(NR)
440 Y(JJ,KK)=YRUF(NR)
450 Y(JJ,KK)=YRUF(NR)
460 Y(JJ,KK)=YRUF(NR)
470 Y(JJ,KK)=YRUF(NR)
480 Y(JJ,KK)=YRUF(NR)
490 Y(JJ,KK)=YRUF(NR)
500 Y(JJ,KK)=YRUF(NR)
510 Y(JJ,KK)=YRUF(NR)
520 Y(JJ,KK)=YRUF(NR)
530 Y(JJ,KK)=YRUF(NR)
540 Y(JJ,KK)=YRUF(NR)
550 Y(JJ,KK)=YRUF(NR)
560 Y(JJ,KK)=YRUF(NR)
570 Y(JJ,KK)=YRUF(NR)
580 Y(JJ,KK)=YRUF(NR)
590 Y(JJ,KK)=YRUF(NR)
600 Y(JJ,KK)=YRUF(NR)
610 Y(JJ,KK)=YRUF(NR)
620 Y(JJ,KK)=YRUF(NR)
630 Y(JJ,KK)=YRUF(NR)
640 Y(JJ,KK)=YRUF(NR)
650 Y(JJ,KK)=YRUF(NR)
660 Y(JJ,KK)=YRUF(NR)
670 Y(JJ,KK)=YRUF(NR)
680 Y(JJ,KK)=YRUF(NR)
690 Y(JJ,KK)=YRUF(NR)
700 Y(JJ,KK)=YRUF(NR)
710 Y(JJ,KK)=YRUF(NR)
720 Y(JJ,KK)=YRUF(NR)
730 Y(JJ,KK)=YRUF(NR)
740 Y(JJ,KK)=YRUF(NR)
750 Y(JJ,KK)=YRUF(NR)
760 Y(JJ,KK)=YRUF(NR)
770 Y(JJ,KK)=YRUF(NR)
780 Y(JJ,KK)=YRUF(NR)
790 Y(JJ,KK)=YRUF(NR)
800 Y(JJ,KK)=YRUF(NR)
810 Y(JJ,KK)=YRUF(NR)
820 Y(JJ,KK)=YRUF(NR)
830 Y(JJ,KK)=YRUF(NR)
840 Y(JJ,KK)=YRUF(NR)
850 Y(JJ,KK)=YRUF(NR)
860 Y(JJ,KK)=YRUF(NR)
870 Y(JJ,KK)=YRUF(NR)
880 Y(JJ,KK)=YRUF(NR)
890 Y(JJ,KK)=YRUF(NR)
900 Y(JJ,KK)=YRUF(NR)
910 Y(JJ,KK)=YRUF(NR)
920 Y(JJ,KK)=YRUF(NR)
930 Y(JJ,KK)=YRUF(NR)
940 Y(JJ,KK)=YRUF(NR)
950 Y(JJ,KK)=YRUF(NR)
960 Y(JJ,KK)=YRUF(NR)
970 Y(JJ,KK)=YRUF(NR)
980 Y(JJ,KK)=YRUF(NR)
990 Y(JJ,KK)=YRUF(NR)
1000 Y(JJ,KK)=YRUF(NR)
1010 Y(JJ,KK)=YRUF(NR)
1020 Y(JJ,KK)=YRUF(NR)
1030 Y(JJ,KK)=YRUF(NR)
1040 Y(JJ,KK)=YRUF(NR)
1050 Y(JJ,KK)=YRUF(NR)
1060 Y(JJ,KK)=YRUF(NR)
1070 Y(JJ,KK)=YRUF(NR)
1080 Y(JJ,KK)=YRUF(NR)
1090 Y(JJ,KK)=YRUF(NR)
1100 Y(JJ,KK)=YRUF(NR)
1110 Y(JJ,KK)=YRUF(NR)
1120 Y(JJ,KK)=YRUF(NR)
1130 Y(JJ,KK)=YRUF(NR)
1140 Y(JJ,KK)=YRUF(NR)
1150 Y(JJ,KK)=YRUF(NR)
1160 Y(JJ,KK)=YRUF(NR)
1170 Y(JJ,KK)=YRUF(NR)

```


- 185 -

AD-A067 297

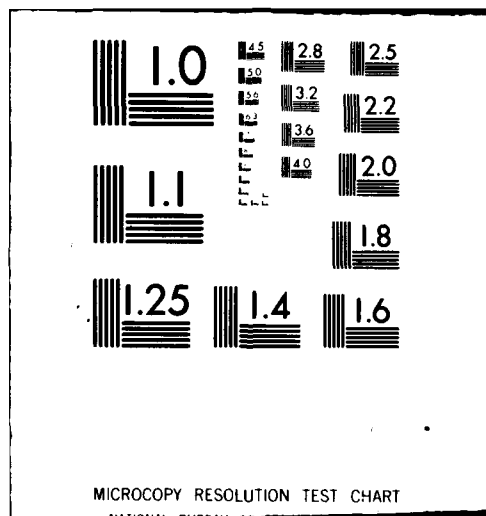
CALIFORNIA UNIV BERKELEY EARTHQUAKE ENGINEERING RES--ETC F/G 13/13
EARTHQUAKE RESPONSE OF CONCRETE GRAVITY DAMS INCLUDING HYDROOYN--ETC(U)
JAN 80 A K CHOPRA, P CHAKRABARTI, S GUPTA DACW73-71-C-0051
UCB/EERC-80/01 NL

UNCLASSIFIED

3 x 3



END
DATE
FILMED
9-80
DTIC



EERC REPORT LISTING

EARTHQUAKE ENGINEERING RESEARCH CENTER REPORTS

NOTE: Numbers in parenthesis are Accession Numbers assigned by the National Technical Information Service; these are followed by a price code. Copies of the reports may be ordered from the National Technical Information Service, 5285 Port Royal Road, Springfield, Virginia, 22161. Accession Numbers should be quoted on orders for reports (PB --- ---) and remittance must accompany each order. Reports without this information were not available at time of printing. Upon request, EERC will mail inquirers this information when it becomes available.

- EERC 67-1 "Feasibility Study Large-Scale Earthquake Simulator Facility," by J. Penzien, J.G. Bouwkamp, R.W. Clough and D. Rea - 1967 (PB 187 905)A07
- EERC 68-1 Unassigned
- EERC 68-2 "Inelastic Behavior of Beam-to-Column Subassemblages Under Repeated Loading," by V.V. Bertero - 1968 (PB 184 888)A05
- EERC 68-3 "A Graphical Method for Solving the Wave Reflection-Refraction Problem," by H.D. McNiven and Y. Mengi - 1968 (PB 187 943)A03
- EERC 68-4 "Dynamic Properties of McKinley School Buildings," by D. Rea, J.G. Bouwkamp and R.W. Clough - 1968 (PB 187 902)A07
- EERC 68-5 "Characteristics of Rock Motions During Earthquakes," by H.B. Seed, I.M. Idriss and F.W. Kiefer - 1968 (PB 188 338)A03
- EERC 69-1 "Earthquake Engineering Research at Berkeley," - 1969 (PB 187 906)A11
- EERC 69-2 "Nonlinear Seismic Response of Earth Structures," by M. Dibaj and J. Penzien - 1969 (PB 187 904)A08
- EERC 69-3 "Probabilistic Study of the Behavior of Structures During Earthquakes," by R. Ruiz and J. Penzien - 1969 (PB 187 886)A06
- EERC 69-4 "Numerical Solution of Boundary Value Problems in Structural Mechanics by Reduction to an Initial Value Formulation," by N. Distefano and J. Schujman - 1969 (PB 187 942)A02
- EERC 69-5 "Dynamic Programming and the Solution of the Biharmonic Equation," by N. Distefano - 1969 (PB 187 941)A03
- EERC 69-6 "Stochastic Analysis of Offshore Tower Structures," by A.K. Malhotra and J. Penzien - 1969 (PB 187 903)A09
- EERC 69-7 "Rock Motion Accelerograms for High Magnitude Earthquakes," by H.B. Seed and I.M. Idriss - 1969 (PB 187 940)A02
- EERC 69-8 "Structural Dynamics Testing Facilities at the University of California, Berkeley," by R.M. Stephen, J.G. Bouwkamp, R.W. Clough and J. Penzien - 1969 (PB 189 111)A04
- EERC 69-9 "Seismic Response of Soil Deposits Underlain by Sloping Rock Boundaries," by H. Dezfulian and H.B. Seed - 1969 (PB 189 114)A03
- EERC 69-10 "Dynamic Stress Analysis of Axisymmetric Structures Under Arbitrary Loading," by S. Ghosh and E.L. Wilson - 1969 (PB 189 026)A10
- EERC 69-11 "Seismic Behavior of Multistory Frames Designed by Different Philosophies," by J.C. Anderson and V. V. Bertero - 1969 (PB 190 662)A10
- EERC 69-12 "Stiffness Degradation of Reinforcing Concrete Members Subjected to Cyclic Flexural Moments," by V.V. Bertero, B. Bresler and H. Ming Liao - 1969 (PB 202 942)A07
- EERC 69-13 "Response of Non-Uniform Soil Deposits to Travelling Seismic Waves," by H. Dezfulian and H.B. Seed - 1969 (PB 191 023)A03
- EERC 69-14 "Damping Capacity of a Model Steel Structure," by D. Rea, R.W. Clough and J.G. Bouwkamp - 1969 (PB 190 663)A06
- EERC 69-15 "Influence of Local Soil Conditions on Building Damage Potential during Earthquakes," by H.B. Seed and I.M. Idriss - 1969 (PB 191 036)A03
- EERC 69-16 "The Behavior of Sands Under Seismic Loading Conditions," by M.L. Silver and H.B. Seed - 1969 (AD 714 982)A07
- EERC 70-1 "Earthquake Response of Gravity Dams," by A.K. Chopra - 1970 (AD 709 640)A03
- EERC 70-2 "Relationships between Soil Conditions and Building Damage in the Caracas Earthquake of July 29, 1967," by H.B. Seed, I.M. Idriss and H. Dezfulian - 1970 (PB 195 762)A05
- EERC 70-3 "Cyclic Loading of Full Size Steel Connections," by E.P. Popov and R.M. Stephen - 1970 (PB 213 545)A04
- EERC 70-4 "Seismic Analysis of the Charaima Building, Caraballeda, Venezuela," by Subcommittee of the SEAONC Research Committee: V.V. Bertero, P.F. Fratessa, S.A. Mahin, J.H. Sexton, A.C. Scordelis, E.L. Wilson, L.A. Wyllie, H.B. Seed and J. Penzien, Chairman - 1970 (PB 201 455)A06

- EERC 70-5 "A Computer Program for Earthquake Analysis of Dams," by A.K. Chopra and P. Chakrabarti - 1970 (AD 723 994)A05
- EERC 70-6 "The Propagation of Love Waves Across Non-Horizontally Layered Structures," by J. Lysmer and L.A. Drake 1970 (PB 197 896)A03
- EERC 70-7 "Influence of Base Rock Characteristics on Ground Response," by J. Lysmer, H.B. Seed and P.B. Schnabel 1970 (PB 197 897)A03
- EERC 70-8 "Applicability of Laboratory Test Procedures for Measuring Soil Liquefaction Characteristics under Cyclic Loading," by H.B. Seed and W.H. Peacock - 1970 (PB 198 016)A03
- EERC 70-9 "A Simplified Procedure for Evaluating Soil Liquefaction Potential," by H.B. Seed and I.M. Idriss - 1970 (PB 198 009)A03
- EERC 70-10 "Soil Moduli and Damping Factors for Dynamic Response Analysis," by H.B. Seed and I.M. Idriss - 1970 (PB 197 869)A03
- EERC 71-1 "Koyna Earthquake of December 11, 1967 and the Performance of Koyna Dam," by A.K. Chopra and P. Chakrabarti 1971 (AD 731 496)A06
- EERC 71-2 "Preliminary In-Situ Measurements of Anelastic Absorption in Soils Using a Prototype Earthquake Simulator," by R.D. Borchardt and P.W. Rodgers - 1971 (PB 201 454)A03
- EERC 71-3 "Static and Dynamic Analysis of Inelastic Frame Structures," by F.L. Porter and G.H. Powell - 1971 (PB 210 135)A06
- EERC 71-4 "Research Needs in Limit Design of Reinforced Concrete Structures," by V.V. Bertero - 1971 (PB 202 943)A04
- EERC 71-5 "Dynamic Behavior of a High-Rise Diagonally Braced Steel Building," by D. Rea, A.A. Shah and J.G. Bouwhuis 1971 (PB 203 584)A06
- EERC 71-6 "Dynamic Stress Analysis of Porous Elastic Solids Saturated with Compressible Fluids," by J. Ghaboussi and E. L. Wilson - 1971 (PB 211 396)A06
- EERC 71-7 "Inelastic Behavior of Steel Beam-to-Column Subassemblages," by H. Krawinkler, V.V. Bertero and E.P. Popov 1971 (PB 211 335)A14
- EERC 71-8 "Modification of Seismograph Records for Effects of Local Soil Conditions," by P. Schnabel, H.B. Seed and J. Lysmer - 1971 (PB 214 450)A03
- EERC 72-1 "Static and Earthquake Analysis of Three Dimensional Frame and Shear Wall Buildings," by E.L. Wilson and H.H. Dovey - 1972 (PB 212 904)A05
- EERC 72-2 "Accelerations in Rock for Earthquakes in the Western United States," by P.B. Schnabel and H.B. Seed - 1972 (PB 213 100)A03
- EERC 72-3 "Elastic-Plastic Earthquake Response of Soil-Building Systems," by T. Minami - 1972 (PB 214 868)A08
- EERC 72-4 "Stochastic Inelastic Response of Offshore Towers to Strong Motion Earthquakes," by M.K. Kaul - 1972 (PB 215 713)A05
- EERC 72-5 "Cyclic Behavior of Three Reinforced Concrete Flexural Members with High Shear," by E.P. Popov, V.V. Bertero and H. Krawinkler - 1972 (PB 214 555)A05
- EERC 72-6 "Earthquake Response of Gravity Dams Including Reservoir Interaction Effects," by P. Chakrabarti and A.K. Chopra - 1972 (AD 762 330)A08
- EERC 72-7 "Dynamic Properties of Pine Flat Dam," by D. Rea, C.Y. Liaw and A.K. Chopra - 1972 (AD 763 928)A05
- EERC 72-8 "Three Dimensional Analysis of Building Systems," by E.L. Wilson and H.H. Dovey - 1972 (PB 222 438)A06
- EERC 72-9 "Rate of Loading Effects on Uncracked and Repaired Reinforced Concrete Members," by S. Mahin, V.V. Bertero, D. Rea and M. Atalay - 1972 (PB 224 520)A08
- EERC 72-10 "Computer Program for Static and Dynamic Analysis of Linear Structural Systems," by E.L. Wilson, K.-J. Bathe, J.E. Paterson and H.H. Dovey - 1972 (PB 220 437)A04
- EERC 72-11 "Literature Survey - Seismic Effects on Highway Bridges," by T. Iwasaki, J. Penzien and R.W. Clough - 1972 (PB 215 613)A19
- EERC 72-12 "SHAKE-A Computer Program for Earthquake Response Analysis of Horizontally Layered Sites," by P.B. Schnabel and J. Lysmer - 1972 (PB 220 207)A06
- EERC 73-1 "Optimal Seismic Design of Multistory Frames," by V.V. Bertero and H. Kamil - 1973
- EERC 73-2 "Analysis of the Slides in the San Fernando Dams During the Earthquake of February 9, 1971," by H.B. Seed, K.L. Lee, I.M. Idriss and F. Makdisi - 1973 (PB 223 402)A14

- EERC 73-3 "Computer Aided Ultimate Load Design of Unbraced Multistory Steel Frames," by M.B. El-Hafez and G.H. Powell 1973 (PB 248 315)A09
- EERC 73-4 "Experimental Investigation into the Seismic Behavior of Critical Regions of Reinforced Concrete Components as Influenced by Moment and Shear," by M. Celebi and J. Penzien - 1973 (PB 215 884)A09
- EERC 73-5 "Hysteretic Behavior of Epoxy-Repaired Reinforced Concrete Beams," by M. Celebi and J. Penzien - 1973 (PB 239 568)A03
- EERC 73-6 "General Purpose Computer Program for Inelastic Dynamic Response of Plane Structures," by A. Kanaan and G.H. Powell - 1973 (PB 221 260)A08
- EERC 73-7 "A Computer Program for Earthquake Analysis of Gravity Dams Including Reservoir Interaction," by P. Chakrabarti and A.K. Chopra - 1973 (AD 766 271)A04
- EERC 73-8 "Behavior of Reinforced Concrete Deep Beam-Column Subassemblages Under Cyclic Loads," by O. Küstü and J.G. Bouwkamp - 1973 (PB 246 117)A12
- EERC 73-9 "Earthquake Analysis of Structure-Foundation Systems," by A.K. Vaish and A.K. Chopra - 1973 (AD 766 272)A07
- EERC 73-10 "Deconvolution of Seismic Response for Linear Systems," by R.B. Reimer - 1973 (PB 227 179)A08
- EERC 73-11 "SAP IV: A Structural Analysis Program for Static and Dynamic Response of Linear Systems," by K.-J. Bathe, E.L. Wilson and F.E. Peterson - 1973 (PB 221 967)A09
- EERC 73-12 "Analytical Investigations of the Seismic Response of Long, Multiple Span Highway Bridges," by W.S. Tseng and J. Penzien - 1973 (PB 227 816)A10
- EERC 73-13 "Earthquake Analysis of Multi-Story Buildings Including Foundation Interaction," by A.K. Chopra and J.A. Gutierrez - 1973 (PB 222 970)A03
- EERC 73-14 "ADAP: A Computer Program for Static and Dynamic Analysis of Arch Dams," by R.W. Clough, J.M. Raphael and S. Mojtahedi - 1973 (PB 223 763)A09
- EERC 73-15 "Cyclic Plastic Analysis of Structural Steel Joints," by R.B. Pinkney and R.W. Clough - 1973 (PB 226 843)A08
- EERC 73-16 "QAD-4: A Computer Program for Evaluating the Seismic Response of Soil Structures by Variable Damping Finite Element Procedures," by I.M. Idriss, J. Lysmer, R. Hwang and H.B. Seed - 1973 (PB 229 424)A05
- EERC 73-17 "Dynamic Behavior of a Multi-Story Pyramid Shaped Building," by R.M. Stephen, J.P. Hollings and J.G. Bouwkamp - 1973 (PB 240 718)A06
- EERC 73-18 "Effect of Different Types of Reinforcing on Seismic Behavior of Short Concrete Columns," by V.V. Bertero, J. Hollings, O. Küstü, R.M. Stephen and J.G. Bouwkamp - 1973
- EERC 73-19 "Olive View Medical Center Materials Studies, Phase I," by B. Bresler and V.V. Bertero - 1973 (PB 235 986)A06
- EERC 73-20 "Linear and Nonlinear Seismic Analysis Computer Programs for Long Multiple-Span Highway Bridges," by W.S. Tseng and J. Penzien - 1973
- EERC 73-21 "Constitutive Models for Cyclic Plastic Deformation of Engineering Materials," by J.M. Kelly and P.P. Gillis 1973 (PB 226 024)A03
- EERC 73-22 "DRAIN - 2D User's Guide," by G.H. Powell - 1973 (PB 227 016)A05
- EERC 73-23 "Earthquake Engineering at Berkeley - 1973," (PB 226 033)A11
- EERC 73-24 Unassigned
- EERC 73-25 "Earthquake Response of Axisymmetric Tower Structures Surrounded by Water," by C.Y. Liaw and A.K. Chopra 1973 (AD 773 052)A09
- EERC 73-26 "Investigation of the Failures of the Olive View Stairtowers During the San Fernando Earthquake and Their Implications on Seismic Design," by V.V. Bertero and R.G. Collins - 1973 (PB 235 106)A13
- EERC 73-27 "Further Studies on Seismic Behavior of Steel Beam-Column Subassemblages," by V.V. Bertero, H. Krawinkler and E.P. Popov - 1973 (PB 234 172)A06
- EERC 74-1 "Seismic Risk Analysis," by C.S. Oliveira - 1974 (PB 235 920)A06
- EERC 74-2 "Settlement and Liquefaction of Sands Under Multi-Directional Shaking," by R. Pyke, C.K. Chan and H.B. Seed 1974
- EERC 74-3 "Optimum Design of Earthquake Resistant Shear Buildings," by D. Ray, K.S. Pister and A.K. Chopra - 1974 (PB 231 172)A06
- EERC 74-4 "LUSH - A Computer Program for Complex Response Analysis of Soil-Structure Systems," by J. Lysmer, T. Udaka, H.B. Seed and R. Hwang - 1974 (PB 236 796)A05

- EERC 74-5 "Sensitivity Analysis for Hysteretic Dynamic Systems: Applications to Earthquake Engineering," by D. Ray 1974 (PB 233 213)A06
- EERC 74-6 "Soil Structure Interaction Analyses for Evaluating Seismic Response," by H.B. Seed, J. Lysmer and R. Hwang 1974 (PB 236 519)A04
- EERC 74-7 Unassigned
- EERC 74-8 "Shaking Table Tests of a Steel Frame - A Progress Report," by R.W. Clough and D. Tang - 1974 (PB 240 869)A03
- EERC 74-9 "Hysteretic Behavior of Reinforced Concrete Flexural Members with Special Web Reinforcement," by V.V. Bertero, E.P. Popov and T.Y. Wang - 1974 (PB 236 797)A07
- EERC 74-10 "Applications of Reliability-Based, Global Cost Optimization to Design of Earthquake Resistant Structures," by E. Vitiello and K.S. Pister - 1974 (PB 237 231)A06
- EERC 74-11 "Liquefaction of Gravelly Soils Under Cyclic Loading Conditions," by R.T. Wong, H.B. Seed and C.K. Chan 1974 (PB 242 042)A03
- EERC 74-12 "Site-Dependent Spectra for Earthquake-Resistant Design," by H.B. Seed, C. Ugas and J. Lysmer - 1974 (PB 240 953)A03
- EERC 74-13 "Earthquake Simulator Study of a Reinforced Concrete Frame," by P. Hidalgo and R.W. Clough - 1974 (PB 241 944)A13
- EERC 74-14 "Nonlinear Earthquake Response of Concrete Gravity Dams," by N. Pal - 1974 (AD/A 006 583)A06
- EERC 74-15 "Modeling and Identification in Nonlinear Structural Dynamics - I. One Degree of Freedom Models," by N. Distefano and A. Rath - 1974 (PB 241 548)A06
- EERC 75-1 "Determination of Seismic Design Criteria for the Dumbarton Bridge Replacement Structure, Vol. I: Description, Theory and Analytical Modeling of Bridge and Parameters," by F. Baron and S.-H. Pang - 1975 (PB 259 407)A15
- EERC 75-2 "Determination of Seismic Design Criteria for the Dumbarton Bridge Replacement Structure, Vol. II: Numerical Studies and Establishment of Seismic Design Criteria," by F. Baron and S.-H. Pang - 1975 (PB 259 408)A11 (For set of EERC 75-1 and 75-2 (PB 259 406))
- EERC 75-3 "Seismic Risk Analysis for a Site and a Metropolitan Area," by C.S. Oliveira - 1975 (PB 248 134)A09
- EERC 75-4 "Analytical Investigations of Seismic Response of Short, Single or Multiple-Span Highway Bridges," by M.-C. Chen and J. Penzien - 1975 (PB 241 454)A09
- EERC 75-5 "An Evaluation of Some Methods for Predicting Seismic Behavior of Reinforced Concrete Buildings," by S.A. Mahin and V.V. Bertero - 1975 (PB 246 306)A16
- EERC 75-6 "Earthquake Simulator Study of a Steel Frame Structure, Vol. I: Experimental Results," by R.W. Clough and D.T. Tang - 1975 (PB 243 981)A13
- EERC 75-7 "Dynamic Properties of San Bernardino Intake Tower," by D. Rea, C.-Y. Liaw and A.K. Chopra - 1975 (AD/A008 406) A05
- EERC 75-8 "Seismic Studies of the Articulation for the Dumbarton Bridge Replacement Structure, Vol. I: Description, Theory and Analytical Modeling of Bridge Components," by F. Baron and R.E. Hamati - 1975 (PB 251 539)A07
- EERC 75-9 "Seismic Studies of the Articulation for the Dumbarton Bridge Replacement Structure, Vol. 2: Numerical Studies of Steel and Concrete Girder Alternates," by F. Baron and R.E. Hamati - 1975 (PB 251 540)A10
- EERC 75-10 "Static and Dynamic Analysis of Nonlinear Structures," by D.P. Mondkar and G.H. Powell - 1975 (PB 242 434)A08
- EERC 75-11 "Hysteretic Behavior of Steel Columns," by E.P. Popov, V.V. Bertero and S. Chandramouli - 1975 (PB 252 365)A11
- EERC 75-12 "Earthquake Engineering Research Center Library Printed Catalog," - 1975 (PB 243 711)A26
- EERC 75-13 "Three Dimensional Analysis of Building Systems (Extended Version)," by E.L. Wilson, J.P. Hollings and H.N. Dovey - 1975 (PB 243 989)A07
- EERC 75-14 "Determination of Soil Liquefaction Characteristics by Large-Scale Laboratory Tests," by P. De Alba, C.K. Chan and H.B. Seed - 1975 (NUREG 0027)A08
- EERC 75-15 "A Literature Survey - Compressive, Tensile, Bond and Shear Strength of Masonry," by R.L. Mayes and R.W. Clough - 1975 (PB 246 292)A10
- EERC 75-16 "Hysteretic Behavior of Ductile Moment Resisting Reinforced Concrete Frame Components," by V.V. Bertero and E.P. Popov - 1975 (PB 246 388)A05
- EERC 75-17 "Relationships Between Maximum Acceleration, Maximum Velocity, Distance from Source, Local Site Conditions for Moderately Strong Earthquakes," by H.B. Seed, R. Murarka, J. Lysmer and I.M. Idriss - 1975 (PB 248 172)A03
- EERC 75-18 "The Effects of Method of Sample Preparation on the Cyclic Stress-Strain Behavior of Sands," by J. Nulilis, C.K. Chan and H.B. Seed - 1975 (Summarized in EERC 75-28)

- EERC 75-19 "The Seismic Behavior of Critical Regions of Reinforced Concrete Components as Influenced by Moment, Shear and Axial Force," by M.B. Atalay and J. Penzien - 1975 (PB 258 842)A11
- EERC 75-20 "Dynamic Properties of an Eleven Story Masonry Building," by R.M. Stephen, J.P. Hollings, J.G. Bouwkamp and D. Jurukovski - 1975 (PB 246 945)A04
- EERC 75-21 "State-of-the-Art in Seismic Strength of Masonry - An Evaluation and Review," by R.L. Mayes and R.W. Clough - 1975 (PB 249 040)A07
- EERC 75-22 "Frequency Dependent Stiffness Matrices for Viscoelastic Half-Plane Foundations," by A.K. Chopra, P. Chakrabarti and G. Dasgupta - 1975 (PB 248 121)A07
- EERC 75-23 "Hysteretic Behavior of Reinforced Concrete Framed Walls," by T.Y. Wong, V.V. Bertero and E.P. Popov - 1975
- EERC 75-24 "Testing Facility for Subassemblages of Frame-Wall Structural Systems," by V.V. Bertero, E.P. Popov and T. Endo - 1975
- EERC 75-25 "Influence of Seismic History on the Liquefaction Characteristics of Sands," by H.B. Seed, K. Mori and C.K. Chan - 1975 (Summarized in EERC 75-28)
- EERC 75-26 "The Generation and Dissipation of Pore Water Pressures during Soil Liquefaction," by H.B. Seed, P.P. Martin and J. Lysmer - 1975 (PB 252 648)A03
- EERC 75-27 "Identification of Research Needs for Improving Aseismic Design of Building Structures," by V.V. Bertero - 1975 (PB 248 136)A05
- EERC 75-28 "Evaluation of Soil Liquefaction Potential during Earthquakes," by H.B. Seed, I. Arango and C.K. Chan - 1975 (NUREG 0026)A13
- EERC 75-29 "Representation of Irregular Stress Time Histories by Equivalent Uniform Stress Series in Liquefaction Analyses," by H.B. Seed, I.M. Idriss, F. Makdisi and N. Banerjee - 1975 (PB 252 635)A03
- EERC 75-30 "FLUSH - A Computer Program for Approximate 3-D Analysis of Soil-Structure Interaction Problems," by J. Lysmer, T. Udaka, C.-F. Tsai and H.B. Seed - 1975 (PB 259 332)A07
- EERC 75-31 "ALUSH - A Computer Program for Seismic Response Analysis of Axisymmetric Soil-Structure Systems," by E. Berger, J. Lysmer and H.B. Seed - 1975
- EERC 75-32 "TRIP and TRAVEL - Computer Programs for Soil-Structure Interaction Analysis with Horizontally Travelling Waves," by T. Udaka, J. Lysmer and H.B. Seed - 1975
- EERC 75-33 "Predicting the Performance of Structures in Regions of High Seismicity," by J. Penzien - 1975 (PB 248 130)A03
- EERC 75-34 "Efficient Finite Element Analysis of Seismic Structure - Soil - Direction," by J. Lysmer, H.B. Seed, T. Udaka, R.N. Hwang and C.-F. Tsai - 1975 (PB 253 570)A03
- EERC 75-35 "The Dynamic Behavior of a First Story Girder of a Three-Story Steel Frame Subjected to Earthquake Loading," by R.W. Clough and L.-Y. Li - 1975 (PB 248 841)A05
- EERC 75-36 "Earthquake Simulator Study of a Steel Frame Structure, Volume II - Analytical Results," by D.T. Tang - 1975 (PB 252 926)A10
- EERC 75-37 "ANSR-I General Purpose Computer Program for Analysis of Non-Linear Structural Response," by D.P. Mondkar and G.H. Powell - 1975 (PB 252 386)A08
- EERC 75-38 "Nonlinear Response Spectra for Probabilistic Seismic Design and Damage Assessment of Reinforced Concrete Structures," by M. Murakami and J. Penzien - 1975 (PB 259 530)A05
- EERC 75-39 "Study of a Method of Feasible Directions for Optimal Elastic Design of Frame Structures Subjected to Earthquake Loading," by N.D. Walker and K.S. Pister - 1975 (PB 257 781)A06
- EERC 75-40 "An Alternative Representation of the Elastic-Viscoelastic Analogy," by G. Dasgupta and J.L. Sackman - 1975 (PB 252 173)A03
- EERC 75-41 "Effect of Multi-Directional Shaking on Liquefaction of Sands," by H.B. Seed, R. Pyke and G.R. Martin - 1975 (PB 258 781)A03
- EERC 76-1 "Strength and Ductility Evaluation of Existing Low-Rise Reinforced Concrete Buildings - Screening Method," by T. Okada and B. Bresler - 1976 (PB 257 906)A11
- EERC 76-2 "Experimental and Analytical Studies on the Hysteretic Behavior of Reinforced Concrete Rectangular and T-Beams," by S.-Y.M. Ma, E.P. Popov and V.V. Bertero - 1976 (PB 260 843)A12
- EERC 76-3 "Dynamic Behavior of a Multistory Triangular-Shaped Building," by J. Petrovski, R.M. Stephen, E. Gartenbaum and J.G. Bouwkamp - 1976 (PB 273 279)A07
- EERC 76-4 "Earthquake Induced Deformations of Earth Dams," by N. Serff, H.B. Seed, F.I. Makdisi & C.-Y. Chang - 1976 (PB 292 065)A08

- EERC 76-5 "Analysis and Design of Tube-Type Tall Building Structures," by H. de Clercq and G.H. Powell - 1976 (PB 252 220)A10
- EERC 76-6 "Time and Frequency Domain Analysis of Three-Dimensional Ground Motions, San Fernando Earthquake," by T. Kubo and J. Penzien (PB 260 556)A11
- EERC 76-7 "Expected Performance of Uniform Building Code Design Masonry Structures," by R.L. Mayes, Y. Omote, S.W. Chen and R.W. Clough - 1976 (PB 270 098)A05
- EERC 76-8 "Cyclic Shear Tests of Masonry Piers, Volume 1 - Test Results," by R.L. Mayes, Y. Omote, R.W. Clough - 1976 (PB 264 424)A06
- EERC 76-9 "A Substructure Method for Earthquake Analysis of Structure - Soil Interaction," by J.A. Gutierrez and A.K. Chopra - 1976 (PB 257 783)A08
- EERC 76-10 "Stabilization of Potentially Liquefiable Sand Deposits using Gravel Drain Systems," by H.B. Seed and J.R. Booker - 1976 (PB 258 820)A04
- EERC 76-11 "Influence of Design and Analysis Assumptions on Computed Inelastic Response of Moderately Tall Frames," by G.H. Powell and D.G. Row - 1976 (PB 271 409)A06
- EERC 76-12 "Sensitivity Analysis for Hysteretic Dynamic Systems: Theory and Applications," by D. Ray, K.S. Pister and E. Polak - 1976 (PB 262 859)A04
- EERC 76-13 "Coupled Lateral Torsional Response of Buildings to Ground Shaking," by C.L. Kan and A.K. Chopra - 1976 (PB 257 907)A09
- EERC 76-14 "Seismic Analyses of the Banco de America," by V.V. Bertero, S.A. Mahin and J.A. Hollings - 1976
- EERC 76-15 "Reinforced Concrete Frame 2: Seismic Testing and Analytical Correlation," by R.W. Clough and J. Gidwani - 1976 (PB 261 323)A08
- EERC 76-16 "Cyclic Shear Tests of Masonry Piers, Volume 2 - Analysis of Test Results," by R.L. Mayes, Y. Omote and R.W. Clough - 1976
- EERC 76-17 "Structural Steel Bracing Systems: Behavior Under Cyclic Loading," by E.P. Popov, K. Takanashi and C.W. Roeder - 1976 (PB 260 715)A05
- EERC 76-18 "Experimental Mode) Studies on Seismic Response of High Curved Overcrossings," by D. Williams and W.G. Godden - 1976 (PB 269 548)A08
- EERC 76-19 "Effects of Non-Uniform Seismic Disturbances on the Dumbarton Bridge Replacement Structure," by F. Baron and R.E. Hamati - 1976 (PB 282 981)A16
- EERC 76-20 "Investigation of the Inelastic Characteristics of a Single Story Steel Structure Using System Identification and Shaking Table Experiments," by V.C. Matzen and H.D. McNiven - 1976 (PB 258 453)A07
- EERC 76-21 "Capacity of Columns with Splice Imperfections," by E.P. Popov, R.M. Stephen and R. Philbrick - 1976 (PB 260 378)A04
- EERC 76-22 "Response of the Olive View Hospital Main Building during the San Fernando Earthquake," by S. A. Mahin, V.V. Bertero, A.K. Chopra and R. Collins - 1976 (PB 271 425)A14
- EERC 76-23 "A Study on the Major Factors Influencing the Strength of Masonry Prisms," by N.M. Mostaghel, R.L. Mayes, R. W. Clough and S.W. Chen - 1976 (Not published)
- EERC 76-24 "GADFLA - A Computer Program for the Analysis of Pore Pressure Generation and Dissipation during Cyclic or Earthquake Loading," by J.R. Booker, M.S. Rahman and H.B. Seed - 1976 (PB 263 947)A04
- EERC 76-25 "Seismic Safety Evaluation of a R/C School Building," by B. Bresler and J. Axley - 1976
- EERC 76-26 "Correlative Investigations on Theoretical and Experimental Dynamic Behavior of a Model Bridge Structure," by K. Kawashima and J. Penzien - 1976 (PB 263 388)A11
- EERC 76-27 "Earthquake Response of Coupled Shear Wall Buildings," by T. Srichatrapimuk - 1976 (PB 265 157)A07
- EERC 76-28 "Tensile Capacity of Partial Penetration Welds," by E.P. Popov and R.M. Stephen - 1976 (PB 262 899)A03
- EERC 76-29 "Analysis and Design of Numerical Integration Methods in Structural Dynamics," by H.M. Hilber - 1976 (PB 264 410)A06
- EERC 76-30 "Contribution of a Floor System to the Dynamic Characteristics of Reinforced Concrete Buildings," by L.E. Malik and V.V. Bertero - 1976 (PB 272 247)A13
- EERC 76-31 "The Effects of Seismic Disturbances on the Golden Gate Bridge," by F. Baron, M. Arikan and R.E. Hamati - 1976 (PB 272 279)A09
- EERC 76-32 "Infilled Frames in Earthquake Resistant Construction," by R.E. Klingner and V.V. Bertero - 1976 (PB 265 892)A13

- UCB/EERC-77/01 "PLUSH - A Computer Program for Probabilistic Finite Element Analysis of Seismic Soil-Structure Interaction," by M.P. Romo Organista, J. Lysmer and H.B. Seed - 1977
- UCB/EERC-77/02 "Soil-Structure Interaction Effects at the Humboldt Bay Power Plant in the Ferndale Earthquake of June 7, 1975," by J.E. Valera, H.B. Seed, C.F. Tsai and J. Lysmer - 1977 (PB 265 795)A04
- UCB/EERC-77/03 "Influence of Sample Disturbance on Sand Response to Cyclic Loading," by K. Mori, H.B. Seed and C.K. Chan - 1977 (PB 267 352)A04
- UCB/EERC-77/04 "Seismological Studies of Strong Motion Records," by J. Shoja-Taheri - 1977 (PB 269 655)A10
- UCB/EERC-77/05 "Testing Facility for Coupled-Shear Walls," by L. Li-Hyung, V.V. Bertero and E.P. Popov - 1977
- UCB/EERC-77/06 "Developing Methodologies for Evaluating the Earthquake Safety of Existing Buildings," by No. 1 - B. Bresler; No. 2 - B. Bresler, T. Okada and D. Zisling; No. 3 - T. Okada and B. Bresler; No. 4 - V.V. Bertero and B. Bresler - 1977 (PB 267 354)A08
- UCB/EERC-77/07 "A Literature Survey - Transverse Strength of Masonry Walls," by Y. Omote, R.L. Mayes, S.W. Chen and R.W. Clough - 1977 (PB 277 933)A07
- UCB/EERC-77/08 "DRAIN-TABS: A Computer Program for Inelastic Earthquake Response of Three Dimensional Buildings," by R. Guendelman-Israel and G.H. Powell - 1977 (PB 270 693)A07
- UCB/EERC-77/09 "SUBWALL: A Special Purpose Finite Element Computer Program for Practical Elastic Analysis and Design of Structural Walls with Substructure Option," by D.Q. Le, H. Peterson and E.P. Popov - 1977 (PB 270 567)A05
- UCB/EERC-77/10 "Experimental Evaluation of Seismic Design Methods for Broad Cylindrical Tanks," by D.P. Clough (PB 272 280)A13
- UCB/EERC-77/11 "Earthquake Engineering Research at Berkeley - 1976," - 1977 (PB 273 507)A09
- UCB/EERC-77/12 "Automated Design of Earthquake Resistant Multistory Steel Building Frames," by N.D. Walker, Jr. - 1977 (PB 276 526)A09
- UCB/EERC-77/13 "Concrete Confined by Rectangular Hoops Subjected to Axial Loads," by J. Vallenias, V.V. Bertero and E.P. Popov - 1977 (PB 275 165)A06
- UCB/EERC-77/14 "Seismic Strain Induced in the Ground During Earthquakes," by Y. Sugimura - 1977 (PB 284 201)A04
- UCB/EERC-77/15 "Bond Deterioration under Generalized Loading," by V.V. Bertero, E.P. Popov and S. Viathanatapa - 1977
- UCB/EERC-77/16 "Computer Aided Optimum Design of Ductile Reinforced Concrete Moment Resisting Frames," by S.W. Zagajeski and V.V. Bertero - 1977 (PB 280 137)A07
- UCB/EERC-77/17 "Earthquake Simulation Testing of a Stepping Frame with Energy-Absorbing Devices," by J.M. Kelly and D.F. Tsztoo - 1977 (PB 273 506)A04
- UCB/EERC-77/18 "Inelastic Behavior of Eccentrically Braced Steel Frames under Cyclic Loadings," by C.W. Roeder and E.P. Popov - 1977 (PB 275 526)A15
- UCB/EERC-77/19 "A Simplified Procedure for Estimating Earthquake-Induced Deformations in Dams and Embankments," by F.I. Makdisi and H.B. Seed - 1977 (PB 276 820)A04
- UCB/EERC-77/20 "The Performance of Earth Dams during Earthquakes," by H.B. Seed, F.I. Makdisi and P. de Alba - 1977 (PB 276 821)A04
- UCB/EERC-77/21 "Dynamic Plastic Analysis Using Stress Resultant Finite Element Formulation," by P. Lukunapvasit and J.M. Kelly - 1977 (PB 275 453)A04
- UCB/EERC-77/22 "Preliminary Experimental Study of Seismic Uplift of a Steel Frame," by R.W. Clough and A.A. Huckelbridge 1977 (PB 278 769)A08
- UCB/EERC-77/23 "Earthquake Simulator Tests of a Nine-Story Steel Frame with Columns Allowed to Uplift," by A.A. Huckelbridge - 1977 (PB 277 944)A09
- UCB/EERC-77/24 "Nonlinear Soil-Structure Interaction of Skew Highway Bridges," by M.-C. Chen and J. Penzien - 1977 (PB 276 176)A07
- UCB/EERC-77/25 "Seismic Analysis of an Offshore Structure Supported on Pile Foundations," by D.D.-N. Liou and J. Penzien 1977 (PB 283 180)A06
- UCB/EERC-77/26 "Dynamic Stiffness Matrices for Homogeneous Viscoelastic Half-Planes," by G. Dasgupta and A.K. Chopra - 1977 (PB 279 654)A06
- UCB/EERC-77/27 "A Practical Soft Story Earthquake Isolation System," by J.M. Kelly, J.M. Eidinger and C.J. Derham - 1977 (PB 276 814)A07
- UCB/EERC-77/28 "Seismic Safety of Existing Buildings and Incentives for Hazard Mitigation in San Francisco: An Exploratory Study," by A.J. Meltner - 1977 (PB 281 970)A05
- UCB/EERC-77/29 "Dynamic Analysis of Electrohydraulic Shaking Tables," by D. Rea, S. Abedi-Hayati and Y. Takahashi 1977 (PB 282 569)A04
- UCB/EERC-77/30 "An Approach for Improving Seismic - Resistant Behavior of Reinforced Concrete Interior Joints," by B. Galunic, V.V. Bertero and E.P. Popov - 1977 (PB 290 870)A06

- UCB/EERC-78/01 "The Development of Energy-Absorbing Devices for Aseismic Base Isolation Systems," by J.M. Kelly and D.F. Tsztsoo - 1978 (PB 284 978)A04
- UCB/EERC-78/02 "Effect of Tensile Prestrain on the Cyclic Response of Structural Steel Connections," by J.G. Bouwkamp and A. Mukhopadhyay - 1978
- UCB/EERC-78/03 "Experimental Results of an Earthquake Isolation System using Natural Rubber Bearings," by J.M. Eidinger and J.M. Kelly - 1978 (PB 281 686)A04
- UCB/EERC-78/04 "Seismic Behavior of Tall Liquid Storage Tanks," by A. Niwa - 1978 (PB 284 017)A14
- UCB/EERC-78/05 "Hysteretic Behavior of Reinforced Concrete Columns Subjected to High Axial and Cyclic Shear Forces," by S.W. Zagajeski, V.V. Bertero and J.G. Bouwkamp - 1978 (PB 283 858)A13
- UCB/EERC-78/06 "Inelastic Beam-Column Elements for the ANSR-I Program," by A. Riahi, D.G. Row and G.H. Powell - 1978
- UCB/EERC-78/07 "Studies of Structural Response to Earthquake Ground Motion," by O.A. Lopez and A.K. Chopra - 1978 (PB 282 790)A05
- UCB/EERC-78/08 "A Laboratory Study of the Fluid-Structure Interaction of Submerged Tanks and Caissons in Earthquakes," by R.C. Byrd - 1978 (PB 284 957)A08
- UCB/EERC-78/09 "Model for Evaluating Damageability of Structures," by I. Sakamoto and B. Bresler - 1978
- UCB/EERC-78/10 "Seismic Performance of Nonstructural and Secondary Structural Elements," by I. Sakamoto - 1978
- UCB/EERC-78/11 "Mathematical Modelling of Hysteresis Loops for Reinforced Concrete Columns," by S. Nakata, T. Sproul and J. Penzien - 1978
- UCB/EERC-78/12 "Damageability in Existing Buildings," by T. Blejwas and B. Bresler - 1978
- UCB/EERC-78/13 "Dynamic Behavior of a Pedestal Base Multistory Building," by R.M. Stephen, E.L. Wilson, J.G. Bouwkamp and M. Button - 1978 (PB 286 650)A08
- UCB/EERC-78/14 "Seismic Response of Bridges - Case Studies," by R.A. Imbsen, V. Nutt and J. Penzien - 1978 (PB 286 503)A10
- UCB/EERC-78/15 "A Substructure Technique for Nonlinear Static and Dynamic Analysis," by D.G. Row and G.H. Powell - 1978 (PB 288 077)A10
- UCB/EERC-78/16 "Seismic Risk Studies for San Francisco and for the Greater San Francisco Bay Area," by C.S. Oliveira - 1978
- UCB/EERC-78/17 "Strength of Timber Roof Connections Subjected to Cyclic Loads," by P. Gülkan, R.L. Mayes and R.W. Clough - 1978
- UCB/EERC-78/18 "Response of K-Braced Steel Frame Models to Lateral Loads," by J.G. Bouwkamp, R.M. Stephen and E.P. Popov - 1978
- UCB/EERC-78/19 "Rational Design Methods for Light Equipment in Structures Subjected to Ground Motion," by J.L. Sackman and J.M. Kelly - 1978 (PB 292 357)A04
- UCB/EERC-78/20 "Testing of a Wind Restraint for Aseismic Base Isolation," by J.M. Kelly and D.E. Chitty - 1978 (PB 292 833)A03
- UCB/EERC-78/21 "APOLLO - A Computer Program for the Analysis of Pore Pressure Generation and Dissipation in Horizontal Sand Layers During Cyclic or Earthquake Loading," by P.P. Martin and H.B. Seed - 1978 (PB 292 835)A04
- UCB/EERC-78/22 "Optimal Design of an Earthquake Isolation System," by M.A. Bhatti, K.S. Pister and E. Polak - 1978 (PB 294 735)A06
- UCB/EERC-78/23 "MASH - A Computer Program for the Non-Linear Analysis of Vertically Propagating Shear Waves in Horizontally Layered Deposits," by P.P. Martin and H.B. Seed - 1978 (PB 293 101)A05
- UCB/EERC-78/24 "Investigation of the Elastic Characteristics of a Three Story Steel Frame Using System Identification," by I. Kaya and H.D. McNiven - 1978
- UCB/EERC-78/25 "Investigation of the Nonlinear Characteristics of a Three-Story Steel Frame Using System Identification," by I. Kaya and H.D. McNiven - 1978
- UCB/EERC-78/26 "Studies of Strong Ground Motion in Taiwan," by Y.M. Hsiung, B.A. Bolt and J. Penzien - 1978
- UCB/EERC-78/27 "Cyclic Loading Tests of Masonry Single Piers: Volume 1 - Height to Width Ratio of 2," by P.A. Hidalgo, R.L. Mayes, H.D. McNiven and R.W. Clough - 1978
- UCB/EERC-78/28 "Cyclic Loading Tests of Masonry Single Piers: Volume 2 - Height to Width Ratio of 1," by S.-W.J. Chen, P.A. Hidalgo, R.L. Mayes, R.W. Clough and H.D. McNiven - 1978
- UCB/EERC-78/29 "Analytical Procedures in Soil Dynamics," by J. Lysmer - 1978

- UCB/EERC-79/01 "Hysteretic Behavior of Lightweight Reinforced Concrete Beam-Column Subassemblages," by B. Forzani, E.P. Popov, and V.V. Bertero - 1979
- UCB/EERC-79/02 "The Development of a Mathematical Model to Predict the Flexural Response of Reinforced Concrete Beams to Cyclic Loads, Using System Identification," by J.F. Stanton and H.D. McNiven - 1979
- UCB/EERC-79/03 "Linear and Nonlinear Earthquake Response of Simple Torsionally Coupled Systems," by C.L. Kan and A.K. Chopra - 1979
- UCB/EERC-79/04 "A Mathematical Model of Masonry for Predicting Its Linear Seismic Response Characteristics," by Y. Mengi and H.D. McNiven - 1979
- UCB/EERC-79/05 "Mechanical Behavior of Light Weight Concrete Confined by Different Types of Lateral Reinforcement," by M.A. Manrique and V.V. Bertero - 1979
- UCB/EERC-79/06 "Static Tilt Tests of a Tall Cylindrical Liquid Storage Tank," by R.W. Clough and A. Niwa - 1979
- UCB/EERC-79/07 "The Design of Steel Energy Absorbing Restrainers and Their Incorporation Into Nuclear Power Plants for Enhanced Safety: Volume 1 - Summary Report," by P.N. Spencer, V.F. Zackay, and E.R. Parker - 1979
- UCB/EERC-79/08 "The Design of Steel Energy Absorbing Restrainers and Their Incorporation Into Nuclear Power Plants for Enhanced Safety: Volume 2 - The Development of Analyses for Reactor System Piping," "Simple Systems" by M.C. Lee, J. Penzien, A.K. Chopra, and K. Suzuki "Complex Systems" by G.H. Powell, E.L. Wilson, R.W. Clough and D.G. Row - 1979
- UCB/EERC-79/09 "The Design of Steel Energy Absorbing Restrainers and Their Incorporation Into Nuclear Power Plants for Enhanced Safety: Volume 3 - Evaluation of Commercial Steels," by W.S. Owen, R.M.N. Pelloux, R.O. Ritchie, M. Faral, T. Ohhashi, J. Toplosky, S.J. Hartman, V.F. Zackay, and E.R. Parker - 1979
- UCB/EERC-79/10 "The Design of Steel Energy Absorbing Restrainers and Their Incorporation Into Nuclear Power Plants for Enhanced Safety: Volume 4 - A Review of Energy-Absorbing Devices," by J.M. Kelly and M.S. Skinner - 1979
- UCB/EERC-79/11 "Conservatism In Summation Rules for Closely Spaced Modes," by J.M. Kelly and J.L. Sackman - 1979

- UCB/EERC-79/12 "Cyclic Loading Tests of Masonry Single Piers Volume 3 - Height to Width Ratio of 0.5," by P.A. Hidalgo, R.L. Mayes, H.D. McNiven and R.W. Clough - 1979
- UCB/EERC-79/13 "Cyclic Behavior of Dense Coarse-Grain Materials in Relation to the Seismic Stability of Dams," by N.G. Banerjee, H.B. Seed and C.K. Chan - 1979
- UCB/EERC-79/14 "Seismic Behavior of R/C Interior Beam Column Subassemblages," by S. Viathanatepa, E.P. Popov and V.V. Bertero - 1979
- UCB/EERC-79/15 "Optimal Design of Localized Nonlinear Systems with Dual Performance Criteria Under Earthquake Excitations," by M.A. Bhatti - 1979
- UCB/EERC-79/16 "OPTDYN - A General Purpose Optimization Program for Problems with or without Dynamic Constraints," by M.A. Bhatti, E. Polak and K.S. Pister - 1979
- UCB/EERC-79/17 "ANSR-II, Analysis of Nonlinear Structural Response, Users Manual," by D.P. Mondkar and G.H. Powell - 1979
- UCB/EERC-79/18 "Soil Structure Interaction in Different Seismic Environments," A. Gomez-Masso, J. Lysmer, J.-C. Chen and H.B. Seed - 1979
- UCB/EERC-79/19 "ARMA Models for Earthquake Ground Motions," by M.K. Chang, J.W. Kwiatkowski, R.F. Nau, R.M. Oliver and K.S. Pister - 1979
- UCB/EERC-79/20 "Hysteretic Behavior of Reinforced Concrete Structural Walls," by J.M. Vallenat, V.V. Bertero and E.P. Popov - 1979
- UCB/EERC-79/21 "Studies on High-Frequency Vibrations of Buildings I: The Column Effects," by J. Lubliner - 1979
- UCB/EERC-79/22 "Bond Deterioration of Reinforcing Bars Embedded in Confined Concrete Blocks," by S. Viathanatepa, E.P. Popov and V.V. Bertero - 1979
- UCB/EERC-79/23 "Shaking Table Study of Single-Story Masonry Houses, Volume 1: Test Structures 1 and 2," by P. Güllan, R.L. Mayes and R.W. Clough - 1979
- UCB/EERC-79/24 "Shaking Table Study of Single-Story Masonry Houses, Volume 2: Test Structures 3 and 4," by P. Güllan, R.L. Mayes and R.W. Clough - 1979
- UCB/EERC-79/25 "Shaking Table Study of Single-Story Masonry Houses, Volume 3: Summary, Conclusions and Recommendations," by R.W. Clough, P. Güllan and R.L. Mayes

- UCB/EERC-79/26 "Recommendations for a U.S.-Japan Cooperative Research Program Utilizing Large-Scale Testing Facilities," by U.S.-Japan Planning Group - 1979
- UCB/EERC-79/27 "Earthquake-Induced Liquefaction Near Lake Amatitlan, Guatemala," by H.B. Seed, I. Arango, C.K. Chan, A. Gomez-Masso, and R. Grant de Ascoli - 1979
- UCB/EERC-79/28 "Infill Panels: Their Influence on Seismic Response of Buildings," by J.W. Axley and V.V. Bertero - 1979
- UCB/EERC-79/29 "3D Truss Bar Element (Type 1) for the ANSR-II Program," by D.P. Mondkar and G.H. Powell - 1979
- UCB/EERC-79/30 "2D Beam-Column Element (Type 5 - Parallel Element Theory) for the ANSR-II Program," by D.G. Row, G.H. Powell, and D.P. Mondkar
- UCB/EERC-79/31 "3D Beam-Column Element (Type 2 - Parallel Element Theory) for the ANSR-II Program," by A. Riahi, G.H. Powell, and D.P. Mondkar - 1979
- UCB/EERC-79/32 "On Response of Structures to Stationary Excitation," by A. Der Kiureghian - 1979
- UCB/EERC-79/33 "Undisturbed Sampling and Cyclic Load Testing of Sands," by S. Singh, H.B. Seed, and C.K. Chan - 1979
- UCB/EERC-79/34 "Interaction Effects of Simultaneous Torsional and Compressional Cyclic Loading of Sand," by P.M. Griffin and W.N. Houston - 1979
- UCB/EERC-80/01 "Earthquake Response of Concrete Gravity Dams Including Hydrodynamic and Foundation Interaction Effects," by A.K. Chopra, P. Charkabarti, and S. Gupta - 1980

